Geometrical Interpretations and Algorithmic Verification of Exact Solutions in Compressed Sensing

Von der
Carl-Friedrich-Gauß-Fakultät
der Technischen Universität Carolo-Wilhelmina zu Braunschweig

zur Erlangung des Grades eines
Doktors der Naturwissenschaften (Dr. rer. nat.)

genehmigte Dissertation

von
Christian Kruschel (M.Sc.)
geboren am 02.05.1984
in Winsen (Luhe)

Eingereicht am:	19.06.2014
Disputation am:	06.10.2014
1. Referent:	Prof. Dr. Dirk A. Lorenz
2. Referent:	Prof. Dr. Marc E. Pfetsch

(2015)

Acknowledgments

I am very grateful for the support and influences of many people without whom the present thesis would not have been possible.

First of all, I would like to express my gratitude to my supervisor Prof Dr. Dirk A. Lorenz for his support, the fruitful discussions and advice, as well as for the opportunity to work in such an interesting field of research on questions I favored.
I would like to offer my special thanks to Prof. Dr. Marc E. Pfetsch for valuable tips and comments on my research work.
I would like to thank Jakob S. Jørgensen for the collaboration, for all the useful comments on my thesis and for the permission to use many graphics from our joint work.
Special thanks also to Nadja S. Worliczek, Andreas M. Tillmann and Maike Götting for their support. Furthermore, I wish to thank all colleagues in the Institute for Analysis and Algebra, especially the Kaffeerunde for supporting me with coffee, cakes and a relaxed and pleasant atmosphere.
I also owe a great debt of gratitude to Inga Paszkowski who supported me in all my decisions during the last years. I also wish to thank my family.
Finally, I acknowledge the financial support I received from the Deutsche Forschungsgemeinschaft (DFG). This work has been funded by the DFG within the project "Sparse Exact and Approximate Recovery" under grant LO 1436/3-1.

Abstract

In an era dominated by the topic *big data*, in which everyone is confronted with spying scandals, personalized advertising, and retention of data, it is not surprising that a topic as *compressed sensing* is of such a great interest. In short, and in the words of Galileo Galilei, 'measure what can be measured...', a huge amount of data is collected and stored such that the comparatively small data storage is a major problem. A well-known example is the digital archive of the Federal Bureau of Investigation (FBI): it consists of 200 million fingerprints which are meanwhile stored in compressed manner and due to the wavelet transform no essential characterizations get lost by reconstructing the compressed data. Compressed sensing has a similar intention: assuming that data only consists of few components, then just these components need to be stored. For instance, not every pixel in a noiseless image needs to be stored, in many cases it is sufficient to store the non-zero elements of the gradient of that image. Thus, the field of compressed sensing is very interesting for problems in signal- and image processing. Similarly, the question arises how many measurements are necessarily required to capture and represent high-resolution signal or objects.

In the thesis at hand, the applicability of three of the most applied optimization problems with linear restrictions in compressed sensing is studied. These are *basis pursuit*, *analysis ℓ_1-minimization* und *isotropic total variation minimization*. Unique solutions of basis pursuit and analysis ℓ_1-minimization are considered and, on the basis of their characterizations, methods are designed which verify whether a given vector can be reconstructed exactly by basis pursuit or analysis ℓ_1-minimization. Further, a method is developed which guarantees that a given vector is the unique solution of isotropic total variation minimization. In addition, results on experiments for all three methods are presented where the linear restrictions are given as a random matrix and as a matrix which models the measurement process in computed tomography.

Furthermore, in the present thesis geometrical interpretations are presented. By considering the theory of convex polytopes, three geometrical objects are examined and placed within the context of compressed sensing. The result is a comprehensive study of the geometry of basis pursuit which contains many new insights to necessary geometrical conditions for unique solutions and an explicit number of equivalence classes of unique solutions. The number of these equivalence classes itself is strongly related to the number of unique solutions of basis pursuit for an arbitrary matrix. In addition, the question is addressed for which linear restrictions do exist the most unique solutions of basis pursuit. For this purpose, upper bounds are developed and explicit restrictions are given under which the most vectors can be reconstructed via basis pursuit.

Zusammenfassung

In Zeiten von *Big Data*, in denen man nahezu täglich mit Überwachungsskandalen, personalisierter Werbung und Vorratsdatenspeicherung konfrontiert wird, ist es kein Wunder dass ein Forschungsgebiet wie *Compressed Sensing* von so grossem Interesse ist. Frei nach den Worten von Galileo Galilei, 'alles messen was messbar ist ...', werden so viele Daten erhoben und gesammelt, dass die vergleichsweise geringe Datenspeicherkapazität häufig ein enormes Problem darstellt. Ein bekanntes Beispiel dafür ist das digitale Archiv des Federal Bureau of Investigation (FBI), das über 200 Millionen Fingerabdrücke verwaltet und diese mittlerweile dank der Verwendung der Wavelettransformation in komprimierter Form speichern kann, ohne dass bei der Wiederherstellung der Daten essenzielle Merkmale verloren gehen. Compressed Sensing ist ähnlich ausgerichtet: Man geht davon aus, dass Daten aus nur wenigen wesentlichen Merkmalen bestehen, die gespeichert werden müssen. Zum Beispiel muss bei rauschfreien Lichtbildern nicht jeder Pixelwert einzeln gespeichert werden, in vielen Fällen reicht es vollkommen die von Null verschiedenen Werte des Gradienten des Bildes zu speichern. Daher zeigt sich Compressed Sensing gerade für Probleme der Signal- und Bildverarbeitung äußerst interessant. In ähnlicher Weise stellt sich die Frage, wie viele Messungen tatsächlich nötig sind, um ein Signal oder ein Objekt hochaufgelöst darstellen zu können.

In der vorliegenden Arbeit wird die Anwendungsmöglichkeit von drei in Compressed Sensing verwendeten Optimierungsprobleme mit linearen Nebenbedingungen untersucht. Hierbei handelt es sich namentlich um *Basis Pursuit*, *Analysis ℓ_1-Minimierung* und *Isotropic Total Variation*. Es werden eindeutige Lösungen von Basis Pursuit und der Analysis ℓ_1-Minimierung betrachtet, um auf der Grundlage ihrer Charakterisierungen Methoden vorzustellen, die Verifizieren ob ein gegebener Vektor exakt durch Basis Pursuit oder der Analysis ℓ_1-Minimierung rekonstruiert werden kann. Für Isotropic Total Variation werden hinreichende Bedingungen aufgestellt, die garantieren, dass ein gegebener Vektor die eindeutige Lösung von Isotropic Total Variation ist. Darüber hinaus werden Ergebnisse zu Experimenten mit Zufallsmatrizen als linearen Nebenbedingungen sowie Ergebnisse zu Experimenten mit Matrizen vorgestellt, die den Aufnahmeprozess bei Computertomographie simulieren.

Weiterhin werden in der vorliegenden Arbeit verschiedene geometrische Interpretationen von Basis Pursuit vorgestellt. Unter Verwendung der konvexen Polytop-Theorie werden drei unterschiedliche geometrische Objekte untersucht und in den Zusammenhang mit Compressed Sensing gestellt. Das Ergebnis ist eine umfangreiche Studie der Geometrie von Basis Pursuit mit vielen neuen Einblicken in notwendige geometrische Bedingungen für eindeutige Lösungen und in die explizite Anzahl von Äquivalenzklassen eindeutiger Lösungen. Darüber hinaus wird der Frage nachgegangen, unter welchen linearen Nebenbedingungen die meisten eindeutigen Lösungen existieren. Zu diesem Zweck werden obere Schranken entwickelt, sowie explizite Nebenbedingungen genannt unter denen die meisten Vektoren exakt rekonstruiert werden können.

Contents

List of Figures **VI**

List of Algorithms **VI**

List of Symbols **VII**

1 Introduction **1**
1.1 Sparsity in Compressed Sensing 2
1.2 Outline of this Thesis 6
1.3 Basic Notation 7

2 Conditions for Exact Recovery **9**
2.1 Strict Source Condition 12
2.2 Null Space Property 21
2.3 Exact Recovery Condition 23
2.4 ℓ_2-Source Condition 24
2.5 Mutual Coherence Condition and Spark 25
2.6 Restricted Isometry Property 29
2.7 Remarks and Future Work 31

3 Equivalence Classes for Exact Recovery **33**
3.1 General Position 35
3.2 Geometrical Interpretation of Basis Pursuit 37
3.3 Polar Interpretation of Basis Pursuit 41
3.4 Adjoint Polar Interpretation of Basis Pursuit 42
3.5 Partial Order of Recoverable Supports 46
3.6 Number of Recoverable Supports for Specific Matrices 50
3.6.1 Minimal Number of Recoverable Supports 50
3.6.2 Stating the Number of Recoverable Supports with a priori Assumptions 52
3.6.3 Equiangular Tight Matrices 54
3.6.4 Gaussian Matrices 57
3.6.5 Upper Bound on the Number of Recoverable Supports 60
3.7 Maximal Number of Recoverable Supports 62
3.7.1 Necessary Conditions on Recovery Matrices 64
3.7.2 Explicit Maximal Numbers of Recoverable Supports 65
3.7.3 Non-trivial Upper Bound on the Maximal Number of Recoverable Supports 68
3.8 Remarks and Future Work 70

4 Verifying Exact Recovery **74**
4.1 Test Instances . . . 76
4.1.1 Construction of Recoverable Supports . . . 76
4.1.2 Constructions of Test Instances for Exact Recovery via Alternating Projections . . . 80
4.1.3 Construction of ℓ_2-Normalized Matrices for Desired Recoverable Supports . . . 84
4.2 Testing Exact Recovery . . . 86
4.2.1 Basis Pursuit . . . 87
4.2.2 Analysis ℓ_1-Minimization / Anisotropic Total Variation Minimization 89
4.2.3 Analysis $\ell_{1,2}$-Minimization / Isotropic Total Variation Minimization 92
4.3 Application to Computed Tomography . . . 96
4.3.1 Imaging Model . . . 96
4.3.2 Results on Basis Pursuit . . . 99
4.3.3 Results on Anisotropic Total Variation Minimization . . . 101
4.3.4 Results on Isotropic Total Variation Minimization . . . 104
4.4 Remarks and Future Work . . . 106

5 Conclusion **108**

Description of Experiments **110**

Index **113**

Bibliography **114**

List of Figures

1.1 Example for more efficient sampling in computed tomography 2
1.2 Geometrical interpretation of ℓ_1- and ℓ_2-minimization 4

2.1 Comparison of different recovery conditions for basis pursuit 11
2.2 Columns of the Mercedes-Benz matrix $A \in \mathbb{R}^{2\times 3}$ and the unit circle in $\mathbb{R}^2$. . 29

3.1 Projected cross-polytope $A\mathcal{C}^4_\triangle$ with the Mercedes-Benz matrix $A \in \mathbb{R}^{3\times 4}$. . 36
3.2 Projected cross-polytope $A\mathcal{C}^3_\triangle$ with a specific matrix $A \in \mathbb{R}^{2\times 3}$. 38
3.3 Counterexample which shows that not each $\mathcal{P}$ is a convex polytope 39
3.4 Three geometrical interpretations of basis pursuit with the Mercedes-Benz matrix $A \in \mathbb{R}^{2\times 3}$ 44
3.5 Relationship between the projected cross-polytope $A\mathcal{C}^3_\triangle$ and $C^3 \cap \mathrm{rg}(A^T)$. 45
3.6 Partially ordered set of all recoverable supports of a specific matrix 47
3.7 Polytope $A\mathcal{C}^4_\triangle$ with a specific $A \in \mathbb{R}^{3\times 4}$ 48
3.8 Comparison of the results in Proposition 3.6.1 and Proposition 3.6.2 52
3.9 Comparison of the different results on the recoverability curve for specific $A \in \mathbb{R}^{10\times 15}$ 54
3.10 Comparison of the recoverability curves for maximal recoverable supports of different minimally redundant matrices 58
3.11 Phase transition curves 59
3.12 Comparison of the upper bound in (3.6.4) 61
3.13 Values of λ_k for certain matrices 62
3.14 Illustration of the proof in Theorem 3.7.3 64
3.15 Partially ordered set of the cube for $n = 2$ and $n = 3$ 67
3.16 Comparison of different upper bounds 71

4.1 Illustration of Algorithm 1 78
4.2 Results on constructing a recoverable support of $A \in \mathbb{R}^{n-1\times n}$ 79
4.3 Generated images with certain D-sparsity 81
4.4 Generated images with certain D-ℓ_2-sparsity 83
4.5 Averaged results from Monte Carlo experiments 89
4.6 Time comparison of (L1p) and (L1d) 90
4.7 Comparison for analysis ℓ_1-minimization 92
4.8 Comparison of (AL12p) and (AL12d) 94
4.9 Line segment method for computed tomography 97
4.10 Illustration of fan-beam computed tomography 98
4.11 Image classes with certain sparsities 99
4.12 Results on the reconstruction rate via basis pursuit 100
4.13 Computational time comparison (L1p) (R) and (L1d) 101

4.14 Image classes with certain D-sparsities 101
4.15 Results on the reconstruction rate via anisotropic total variation minimization 102
4.16 Comparison of the phase transition with images generated via alternating projections and with images of the truncated uniform image 103
4.17 Computational time comparison for (AL1p) and (AL1d) 104
4.18 Image classes with certain $D - \ell_2$-sparsities 104
4.19 Results on the reconstruction rate via isotropic total variation minimization 105

List of Algorithms

1 Computing a recoverable support of a given matrix A with a desired size k . 77
2 Constructing a vector $x^* \in \mathbb{R}^n$ with D-sparsity k 80
3 Constructing Test Instance with desired D-ℓ_2-sparsity 82
4 Computing a matrix $A \in \mathbb{R}^{m \times n}$ with ℓ_2-normalized columns such that for given $(I, s) \in \mathcal{S}_{n,k}$, $w \in \mathbb{R}^m, m < n$, the pair (I, s) is a recoverable support of A and w is a dual certificate of (I, s) 85

List of Symbols

Spaces

ℓ_1	Space of absolutely convergent sequences
ℓ_2	Space of square-summable sequences
ℓ_∞	Space of bounded sequences

Elements of Spaces

$\mathbf{1}_n$	$\mathbf{1_n} \in \mathbb{R}^n$ with $\mathbf{1}_i = 1$ for all $i = 1, ..., n$
a_i	i-th column of a given matrix A
d_i	i-th column of a given matrix D
y_I	Subvector $y_I \in \mathbb{R}^I$ with $y \in \mathbb{R}^n, I \subset \{1, ..., n\}$

Functions

$\binom{n}{k}$	Binomial coefficient, i.e. $\binom{n}{k} \equiv \frac{n!}{k!(n-k)!}$
$y!$	Factorial, i.e. $y! \equiv \prod_{i=1}^{y} i$ for $y \in \mathbb{N}$
$\kappa(M)$	Condition number of a matrix M
$\Lambda(A, k)$	Number of recoverable supports of a matrix A with size k
$\lfloor y \rfloor$	Floor function, i.e. $\lfloor y \rfloor \equiv \max\{x \in \mathbb{N} : x \leq y\}$
$\lvert I \rvert$	Cardinality of an index set I
$\lvert y \rvert_0$	Number of non-zeros of $y \in \mathbb{R}^n$, i.e. $\lvert y \rvert_0 \equiv \lvert \text{supp}(y) \rvert$
$\mathbb{E}$	Expected value
$\lVert y \rVert_1$	ℓ_1-norm of $y \in \ell_2$, cf. page 10
$\lVert y \rVert_2$	ℓ_2-norm of $y \in \ell_2$
$\lVert y \rVert_2$	ℓ_2-norm of $y \in \mathbb{R}^n$, i.e. $\lVert y \rVert_2 \equiv \sum_{i=1}^{n} \lvert y_i \rvert^2$
$\lVert y \rVert_\infty$	ℓ_∞-norm of $y \in \ell_2$
$\lVert y \rVert_\infty$	ℓ_∞-norm of $y \in \mathbb{R}^n$
ϕ	Function $\Phi : \mathcal{S}_{n,k} \to \mathcal{F}_{n-k}(C^n)$ in Lemma 3.4.1
$\langle x, y \rangle$	Inner product in $\mathbb{R}^n$, i.e. $\langle x, y \rangle \equiv \sum_{i=1}^{n} x_i y_i$
$\langle x, y \rangle_2$	Inner product in ℓ_2, i.e. $\langle x, y \rangle \equiv \sum_{i \in \Gamma} x_i y_i$
$\text{supp}(y)$	Support of $y \in \mathbb{R}^n$, i.e. $\text{supp}(y) \equiv \{i : y_i \neq 0\}$
$\Xi(m, n, k)$	$\Xi(m, n, k) \equiv \max\{\Lambda(A, k) : A \in \mathbb{R}^{m \times n}\}$
F^*	Fenchel conjugate of $F : \mathcal{X} \to \mathbb{R}_\infty$
$\lVert y \rVert_1$	ℓ_1-norm of $y \in \mathbb{R}^n$, i.e. $\lVert y \rVert_1 \equiv \sum_{i=1}^{n} \lvert y_i \rvert$
erf	Gauss error function

Operators

A^*	Adjoint operator of a linear and bounded operator A
$A^\dagger$	Pseudo-inverse of an operator A
A^T	Transposed matrix of a matrix A
A_I	Restriction of an operator $A : \ell_2 \to \mathcal{Y}$ to $\text{span}(\{e_i\}_{i\in\Gamma}), I \subset \Gamma$
A_I	Submatrix of a matrix $A \in \mathbb{R}^{m\times n}$ with columns indexed by $I \subset \{1, ..., n\}$
P_I	Orthonormal projection onto $\text{span}(\{e_i\}_{i\in I})$
P_Y	Orthonormal projection onto a set Y

Sets

$\text{aff}(Y)$	Affine hull of a set Y
$\text{clo}(Y)$	Topological closure of a set Y
$\text{conv}(Y)$	Convex hull of a set Y
$\mathcal{C}^n_\triangle$	n-dimensional cross-polytope
Γ	Countable index set which belongs to ℓ_1 and ℓ_2
$\ker(A)$	Null space of a linear operator A or a matrix A
$\mathbb{N}$	Set of positive integers
$\mathbb{R}$	Set of real numbers
$\mathbb{R}^n$	Set of n-dimensional real vectors
$\mathbb{R}_+$	Set of real, positive numbers
$\mathbb{R}_\infty$	$\mathbb{R}_\infty \equiv \mathbb{R} \cup \{\infty\}$
$\mathcal{F}_k(P)$	Set of k-dimensional faces of a polytope P
$\mathcal{P}$	$\mathcal{P} \equiv \{Ax^* : x^* \in \mathcal{C}^n_\triangle \text{ solves (L1) uniquely}\}$
$\mathcal{U}^\perp$	Orthogonal complement of a subset U
$\text{cone}(Y)$	Conical hull a set Y
$\text{Sign}(y)$	$\{v \in \ell_2 : v_i = \text{sign}(y_i) \text{ if } y_i \neq 0, \|v\|_\infty \leq 1\}$
$\Omega(g)$	$\Omega(g) \equiv \{f : \mathbb{N} \to \mathbb{R} : \liminf_{k\to\infty} \lvert f(k)/g(k)\rvert > 0\}$ for a function $g : \mathbb{N} \to \mathbb{R}$
$\text{relint}(Y)$	Relative interior of a set Y
$\text{rg}(A)$	Range of an operator A or a matrix A
$\mathcal{S}_{n,k}$	$\{(I, s) : I \subset \{1, ..., n\}, \lvert I\rvert = k, s \in \{-1, +1\}^I\}$ for positive integer n, k
$\text{span}(Y)$	Linear span of a set Y
$\{e_i\}_{i=1}^\infty$	Standard basis of $\mathbb{R}^n$ with $e_i = (\delta_{i,j})_{j=1}^n, 1 \leq i \leq n$
$\{e_i\}_{i\in\Gamma}$	Basis of ℓ_2 with $e_i = (\delta_{i,j})_{j\in\Gamma}, i \in \Gamma$
C^n	n-dimensional cube, i.e. $C^n \equiv [-1, +1]^n$
C^n_+	n-dimensional unit cube, i.e. $C^n_+ \equiv [0, +1]^n$
I^c	Complement of an index set I
P^*	Polar polytope of a polytope P
Y^*	Polar set of a set Y

Other Symbols

$(a, b]$	$(a, b] \equiv \{x \in \mathbb{R} : a < x \leq b\}$ if $a, b \in \mathbb{R}, a < b$

$[a, b]$	$(a, b) \equiv \{x \in \mathbb{R} : a < x < b\}$ if $a, b \in \mathbb{R}, a < b$
$[a, b]$	$[a, b) \equiv \{x \in \mathbb{R} : a \leq x < b\}$ if $a, b \in \mathbb{R}, a < b$
$[a, b]$	$[a, b] \equiv \{x \in \mathbb{R} : a \leq x \leq b\}$ if $a, b \in \mathbb{R}, a \leq b$
$\delta_{i,j}$	Kronecker delta
$\equiv$	$X \equiv Y$ means that the symbol X is defined by the object Y
$\forall$	means 'for all'
λ_k	$\lambda_k \equiv \Lambda(A, -k-1)^{-1} k \Lambda(A, k)$
$\ll$	$a \ll b$ means 'a is much smaller than b'
$\subset$	$X \subset Y \Leftrightarrow \forall x \in X : x \in Y$
$\supset$	$X \supset Y \Leftrightarrow \forall y \in Y : y \in X$

CHAPTER 1

Introduction

Solving a linear system of equations $Ay = b$ with a full rank matrix $A \in \mathbb{R}^{m \times n}$ and a right-hand side $b \in \mathbb{R}^m$ provides three situations: there is no solution, there is exactly one solution, or there are infinitely many solutions. If the matrix A is underdetermined, that is $m < n$, only the third situation occurs. This means that, in general and without any further assumptions, it is difficult or impossible to reconstruct a given vector $x^* \in \mathbb{R}^n$ from $b \equiv Ax^*$. Since in several applications only solutions are required which satisfy a certain model, the restriction to specific properties may reduce the number of possible and desired solutions – ideally, only one solution x^* is left. In signal processing, if the information acquisition process is linear and the underdetermined matrix A models the linear measurement process, one speaks frequently of *compressed sensing*. This term stands for a research area in which an object is captured perfectly by a small number of measurements.

The research on non-adaptive compressed acquisition of data has been concerning many researchers since the beginning of the new millennium. For example the use of standard methods in x-ray computed tomography for medical diagnosis requires many measurements which are used to get good image quality and a precise insight into the patient's body. But a high x-ray dose may have impact on the patient's health, that is why there is great interest in using as few as possible measurements. As one may observe in Figure 1.1, with the use of a specific solver method, only few measurements are sufficient to reconstruct the considered object in perfect image quality from measured data. This means that although a large number of measurements is sufficient to capture an object perfectly, under certain circumstances many of these measurements are redundant. In the following, the term *redundancy* stands for the quotient of the number m of measurements divided by the length n of the signal, i.e. m/n. An other issue to note is that capturing a high-dimensional signal is very expensive in time and memory. To that end, the direct acquisition of a compressed version of a signal or an object via significantly fewer measured data than the dimension of the signal is an important topic in modern applied science.

Three models of solutions concerning compressed sensing came to the fore which all have in common that only little information is required to represent a signal of interest. In these models, the location of the required information is not known a priori; the term *sparsity* is mostly associated with these models. One of the main challenges in compressed sensing is to study the measurements with regard to the corresponding model. This task brings two perspectives of research which are relevant in dependency of the object of research. On the one hand, the task is to design a matrix $A \in \mathbb{R}^{m \times n}$ for an arbitrary n and the smallest possible m such that all vectors $x^* \in \mathbb{R}^n$ of a certain model can be reconstructed exactly from $b \equiv Ax^*$. The advantage of such a matrix may bring, for example, new techniques to compress data, but the feasibility of such new techniques

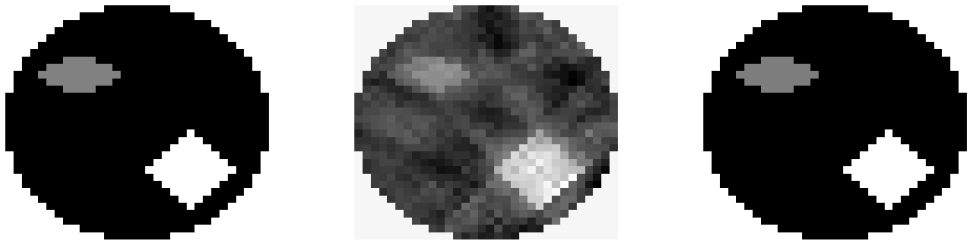

Figure 1.1: Computed tomography reconstructions of a disk-shaped, two-dimensional object with $n \equiv 812$ pixel arrays; the measurements are modeled by $A \in \mathbb{R}^{m\times 812}$ with $m \equiv 320$ measurements. On the left-hand side, the original object x^* is given; in the center the solution with smallest ℓ_2-norm is given; on the right-hand side, the solution with the smallest ℓ_1-norm is given. For a unique solution of $Ay = Ax^*$, it is necessary that A consists of at least $m \approx 812$ measurements, but less than half are sufficient to capture the object. The experiment is described on page 110.

depends strongly on whether A can be constructed in appropriate time. On the other hand, the task is to identify a model of solutions such that for a given measurement matrix $A \in \mathbb{R}^{m\times n}$, all $x^* \in \mathbb{R}^n$ which satisfy this model can be reconstructed from the measured data $b \equiv Ax^*$. The present thesis contains both perspectives.

1.1 Sparsity in Compressed Sensing

A classic model used in compressed sensing is that solutions are considered which have only a few non-zero entries. The model behind this assumption considers that each vector can be represented as a non-negative, linear combination of elements of a set $\mathcal{A}$, and that such a representation can be made by only a few elements of $\mathcal{A}$, not all. This means that, for a given set $\mathcal{A} \subset \mathbb{R}^n$, an element $y \in \mathbb{R}^n$ is related to the model concerning $\mathcal{A}$ if there is a finite subset $\mathcal{S} \subset \mathcal{A}$ and a non-negative sequence $\{q_e\}_{e\in\mathcal{S}}, q_e \geq 0$, such that

$$y = \sum_{e\in\mathcal{S}} q_e e. \tag{1.1.1}$$

Such a vector y is called *sparse*. As their chemical analogue, the elements in $\mathcal{A}$ are called *atoms*, the set $\mathcal{A}$ itself is mostly named *atomic set* [38] or, as in similar applications [52], *dictionary*. In fact, the results on regularization methods with sparsity constraints [46] for ill-posed, inverse problems [74] suggest that their solutions can be compounded by only a few atoms [125].

Let $\mathcal{B}$ denote the standard basis in $\mathbb{R}^n$ and consider the atomic set $\mathcal{E} \equiv \mathcal{B} \cup -\mathcal{B}$. With the notation that $|I|$ describes the cardinality of a finite set I, a vector $y \in \mathbb{R}^n$ which satisfies (1.1.1) with a finite subset $\mathcal{S} \subset \mathcal{E}$ and a non-negative sequence $\{q_e\}_{e\in\mathcal{S}}$ is called *k-sparse* if $k \equiv |\mathcal{S}|$. Further, the cardinality of such a set $\mathcal{S}$ is also called *sparsity*. Let $A \in \mathbb{R}^{m\times n}$ be a matrix with $m < n$, let $x^* \in \mathbb{R}^n$, and let $|y|_0$ denote the number of non-zero entries of $y \in \mathbb{R}^n$. The number $|y|_0$ coincides with the smallest number of atoms in $\mathcal{E}$, denoted by $\mathcal{S}$, such that (1.1.1) holds for a non-negative sequence $\{q_e\}_{e\in\mathcal{S}}$. To find a solution of the linear system of equations $Ay = Ax^*$ with the smallest number of non-zero entries, the sparse optimization problem with affine constraints

$$\min_y |y|_0 \text{ subject to } Ay = Ax^* \tag{L0}$$

is considered. Since the problem (L0) is, in general, NP-hard, cf. [67, Section A6, Mp5], it is of peculiar interest to replace $|\cdot|_0$ by a more computational tractable function. Incorporating the decomposition in atoms, a good substitute might be the gauge function [109, Example 3.50] of $\mathcal{E}$, i.e.

$$\|x\|_{\mathcal{E}} \equiv \inf\left\{t > 0 : t^{-1}x \in \operatorname{conv}(\mathcal{E})\right\} \text{ for } x \in \mathbb{R}^n,$$

where the convex hull of all elements in $\mathcal{E}$ is denoted by $\operatorname{conv}(\mathcal{E})$. By [25, Theorem 1], it follows that

$$\|x\|_{\mathcal{E}} = \inf\left\{\sum_{a\in\mathcal{E}} c_a : x = \sum_{a\in\mathcal{E}} c_a a, c_a \geq 0 \ \forall a \in \mathcal{E}\right\},$$

which corresponds to the ℓ_1-norm, cf. [38]. The convex hull $\operatorname{conv}(\mathcal{E})$ is equal to the cross-polytope. Indeed, the ℓ_1-norm appears to be a good substitute for $|\cdot|_0$: the problem

$$\min_y \|y\|_1 \text{ subject to } Ay = Ax^* \tag{L1}$$

can be attacked by using linear programming, cf. [22], and, therefore, it is computational tractable, cf. [100]. The problem (L1) is called *basis pursuit*. One may observe in the example given in Figure 1.2 that, on the left-hand side, the two-dimensional cross-polytope touches the one-dimensional affine space of solutions of the linear equation only in one coordinate: x_2. This means that a solution of (L0) coincides with the solution of (L1). Replacing the ℓ_1-norm in (L1) by the ℓ_2-norm may lead to the situation in the center of Figure 1.2: the ℓ_2-ball touches the affine space of solutions in both coordinates. Hence, the solution x^{ℓ_2} of $Ay = b$ with the smallest ℓ_2-norm does not coincide with a solution of (L0). As stated in [38, Proposition 2.1], a vector $x^* \in \mathbb{R}^n$ solves (L1) uniquely if and only if the intersection of the null space of A and the tangent cone at x^* with respect to the scaled cross-polytope $\|x^*\|_1\operatorname{conv}(\mathcal{E})$, i.e. $T_{\mathcal{E}}(x^*) \equiv \operatorname{cone}\{z - x^* : \|z\|_1 \leq \|x^*\|_1\}$, is trivial, i.e. $\ker(A) \cap T_{\mathcal{E}}(x^*) = \{0\}$. On the right-hand side in Figure 1.2, one may observe that this condition is similar to the geometrical interpretation on the left-hand side of Figure 1.2. Further, one may observe on the right-hand side of Figure 1.2 that these sufficient and necessary conditions depend on the angle α: if α is the open interval between zero and forty-five, then $\ker(A)\cap T_{\mathcal{E}}(x^*) \supsetneq \{0\}$ and x^* is not a solution of (L1). In three dimensions or higher, solutions of (L0) and (L1) do not coincide necessarily: for the linear system $Ay = Ax^*$ with

$$A \equiv \begin{pmatrix} 1 & 0 & 4 \\ 0 & -1 & 1 \end{pmatrix}, x^* \equiv \begin{pmatrix} 2 & 0 & 0 \end{pmatrix}^T, \tag{1.1.2}$$

the solution of (L1) is the vector $x_1 \equiv \begin{pmatrix} 0 & 1/2 & 1/2 \end{pmatrix}^T$ which is, obviously, not a solution of (L0). So far, it is not clear in which case a solution of (L0) really coincides with a global minimizer of (L1); however, one can state: if $x^* \in \mathbb{R}^n$ solves (L1) uniquely for $A \in \mathbb{R}^{m\times n}, m < n$, then x^* is necessarily at most m-sparse [104].

The model behind the optimization problems in (L0) and (L1) is the so-called *synthesis model* and addresses the situation in which a considered solution is sparse. In some applications, the sparsity of an element itself is not relevant, but some properties may be realized via sparsity. If, for example, it is known that the gradient of a vector is sparse, with D^T as an approximation of finite difference operator, one considers $|D^T y|_0$ and $\|D^T y\|_1$ in (L0) and (L1), respectively, as the objective functions to be minimized. In

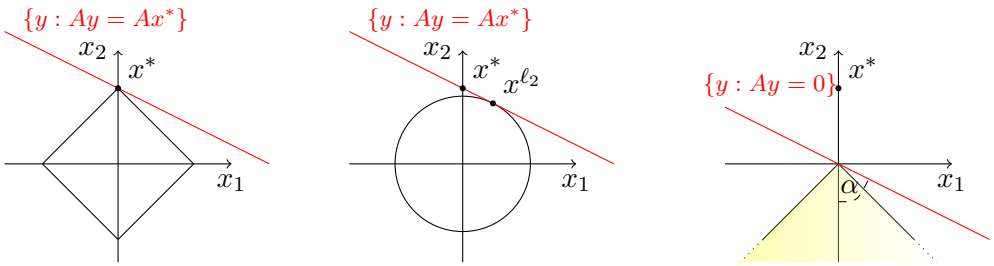

Figure 1.2: Geometrical interpretation of ℓ_1- and ℓ_2-minimization with linear restrictions in $\mathbb{R}^2$. On the left-hand side, the ℓ_1-ball touches the one-dimensional solution space $\{y : Ay = Ax^*\}$ in one coordinate; in the center, the ℓ_2-ball touches the solution space in both coordinates; on the right-hand side, the sufficient and necessary condition $\ker(A) \cap T_{\mathcal{E}}(x^*) = \{0\}$ for x^* being the unique solution of (L1) is illustrated, where $T_{\mathcal{E}}(x^*)$ is exemplified as the yellow-shaped cone.

general, for given $A \in \mathbb{R}^{m\times n}, m < n, D \in \mathbb{R}^{n\times p}$, and $x^* \in \mathbb{R}^n$ one considers

$$\min_y \|D^T y\|_1 \text{ subject to } Ay = Ax^*. \tag{AL1}$$

This model is called the *analysis model* and (AL1) is called *analysis ℓ_1-minimization*. Several applications as decompression [90] and object classification [129] can be realized via the synthesis model, while applications concerning for example signal reconstruction in magnetic resonance imaging [89], limited angle computed tomography [79], and synthetic aperture radar imaging [102] are often realized via the analysis model. In image processing, where $x^* \in \mathbb{R}^n$ can be considered as an image $X \in \mathbb{R}^{N\times N}$ with $n \equiv N^2$, the choice of $D^T \in \mathbb{R}^{2n\times n}$ as the two-dimensional derivate forward operator in the analysis model is closely related to total variation minimization [111]: such a choice of D^T in the analysis model (AL1) is also named *anisotropic total variation minimization*.

Anisotropic total variation minimization plays a crucial role in image processing: since natural images are mostly piecewise-constant, the gradient of such an image is sparse. In fact, considering anisotropic total variation minimization may decrease the number of sufficient measurements: the acquisition process in the example of Figure 1.1 requires only 192 measurements such that (AL1) recovers the original object in perfect image quality. In comparison, in the same example 320 measurements are required for using the ℓ_1-minimization in (L1).

Similar to analysis ℓ_1-minimization, the following problem is considered in compressed sensing. In the following, for given $A \in \mathbb{R}^{m\times n}, m < n, D \in \mathbb{R}^{n\times pn}, p \in \mathbb{N}$, and $x^* \in \mathbb{R}^n$ the optimization problem

$$\min_y \sum_{i=1}^{n} \left(\sum_{j=0}^{p-1} (d_{i+jn}^T y)^2 \right)^{1/2} \text{ subject to } Ay = Ax^* \tag{AL12}$$

is called *analysis $\ell_{1,2}$-minimization*; the $\ell_{1,2}$-norm is defined as

$$\|X\|_{1,2} \equiv \sum_{i=1}^{n} \|x_i\|_2 \text{ for all } X \in \mathbb{R}^{n\times m} \text{ with the } i\text{-th column } x_i \in \mathbb{R}^m.$$

The problem (AL12) can be related to *group sparsity* [7, 70] if D^T consists of permutation matrices. If the matrix $D^T \in \mathbb{R}^{2n\times n}$ is the two-dimensional derivate forward operator,

the problem (AL12) is called *isotropic total variation minimization*. In the present thesis, only isotropic total variation minimization is considered for (AL12). The term sparsity can also be related to (AL1) and (AL12): as in (L1), the sparsity with respect to (AL1) and (AL12), respectively, is associated with the number of non-zero terms of the (outer) sum at the considered objective function. The results in Chapter 2 and Chapter 4 emphasize this definition.

It is well-known [49, 53] that for a certain number m of randomly chosen measurements $A \in \mathbb{R}^{m\times n}, m < n$, all vectors $x^* \in \mathbb{R}^n$ up to a certain sparsity k can be reconstructed perfectly via (L1) from the measurements $b \equiv Ax^*$. Further, it is known [104] that the reconstruction of an arbitrary $x^* \in \mathbb{R}^n$ via (L1) depends only on, loosely speaking, the matrix A, the support and the sign pattern of x^*. But up to now, the smallest possible number of measurements, regardless of what kind of measurements, is not known such that an arbitrary $x^* \in \mathbb{R}^n$ with a certain sparsity can be reconstructed perfectly from $b \equiv Ax^*$. Vice versa, it is not known up to which sparsity a signal can be reconstructed perfectly by given measurements. The present work addresses both issues. On the one hand, several geometrical interpretations are considered to develop theoretical statements on the (maximal possible) number of different pairs of sign pattern and supports. With such results, statements about the (maximal possible) reconstruction rate of vectors with a certain sparsity can be made, which declare, for example, the applicability of the optimization problem in (L1). On the other hand, testing procedures are developed and applied which verify whether a given vector $x^* \in \mathbb{R}^n$ solves (L1) and (AL1), respectively, uniquely for given $A \in \mathbb{R}^{m\times n}, m < n, D \in \mathbb{R}^{n\times p}$. Another method guarantees that a given vector $x^* \in \mathbb{R}^n$ solves (AL12) uniquely for given $A \in \mathbb{R}^{m\times n}, m < n, D \in \mathbb{R}^{n\times pn}, p \in \mathbb{N}$. In contrast to the other mentioned procedures, with the method for analysis $\ell_{1,2}$-minimization no statement can be made which negates the question whether the considered vector solves (AL12) uniquely.

It is worth pointing out that only the optimization problems in (L1), (AL1), and (AL12) are considered in the present thesis. Please note, such linear restrictions mostly occur in idealized situations. In more realistic settings, a solution x^* of one of the three considered optimization problems may not be sparse but may be close to a sparse vector $x^\#$. The term *stability* refers to the property that the distance $\|x^* - x^\#\|_1$ can be controlled by a value δ.
Further, in real-world applications, it can reasonably be concluded that a measured vector b is corrupted by noise, see for instance in [30], this means that for a given matrix $A \in \mathbb{R}^{m\times n}$, which models the measurement process, and an original object $x^* \in \mathbb{R}^n$, a measured vector $b \in \mathbb{R}^m$ is an approximation of Ax^* with $\|Ax^* - b\|_2 \leq \eta$ for some $\eta \geq 0$. The term *robustness* refers to the property that the distance $\|Ax^* - b\|_2$ can be controlled by a value $\bar{\delta}$. In such a situation, the linear restriction in (L1), (AL1), and (AL12), respectively, is replaced by $\|Ay - b\|_2 \leq \bar{\delta}$ for a predefined $\bar{\delta} \geq 0$.
Since only the case of exact sparse solutions of linear systems of equations are considered in the present thesis, the terms stability and robustness are not addressed but it should be emphasized that these are important topics in compressed sensing. Further, only Mosek [5] is used as a solver for the considered problems, but many other solvers do exist. For example in [87] an extensive comparison for solvers of the optimization problem in (L1) is given.

1.2 Outline of this Thesis

The journey of this thesis began with the question how to identify and how to construct a unique solution $x^* \in \mathbb{R}^n$ of (L1) for a given $A \in \mathbb{R}^{m\times n}, m < n$, and a desired sparsity of x^*. The study on several sufficient conditions, in particular the necessary and sufficient conditions in [71], led to the design of an optimization problem whose solution may be used to judge whether a given x^* solves (L1) uniquely for a given underdetermined matrix A, and to the design of an iterative algorithm which constructs a support I, with a desired cardinality k, and a sign pattern $s \in \{-1, +1\}^I$ such that each k-sparse vector $x^* \in \mathbb{R}^n$ with $I = \operatorname{supp}(x^*)$ and $s = \operatorname{sign}(x^*_I)$ solves (L1) uniquely for a given matrix $A \in \mathbb{R}^{m\times n}, m < n$. On the basis of this iterative algorithm, the question arose how many different pairs (I, s) do exist such that each k-sparse vector $x^* \in \mathbb{R}^n$ with $I = \operatorname{supp}(x^*)$ and $s = \operatorname{sign}(x^*_I)$ is the unique solution of (L1) for a given underdetermined matrix A. This led to the connection between the necessary and sufficient conditions in [71] and the intersection of the unit cube in $\mathbb{R}^n$ with hyperplanes, cf. Section 3.4, as well as to the partition of unique solutions of (L1) into equivalence classes in dependency of the considered matrix $A \in \mathbb{R}^{m\times n}$ and the sparsity k. The results are summarized partially in a joint paper [84] with Dirk A. Lorenz. The verification test whether a vector $x^* \in \mathbb{R}^n$ solves (L1) uniquely for a given underdetermined matrix A found an unexpected application at the SIAM Imaging Science conference in 2012 when I got to know Jakob Jørgensen; he did a quantitative verification study on solutions x^* of (L1) with matrices A which model the measurements for computed tomography [81] by solving (L1) straightforwardly (as described in Section 4.2). During the following months, we complemented his original study by ensuring uniqueness, as well as anisotropic and isotropic total variation minimization. In this context, constructions of test instances $x^* \in \mathbb{R}^n$ with a desired corresponding sparsity were developed. The theoretical development of the conditions and the test instances have been mainly my contribution. The results are summarized in [80] which is a joint work with Jakob S. Jørgensen and Dirk A. Lorenz. At the time of the submission of the present thesis, this joint work is close to completion. Simultaneously, I continued the work on the geometrical interpretation of basis pursuit by considering results concerning convex polytopes, in particular, simplicial as well as centrally symmetric polytopes. Besides a full characterization for the matrix $A \in \mathbb{R}^{n-1\times n}$ which reconstructs the most $x^* \in \mathbb{R}^n$ via (L1), these considerations brought new insights to non-trivial upper bounds on the maximal possible of vectors which can be reconstructed via basis pursuit for matrices of arbitrary size.
The present thesis summarizes my recent work and is organized as follows.

Chapter 2. In Chapter 2 several conditions are introduced which guarantee that a certain element x^* solves (L1) uniquely for a given measurement operator A. The conditions *strict source condition*, *null space property*, *exact recovery condition* and *mutual coherence* are introduced and sorted by implication to each other. Additionally, a new recovery condition is introduced: the *ℓ_2-source condition*. Further, sufficient conditions for unique solutions of (AL1) and (AL12) are introduced.

Chapter 3 summarizes my studies on a connection between (L1) and convex polytopes. In this chapter, unique solutions x^* of (L1) are partitioned in equivalence classes in dependency of a matrix A and the sparsity k of the considered vector x^*. Due to the theory of convex polytopes, insights on the number of equivalence classes are given. This number gives further insights whether and how many vectors x^* solves (L1) uniquely. For this purpose specific matrices are considered and the

maximal possible number of equivalence classes is examined.

Chapter 4. In Chapter 4 two types of algorithms are developed: test instances and methods which verify or guarantee uniqueness for basis pursuit, analysis ℓ_1-minimization and analysis $\ell_{1,2}$-minimization. The first method for test instances delivers unique solutions x^* of (L1) for an arbitrary matrix and x^* has a desired sparsity. The second method delivers for a given vector $x^* \in \mathbb{R}^n$ a matrix $A \in \mathbb{R}^{m\times n}$ such that x^* solves (L1) uniquely with regards to A. Further, vectors with a corresponding sparsity for analysis ℓ_1-minimization and analysis $\ell_{1,2}$-minimization are designed. Additionally, methods to verify whether a given $x^* \in \mathbb{R}^n$ solves (L1) and (AL1) uniquely for given $A \in \mathbb{R}^{m\times n}, m < n, D \in \mathbb{R}^{n\times p}$ are designed, as well as an algorithm to guarantee that a given $x^* \in \mathbb{R}^n$ solves (AL12) uniquely is stated. Finally, these methods and generated test instances are used to examine how many vectors with corresponding sparsity are unique solutions of basis pursuit, anisotropic total variation and isotropic total variation, respectively, if the matrix A is modeled for computed tomography with few measurements.

Finally, at the end of each chapter, some remarks and ideas for future work on the considered topic are presented.

1.3 Basic Notation

In the following of the present thesis, no mathematical basics are introduced in a separate chapter. Since the theory in Chapter 2 and Chapter 3 can be assigned to functional analysis and convex polytopes, respectively, at the beginning of each chapter, the most important terms are introduced and further terms are defined when and where they are needed. For simplification, a list of symbols can be found at the beginning of this thesis. To refer to well-known results, the following textbooks are mostly considered:

- for functional analysis: *Linear and Nonlinear Functional Analysis with Applications* by Ciarlet [41],
- for convex analysis: *Convex Analysis and Monotone Operator Theory in Hilbert Spaces* by Bauschke and Combettes [17], and
- for convex polytopes: *Convex Polytopes* by Grünbaum [73].

However, some notations are used in each chapter. In the following, these notations are introduced. Most of the used notations are standard: for example, the symbol $\mathbb{N}$ denotes the set of positive integers, the set of real numbers is denoted by $\mathbb{R}$, and $\mathbb{R}^{m\times n}$ denotes the set of all real matrices with m rows and n columns.

In the present chapter and subsequently, $\equiv$ stands for the definition of a symbol by an object: an arbitrary symbol on the left-hand side is denoted by the object on the right-hand side. For example, if n is a positive integer, then $\mathbb{R}^n \equiv \{(v_i)_{i=1}^n : v_i \in \mathbb{R}\}$ which means that the set of all n-dimensional, real vectors is denoted by $\mathbb{R}^n$. Further, for an index set $I \subset \{1, ..., n\}$ the set

$$\mathbb{R}^I \equiv \{(v_i)_{i\in I} : (v_i)_{i=1}^n \in \mathbb{R}^n\}$$

denotes the set of all real vectors only indexed by I. This notation will cause no confusion to congruence in modular arithmetic.

As in standard notation, for $(v_i)_{i=1}^n \in \mathbb{R}^n$ the symbol $v \in \mathbb{R}^n$ is used. The notations in the previous paragraph do actually hold in the present thesis. The same notation is used for subsets of $\mathbb{R}$, for example

$$\{-1,+1\}^I \equiv \{(v_i)_{i\in I} : v_i \in \{-1,+1\}\}.$$

For such an index set $I \subset \{1,...,n\}$, the complement of I is denoted by I^c, i.e. $I^c \equiv \{1,...,n\}\backslash I$. Further for $v \in \mathbb{R}^n$, the symbol v_I denotes the entries of v indexed by I, i.e.

$$v_I \equiv (v_i)_{i\in I}.$$

For $v \in \mathbb{R}^n$, the support of v is denoted by $\operatorname{supp}(v) \equiv \{i : v_i \neq 0\}$ and the sign of v restricted to its support I is denoted by

$$\operatorname{sign}(v_I) \equiv \left(\frac{v_i}{|v_i|}\right)_{i\in I}.$$

The vector $\operatorname{sign}(v_I)$ is also called *sign pattern of* v.

Matrices are only denoted in upper case letters, their corresponding columns are denoted by the same letter but all in lower case equipped with an index. For example the matrix $A \in \mathbb{R}^{m\times n}$ has columns $a_1,...,a_n \in \mathbb{R}^m$. For an index set $I \subset \{1,...,n\}$, the matrix A_I denotes the restriction of the matrix $A \in \mathbb{R}^{m\times n}$ to columns only indexed by I.

Finally, for a real Hilbert space $\mathcal{X}$ and a convex function $f : \mathcal{X} \to \mathbb{R}$, the subdifferential of f at $x^* \in \mathcal{X}$ is denoted by

$$\partial f(x^*) \equiv \{v \in \mathcal{X} : f(x^*) + \langle v, y - x^*\rangle_{\mathcal{X}} \leq f(y) \text{ for all } y \in \mathcal{X}\}.$$

An important theorem is the optimality condition concerning the subdifferential, see for instance [16, Theorem 16.2]:

$$x^* \in \mathcal{X} \text{ solves } \min_y f(y) \text{ if and only if } 0 \in \partial f(x^*).$$

This result is applied several times in the present thesis.

CHAPTER 2

Conditions for Exact Recovery

In this chapter, several conditions which guarantee that a given vector $x^* \in \mathbb{R}^n$ solves (L1) uniquely for a given matrix $A \in \mathbb{R}^{m \times n}, m < n$, are introduced and related to each other by implication. Most of the results stated in the present chapter are well-known in the field of compressed sensing. The contribution to the present thesis is the elaboration of the relationship of these conditions to each other. Further, a new condition is introduced: the *ℓ_2-source condition*.

A condition is called *recovery condition* if it states sufficient conditions on a matrix A or a vector x^* such that x^* solves (L1) uniquely; one may well refer to *recoverability*. For a given matrix $A \in \mathbb{R}^{m \times n}, m < n$, the result in Corollary 2.1.11 below implies that $x^* \in \mathbb{R}^n$ solving (L1) uniquely depends on its support and the signs of its entries. Therefore, the following three levels of recoverability are distinguished. Let k be a positive integer.

> *Global recoverability* means, for all subsets $I \subset \{1, ..., n\}$ with $|I| = k$, all x^* with $I = \operatorname{supp}(x^*)$ solve (L1) uniquely.
>
> *Local recoverability* means that for a given subset $I \subset \{1, ..., n\}$ with $|I| = k$, all x^* with $I = \operatorname{supp}(x^*)$ solve (L1) uniquely.
>
> *Individual recoverability* means that for a given subset $I \subset \{1, ..., n\}$ with $|I| = k$ and $s \in \{-1, +1\}^I$, all x^* with $I = \operatorname{supp}(x^*)$ and $s = \operatorname{sign}(x^*)_I$ solve (L1) uniquely.

In global recoverability all supports of a certain size k are considered, while in local recoverability a fixed support I is regarded but not a certain sign pattern $s \in \{-1, +1\}^I$. It follows easily that global recoverability implies local recoverability, and local recoverability implies individual recoverability; the converse does not hold. This distinction was first considered in [49].

Recovery conditions concerning the constrained ℓ_1-minimization in (L1) were also introduced for complex numbers [63, 124] as well as for real, infinite-dimensional Hilbert spaces [71, 88]. Impressively, adapting the recovery conditions from a real, finite-dimensional setting to a real, infinite-dimensional Hilbert space does not alter the conditions significantly. For this reason, the recovery conditions, with two exceptions, are introduced for a real, separable Hilbert space setting in this chapter. The three terms of recoverability can easily be transfered to this setting by considering the index set I as a finite subset of a countable index set Γ.

In the following, basic results from functional analysis are repeated; most results can

be found in [41]. With a countable index set Γ, the space of square-summable sequences

$$\ell_2 \equiv \left\{ x = (x_i)_{i\in\Gamma} : \sum_{i\in\Gamma} x_i^2 < \infty \text{ with } x_i \in \mathbb{R} \text{ for all } i \in \Gamma \right\} \tag{2.0.1}$$

is considered. In the following and without further mentioning, the countable index set Γ is associated with the definition of ℓ_2 in (2.0.1). The space ℓ_2 is a separable Hilbert space [41, Theorem 2.4-2]. Since each separable, infinite-dimensional, and real Hilbert space $\mathcal{X}$ is isometrically isomorphic to ℓ_2 [41, Theorem 4.9-4], one can also consider other separable, infinite-dimensional, and real Hilbert spaces instead of ℓ_2. In the following and without further mentioning, the space ℓ_2 is equipped with the orthonormal basis $\{e_i\}_{i\in\Gamma}$, where $e_{i,j} = \delta_{i,j}$ with $\delta_{i,j}$ as the Kronecker delta. The topological closure of a space $\mathcal{U}$ is denoted by $\mathrm{clo}(\mathcal{U})$. Due to the optimization problem in (L1), the space

$$\ell_1 \equiv \left\{ x = (x_i)_{i\in\Gamma} : \sum_{i\in\Gamma} |x_i| < \infty \text{ with } x_i \in \mathbb{R} \text{ for all } i \in \Gamma \right\}$$

is also considered. Since $\ell_1 \subsetneq \ell_2$, i.e. not all elements in ℓ_2 are absolutely convergent, the ℓ_1-norm is extended to $\|\cdot\|_1 : \ell_2 \to \mathbb{R}_\infty$ with $\mathbb{R}_\infty \equiv \mathbb{R} \cup \{\infty\}$ by setting

$$\|x\|_1 \equiv \begin{cases} \sum_{i\in\Gamma} |x_i| & , \text{ if } x \in \ell_1 \\ \infty & , \text{ if } x \in \ell_2 \backslash \ell_1 \end{cases} \quad \text{for all } x \in \ell_2.$$

These adaptions imply that $\langle e_i, x\rangle_2 = x_i$ for $i \in \Gamma$. For a Hilbert space $\mathcal{X}$, a linear and bounded operator $D : \ell_2 \to \mathcal{X}$, and an index set $I \subset \Gamma$, the topological closure of the linear span of $\{De_i\}_{i\in I}$ is denoted by

$$\mathcal{X}_I^D \equiv \mathrm{clo}(\mathrm{span}(\{De_i\}_{i\in I})).$$

For all $I \subset \Gamma$ it follows that $\mathcal{X}_I \subset \mathcal{X}$, and $\mathcal{X}_I$ is finite-dimensional if I is finite. Further, for a Hilbert space $\mathcal{Y}$ and a linear and bounded operator $A : \mathcal{X} \to \mathcal{Y}$, the restriction of A to the domain $\mathcal{X}_I^D$ is denoted by

$$A_I^D : \mathcal{X}_I^D \to \mathcal{Y}.$$

Except for Theorem 2.1.3, the operator D is considered as the identity operator; to that end, if $D : \ell_2 \to \ell_2$ with $Dx = x$ for all $x \in \ell_2$, the notations

$$\mathcal{X}_I \equiv \mathcal{X}_I^D \text{ and } A_I \equiv A_I^D$$

are used. An important tool is the *direct sum theorem* [41, Theorem 4.5-2] stating that each Hilbert space $\mathcal{X}$ can be represented as the direct sum of the topological closure of a subspace $\mathcal{U} \subset \mathcal{X}$ and its orthogonal complement

$$\mathcal{U}^\perp \equiv \{y \in \mathcal{X} : \langle x, y\rangle_{\mathcal{X}} = 0 \text{ for all } x \in \mathcal{U}\}.$$

The orthogonal complement is closed [41, Theorem 4.5-1]. Hence, for all $x \in \mathcal{X}$ there exists $u \in \mathrm{clo}(\mathcal{U})$ and $v \in \mathcal{U}^\perp$ such that $x = u + v$. For each linear and bounded operator $A : \mathcal{X} \to \mathcal{Y}$, the null space of A is denoted by $\ker(A)$ and the the range of A is denoted by $\mathrm{rg}(A)$. The adjoint of A is the operator $A^* : \mathcal{Y} \to \mathcal{X}$ which satisfies $\langle Ax, y\rangle_{\mathcal{Y}} = \langle x, A^*y\rangle_{\mathcal{X}}$ for $x \in \mathcal{X}, y \in \mathcal{Y}$. It follows that $\ker(A) = \mathrm{rg}(A^*)^\perp$ [41, Theorem 4.7-2]. The null space of A is a closed subset of $\mathcal{X}$, the range of A is not closed if $\mathcal{X}$ is infinite-dimensional. For the

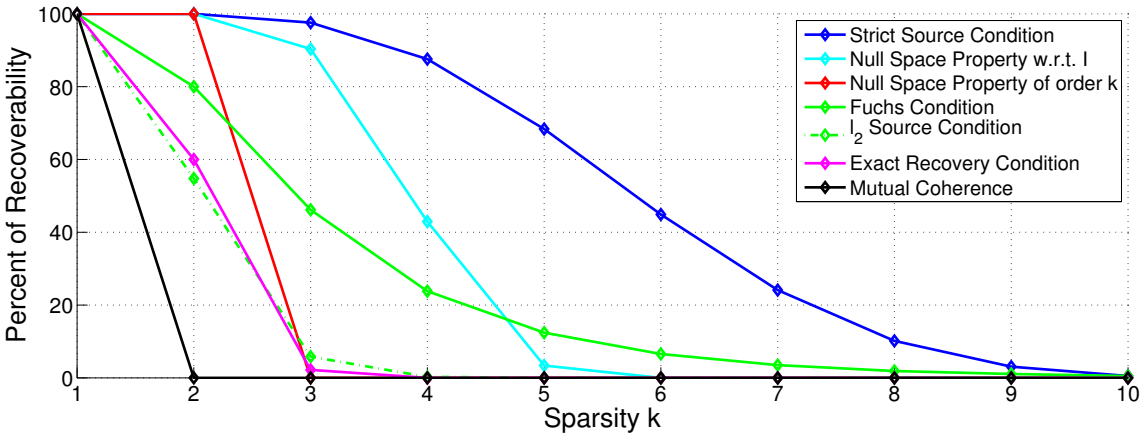

Figure 2.1: Comparison of different recovery conditions of (L1) on a matrix $A \in \mathbb{R}^{10\times 15}$ whose entries are independent standard normal distributed random variables. The graphs illustrate how many percent of the considered vectors $x^* \in \mathbb{R}^{15}$ satisfy the corresponding recovery condition. Details can be found on page 110.

orthogonal projection $P_{\mathcal{U}} : \mathcal{X} \to \mathcal{U}$ onto an arbitrary subspace $\mathcal{U} \subset \mathcal{X}$, the pseudo-inverse of A is denoted by $A^\dagger : \mathrm{rg}(A) \oplus \mathrm{rg}(A)^\perp \to \ell_2$ with the properties

$$AA^\dagger A = A, A^\dagger AA^\dagger = A^\dagger, AA^\dagger = P_{\mathrm{clo}(\mathrm{rg}(A))}, A^\dagger A = P_{\mathrm{clo}(\mathrm{rg}(A^*))}.$$

In finite dimension, instead of operators A and D, one considers matrices $A \in \mathbb{R}^{m\times n}, D \in \mathbb{R}^{n\times p}$, where A^T denotes the transposed matrix of A. Further, it follows that $\mathbb{R}^m = \mathrm{rg}(A) \oplus \ker(A^T)$ for $A \in \mathbb{R}^{m\times n}$ since in finite dimension, the range of A is closed. The rest remains as in the infinite-dimensional setting.

The present chapter is organized as follows. In each section, one recovery condition for (L1) is introduced. An exception is given in Section 2.1, in which sufficient conditions on the unique solution $x^* \in \mathcal{X}$ of the problem

$$\min_{y\in\mathcal{X}} \mathcal{R}(y) \text{ subject to } Ay = Ax^*$$

are examined, where one of the following situations occurs.

- With Hilbert spaces $\mathcal{X}$ and $\mathcal{Y}$, a countable sequence $(\mathcal{X}_i)_{i=1}^\infty$ of Hilbert spaces with $\|\cdot\|_{(i)}$ as the norm induced by the inner products of $\mathcal{X}_i$, a linear and bounded operator $A : \mathcal{X} \to \mathcal{Y}$, and a countable sequence of bounded and linear operators $\{\Phi_i\}_{i=1}^\infty$ with $\Phi_i : \mathcal{X} \to \mathcal{X}_i$, the functional $\mathcal{R} : \mathcal{X} \to \mathbb{R}_\infty$ with

  $$\mathcal{R}(y) \equiv \sum_{i=1}^{\infty} \|\Phi_i y\|_{(i)}$$

  is considered. The resulting problem is related to analysis $\ell_{1,2}$-minimization.

- With Hilbert spaces $\mathcal{X}$ and $\mathcal{Y}$, and linear and bounded operators $D : \ell_2 \to \mathcal{X}$ and $A : \mathcal{X} \to \mathcal{Y}$, the functional $\mathcal{R} : \mathcal{X} \to \mathbb{R}_\infty$ with

  $$\mathcal{R}(y) \equiv \sum_{i\in\Gamma} |\langle De_i, y\rangle|$$

  is considered. The resulting problem is called analysis ℓ_1-minimization.

- With a Hilbert space $\mathcal{Y}$, a linear and bounded operator $A : \ell_2 \to \mathcal{Y}$, the functional $\mathcal{R} : \ell_2 \to \mathbb{R}_\infty$ with
$$\mathcal{R}(y) \equiv \sum_{i \in \Gamma} |\langle e_i, y \rangle|$$
is considered. The resulting optimization problem is called basis pursuit.

Additionally, all three cases above are adapted to the finite-dimensional case. The sufficient conditions for basis pursuit and analysis ℓ_1-minimization in Section 2.1 are also necessary conditions for the existence of unique solutions of the considered optimization problems. In Section 2.2 and the subsequent sections only recovery conditions for basis pursuit are considered. The results on recovery conditions of basis pursuit in Figure 2.1 suggest that the presented conditions can be ordered from the weakest condition to the strongest considered condition. In fact, as shown in the present chapter, all considered conditions can be ordered by *implication*; this means if a recovery condition is satisfied, then a different recovery condition is also satisfied. Therefore, the sections are sorted by implication of the recovery conditions for basis pursuit. An exception to the implication is the *restricted isometry condition* which is introduced in the last section. Since this condition is not only a recovery condition but additionally a condition which implies stability and robustness, this condition is presented out of sequence. In the Sections 2.1 – 2.3, the conditions are presented in a finite-dimensional and infinite-dimensional setting, the subsequent conditions are only introduced in a finite-dimensional setting. All considered spaces are real-valued.

2.1 Strict Source Condition

In this section, the *strict source condition* is introduced as a sufficient and necessary condition on an element $x^* \in \mathcal{X}$ of a Hilbert space $\mathcal{X}$ which solves (L1) uniquely for a linear and bounded operator A mapping from $\mathcal{X}$ into another Hilbert space $\mathcal{Y}$. Up to equivalences, it is the weakest condition for individual recoverability, and it is also known as the *strong source condition* [71]. This condition is one of the linchpins of the present thesis and will also be adapted to *analysis ℓ_1-minimization* in (AL1), where the ℓ_1-norm in (L1) is replaced by the composition of the ℓ_1-norm and the adjoint of a linear and bounded operator $D : \ell_2 \to \mathcal{X}$. Further, a generalization to semi-norms is considered, which can be related to analysis $\ell_{1,2}$-minimization. In Section 4.2.3, the derived sufficient condition on a unique solution of analysis $\ell_{1,2}$-minimization is used for *isotropic total variation minimization* in (AL12).

In the end of the present section, the strict source condition for (L1) is introduced. Priorly, characterizations for solving analysis ℓ_1-minimization uniquely are introduced. But first, an adaption to analysis $\ell_{1,2}$-minimization is considered. The following proposition gives a general result and can be adapted easily to analysis $\ell_{1,2}$-minimization and, in particular, isotropic total variation. The direct product of a countable collection of Hilbert spaces $\{\mathcal{X}_i\}_{i=1}^\infty$, denoted by $\prod_{i=1}^\infty \mathcal{X}_i$, is considered, where for $V = (V_j)_{j=1}^\infty \in \prod_i \mathcal{X}_i$ the j-th component of V is denoted by V_j; hence $V_j \in \mathcal{X}_j$. The result in Proposition 2.1.1 is similar to the result in [70, Proposition 7.1].

Proposition 2.1.1 *Let $\mathcal{X}$ and $\mathcal{Y}$ be real Hilbert spaces, and let $(\mathcal{X}_i)_{i=1}^\infty$ be a countable sequence of real Hilbert spaces. Let $\|\cdot\|_{(i)}$ denote the norm induced by the inner product of*

$\mathcal{X}_i$, consider a countable sequence of linear and bounded operators $(\Phi_i)_{i=1}^{\infty}$ with $\Phi_i : \mathcal{X} \to \mathcal{X}_i$, and let $A : \mathcal{X} \to \mathcal{Y}$ be a linear and bounded operator. Further, consider the mapping

$$\Phi : \mathcal{X} \to \prod_{i=1}^{\infty} \mathcal{X}_i \ , x \mapsto (\Phi_1 x, \Phi_2 x, ...).$$

Let $x^* \in \mathcal{X}$, let $I \equiv \{i : \|\Phi_i x^*\|_{(i)} \neq 0\}$ be finite, and let there exist $j \notin I$. Then x^* solves

$$\min_y \sum_{i=1}^{\infty} \|\Phi_i y\|_{(i)} \text{ subject to } Ay = Ax^* \tag{2.1.1}$$

uniquely if there exists $V \in \prod_{i=1}^{\infty} \mathcal{X}_i$ such that

$$\Phi^* V \in \mathrm{rg}(A^*),\ V_i = \frac{\Phi_i x^*}{\|\Phi_i x^*\|_{(i)}} \text{ for } i \in I,\ \|V_j\|_{(j)} < 1 \text{ for } j \notin I,$$

and A is injective on $\mathcal{S} \equiv \{y \in \mathcal{X} : \|\Phi_j y\|_{(j)} = 0 \text{ for } j \notin I\}$.

Proof. Let $w \in \mathcal{Y}$ satisfy $A^* w = \Phi^* V$, and let $y \in \mathcal{X}, y \neq x^*$, satisfy $Ay = Ax^*$. Since the inner product of $\prod_{i=1}^{\infty} \mathcal{X}_i$ is the sum of the inner products of $\mathcal{X}_i$, it follows that

$$\sum_{i=1}^{\infty} \|\Phi_i x^*\|_{(i)} = \langle V, \Phi x^* \rangle = \langle A^* w, x^* \rangle_{\mathcal{X}} = \langle w, Ax^* \rangle_{\mathcal{Y}} = \langle A^* w, y \rangle_{\mathcal{X}} = \langle V, \Phi y \rangle$$

$$\leq \sum_{i \in I} \underbrace{\|V_i\|_{(i)}}_{=1} \|\Phi_i y\|_{(i)} + \sum_{j \notin I} \underbrace{\|V_j\|_{(j)}}_{<1} \|\Phi_j y\|_{(j)} < \sum_{i=1}^{\infty} \|\Phi_i y\|_{(i)}.$$

Indeed, the previous inequality is strict due to the injectivity: if $\|\Phi_j y\|_{(j)} = 0$ holds for all $j \notin I$, then $y = x^*$. □

Note that in the situation of the previous proposition, it is not necessary that $\|V_j\|_{(j)} < 1$ holds for all $j \notin I$. In the same manner one can also require the existence of $V \in \prod_{i=1}^{\infty} \mathcal{X}_i$ with $\|V_j\|_{(j)} < 1$ for at least one $j \notin I$,

$$\Phi^* V \in \mathrm{rg}(A^*),\ V_i = \frac{\Phi_i x^*}{\|\Phi_i x^*\|_{(i)}} \text{ for } i \in I,\ \|V_j\|_{(j)} \leq 1 \text{ for } j \notin I,$$

and A is injective on $\bar{\mathcal{S}} \equiv \{y \in \mathcal{X} : \|\Phi_j y\|_{(j)} = 0 \text{ for } j \notin I \text{ satisfying } \|V_j\|_{(j)} < 1\}$ as a sufficient condition for $x^* \in \mathcal{X}$ solving (2.1.1) uniquely for a corresponding operator A. This statement can be found in [70].

The previous proposition is consulted in Section 4.2.3. Problem (2.1.1) can be adapted to total variation minimization, analysis ℓ_1-minimization and also basis pursuit. Analysis ℓ_1-minimization and basis pursuit are considered separately in Theorem 2.1.3 and Corollary 2.1.5, respectively. The result of Proposition 2.1.1 can be applied to isotropic total variation minimization, which can be derived by choosing Φ as a discrete gradient as proposed in [37], cf. Section 4.2.3. Several recovery conditions for isotropic total variation minimization have been developed, e.g. [70, 99], but, so far, no necessary conditions for unique solutions x^* of (AL12) are known. In anticipation of the proof of Theorem 2.1.3 below, in which necessary conditions for the unique solution of analysis ℓ_1-minimization are proved, the piecewise linearity of the corresponding optimization problem is used; but

in (2.1.1), the optimization problem is not necessarily piecewise linear. However, since the problem (2.1.1) is a convex optimization problem, one can still formulate necessary (and sufficient) conditions to guarantee that a given $x^* \in \mathcal{X}$ is one solution, but not necessarily the only solution, of (2.1.1).

Proposition 2.1.2 *Consider the same situation as in Proposition 2.1.1. Then $x^* \in \mathcal{X}$ solves* (2.1.1) *if and only if there exists $V \in \prod_{i=1}^{\infty} \mathcal{X}_i$ such that*

$$\Phi^* V \in \mathrm{rg}(A^*),\ V_i = \frac{\Phi_i x^*}{\|\Phi_i x^*\|_{(i)}} \text{ for } i \in I,\ \|V_j\|_{(j)} \leq 1 \text{ for } j \notin I.$$

Proof. This directly follows from the optimality conditions concerning the subdifferential, see for instance [17, Theorem 16.2] with the functional in (2.1.1). □

In the following, the analysis ℓ_1-minimization is considered, where the subdifferential of the ℓ_1-norm is used: for $y \in \ell_1$, it is

$$\partial \|y\|_1 = \mathrm{Sign}(y) \equiv \{v \in \ell_2 : v_j \in [-1, +1]\ \forall j \in \Gamma \text{ and } v_i = \mathrm{sign}(y_i) \text{ if } y_i \neq 0\}.$$

The result in the following theorem is a generalization of the sufficient and necessary condition for unique solutions of basis pursuit which is published in [71]. The argument for proving the necessary conditions is similar to the proof in [71, Lemma 4.5].

Theorem 2.1.3 *Let $\mathcal{X}$ and $\mathcal{Y}$ be real Hilbert spaces, let $A : \mathcal{X} \to \mathcal{Y}, D : \ell_2 \to \mathcal{X}$ be linear and bounded operators, and consider the functional*

$$\mathcal{R} : \mathcal{X} \to \mathbb{R}_\infty, x \mapsto \sum_{i \in \Gamma} |\langle De_i, x \rangle_{\mathcal{X}}|.$$

Finally, let $x^* \in \mathcal{X}$ such that the index set $I \equiv \{i \in \Gamma : \langle De_i, x^* \rangle_{\mathcal{X}} \neq 0\}$ is finite. Then x^* is the unique solution of

$$\min_{y \in \mathcal{X}} \mathcal{R}(y) \text{ subject to } Ay = Ax^* \tag{2.1.2}$$

if and only if there exists $v \in \ell_2$ such that

$$\begin{aligned} &Dv \in \mathrm{rg}(A^*), \\ &\langle e_i, v \rangle_2 = \mathrm{sign}(\langle De_i, x^* \rangle_{\mathcal{X}}) \text{ for } i \in I, \\ &|\langle e_j, v \rangle_2| < 1 \text{ for } j \notin I, \end{aligned} \tag{2.1.3}$$

and the operator A restricted to $S \equiv \{y \in \mathcal{X} : \langle e_j, D^* y \rangle_2 = 0\ \forall j \notin I\}$ is injective.

Proof. This proof is divided into two parts, in each part one direction of the equivalence is proved.

First, it is shown that, under the stated conditions, the element x^* solves (2.1.2) uniquely. Let $w \in \mathcal{Y}$ satisfy $A^* w = Dv$, and let $y \in \mathcal{Y}, y \neq x^*$, satisfy $Ay = Ax^*$. Then there is $j \notin I$ such that $\langle e_j, D^* y \rangle_2 \neq 0$. Indeed, if $\langle e_j, D^* y \rangle_2 = 0$ for all $j \notin I$, then $y \in S$ and, due to the injectivity of A restricted to S, it follows that $x^* = y$. Further, the

conditions in (2.1.3) imply

$$\begin{aligned}\mathcal{R}(x^*) &= \sum_{i\in I} |\langle e_i, D^*x^*\rangle_2| = \sum_{i\in I} \langle e_i, v\rangle_2 \langle e_i, D^*x^*\rangle_2 \\ &= \langle v, D^*x^*\rangle_2 = \langle w, Ax^*\rangle_{\mathcal{Y}} = \langle v, D^*y\rangle_2 \\ &= \sum_{i\in\Gamma} \langle e_i, v\rangle_2 \langle e_i, D^*y\rangle_2 \\ &\leq \sum_{i\in I} \underbrace{|\langle e_i, v\rangle_2|}_{=1} |\langle e_i, D^*y\rangle_2| + \sum_{j\notin I} \underbrace{|\langle e_j, v\rangle_2|}_{<1} |\langle e_j, D^*y\rangle_2| \\ &< \sum_{i\in\Gamma} |\langle e_i, D^*y\rangle_2| = \mathcal{R}(y).\end{aligned}$$

The strict inequality holds since, as seen previously, there is at least one $j \notin I$ such that $\langle e_j, D^*y\rangle_2 \neq 0$. This proves one direction.
The converse direction is proved in two separated parts: first, it is shown that the injectivity statement holds true. Then the remaining conditions in (2.1.3) are proved. Assume that x^* solves (2.1.2) uniquely. Then, for all $z \in \ker(A)\backslash\{0\}$ and all real $t \neq 0$, it follows that $\mathcal{R}(x^*) < \mathcal{R}(x^*+tz)$. Fix $z \in \ker(A)\backslash\{0\}$. Since I is finite, the mapping $t \mapsto \mathcal{R}(x^*+tz)$ is piecewise linear. Considering its one-sided directional derivative with respect to t, it follows that

$$\begin{aligned}0 &< \lim_{t\to 0, t>0} \frac{1}{t} \left[\sum_{i\in I} |\langle e_i, D^*x^*\rangle_2 + t\langle e_i, D^*z\rangle_2| + |t| \sum_{j\notin I} |\langle e_j, D^*z\rangle\rangle_2| - \sum_{i\in I} |\langle e_i, D^*x^*\rangle_2| \right] \\ &= \sum_{j\notin I} |\langle e_j, D^*z\rangle_2| + \lim_{t\to 0, t>0} \frac{1}{t} \sum_{i\in I} |\langle e_i, D^*x^*\rangle_2 + t\langle e_i, D^*z\rangle_2| - |\langle e_i, D^*x^*\rangle_2| \\ &= \sum_{j\notin I} |\langle e_j, D^*z\rangle_2| + \sum_{i\in I} \operatorname{sign}(\langle e_i, D^*x^*\rangle_2) \langle e_i, D^*z\rangle_2.\end{aligned}$$

Since the previous inequality also holds for $-z$, for all $z \in \ker(A)\backslash\{0\}$ the strict inequality

$$\left| \sum_{i\in I} \operatorname{sign}(\langle e_i, D^*x^*\rangle_2) \langle e_i, D^*z\rangle_2 \right| < \sum_{j\notin I} |\langle e_j, D^*z\rangle_2| \tag{2.1.4}$$

holds. Moreover,

$$\text{for all } z \in \ker(A)\backslash\{0\} \ \exists j \notin I \ : \ \langle e_j, D^*z\rangle_2 \neq 0. \tag{2.1.5}$$

Assume that A is not injective on S, then there is $y \in \mathcal{X}, y \neq x^*$, such that $Ax^* = Ay$ and $\langle e_j, D^*y\rangle_2 = 0$ for all $j \notin I$. With $z \equiv y - x^* \in \ker(A)\backslash\{0\}$, for all $j \notin I$, it follows that

$$\langle e_j, D^*z\rangle_2 = \langle e_j, D^*y\rangle_2 - \langle e_j, D^*x^*\rangle_2 = 0,$$

which contradicts (2.1.5); hence, A is injective on S, which proves one necessary condition. With the indicator functional $\mathcal{I} : \mathcal{X} \to \{0, \infty\}$,

$$\mathcal{I}(x) \equiv \begin{cases} 0, & \text{if } Ax = Ax^* \\ \infty, & \text{else} \end{cases} \quad \text{for all } x \in \mathcal{X},$$

consider the subdifferential of the functional $\mathcal{R}+\mathcal{I}$. Since x^* solves (2.1.2), one can deduce from the optimality conditions [17, Theorem 16.2] concerning the subdifferential that there is $\tilde{v} \in \ell_2$ such that $D\tilde{v} \in \mathrm{rg}(A^*)$, $\tilde{v}_i = \mathrm{sign}(\langle e_i, D^*x^*\rangle)$ for $i \in I$ and $|\tilde{v}_j| \leq 1$ for $j \notin I$. Consider $I' \equiv \{i \in \Gamma : |\tilde{v}_i| = 1, i \notin I\}$. Since $\tilde{v}$ is square-summable, the index set I' is finite and, further, it follows that $\mathrm{rg}((A^D_{I\cup I'})^*) = \ker(A^D_{I\cup I'})^\perp$.
The strict inequality (2.1.4) and finiteness of $I \cup I'$ imply the existence of $\nu \in (0,1)$ such that for all $z \in \ker(A)\backslash\{0\}$ which are spanned by $\{De_i\}_{i\in I\cup I'}$ it follows that

$$\left|\sum_{i\in I} \mathrm{sign}(\langle e_i, D^*x^*\rangle_2)\langle e_i, D^*z\rangle_2\right| \leq \nu \sum_{j\in I'} |\langle e_j, D^*z\rangle_2|. \tag{2.1.6}$$

Consider $\eta \in \mathrm{span}\{e_i : i \in I \cup I'\}$ with $\eta_i = \mathrm{sign}(\langle e_i, D^*x^*\rangle_2)$ for $i \in I$ and $\eta_j = 0$ for $j \in I'$. Assume $D\eta \notin \mathrm{rg}((A^D_{I\cup I'})^*)$, otherwise set $\bar{v} = \eta$ and go to the end of the proof. Choose a basis $\{z^{(l)}\}_{1\leq l\leq s}$ of the null space of $A^D_{I\cup I'}$ with

$$\begin{aligned} 1 = \langle D\eta, z^{(l)}\rangle_{\mathcal{X}} &= \sum_{i\in I}\langle e_i, \eta\rangle_2\langle e_i, D^*z^{(l)}\rangle_2 + \underbrace{\sum_{j\in I'}\langle e_j, \eta\rangle_2\langle e_j, D^*z^{(l)}\rangle_2}_{=0} \\ &= \sum_{i\in I} \mathrm{sign}(\langle e_i, D^*x^*\rangle_2)\langle e_i, D^*z^{(l)}\rangle_2 \text{ for all } l = 1, ..., s, \end{aligned} \tag{2.1.7}$$

and consider the optimization problem

$$\min_{\xi\in\mathrm{span}(\{e_j\}_{j\in I'})} \max_{j\in I'} |\langle e_j, \xi\rangle_2| \text{ subject to } \langle \xi, D^*z^{(l)}\rangle_2 = -1 \;\forall\; 1 \leq l \leq s, \tag{2.1.8}$$

and, with $F : x \in \ell_2 \mapsto \max_{j\in I'} |\langle e_j, x\rangle_2|$, the set

$$K = \{y \in \mathcal{X} : \langle y, z^{(l)}\rangle_{\mathcal{X}} = -1 \;\forall\; 1 \leq\; l \leq\; s\},$$

and the indicator functional $\mathcal{I}_K$ on K, its dual problem

$$\max_{\mu\in\ker(A^D_{I\cup I'})} -F^*(-D^*\mu) - \mathcal{I}^*_K(\mu),$$

where the superscript $*$ denotes the Fenchel conjugate [17, Definition 13.1] of the corresponding functional. Note that in (2.1.8), the operator D^* can be restricted to the domain $\ker(A^D_{I\cup I'})$. Since F is a norm, the Fenchel conjugate of F is

$$F^*(z) = \begin{cases} 0 & , \text{ if } \sum_{j\in I'} |\langle e_j, z\rangle_2| \leq 1 \\ \infty & , \text{ else} \end{cases}.$$

Let $z \in \ker(A^D_{I\cup I'})$ have the representation $z = \sum_{l=1}^s q_l z^{(l)}$ with $q \in \mathbb{R}^s$, then the Fenchel conjugate of the indicator functional $\mathcal{I}_K$ is

$$\mathcal{I}^*_K(z) = \sup_{y\in K}\langle z, y\rangle_{\mathcal{X}} = \sup_{y\in K} \sum_{l=1}^s q_l \underbrace{\langle \omega^{(l)}, y\rangle_{\mathcal{X}}}_{=-1} = -\sum_{l=1}^s q_l.$$

With the Fenchel-Rockafellar duality [17, Section 15.3], the optimal value of (2.1.8) is equal to the optimal value of

$$\min_{q\in\mathbb{R}^s} \sum_{l=1}^s q_l \text{ subject to } \sum_{j\in I'} \left|\sum_{l=1}^s q_l\langle e_j, D^*z^{(l)}\rangle_2\right| \leq 1. \tag{2.1.9}$$

Let q^* be a solution of (2.1.9) and consider $z^* \equiv \sum_{l=1}^{s} q_l^* z^{(l)} \in \ker(A^D_{I\cup I'})$. From (2.1.7) and (2.1.6) it follows that

$$\begin{aligned}\left|\sum_{l=1}^{s} q_l^*\right| &= \left|\sum_{i\in I} \operatorname{sign}(\langle e_i, D^*x^*\rangle_2)\langle e_i, D^*z^*\rangle_2\right| \\ &\leq \nu \sum_{j\in I'} \left|\sum_{l=1}^{s} q_l \langle e_j, D^*z^{(l)}\rangle_2\right| \leq \nu < 1.\end{aligned}$$

For a solution ξ^* of (2.1.8) and for $\bar{v} \equiv \eta + \xi^*$ it follows that $D\bar{v} \in \operatorname{rg}((A^D_{I\cup I'})^*)$, since

$$\langle D^*z, (\eta + \xi^*)\rangle_2 = \langle z, D\eta\rangle_{\mathcal{X}} + \langle z, D\xi^*\rangle_{\mathcal{X}} = 0$$

holds for all $z \in \ker(A_{I\cup I'})\backslash\{0\}$. This means that $D(\eta+\xi^*)$ is orthogonal to the null space of $A^D_{I\cup I'}$.
Consider $v = (\tilde{v} + \bar{v})/2$. It follows that $Dv \in \operatorname{rg}(A^*)$ and since $\bar{v} \in \operatorname{span}(\{e_i\}_{i\in I\cup I'})$ it further follows that

$$\begin{aligned}v_i &= \frac{1}{2}\tilde{v}_i + \frac{1}{2}\bar{v}_i = \operatorname{sign}(\langle e_i, D^*x^*\rangle_2) \text{ for } i \in I, \\ |v_j| &\leq \frac{1}{2}\underbrace{|\tilde{v}_j|}_{=1} + \frac{1}{2}\underbrace{|\bar{v}_j|}_{<1} < 1 \text{ for } j \in I', \\ |v_j| &\leq \frac{1}{2}\underbrace{|\tilde{v}_j|}_{<1} + \frac{1}{2}\underbrace{|\bar{v}_j|}_{=0} < 1 \text{ for } j \notin I \cup I',\end{aligned}$$

which proves the assertion. □

The previous theorem states a sufficient and necessary condition for an element x^* to solve analysis ℓ_1-minimization in (AL1) uniquely, even if D is a redundant, non-tight frame operator as discussed in [76].

Remark 2.1.4 In Section 4.2.2, the conditions from the previous theorem are used to formulate a test whether, for given matrices $D \in \mathbb{R}^{n\times p}, A \in \mathbb{R}^{m\times n}, m < n$, a given vector $x^* \in \mathbb{R}^n$ solves

$$\min_y \|D^T y\|_1 \text{ subject to } Ay = Ax^* \tag{AL1}$$

uniquely. To that end, the situation in Theorem 2.1.3 can be simplified by setting $\mathcal{X} = \mathbb{R}^n, \mathcal{Y} = \mathbb{R}^m$, and considering $\mathbb{R}^p$ instead of ℓ_2. Let $x^* \in \mathbb{R}^n$ as well as $D \in \mathbb{R}^{n\times p}, A \in \mathbb{R}^{m\times n}$ be given. With d_i as the i-th column of D, consider $I \equiv \{i : d_i^T x^* \neq 0\}$ and assume x^* and D are given such that the complement of I is not empty, i.e. $I^c \neq \emptyset$, with $I^c \equiv \{1, ..., p\}\backslash I$. Then x^* solves (AL1) uniquely if and only if there are $w \in \mathbb{R}^m$ and $v \in \mathbb{R}^p$ such that

$$\begin{aligned}A^T w + Dv &= 0, \\ v_i = \operatorname{sign}(d_i^T x^*) &\text{ for } i \in I, \\ |v_j| < 1 &\text{ for } j \in I^c,\end{aligned} \tag{2.1.10}$$

and A is injective on $\{y \in \mathbb{R}^n : d_j^T y = 0 \text{ for } j \in I^c\}$. Note, that $I^c \neq \emptyset$ is required for uniqueness: if I^c is empty, then, in the proof for the sufficient and necessary condition, the statements $\mathcal{R}(x^*) < \mathcal{R}(y)$ and (2.1.4), respectively, can not be guaranteed.

Analysis ℓ_1-minimization will be considered again in Section 4.2.2, until then only (L1) is considered. From now on and until the end of this chapter, *solving* (L1) *uniquely* is considered, which means that for a given linear and bounded operator $A : \ell_2 \to \mathcal{Y}$ and a given $x^* \in \ell_2$, solving the problem

$$x^* = \arg\min_{y \in \ell_2} \|y\|_1 \text{ such that } Ay = Ax^*$$

is considered. For that purpose, several conditions on x^* are considered. In the following corollary, the condition in Theorem 2.1.3 is adapted to (L1). The same result is published in [71]. Up to equivalences, it is the weakest condition for individual recoverability.

Corollary 2.1.5 *[71, Theorem 4.7] Let $\mathcal{Y}$ be a real Hilbert space, let $A : \ell_2 \to \mathcal{Y}$ be a linear and bounded operator, and $x^* \in \ell_2$ with $I \equiv \{i \in \Gamma : x_i^* \neq 0\}$ finite. Then x^* solves*

$$\min_y \|y\|_1 \text{ subject to } Ay = Ax^*$$

uniquely if and only if A restricted to $\{y \in \ell_2 : \ y_i = 0 \ \forall i \notin I\}$ is injective and there exists $w \in \mathcal{Y}$ such that

$$\begin{aligned} &\langle e_i, A^*w\rangle_2 = \operatorname{sign}(x_i^*), && \text{for } i \in I, \\ &|\langle e_j, A^*w\rangle_2| < 1, && \text{for } j \notin I. \end{aligned} \tag{2.1.11}$$

Remark 2.1.6 The conditions in (2.1.3) can be adopted to (L1) such that they imply the conditions in (2.1.11): in the context of Theorem 2.1.3, set $\mathcal{X} \equiv \ell_2$ and D as the identity operator, i.e. $Dx = x$ for all $x \in \ell_2$. Then there exists $w \in \mathcal{Y}$ with $A^*w = v$ and (2.1.11) holds.
Vice versa, the conditions in (2.1.11) do not imply the conditions in (2.1.3): for an operator $D : \ell_2 \to \mathcal{X}$ with $\mathcal{X}$ as a separable Hilbert space, an orthonormal basis $\{e_i\}_{i\in\Gamma}$ of ℓ_2 has to be chosen such that the set $\{De_i\}_{i\in\Gamma}$ is an orthonormal basis of $\mathcal{X}$. This is not valid if the null space of D^* contains more than the trivial null space element, i.e. $\{0\} \neq \ker(D^*)$, since only the elements in $\operatorname{rg}(D) \subset \mathcal{X}$ can be generated by the linear span of $\{De_i\}_{i\in\Gamma}$.

The condition given in Corollary 2.1.5 is called *strict source condition*, see Definition 2.1.12 below. Similarly to Proposition 2.1.2, a condition can be deduced from the optimality conditions concerning the subdifferential, see for instance [17, Theorem 16.2], which guarantees that a considered element x^* solves (L1). This condition is called *source condition*.

Corollary 2.1.7 *Let $\mathcal{Y}$ be a real Hilbert space, let $A : \ell_2 \to \mathcal{Y}$ be a linear and bounded operator, and $x^* \in \ell_2$ with $I \equiv \{i \in \Gamma : x_i^* \neq 0\}$. Then x^* solves*

$$\min_y \|y\|_1 \text{ subject to } Ay = Ax^*$$

if and only if there exists $w \in \mathcal{Y}$ such that

$$\begin{aligned} &\langle e_i, A^*w\rangle_2 = \operatorname{sign}(x_i^*), && \text{for } i \in I, \\ &|\langle e_j, A^*w\rangle_2| \leq 1, && \text{for } j \notin I. \end{aligned}$$

The sufficient and necessary condition in Corollary 2.1.5 shows that the recoverability of an element x^* via (L1) depends only on the support and the sign of x^*, but not on the magnitude of its non-zero entries. In other words, changing the entries of a solution on

its support with maintaining signs does not influence whether the changed element solves (L1). The following corollary states that the solutions of the constrained ℓ_1-minimization are *nested*, i.e. in the context of Corollary 2.1.5, if $x^* \in \ell_2$ with a finite support $I \equiv \{i \in \Gamma : x_i^* \neq 0\}$ solves (L1) uniquely for a linear and bounded operator $A : \ell_2 \to \mathcal{Y}$, then each $\bar{x}^* \in \ell_2$ with $\operatorname{supp}(\bar{x}^*) \subset I$ and $\operatorname{sign}(x_i^*) = \operatorname{sign}(\bar{x}_i^*)$ for $\bar{x}_i^* \neq 0$ is the unique solution of

$$\min_y \|y\|_1 \text{ subject to } Ay = A\bar{x}^*. \tag{2.1.12}$$

The following extension for guaranteeing that $\bar{x}^*$ is the unique solution of (2.1.12) is published in [84, Theorem 2.1] for the real, finite-dimensional case.

Proposition 2.1.8 *Let $\mathcal{Y}$ be a real Hilbert space, let $A : \ell_2 \to \mathcal{Y}$ be a linear and bounded operator, and let $x^* \in \ell_2$ with a finite support $I \equiv \{i \in \Gamma : x_i^* \neq 0\}$ be the unique solution of* (L1)*. Then each $\bar{x}^* \in \ell_2$ with $J \equiv \{i \in \Gamma : \bar{x}_i^* \neq 0\}$ which satisfies*

$$J \subset I \text{ and } \operatorname{sign}(x_i^*) = \operatorname{sign}(\bar{x}_i^*) \text{ for } i \in J$$

solves (2.1.12) *uniquely.*

Proof. It is sufficient to show that the statement holds for $J \equiv I \backslash \{j_0\}$ with $j_0 \in I$; the full result can be achieved by applying the following recursively.
By Corollary 2.1.5, let $w \in \mathcal{Y}$ satisfy (2.1.11). Since $\ker(A_I^*) \subsetneq \ker(A_J^*)$, there is $z \in \ker(A_J^*) \backslash \{0\}$ with $\langle e_{j_0}, A^* z \rangle_2 \neq 0$. Choose $\gamma \neq 0$ sufficiently small such that

$$|\gamma| < \frac{1 - |\langle e_j, A^* w \rangle_2|}{|\langle e_j, A^* z \rangle_2|} \text{ for all } j \notin I \text{ with } \langle e_j, A^* z \rangle_2 \neq 0$$

and

$$\gamma \langle e_{j_0}, A^* z \rangle_2 \in \begin{cases} (-2, 0) & , \text{ if } \langle e_{j_0}, A^* w \rangle_2 = +1 \\ (0, 2) & , \text{ if } \langle e_{j_0}, A^* w \rangle_2 = -1 \end{cases}$$

hold. By construction, it follows that

$$\begin{aligned} &|\langle e_{j_0}, A^* w + \gamma A^* z \rangle_2| < 1, \\ &\langle e_i, A^* w + \gamma A^* z \rangle_2 = \langle e_i, A^* w \rangle_2 \text{ for } i \in J, \\ &|\langle e_j, A^* w + \gamma A^* z \rangle_2| \leq |\langle e_j, A^* w \rangle_2| + |\gamma| |\langle e_j, A^* z \rangle_2| < 1 \text{ for } j \notin I. \end{aligned}$$

Hence, for $\bar{w} \in \mathcal{Y}$ with $\bar{w} \equiv w + \gamma z$, it follows that

$$\langle e_i, A^* \bar{w} \rangle_2 = \operatorname{sign}(\bar{x}_i^*), \text{ for } i \in J, \ |\langle e_j, A^* \bar{w} \rangle_2| < 1 \text{ for } j \notin J.$$

Further, if A_I is injective, the operator A_J is injective too. With Corollary 2.1.5 the element $\bar{x}^*$ is the unique solution of (2.1.12). □

Up to equivalences, Corollary 2.1.5 presents the weakest conditions of solving (L1) uniquely. A stronger condition is introduced by Fuchs [66], in which a certain element $w \in \mathcal{Y}$ is considered for the condition in Corollary 2.1.5. The following corollary provides this condition.

Corollary 2.1.9 *Let $\mathcal{Y}$ be a real Hilbert space, let $A : \ell_2 \to \mathcal{Y}$ be linear and bounded, and let $x^* \in \ell_2$ have finite support $I \equiv \{i \in \Gamma : x_i^* \neq 0\}$. Consider $s \in \operatorname{span}(\{e_i\}_{i \in I})$ with $s_i = \operatorname{sign}(x_i^*)$ for all $i \in I$. If A_I is injective and*

$$|\langle A_I^\dagger A e_j, s \rangle_2| < 1$$

holds for all $j \notin I$, then x^* is the unique solution of (L1).

Proof. For $w \equiv (A_I^*)^\dagger s$, it follows that $1 > |\langle A_I^\dagger A e_j, s\rangle_2| = |\langle e_j, A^* w\rangle_2|$. Further, since A_I is injective with a finite-dimensional domain, $\mathrm{rg}(A_I^*) = \mathrm{span}(\{e_i\}_{i\in I})$, and therefore, the operator $A_I^\dagger A$ restricted to the linear span of $\{e_i\}_{i\in I}$ is the identity operator. For $i \in I$ it follows that

$$\langle e_i, A^* w\rangle_2 = \langle A_I^\dagger A e_i, s\rangle_2 = \langle e_i, s\rangle_2 = \mathrm{sign}(x^*)_i.$$

□

Remark 2.1.10 In Corollary 2.1.9, the solution of $A_I^* w = s$ with the smallest ℓ_2-norm is considered, but such a solution does not necessarily fulfill $|\langle A_I^\dagger A e_j, s\rangle_2| < 1$. Therefore, the condition in Corollary 2.1.9 is stronger than the condition in Corollary 2.1.5 for individual recoverability.

The following corollary transfers Corollary 2.1.5 to finite dimension. In [66, Theorem 4] the conditions are proved to be sufficient, in [104, Theorem 2], it is shown that these conditions are also necessary.

Corollary 2.1.11 *Let $A \in \mathbb{R}^{m\times n}, m < n$, and $x^* \in \mathbb{R}^n$ with $I \equiv \{i : x_i^* \neq 0\}$. Then x^* solves* (L1) *uniquely if and only if A_I is injective and there exists $w \in \mathbb{R}^m$ satisfying*

$$\begin{aligned} &A_I^T w = \mathrm{sign}(x^*)_I, \\ &\|A_{I^c}^T w\|_\infty < 1. \end{aligned} \tag{2.1.13}$$

The existence of an element $w \in \mathbb{R}^m$ satisfying (2.1.13) in the setting of the previous corollary is important to state sufficient and necessary conditions for individual recoverability.

Definition 2.1.12 *Let $A \in \mathbb{R}^{m\times n}, m < n$, let $I \subset \{1, ..., n\}$, and let $s \in \{-1, +1\}^I$. Then A, I, and s are said to satisfy the* strict source condition *if A_I is injective and there exists an element $w \in \mathbb{R}^m$ such that the conditions in* (2.1.13) *are satisfied. Such an element $w \in \mathbb{R}^m$ is called* dual certificate.

In finite dimension, Fuchs' condition is also a stronger condition for individual recoverability than the condition in Corollary 2.1.11 for the same reason explained in Remark 2.1.10. In the situation of Corollary 2.1.11, the condition in (2.1.13) requires a solution $w^* \in \mathbb{R}^m$ of the linear system of equations $A_I^T w = s \equiv \mathrm{sign}(x^*)_I$ which satisfies $\|A_{I^c}^T w^*\|_\infty < 1$. Each solution of this linear system of equations can be represented as $w = (A_I)^\dagger s + z$ with $z \in \ker(A_I^T)$; Fuchs' condition considers $z = 0$. Note, if A_I is injective, then $\ker(A_I^T)$ has the dimension $(m - |I|)$. With this representation, Fuchs' condition can be made weaker, as shown in the following corollary.

Corollary 2.1.13 *Let $A \in \mathbb{R}^{m\times n}, m < n$, and $x^* \in \mathbb{R}^n$ with $I \equiv \{i : x_i^* \neq 0\}$. The element x^* solves* (L1) *uniquely if and only if A_I is injective and there is $z \in \ker(A_I^T)$ such that*

$$\|A_{I^c}^T (A_I^T)^\dagger \mathrm{sign}(x^*)_I + A_{I^c}^T z\|_\infty < 1.$$

Note, if for $A \in \mathbb{R}^{m\times n}, m < n$, and $x^* \in \mathbb{R}^n$ satisfies $|\mathrm{supp}(x^*)| = \mathrm{rk}(A)$, Fuchs' condition and Corollary 2.1.13 are identical, since $z = 0$ is the only null space element of $A_I^T, I \equiv \mathrm{supp}(x^*)$. The previous corollary can also be adapted to a Hilbert space setting as in Corollary 2.1.5. It seems that verifying individual recoverability is not made easier or

clearer with Corollary 2.1.13 than in the expression of Corollary 2.1.5: one searches for a certain null space element of A_I^T instead of a dual certificate. In some cases, the condition for individual recoverability in Corollary 2.1.13 is expressed briefly and succinctly: for one thing, the representation of all solutions of the linear system $A_I^T w = \operatorname{sign}(x^*)_I$ can be used for statements about existence, see for instance Proposition 4.1.1; for another thing, if the null space has small dimension, for instance $\ker(A_I^T)$ is one-dimensional, the expression in Corollary 2.1.13 may faster or directly show whether an element $x^* \in \mathbb{R}^n$ solves (L1) uniquely.

2.2 Null Space Property

In the previous section, up to equivalences the weakest condition for individual recoverability is considered; in the present section, up to equivalences the weakest conditions for local and global recoverability are discussed. It was first introduced in [52]. Without further mentioning, only real spaces are considered; for the complex case, the reader may consult [72, 122].

Let $\mathcal{Y}$ be a Hilbert space, $x^* \in \ell_1$ and $A : \ell_2 \to \mathcal{Y}$ linear, bounded. If A is not injective, the linear system of equations $Ay = Ax^*$ has infinitely many solutions of the form $x^* + z$ for $z \in \ker(A)$. In (L1) only elements with the smallest ℓ_1-norm are of interest, but one can not verify that each solution of $Ay = Ax^*$ is absolutely convergent. For this reason, the null space of A restricted to ℓ_1 is considered, i.e.

$$\ker(A) \cap \ell_1 = \{z \in \ell_1 : Az = 0\},$$

from now on and until the end of this section. This is similar to the case in [72]. For $I \subset \Gamma$, the operator

$$P_I : \ell_1 \to \operatorname{span}(\{e_i\}_{i\in I}), (x_i)_{i\in\Gamma} \mapsto (x_i)_{i\in I} \tag{2.2.1}$$

denotes the orthogonal projection onto the linear span of $\{e_i\}_{i\in I}$, and $I^c \equiv \Gamma\backslash I$ denotes all indices which are not contained in I.

Definition 2.2.1 *Let $\mathcal{Y}$ be a Hilbert space, let $A : \ell_2 \to \mathcal{Y}$ be a linear and bounded operator, and let $I \subset \Gamma$ be an index set. Then A satisfies the* null space property relative to I *if*

$$\|P_I z\|_1 < \|P_{I^c} z\|_1 \text{ for all } z \in (\ker(A) \cap \ell_1)\backslash\{0\}.$$

Further, the operator A is said to satisfy the null space property of order k *if for all finite subsets $J \subset \Gamma$ with $|J| \leq k$ the operator A satisfies the null space property relative to J.*

Alternatively, one can express both terms of the null space property as follows: there exists $\Theta < \frac{1}{2}$ such that

$$\|P_I z\|_1 \leq \Theta \|z\|_1 \text{ for all } z \in \ker(A) \cap \ell_1.$$

The null space property is a condition which is used to state one of the most considered recovery conditions. Up to equivalences, the following theorem gives the weakest condition for local recoverability.

Theorem 2.2.2 *[72, Lemma 4, Lemma 5] Let $\mathcal{Y}$ be a Hilbert space, let $A : \ell_2 \to \mathcal{Y}$ be a linear and bounded operator, and let $I \subset \Gamma$ be a finite index set. Then every $x^* \in \ell_1$ with* $\operatorname{supp}(x^*) \subset I$ *solves* (L1) *uniquely if and only if A satisfies the null space property relative to I.*

In contrast to the strict source condition, in local recoverability, one does not necessarily need a finite support of the unique solution x^* of (L1) but instead $x^* \in \ell_1$. The object of the null space property of order k is to give a condition for global recoverability, this means only finite subsets of Γ are considered as supports of unique solutions x^* of (L1). The following theorem is done by adapting [43, Corollary 3.3] to Hilbert spaces.

Theorem 2.2.3 *Let $\mathcal{Y}$ be a Hilbert space, let $A : \ell_2 \to \mathcal{Y}$ be a linear and bounded operator, and let k be a positive integer. Then every $x^* \in \ell_2$ with $|\mathrm{supp}(x^*)| \leq k$ solves* (L1) *uniquely if and only if A satisfies the null space property of order k.*

The previous theorem can be proved by considering Theorem 2.2.2 for each $I \subset \Gamma$ with $|I| \leq k$. Both terms of the null space property give an impression about the difference between global and local recoverability: if a corresponding linear and bounded operator A satisfies the null space property of a certain order k (global recoverability), then the null space property relative to each subset with cardinality k is satisfied (local recoverability); the opposite direction does not hold in general. The effect on recoverability may be observed in Figure 2.1. Consequently, both terms of recoverability do not depend on the signs of the entries as in individual recoverability. The null space property appeared also in earlier publications (e.g. [52, 58]). For finite index sets, Theorem 2.2.2 can also be used for individual recoverability in the setting of Section 2.1.

Corollary 2.2.4 *Let $\mathcal{Y}$ be a Hilbert space, let $A : \ell_2 \to \mathcal{Y}$ be a linear and bounded operator, and let $x^* \in \ell_2$ with finite support $I \equiv \mathrm{supp}(x^*) \subset \Gamma$. Then x^* solves* (L1) *uniquely if A satisfies the null space property relative to I.*

Up to equivalences, the null space property is the weakest condition for global and local recoverability, but for individual recoverability it is stronger than the strict source condition. Similarly to Section 2.1, both terms of the null space property can be adapted to the finite-dimensional, real case. Considering the matrix

$$A \equiv \begin{pmatrix} 1 & 0 & 1 \\ 0 & 1 & 1 \end{pmatrix}$$

and observe A does not satisfy the null space property of order $k = 2$, but A, $I \equiv \{2, 3\}$, and $s \equiv [1, 1]^T$ satisfy the strict source condition, with $w = [0, 1]^T$ as the corresponding dual certificate; hence, neither of both concepts of the null space property imply the strict source condition. However, the strict source condition has also been adapted to local recoverability: for a corresponding operator A and a finite index set $I \subset \Gamma$ all $J \subset I$ and all $s \in \mathrm{span}(\{e_j\}_{j \in J})$ with $|s_j| = 1, j \in J$, satisfy the strict source condition. This condition is called *uniform strict source condition* and is equivalent to the null space property relative to I [88, Proposition 5.2].

In the following, the finite-dimensional, real case is considered. To verify the null space property of order k, it is sufficient to show that $\|w_I\|_1 < \|w_{I^c}\|_1$ holds for all $w \in \ker(A) \backslash \{0\}$ and all $I \subset \{1, ..., n\}, |I| = k$, since the condition implies for $J \subsetneq I$ that $\|w_J\|_1 \leq \|w_I\|_1 < \|w_{I^c}\|_1 \leq \|w_{J^c}\|_1$ for all $w \in \ker(A) \backslash \{0\}$. Similarly to the strict source condition, this can be interpreted as *nestedness* of the null space property. But even reformulating the condition to $\|w_I\|_1 < \frac{1}{2}\|w\|_1$ and considering the k largest entries in absolute value on the left-hand side does not simplify the problem: as shown in [121, Corollary 7], the verification whether an underdetermined matrix $A \in \mathbb{Q}^{m \times n}$ satisfies the null space property of order k is NP-hard. However, constructing algorithms for verification is an active research field [39, 45, 83].

On the right-hand side of Figure 1.2 on page 4, one may see a geometrical interpretation of the null space property relative to $I \subset \{1, ..., n\}$, see also [62, Section 2.2.1]. Consider $x^* = [0, 1]^T, I \equiv \{2\}$, and $A \in \mathbb{R}^{1\times 2}$ such that the red line represents the null space of A. If the angle α between the x_2-axis and $\ker(A)$ is in the open interval from forty-five to ninety degrees, for each element $z \in \mathbb{R}^2$ of the null space of A, it follows that

$$|z_2| = |\cos\alpha|\|z\|_2 < |\sin\alpha|\|z\|_2 = |z_1|$$

and with $y \equiv x^* + z$, which also satisfies $Ay = Ax^*$, it follows that

$$\|x^*\|_1 \leq |x_2^* - y_2| + |y_2| = |z_2| + |y_2| < |z_1| + |y_2| = \|y\|_1,$$

i.e. the vector x^* is the unique solution of (L1). This argument can be used to prove one direction in Theorem 2.2.2 [72].

Theorem 2.2.3 also gives a relation between (L0) and (L1). Assume that a linear and bounded operator $A : \ell_2 \to \mathcal{X}$ satisfies the null space property of order k and $x_0 \in \ell_2$ solves (L0), then each $x_1 \in \ell_2$ with $|x_1|_0 \leq k$ solves (L1) uniquely and $|x_0|_0 \leq |x_1|_0 = k$. Hence, the support of x_0 has at most cardinality k.

2.3 Exact Recovery Condition

The exact recovery condition, introduced by Tropp [123], is defined as follows.

Definition 2.3.1 *Let $\mathcal{Y}$ be a Hilbert space, let $A : \ell_2 \to \mathcal{Y}$ be a linear and bounded operator, and let $I \subset \Gamma$ be an index set. Then A and I satisfy the* exact recovery condition *if*

$$\sup_{j\in I^c} \|A_I^\dagger A e_j\|_1 < 1$$

holds and A_I is injective.

The exact recovery condition is a sufficient condition for local recoverability; this can be proved directly [123, Theorem 3.3] or, as in the following proposition, it can be proved by showing the implication to the null space property with respect to a corresponding subset I. The following proposition states that the exact recovery condition is a condition for local recovery.

Proposition 2.3.2 *[88, Proposition 5.1, Proposition 5.3] Let $\mathcal{Y}$ be a Hilbert space, let $A : \ell_2 \to \mathcal{Y}$ be a linear and bounded operator, and let $I \subset \Gamma$ be an index set. Further, let A and I satisfy the exact recovery condition. Then A satisfies the null space property relative to I.*

The opposite direction is not true: considering, as in the previous sections, the real, finite-dimensional case, then the matrix

$$A^{(1)} \equiv \begin{pmatrix} 1 & 1 & 0 \\ 1 & 0 & 1 \end{pmatrix}$$

satisfies the null space property relative to $\{3\}$, but $A^{(1)}$ and $\{3\}$ do not satisfy the exact recovery condition. Moreover, the exact recovery condition is not nested, as the matrix

$$A^{(2)} \equiv \begin{pmatrix} 2 & 5 & 0 \\ 0 & 1 & 1 \end{pmatrix}$$

and the index set $\{2, 3\}$ satisfy the exact recovery condition while $A^{(2)}$ and $\{3\}$ do not satisfy the exact recovery condition. This phenomenon has been observed in [104, Theorem 10] for squared matrices, a follow-up paper [119] proposes the idea to add a normalization of the atoms to this condition.

Similarly to the null space property, one can easily see that the exact recovery condition also implies Fuchs' condition in Corollary 2.1.9. For a Hilbert space $\mathcal{Y}$, a linear and bounded operator $A : \ell_2 \to \mathcal{Y}$, a finite index set $I \subset \Gamma$, and $s \in \operatorname{span}(\{e_i\}_{i\in I})$ with $|s_i| = 1$ for all $i \in I$, it follows that

$$\sup_{j\in I^c} |\langle A_I^\dagger A e_j, s\rangle| \leq \sup_{j\in I^c} \|A_I^\dagger A e_j\|_1 \underbrace{\|s\|_\infty}_{=1} < 1$$

if A and I satisfy the exact recovery condition. Therefore, the exact recovery condition is a stronger condition than the strict source condition.

2.4 ℓ_2-Source Condition

As stated in Corollary 2.1.7, the source condition provides a characterization of a solution $x^* \in \ell_2$ of (L1) for a given linear and bounded operator $A : \ell_2 \to \mathcal{Y}$, with $\mathcal{Y}$ as a Hilbert space. Therefore, the existence of an element $w \in \mathcal{Y}$ such that $A^*w \in \partial\|x^*\|_1$ is sufficient and necessary such that x^* is a solution of (L1). In contrast, for a unique solution x^* of (L1), such an element $w \in \mathcal{Y}$ has to satisfy additionally $|\langle e_j, A^*w\rangle_2| < 1$ for all $j \notin I$. One may ask whether certain properties on the element w can be assumed such that w satisfies these requirements. The following theorem gives an answer to this question.

Theorem 2.4.1 *Let $\mathcal{Y}$ be a Hilbert space, let $A : \ell_2 \to \mathcal{Y}$ be a linear and bounded operator, and let $x^* \in \ell_2$ with a finite and non-empty support $I \equiv \operatorname{supp}(x^*)$ such that A_I is injective. Let $\mathcal{P}_I : \mathcal{Y} \to \operatorname{rg}(A_I)$ denote the projection onto the range of A_I. Then x^* solves* (L1) *uniquely if there is $w \in \mathcal{Y}$ such that $A^*w \in \partial\|x^*\|_1$ and*

$$\sup_{j\in I^c} \|\mathcal{P}_I A e_j\|_{\mathcal{Y}} < \|w\|_{\mathcal{Y}}^{-1}. \tag{2.4.1}$$

Proof. In this proof, the statement (2.4.1) is related directly to the strict source condition. Note, that x^* is already a solution of (L1). Since $\mathcal{P}_I$ is a projection, its norm is equal to 1 and for all $j \notin I$ it follows that

$$|\langle A^*w, e_j\rangle_2| = |\langle \mathcal{P}_I w, \mathcal{P}_I A e_j\rangle_{\mathcal{Y}}| \leq \|\mathcal{P}_I\|\|w\|_{\mathcal{Y}}\|\mathcal{P}_I A e_j\|_{\mathcal{Y}} < 1,$$

which implies the strict source condition in Corollary 2.1.5. □

The previous theorem introduces a condition for individual recoverability. The underlying condition is called *ℓ_2-source condition.*

Definition 2.4.2 *Let $\mathcal{Y}$ be a Hilbert space, let $A : \ell_2 \to \mathcal{Y}$ be a linear and bounded operator, let $I \subset \Gamma$ be a finite subset, and let $s \in \operatorname{span}(\{e_i\}_{i\in I})$ satisfy $|s_i| = 1$ for all $i \in I$. If A_I is injective and there exists $w \in \mathcal{Y}$ such that $A_I^* w = s, \|A^*w\|_\infty \leq 1$ and* (2.4.1) *holds, then A, I, and s are said to satisfy the* ℓ_2-source condition.

So far, this condition is not published as a recovery condition. In Figure 2.1, one may observe that the ℓ_2-source condition delivers almost similar recoverability as the exact recovery condition. Consider the matrix

$$A^{(1)} \equiv \begin{pmatrix} \frac{1}{2} & \frac{1}{2} & 0 \\ 0 & \frac{1}{2} & \frac{1}{2} \end{pmatrix},$$

the index set $I \equiv \{2,3\}$, and $s \equiv [1,1]^T$, then, with $\mathcal{P}_I$ as the orthogonal projection onto the range of $A_I^{(1)}$, it follows that $\|\mathcal{P}_I A^{(1)} e_1\|_2 = \frac{1}{2}$ and there is $w_1 = [0,1]^T$ such that $(A^{(1)})_I^T w_1 = s$ and $\|(A^{(1)})^T w_1\|_\infty \leq 1$. Hence, the ℓ_2-source condition is satisfied by A, I, and s, but the exact recovery condition is not satisfied by $A^{(1)}$ and I since

$$\|(A_I^{(1)})^\dagger A^{(1)} e_1\|_1 = 2 > 1.$$

Vice versa, the matrix

$$A^{(2)} \equiv \begin{pmatrix} 2 & 5 & 0 \\ 0 & 0 & 1 \end{pmatrix},$$

the index set $J \equiv \{2,3\}$, and $s \equiv [1,1]^T$ give a counterexample which shows that the exact recovery condition does not imply the ℓ_2-source condition. But by bounding the operator norm of A_I in dependency of w, the exact recovery condition implies the ℓ_2-source condition.

Proposition 2.4.3 *Let $\mathcal{Y}$ be a Hilbert space, let $A : \ell_2 \to \mathcal{Y}$ be a linear and bounded operator, let $I \subset \Gamma$ be a finite subset, and let $s \in \operatorname{span}(\{e_i\}_{i \in I})$ with $|s_i| = 1$ for all $i \in I$. Let $\mathcal{P}_I : \mathcal{Y} \to \operatorname{rg}(A_I)$ denote the projection onto the range of A_I. Further, let A and I satisfy the exact recovery condition. If there exists $w \in \mathcal{Y}$ such that $A_I^* w = s$, $\|A^* w\|_\infty \leq 1$, and $\|A_I\| \leq \|w\|_2^{-1}$, then A, I and s satisfy the ℓ_2-source condition.*

Proof. It follows that

$$\sup_{j \notin I} \|\mathcal{P}_I A e_j\|_1 = \sup_{j \notin I} \|A_I A_I^\dagger A e_j\|_1 \leq \|A_I\| \sup_{j \notin I} \|A_I^\dagger A e_j\|_1 < \|w\|_2^{-1}.$$

□

Verifying whether a given matrix $A \in \mathbb{R}^{m \times n}, m < n$, a given index set $I \subset \{1, ..., n\}$, and a given $s \in \{-1, +1\}^I$ satisfy the ℓ_2-source condition can be done by checking whether the solution of the quadratic optimization problem

$$\min_w \frac{1}{2}\|w\|_2^2 \text{ subject to } A_I^T w = s, \|A^T w\|_\infty \leq 1$$

satisfies (2.4.1). Note in Fuchs' condition, only the solution of $A_I^T w = s$ with the smallest ℓ_2-norm is considered.

2.5 Mutual Coherence Condition and Spark

In this section, a condition to guarantee global recoverability is introduced: the *mutual coherence condition*. Further, the *spark of a matrix* is introduced which gives a characterization on solutions of (L0) and which is related to the mutual coherence condition.

In contrast to the previous sections, only the finite-dimensional, real case is considered in the present section. The terms of mutual coherence and the spark, see Definition 2.5.1 and Definition 2.5.5, respectively, and the corresponding recovery condition can also be introduced in a general Hilbert space setting, see for instance [106], but since some results, as the Welch bound in Theorem 2.5.8, can not be adapted to infinite-dimensional Hilbert spaces, only finite-dimensional spaces are considered in the present section.

First, a recovery condition based on the maximal coherence between columns of a matrix is introduced. The following methods usually require the introduction to the concept of *frames*, but since the tools from frame theory only appear indirectly, a full introduction has been waived but can be found in [40, 36]. A family of vectors $\{a_i\}_{i=1}^n \subset \mathbb{R}^m$ is called *frame* if there exist positive constants $0 < c_1 \leq c_2$ such for all $b \in \mathbb{R}^m$ it follows that

$$c_1\|b\|_2^2 \leq \sum_{i=1}^{n} |\langle b, a_i\rangle|^2 \leq c_2\|b\|_2^2.$$

An intuition about frames is that a frame is a natural generalization of orthonormal bases by adding redundant elements. Since in the present case the number of frame elements is finite, one may also speak of a *finite frame*. In the present section, matrices $A \in \mathbb{R}^{m\times n}, m < n$, are considered such that the columns a_i build a frame. If a matrix A satisfies $AA^T = \mathrm{Id}$, then A is called *tight*. Note that in the following and without further mentioning, matrices whose entries are all equal to 0 are not considered.

The following term gives the maximum absolute value of the cross-correlation between pairwise different columns of a matrix; it was introduced in [52].

Definition 2.5.1 *Let $A \in \mathbb{R}^{m\times n}$. Then the* mutual coherence *of A is defined by*

$$\mu(A) = \max_{i\neq j} \frac{|\langle a_i, a_j\rangle|}{\|a_i\|_2\|a_j\|_2}.$$

The mutual coherence characterizes the dependency between normalized columns of a matrix: if the columns of a matrix build an orthogonal system, then its mutual coherence is 0. For all matrices $A \in \mathbb{R}^{m\times n}$, an upper bound for the mutual coherence is $\mu(A) \leq 1$.

The mutual coherence can be connected directly to (L1). The sufficient condition in the following theorem first appeared in [52, Theorem 7.1] for A consisting of two orthonormal bases and in [51, Theorem 12] for general A.

Theorem 2.5.2 *Let $A \in \mathbb{R}^{m\times n}$ with $m < n$. If $x^* \in \mathbb{R}^n$ satisfies*

$$|x^*|_0 < \frac{1}{2}\left(1 + \mu(A)^{-1}\right), \tag{2.5.1}$$

then x^* solves (L1) *uniquely.*

Theorem 2.5.2 gives a result for global recoverability: if $k < \frac{1}{2}(1 + \mu(A)^{-1})$, then each k-sparse vector can be recovered via (L1).

Definition 2.5.3 *Let $A \in \mathbb{R}^{m\times n}$ with $m < n$, and let k be a positive integer. Then A and k satisfy the* mutual coherence condition *if*

$$k < \frac{1}{2}\left(1 + \mu(A)^{-1}\right).$$

An advantage of the mutual coherence condition is that it is easily computable. Further, if a matrix $A \in \mathbb{R}^{m\times n}, m < n$, has pairwise different columns, one can deduce that $\mu(A) < 1$, thus, every 1-sparse vector $x^* \in \mathbb{R}^n$ solves (L1) uniquely. Moreover, the condition (2.5.1) implies the exact recovery condition in Section 2.3.

Proposition 2.5.4 *[124] Let $A \in \mathbb{R}^{m\times n}$ with $m < n$ have ℓ_2-normalized columns. If $x^* \in \mathbb{R}^n$ satisfies* (2.5.1)*, then A and $I \equiv \mathrm{supp}(x^*)$ satisfy the exact recovery condition.*

Direct relationships to Fuchs' condition [66, Theorem 3] and the null space property of order k [57, Theorem 4.5] are also known.

As mentioned in the beginning of this section, the concept of the spark can be related to the mutual coherence of a matrix.

Definition 2.5.5 *Let $A \in \mathbb{R}^{m\times n}, m < n$. The spark of A is defined by*

$$\mathrm{spark}(A) \equiv \min\{|z|_0 : z \in \ker(A)\backslash\{0\}\}.$$

In other words, the spark of a matrix is the smallest number of its columns which are linearly dependent. The spark was first introduced in [51]. In general, computing the spark of a matrix is NP-hard [121, Corollary 1]. For all matrices $A \in \mathbb{R}^{m\times n}, m < n$, it follows that $\mathrm{spark}(A) \leq \mathrm{rk}(A) + 1$; if $A \in \mathbb{R}^{m\times n}, m < n$, satisfies $\mathrm{spark}(A) = m + 1$, then A is called *full spark matrix*. Please note, that the term full spark matrix is adopted from frame theory; in some publications concerning compressed sensing, a matrix with such a property is still named full spark frame [3]. Every full spark matrix A has the advantageous property that each submatrix A_I with $I \subset \{1, ..., n\}, |I| = m$, is invertible; for example, if $x^* \in \mathbb{R}^n$ with $I \equiv \mathrm{supp}(x^*)$ and $|I| = m$ solves (L1) uniquely with $A \in \mathbb{R}^{m\times n}, m < n$, then there is only one dual certificate, namely $w = (A_I^T)^{-1}\mathrm{sign}(x^*)_I$.

The following proposition shows the relationship between the spark and the mutual coherence of a matrix. It applies the Gershgorin Disc Theorem [68, Theorem 2].

Proposition 2.5.6 *Let $A \in \mathbb{R}^{m\times n}, m < n$, then*

$$\mathrm{spark}(A) \geq 1 + \mu(A)^{-1}.$$

Before the focus is put back to the mutual coherence, it should be emphasized that the spark is a sufficient and necessary condition for x^* solving (L0).

Theorem 2.5.7 *[51, Corollary 1] Let $A \in \mathbb{R}^{m\times n}, m < n$. Then every k-sparse vector $x^* \in \mathbb{R}^n$ solves* (L0) *if and only if $2k < \mathrm{spark}(A)$.*

By the previous theorem, one can deduce that x^* which satisfies (2.5.1) for a matrix $A \in \mathbb{R}^{m\times n}, m < n$, solves (L0) and (L1) uniquely. This may give an intuitional guess that a matrix with a small mutual coherence is an appropriate candidate for a *recovery matrix*, which is a matrix A for which the most vectors x^* solve (L1) uniquely. In the end of the present and the following section, this aspect is taken up. In [128, 110], a lower bound on the mutual coherence is established.

Theorem 2.5.8 *Let $A \in \mathbb{R}^{m\times n}$, then*

$$\mu(A) \geq \sqrt{\frac{n-m}{m(n-1)}}. \tag{2.5.2}$$

The lower bound in (2.5.2) is called *Welch bound*. In fact, there are pairs $(m,n) \in \mathbb{N}\times\mathbb{N}$ for which a matrix $A \in \mathbb{R}^{m\times n}$ satisfying the Welch bound (2.5.2) can not be found, cf. [18, Theorem VI.7]. A matrix $A \in \mathbb{R}^{m\times n}$ which solves $\min \mu(A)$ is called *Grassmannian*; if there is a constant c such that $c = |\langle a_i, a_j\rangle|$ for all $i \neq j$, then A is called *equiangular*. Malezemov and Pevnyi show in [91, Theorem 5] how important it is to consider the absolute value of the coherence at equiangular matrices: there is no matrix $A \in \mathbb{R}^{m\times n}$ with ℓ_2-normalized columns, $m < n-1$, and $\langle a_i, a_j\rangle = c, i \neq j$, for $c \neq 1$. The following theorem gives a necessary condition on n such that the Welch bound is achieved.

Theorem 2.5.9 *[118, Theorem 2.3] Let $A \in \mathbb{R}^{m\times n}$ with $m < n$ have ℓ_2-normalized columns. Then A is equiangular and tight if and only if equality in* (2.5.2) *holds. Furthermore, equality in* (2.5.2) *can only hold if*

$$n \leq \frac{m(m+1)}{2}. \tag{2.5.3}$$

In other words, the previous theorem states that at high redundancy, i.e. $m \ll n$, it is impossible that the Welch bound (2.5.2) is met.

Remark 2.5.10 Let k be a positive integer and let $n \geq 2m$. From Theorem 2.5.9, one may imply that $m \in \Omega(k^2)$ measurements are necessary such that the corresponding matrix $A \in \mathbb{R}^{m\times n}$, modeled by the measurements, and k satisfy the mutual coherence condition, i.e. every k-sparse vector $x^* \in \mathbb{R}^n$ solves (L1) uniquely. Assume $m \leq \frac{1}{2}(2k-1)^2$. Then, with the Welch bound (2.5.2) and Theorem 2.5.2, it follows that

$$1 > \sqrt{\frac{n-m}{m(n-1)}}(2k-1) \geq \sqrt{\frac{n}{2m(n-1)}}(2k-1) > \sqrt{\frac{1}{2m}}(2k-1) \geq 1,$$

which is a contradiction; hence, at high redundancy $m/n \leq 1/2$ more than $\frac{1}{2}(2k-1)^2$ measurements are required for applying Theorem 2.5.2. This phenomenon is called *squared bottleneck*.

However, constructing Grassmannian, redundant matrices is still an active field in research; so far, only a few deterministic constructions are known [44, 60]. In case of minimally redundancy, i.e. $m = n-1$, one can characterize Grassmannian matrices.

Proposition 2.5.11 *[118, Corollary 2.5] Let $A \in \mathbb{R}^{n-1\times n}$. The matrix A is Grassmannian if and only if A is tight and has ℓ_2-normalized columns.*

Remark 2.5.12 In [78, 91] a tight, minimally redundant matrix $A \in \mathbb{R}^{n-1\times n}$ is constructed iteratively. The constructed matrix possesses the properties that $\langle a_i, a_j\rangle = -n^{-1}$ for all $i \neq j$ and $\sum_{i=1}^n a_i = 0$. Such a matrix is called *Mercedes-Benz matrix*; note that in frame theory, it is called Mercedes-Benz frame. In Figure 2.2, the columns of the Mercedes-Benz matrix for $n = 3$ are illustrated.

Besides other special matrices, Mercedes-Benz matrices possess a property which is relevant in Chapter 3. To that end, the element $\mathbf{1}_n \in \mathbb{R}^n$ whose entries are all equal to 1 is required. Since $\sum_{i=1}^n a_i = 0$ for a_i as the i-th column of a Mercedes-Benz matrix $A \in \mathbb{R}^{n-1\times n}$, it follows that $\ker(A) = \operatorname{span}(\mathbf{1}_n)$.

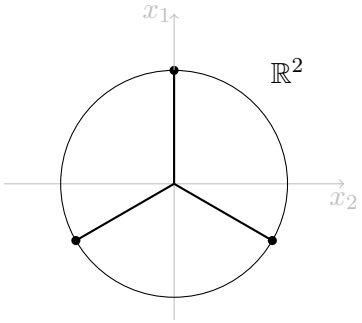

Figure 2.2: Columns of the Mercedes-Benz matrix $A \in \mathbb{R}^{2\times 3}$ and the unit circle in $\mathbb{R}^2$.

Proposition 2.5.13 *Let $A \in \mathbb{R}^{n-1\times n}$ with $\ker(A) = \operatorname{span}(\mathbf{1}_n)$. Then for $y \in \mathbb{R}^n$ it follows that $y \in \operatorname{rg}(A^T)$ if and only if $\sum_{i=1}^n y_i = 0$.*

Proof. The proof is done by considering the direct sum theorem [41, Theorem 4.5-2] and the statement $\operatorname{rg}(A^T) = \ker(A)^\perp$ in finite spaces. □

2.6 Restricted Isometry Property

Since the *restricted isometry property* is not figured prominently in this thesis, it will only be introduced briefly and a lot of important aspects for the compressed sensing are disregarded. For a more detailed account, please consult for example [23]. In this section, the restricted isometry property will only be considered as a recovery condition, as introduced in [35, 34]. It is a promising tool for constructing recovery matrices which also regard stability and robustness. This aspect is considered at the end of this section. In the following, only the finite-dimensional case is considered, a generalized setting can be found, for example, in [71].

Definition 2.6.1 *Let $A \in \mathbb{R}^{m\times n}, m < n$, and let k be a positive integer. The* restricted isometry property of order k *is satisfied by A if there exists $\delta \in (0,1)$ such that for all k-sparse vectors $x \in \mathbb{R}^n$ it follows that*

$$(1-\delta)\|x\|_2^2 \leq \|Ax\|_2^2 \leq (1+\delta)\|x\|_2^2. \tag{2.6.1}$$

The k-th restricted isometry constant $\delta = \delta_k(A)$ *is the smallest $\delta \geq 0$ such that A satisfies the restricted isometry property of order k.*
The matrix A has the (k,δ)-RIP *if* (2.6.1) *is satisfied for all k-sparse vectors for the given δ.*

In general, deciding whether a matrix $A \in \mathbb{Q}^{m\times n}$ is (k,δ)-RIP hard [121, Theorem 3]. The inequality (2.6.1) may be interpreted as a matrix A approximately preserves the distance between any pair of k-sparse vectors. An equivalent description of the k-th restricted isometry constant is given by

$$\delta_k = \max_{I\subset\{1,\dots,n\},|I|\leq k} \|A_I^T A_I - \mathrm{Id}_I\|_2^2.$$

Providing $\delta_k < 1$, each submatrix A_I with $|I| \leq k$ has all its singular values in the interval $[1-\delta_k, 1+\delta_k]$. Moreover, if $\delta_{2k} < 1$, then every two k-sparse vectors $x_1, x_2 \in \mathbb{R}^n$ with different supports satisfy $\|A(x_1 - x_2)\|_2^2 > 0$, which means that distinct k-sparse vectors have distinct measurements. Actually, the function $\delta(A) : k \mapsto \delta_k$ is monotonically nondecreasing for fixed $A \in \mathbb{R}^{m\times n}$, see for instance [64, Chapter 6].

The following theorem gives a recovery condition for global recoverability.

Theorem 2.6.2 *[31] Let $A \in \mathbb{R}^{m\times n}, m < n$. If A is (k,δ)-RIP with $\delta < \frac{1}{3}$, then every k-sparse vector $x^* \in \mathbb{R}^n$ is the unique solution of* (L1).

Theorem 2.6.2 is not the only recovery condition using the restricted isometry constants, other bounds on the restricted isometry constant also imply global recoverability, e.g. [34] or [33].

The restricted isometry constant can also be linked directly to the mutual coherence by using the Gershogorin circle theorem [68].

Proposition 2.6.3 *[64, Proposition 6.2] Let $A \in \mathbb{R}^{m\times n}, m < n$, with ℓ_2-normalized columns. Then A is (k,δ)-RIP with $\delta \leq (k-1)\mu(A)$ for all $k \geq 2$ and $\mu(A) = \delta$ if $k = 1$.*

With the previous proposition, one can connect the mutual coherence and the restricted isometry constant.

Corollary 2.6.4 *Let $A \in \mathbb{R}^{m\times n}, m < n$, with ℓ_2-normalized columns and $k \geq 2$. If A and k satisfy the mutual coherence condition, then A is $(2k,\delta)$-RIP with $\delta < 1$.*

The restricted isometry property is often considered as a promising tool for finding a recovery matrix which also regards stability and robustness. Studying *random matrices*, i.e. matrices whose entries are random variables, are often considered as objects of research in compressed sensing. For example, if the entries of $A \in \mathbb{R}^{m\times n}$ are drawn randomly from the standard normal distribution, and if $m \in \Omega(k\delta^{-2}\log(n/k))$, then A is $(2k,\delta)$-RIP with probability at least $1-2\exp(-C\delta^2 m)$ with a constant C [59, Theorem 5.65]. This matches with the lower bound for the measurements $m \geq Ck\log(n/k)$ in [47, Theorem 3.5] up to a constant if $A \in \mathbb{R}^{m\times n}$ is $(2k,\delta)$-RIP with $\delta \leq \frac{1}{2}$.

Finding deterministic matrices which can be computed in polynomial time and which satisfy $\delta_k \leq \delta$ for a given δ is a major open problem. So far, estimates on δ_k combine an estimate of the mutual coherence μ and $\delta_k \leq (k-1)\mu$, which leads to the squared bottleneck, see Remark 2.5.10. The difficulty in bounding the restricted isometry constants of an explicit matrix A lies in the use of Gershgorin's disc theorem, which is a basic tool for estimating eigenvalues of $A_I^T A_I - \mathrm{Id}$. Consequently, by using Gershgorin's disc theorem, the squared bottleneck is unavoidable. However, in [26] a construction for a matrix is given which cuts through the squared bottleneck with $m \in \Omega(k^{2-\epsilon})$ for small $\epsilon > 0$ and certain n.

Finally, some limiting properties about the matrices satisfying the restricted isometry property are considered which partially give a pessimistic view on applications. Considering the strict source condition, one may observe that adding rows to a matrix does not deteriorate the recoverability. Indeed, if $A \in \mathbb{R}^{m\times n}, m < n$, and $x^* \in \mathbb{R}^n$ is a k-sparse vector with $k < m$ which solves (L1) uniquely, then there is a dual certificate $w \in \mathbb{R}^m$. For any $B \in \mathbb{R}^{q\times n}$, the vector x^* also solves (L1) uniquely for $\bar{A} = \begin{bmatrix} A \\ B \end{bmatrix}$, since with the dual

certificate $\bar{w}^T = [w^T, 0^T]$, it follows that $[A^T, B^T]\bar{w} = \text{sign}(x^*)_I$. In other words, adding further measurements does not violate the recoverability. As highlighted in [64, Page 147], adding rows to a matrix with restricted isometry constant δ_k may increase the restricted isometry constant, for example by adding the row $\sqrt{1+\delta}e_n^T$, with $\delta > \delta_k$ and the i-th unit vector e_n, to a matrix with n columns. In other words, measuring too much may improve the recoverability but may corrupt the restricted isometry constant.

2.7 Remarks and Future Work

In this chapter, several recovery conditions have been considered and have been related to each other, namely the strict source condition, the null space property, the exact recovery condition, the mutual coherence and the spark. Further, a brief introduction to the restricted isometry condition was given, and the ℓ_2-Source Condition was introduced the first time. It should be emphasized that many other recovery conditions do exist, as for example the conditions proposed in [54, 32, 130]. To complement the picture, further recovery conditions may be considered and related to the presented conditions.

Examine the Influence on Dual Certificates and the ℓ_2-Source Condition
As one may observe in Figure 2.1, the exact recovery condition and the ℓ_2-source condition deliver similar results on the recoverability under consideration of the same instances. Both curves in Figure 2.1 and the results in Section 2.4 do not display any relationship between both recovery conditions without further assumptions. Moreover, the ℓ_2-source condition can only be adapted to the strict source condition; a clear relationship to Fuchs' condition is not known so far. In contrast, the exact recovery condition can be connected directly to Fuchs' condition [88, Proposition 5.1]. A clearer classification of the ℓ_2-source condition with respect to the other recovery conditions is the aim of further research. So far, the advantage of this condition over the strict source condition is not clear, but it may be interesting whether this condition gives new insights to stability when the right-hand side of the considered linear system is disturbed by noise.

Relationship between Recovery Conditions for Analysis ℓ_1-Minimization
In the present chapter, recovery conditions for (L1) are mainly considered. In [97], the null space property relative to $I \subset \{1, ..., n\}$, the exact recovery condition, and the spark are adapted to analysis ℓ_1-minimization as in (AL1). The authors in [127] suggest a different variant of the exact recovery condition in analysis ℓ_1-minimization. Establishing implications which relate recovery conditions for analysis ℓ_1-minimization to each other and in regard to [97], [127], and further works on conditions is an idea for future work.

Additionally, developing a variant of Fuchs' condition with respect to analysis ℓ_1-minimization might be a helpful strategy for verifying unique solutions. In basis pursuit, Fuchs' condition is satisfied if $w \equiv (A_I^T)^\dagger \text{sign}(x^*)_I$ is a dual certificate. Following this strategy, several corresponding elements v and w as positive candidates for satisfying (2.1.10) can be constructed, cf. [42].

Recovery Conditions for Analysis $\ell_{1,2}$-Minimization
In this thesis, recovery conditions concerning (2.1.1) are not examined extensively. Further, a necessary condition of unique solutions of (2.1.1), which is similar to the sufficient condition in Proposition 2.1.1, is not known. By applying similar arguments as in the case of analysis ℓ_1-minimization, the development of such a necessary condition was not possible, since (2.1.1) is a conic optimization problem and, in general, not piecewise linear.

Nevertheless, finding necessary conditions, which are also sufficient, is an interesting topic for future work.

CHAPTER 3

Equivalence Classes of Exact Recovery Solutions

In this chapter, basis pursuit is connected to the theory of convex polytopes. For that purpose, equivalence classes of unique solutions of basis pursuit are considered. The sufficient and necessary condition in Corollary 2.1.11 implies that the recoverability of every $x^* \in \mathbb{R}^n$ via (L1) for a matrix $A \in \mathbb{R}^{m \times n}, m < n$, does only depend on its support $I \equiv \operatorname{supp}(x^*)$ and its restricted sign-vector $s \equiv \operatorname{sign}(x^*)_I$. If x^* solves (L1) uniquely, then each $\bar{x}^* \in \mathbb{R}^n$ with $\operatorname{supp}(\bar{x}^*) = I$ and $\operatorname{sign}(\bar{x}^*)_I = s$ also solves (L1) uniquely. Consequently, the vectors x^* and $\bar{x}^*$ are in the same equivalence class, introduced in Definition 3.0.1, if their support and their sign pattern coincide. In the course of this chapter, three different geometrical interpretations of basis pursuit are considered which enables the connection of basis pursuit to convex polytopes such that several results from the field of convex polytopes can be applied to the equivalence classes of solutions. Adaptions to convex polytopes were also done by Donoho [49], see Sections 3.2 and 3.6.4, and Plumbley [104], see Section 3.3, but they have not been studied as extensive as in this chapter. A further contribution of the present thesis is a geometrical interpretation on the basis of the strict source condition. Considering these geometrical interpretations, numbers and maximal possible numbers of these equivalence classes are studied, as well as necessary (geometrical) conditions for instances which reach the maximal possible number of equivalence classes.

The following definition separates different unique solutions of (L1) into equivalence classes.

Definition 3.0.1 *Let $A \in \mathbb{R}^{m \times n}$ with $m < n$, let $I \subset \{1, ..., n\}$ with $|I| = k$ for a positive integer k, and $s \in \{-1, +1\}^I$. The pair (I, s) is called* recoverable support of A with size k *if A_I is injective and there exists $w \in \mathbb{R}^m$ such that*

$$A_I^T w = s,$$
$$\|A_{I^c}^T w\|_\infty < 1.$$

Such an element $w \in \mathbb{R}^m$ is called dual certificate of (I, s).
Further, if (I, s) is a recoverable support of A and there is no recoverable support $(J, \bar{s})$ with $J \supset I$ and $\bar{s}_I = s_I$, then (I, s) is called maximal recoverable support of A.

Both terms in the previous definition are introduced in [84]; in [49], a similar pair (I, s) with I as the support and s as the sign pattern of a solution of (L1) is introduced as a *signed support*. Corollary 2.1.11 implies the connection between recoverable supports and unique solutions of basis pursuit, which is given in the following corollary.

Corollary 3.0.2 *Let $A \in \mathbb{R}^{m\times n}$ with $m < n$, $I \subset \{1,...,n\}$ with $k \equiv |I|$ and a positive integer k, and $s \in \{-1,+1\}^I$. Then (I,s) is a recoverable support of A with size k if and only if every $x^* \in \mathbb{R}^n$ with $\operatorname{supp}(x^*) = I$ and $\operatorname{sign}(x^*)_I = s$ solves* (L1) *uniquely.*

The set

$$\mathcal{S}_{n,k} \equiv \left\{(I,s) : I \subset \{1,...,n\}, |I| = k, s \in \{-1,+1\}^I\right\}$$

is considered as the set which contains all possible candidates for being a recoverable support of size k. One may see this definition as redundant since, strictly speaking, the conditions in Corollary 2.1.11 can also be characterized only by a vector $\bar{s} \in [-1,+1]^n$ which would state a clear relationship to the subdifferential of the ℓ_1-norm. However, since stating $I \equiv \{i : \bar{s}_i \neq 0\}$ is mostly necessary, for the sake of brevity, the notation above is chosen. Note that the set $\mathcal{S}_{n,k}$ has the cardinality $|\mathcal{S}_{n,k}| = 2^k\binom{n}{k}$.

In the present chapter, the focus is on recoverable supports which can be seen as equivalence classes since, for a given matrix A, they partition unique solutions x^* of (L1) on the basis of their supports and signs. For a given matrix $A \in \mathbb{R}^{m\times n}$ and a positive integer k, the following numbers are considered in the present chapter:

$$\Lambda(A,k) \equiv |\{(I,s) : (I,s) \text{ is a recoverable support of } A \text{ with size } k\}|,$$
$$\Xi(m,n,k) \equiv \max\{\Lambda(A,k) : A \in \mathbb{R}^{m\times n}\}.$$

The number $\Lambda(A,k)$ is the number of recoverable supports of A with size k. The maximal possible number of recoverable supports of any $(m \times n)$-matrix with size k is denoted with $\Xi(m,n,k)$. It follows easily that $\Lambda(A,k) \leq 2^k\binom{n}{k}$ for any $A \in \mathbb{R}^{m\times n}$ as well as $\Xi(m,n,k) \leq 2^k\binom{n}{k}$. Both terms can be adapted to the achievements in Chapter 2; in particular for a positive integer k, the matrix $A \in \mathbb{R}^{m\times n}$ which solves $\Xi(m,n,k) = \Lambda(A,k)$ is declared as a *recovery matrix*. Loosely speaking, such a matrix guarantees that most k-sparse vectors $x^* \in \mathbb{R}^n$ can be recovered via (L1). Note that the transfer of the results in Chapter 2 to Λ and Ξ can easily be done.

In this chapter, most results on Λ and Ξ are achieved by considering the geometry of basis pursuit, especially convex polytopes play a decisive role. For a full introduction to convex polytopes, the reader may consult the book by Branko Grünbaum [73] as well as the book by Günter M. Ziegler [132]; for clarification, only a few concepts are introduced in this paragraph. For a set $Y \equiv \{v_1,...,v_r\} \subset \mathbb{R}^d$ of r points the *affine hull* of Y is defined as the set

$$\operatorname{aff}(Y) \equiv \left\{\sum_{i=1}^r q_i v_i : q_i \in \mathbb{R}, \sum_{i=1}^r q_i = 1\right\}$$

and the *convex hull* of Y is defined as the set

$$\operatorname{conv}(Y) \equiv \left\{\sum_{i=1}^r q_i v_i : q_i \in \mathbb{R}, q_i \geq 0, \sum_{i=1}^r q_i = 1\right\}.$$

The set Y is said to be *affinely independent* if for all $v \in Y$ it follows that $v \notin \operatorname{aff}(Y\backslash\{v\})$. The dimension of $\operatorname{aff}(Y)$ is defined as the dimension of corresponding vector space. Note that $\operatorname{conv}(Y) \subset \operatorname{aff}(Y)$ and that Y is affinely independent if Y is linearly independent. A *polytope* P is the convex hull of a finite point set $Y \subset \mathbb{R}^d$, i.e. $P \equiv \operatorname{conv}(Y)$. If the affine hull of P has dimension d, then P is said to be *d-dimensional*. This means that a *d-polytope* is a polytope of dimension d in some $\mathbb{R}^m, m \geq d$. For $w \in \mathbb{R}^d$, the set

$$H_w \equiv \left\{y \in \mathbb{R}^d : \langle y, w\rangle = 1\right\}$$

is called *hyperplane*. For a polytope $P \subset \mathbb{R}^d$ and for a set $W \subset \mathbb{R}^d$, the set $F \equiv \{y \in P : \langle y, w\rangle = 1 \text{ for all } w \in W\}$ is called *face of* P if for all $b \in P \backslash F$ it follows that $\langle b, w\rangle < 1$ for all $w \in W$. Note, that each face of a polytope is also a polytope. The set of all k-dimensional faces of a polytope P is denoted by $\mathcal{F}_k(P)$, and the number of different k-dimensional faces by $f_k(P) \equiv |\mathcal{F}_k(P)|$. If $F \in \mathcal{F}_0(P)$, then F is called *vertex* of P. A face $F \in \mathcal{F}_1(P)$ is named an *edge* of P and a *facet* F is an $(d-1)$-dimensional face of P if P is d-dimensional. Further, for a d-dimensional polytope P and $F \in \mathcal{F}_k(P)$ with $0 \leq k \leq d-1$, the face F is a *proper* face; in contrast, it might be useful to regard $\emptyset$ and P also as faces of P, these are called *improper* faces. The union of all faces is denoted by $\mathcal{F}(P) = \bigcup_k \mathcal{F}_k(P)$. During this chapter, further concepts are introduced when and where they are needed.

Before the geometrical interpretation of basis pursuit is considered, an important concept is introduced in the following section.

3.1 General Position

In this section, a concept is introduced which will be confirmed as a necessary condition for the geometrical interpretation of basis pursuit when uniqueness is examined. This term is based on a similar term in geometry and its closely related fields, see for instance [95, 132].

Definition 3.1.1 *Let $A \in \mathbb{R}^{m\times n}, m < n$, and $(I, s) \in \mathcal{S}_{n,k}$ for a positive integer k. Then A is in* general position with respect to (I, s) *if the set $\{a_i\}_{i\in I}$ is linearly independent, and for the $(k-1)$-dimensional affine hull $\mathcal{H} \equiv \operatorname{aff}(\{s_i a_i\}_{i\in I})$ it follows that $\pm a_j \notin \mathcal{H}$ for all $j \in I^c$.*
The matrix A is said to be in global general position *if for every $(I, s) \in \bigcup_{k\leq \operatorname{rk}(A)} \mathcal{S}_{n,k}$ the matrix A is in general position with respect to (I, s).*

Remark 3.1.2 Please note that the term *general position* needs to be read carefully in further literature! Recently, this term also appeared in compressed sensing and frame theory, but there it is occupied by a different definition: in [49], a matrix A is said to be in general position if for all $I \subset \{1, ..., n\}$ with $|I| = m$ the submatrix A_I is injective. In this thesis, such a matrix is called *full spark matrix*, cf. Section 2.5. A simple counterexample shows that both concepts, the term in Definition 3.1.1 and a full spark matrix, are not equivalent: taking $a_1 = [1, 0]^T, a_2 = [0, 1]^T, a_3 = (a_1 + a_2)/2$, and $a_4 = (a_1 - a_2)/2$, then the corresponding matrix A is a full spark matrix, but it is not in general position with respect to $(\{1, 2\}, [1, 1]^T)$. Full spark matrices only consider the subsets I with $|I| = m$, but do not consider the entire set $\{1, ..., n\}$. Vice versa, general position with respect to (I, s) takes only one subset I and one vector $s \in \{-1, +1\}^I$ into account – not each. The matrix

$$A = \begin{pmatrix} 1 & 0 & 0 & \frac{1}{2} \\ 0 & 1 & 0 & \frac{1}{2} \\ 0 & 0 & 1 & 0 \end{pmatrix}$$

is obviously not a full spark matrix but it is in general position with respect to the recoverable support $(\{1, 2, 3\}, [1, 1, 1]^T)$.

Although the collision of both names is known, it is reasonable to call the concept in Definition 3.1.1 *general position* to give a clear connection between geometry and compressed sensing.

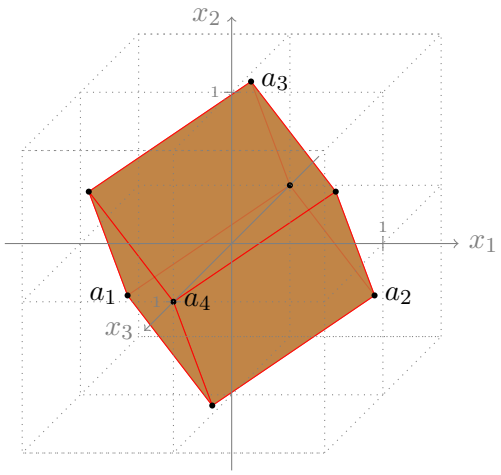

Figure 3.1: Projected cross-polytope $AC^4_\triangle$ with the Mercedes-Benz matrix $A \in \mathbb{R}^{3\times 4}$.

However, the concept in Definition 3.1.1 is slightly different from the term being used in geometry: for example in [95, page 81], a set $X \subset \mathbb{R}^m$ of points is said to be in general position if every subset $Y \subset X$ with $m+1$ or fewer points is affinely independent. Let $A \in \mathbb{R}^{m\times n}, m < n$, be in general position with respect to some $(I,s) \in \mathcal{S}_{n,m}$. Then $\{s_i a_i\}_{i\in I}$ is linearly independent and, moreover for all $j \in I^c$ and $|\lambda| = 1$ it follows that $\{s_i a_i\}_{i\in I} \cup \{\lambda a_j\}$ is affinely independent, since $\lambda a_j \notin \operatorname{aff}(\{s_i a_i\}_{i\in I})$. This means that in Definition 3.1.1 the subset Y from the definition in [95, page 81] is restricted and has to contain the set $\{s_i a_i\}_{i\in I}$. In fact, the definition from [95, page 81] is equivalent to the term global general position.

Proposition 3.1.3 *Let $A \in \mathbb{R}^{m\times n}, m < n$, be in general position with respect to all $(I,s) \in \mathcal{S}_{n,m}$. Then A is a full spark matrix.*

Proof. For each $(I,s) \in \mathcal{S}_{m,n}$, the affine hull $\{s_i a_i\}_{i\in I}$ is $(m-1)$-dimensional since the set $\{a_i\}_{i\in I}$ is linearly independent. □

From [82, Section 3], one can deduce that matrices whose columns are independently and uniformly chosen at random are in global general position with high probability. Please note that matrices whose columns are pairwise different and placed on the ℓ_2-unit sphere are not necessarily in global general position: for a positive integer k and $(I,s) \in \mathcal{S}_{n,k}$ it follows that $\|\sum_{i\in I} q_i s_i a_i\|_2 < \sum_{i\in I} q_i \|s_i a_i\|_2 = 1$ for $q \in \mathbb{R}^I_+$ with $\sum_{i\in I} q_i = 1$; but the same does not hold for $q \in \mathbb{R}^I$ with $\sum_{i\in I} q_i = 1$. For example one may observe that in Figure 3.1 the cross-polytope projected via the Mercedes-Benz matrix $A \in \mathbb{R}^{3\times 4}$ is a three-dimensional cube and, therefore, the matrix A is not in global general position.

Proposition 3.1.4 *Let k be a positive integer and $A \in \mathbb{R}^{m\times n}, m < n$, be in general position with respect to $(I,s) \in \mathcal{S}_{n,k}$. Then for each $(J,\bar{s}) \in \mathcal{S}_{n,l}$ with $l \le k, J \subset I$, and $\bar{s}_J = s_J$, the matrix A is in general position with respect to $(J,\bar{s})$.*

Proof. Assume that A is not in general position with respect to a given $(J,\bar{s})$. Then the set $\{\bar{s}_j a_j\}_{j\in J}$ is linearly independent since $\{s_i a_i\}_{i\in I}$ is linearly independent. For $j_0 \in I^c$

and each λ with $|\lambda| = 1$, it follows that $\lambda a_{j_0} \notin \text{aff}(\{s_j a_j\}_{j\in J})$. Further, there are $j_0 \notin J$ and λ with $|\lambda| = 1$ which satisfy $\lambda a_{j_0} = \sum_{j\in J} q_j s_j a_j$ for $q \in \mathbb{R}^J, \sum_{j\in J} q_j = 1$, i.e. $\lambda a_{j_0} \in \text{aff}(\{s_j a_j\}_{j\in J})$. If $j_0 \in I\backslash J$, then for $q_i = 0, i \in I\backslash J$, it follows that

$$\lambda a_{j_0} = \sum_{i\in J} q_i s_i a_i = \sum_{i\in J} q_i s_i a_i + \sum_{i\in I\backslash J, i\neq j_0} \underbrace{q_i}_{=0} s_i a_i = \sum_{i\in I\backslash\{j_0\}} q_i s_i a_i.$$

This means that $\lambda a_{j_0} \in \text{aff}(\{s_i a_i\}_{i\in I}\backslash\{\lambda a_{j_0}\})$ and $\{s_i a_i\}_{i\in I}$ is not affinely independent. Further, the set $\{s_i a_i\}_{i\in I}$ is not linearly independent, which is a contradiction. □

One can state that for each $I \subset \{1, ..., n\}$ and $s \in \{-1, +1\}^I, |I| \leq m$, the affine hull of $\{s_i a_i\}_{i\in I}$ is contained in at least one hyperplane.

Lemma 3.1.5 *Let $A \in \mathbb{R}^{m\times n}, m < n$, and let $(I, s) \in \mathcal{S}_{n,k}$ for a positive integer $k \leq m$. Further, let A be in general position with respect to (I, s). Then there exists $w \in \mathbb{R}^m$ such that*

$$\text{aff}(\{s_i a_i\}_{i\in I}) \subset H_w. \tag{3.1.1}$$

Proof. For $k \leq m$, the linear system $\{\langle s_i a_i, \bar{w}\rangle = 1\}_{i\in I}$ has full rank and there is at least one solution $w \in \mathbb{R}^m$. For each $y \in \text{aff}(\{s_i a_i\}_{i\in I})$, with $q \in \mathbb{R}^I$ and $\sum_{i\in I} q_i = 1$, it follows that

$$\langle y, w\rangle = \sum_{i\in I} q_i \langle s_i a_i, w\rangle = 1,$$

therefore $y \in H_w$. □

Note that the derived element $w \in \mathbb{R}^m$ in Lemma 3.1.5 is a dual certificate of the considered pair (I, s). For the rest of this chapter, the previous lemma is used to link the term general position with the conditions stated in (2.1.13).

3.2 Geometrical Interpretation of Basis Pursuit

In this section, the geometry of the optimization problem in (L1) is considered, which was first done in [49]. As mentioned in Chapter 1, the convex hull of the union of the positive and negative standard basis, i.e. $\mathcal{E} \equiv \{e_i\}_{i=1}^n \cup \{-e_i\}_{i=1}^n$, is the cross-polytope

$$\mathcal{C}_\triangle^n \equiv \{y \in \mathbb{R}^n : \|y\|_1 \leq 1\}.$$

In the present section, a matrix $A \in \mathbb{R}^{m\times n}$ is associated with the convex polytope

$$P \equiv A\mathcal{C}_\triangle^n = \{Ay : \|y\|_1 \leq 1\}$$

which is the convex hull of the positive and negative columns of A, i.e.

$$A\mathcal{C}_\triangle^n = \text{conv}(\{\pm a_i\}_{i=1}^n),$$

since $\mathcal{C}_\triangle^n = \text{conv}(\mathcal{E})$ and $A\mathcal{C}_\triangle^n = A\text{conv}(\mathcal{E})$. This polytope is called *projected cross-polytope*. Obviously, the projected cross-polytope is symmetrical with respect to the origin, i.e. for all $b \in P$ it follows that $-b \in P$. Such a polytope is called *centrally symmetric*. A set $S \subset \{\pm a_i\}_{i=1}^n$ is called *antipodal* if for all $v \in S$ it follows that $-v \notin S$. Recall, if $b \in A\mathcal{C}_\triangle^n$, then there is $y \in \mathbb{R}^n$ with $b = Ay$ and $\|y\|_1 \leq 1$.

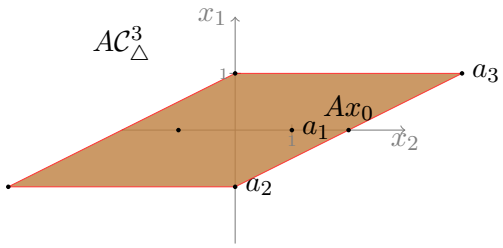

Figure 3.2: Projected cross-polytope $A\mathcal{C}^3_\triangle$ with $A \in \mathbb{R}^{2\times 3}$ from (1.1.2).

In the following theorem, the relationship between $A\mathcal{C}^n_\triangle$ and the optimization problem in (L1) is revealed. It is based on [49, Theorem 1] and requires the concepts of *neighborliness* saying that P is called k-*neighborly* if each antipodal set of k vertices of P determines a face of P.

Theorem 3.2.1 *Let $A \in \mathbb{R}^{m\times n}$ with $m < n$ and let $k \geq 1$ be a positive integer. Then the following two statements are equivalent.*

- *The polytope $A\mathcal{C}^n_\triangle$ has $2n$ vertices and is k-neighborly.*
- *Every pair $(I, s) \in \mathcal{S}_{n,k}$ is a recoverable support of A with size k.*

A different proof can be found in [64, Theorem 4.39]. Theorem 3.2.1 gives geometrical conditions on global recovery: if each antipodal set of k vertices forms a $(k-1)$-dimensional face of $P \equiv A\mathcal{C}^n_\triangle$ for a matrix $A \in \mathbb{R}^{m\times n}, m < n$, then P has $2^k\binom{n}{k}$ faces of the dimension $(k-1)$. Consequently, the number of $(k-1)$-dimensional faces of $A\mathcal{C}^n_\triangle$ and $\mathcal{C}^n_\triangle$ is the same, i.e. $f_{k-1}(A\mathcal{C}^n_\triangle) = f_{k-1}(C^n_\triangle)$. Further, it follows that $\Lambda(A,k) = 2^k\binom{n}{k}$ if A is k-neighborly. In general, it follows that $f_{k-1}(A\mathcal{C}^n_\triangle) \leq f_{k-1}(\mathcal{C}^n_\triangle)$, cf. [49, Section 2], which implies that, under the mapping $A : \mathbb{R}^n \to \mathbb{R}^m$, some $(k-1)$-dimensional faces could get lost: hence $\Lambda(A,k) \leq f_{k-1}(A\mathcal{C}^n_\triangle)$. The previous theorem can also be adapted to individual recovery.

Theorem 3.2.2 *Let $A \in \mathbb{R}^{m\times n}$ with $m < n$, and let $(I, s) \in \mathcal{S}_{n,k}$ for a positive integer k. Then (I, s) is a recoverable support of A with size k if and only if A is in general position with respect to (I, s) and the set $F \equiv \operatorname{conv}(\{s_i a_i\}_{i\in I})$ is a $(k-1)$-dimensional face of $A\mathcal{C}^n_\triangle$.*

Proof. Each direction is proved separately. With (I, s) being a recoverable support of A with size k, necessarily, there is a dual certificate $w \in \mathbb{R}^m$ of (I, s). Consider $b \in A\mathcal{C}^n_\triangle$ with $y \in \mathbb{R}^n$ satisfying $b = Ay$, and, without loss of generality, assume $\|y\|_1 = 1$ – otherwise, in the following inequality the vector $\tilde{w} = w/\|y\|_1$ needs to be used instead of w. With the Hölder inequality, it follows that

$$\begin{aligned}\langle b, w\rangle &= \langle y, A^T w\rangle = \langle y_I, A_I^T w\rangle + \langle y_{I^c}, A_{I^c}^T w\rangle \\ &\leq \|y_I\|_1 \underbrace{\|A_I^T w\|_\infty}_{=1} + \|y_{I^c}\|_1 \underbrace{\|A_{I^c}^T w\|_\infty}_{<1} \leq \|y\|_1 = 1.\end{aligned}$$

The inequality can not be stated strictly since $\|y_{I^c}\|_1 \neq 0$ does not hold necessarily. Further, the previous inequality shows that

$$\bar{F} \equiv \{b \in A\mathcal{C}^n_\triangle : \langle b, w\rangle = 1, \exists y : b = Ay, \|y\|_1 = 1, \operatorname{supp}(y) = I, \operatorname{sign}(y)_I = s\}$$

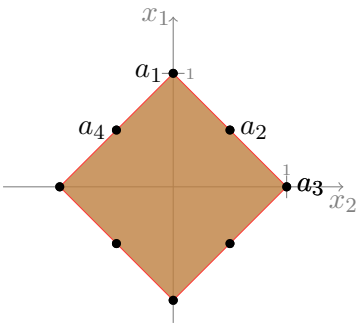

$A\mathcal{C}^4_\triangle$

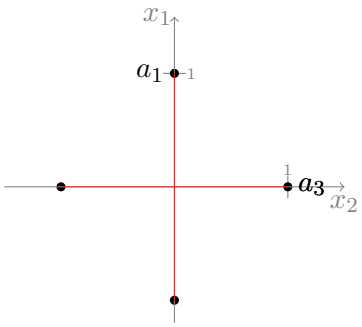

$\mathcal{P} \equiv \{Ax^* : x^* \in \mathcal{C}^4_\triangle \text{ solves (L1) uniquely}\}$

Figure 3.3: Counterexample which shows that not each $\mathcal{P}$ is a convex polytope. Left: projected cross-polytope with a certain matrix $A \in \mathbb{R}^{2\times 4}$ with columns $a_1 = e_1, a_2 = (e_1 + e_2)/2, a_3 = e_2$, and $a_4 = (e_1 - e_2)/2$. Right: the set of all unique solutions $x^* \in \mathbb{R}^2$ of (L1) with the same matrix $A \in \mathbb{R}^{2\times 4}$.

is a face of $A\mathcal{C}^n_\triangle$, since for all $b \in A\mathcal{C}^n_\triangle$ it follows that $\langle b, w\rangle \leq 1$. Further, one can deduce that $\bar{F} \subset F$, since for $b \in \bar{F}$ with a corresponding $y \in \mathbb{R}^n$ and $q_i = |y_i|$ for all $i \in I$, it follows that $b = \sum_{i\in I} a_i y_i = \sum_{i\in I} q_i s_i a_i$ with $\sum_{i\in I} q_i = \|y\|_1 = 1$. Actually, it is $F = \bar{F}$ since $\langle b, w\rangle = \sum_{i\in I} q_i \langle s_i a_i, w\rangle = 1$ for $b \in F$, a corresponding $q \in \mathbb{R}^I, \sum_{i\in I} q_i = 1$, and a corresponding $y \in \mathbb{R}^n$, $y_i = s_i q_i$ for $i \in I$ and $y_j = 0$ for $j \notin I$ such that $Ay = b$. Let $w \in \mathbb{R}^m$ satisfy (3.1.1) and assume for $j_0 \in I^c$ with $|\lambda| = 1$ it holds that $\lambda a_{j_0} \in H_w$. Note that $F \subset H_w$. Then it follows that $|\langle w, a_{j_0}\rangle| = 1$, which contradicts (I, s) being a recoverable support of A. Finally, the face F is $(k-1)$-dimensional since A_I is injective; this completes the proof concerning the first direction.
Assume F is a $(k-1)$-dimensional face of $A\mathcal{C}^n_\triangle$, then there is $w \in \mathbb{R}^m$ such that $F = \{b \in A\mathcal{C}^n_\triangle : \langle b, w\rangle = 1\}$. Especially, for all $i \in I$ it follows that $1 = \langle s_i a_i, w\rangle$, which implies $A_I^T w = \operatorname{sign}(x^*)_I$. Since $\pm a_j \notin F$ for $j \in I^c$ and F is a face, it follows that $|\langle a_j, w\rangle| < 1$ for all $j \in I^c$, hence $\|A_{I^c}^T w\|_\infty < 1$. Finally, since F is $(k-1)$-dimensional, the submatrix A_I is injective. □

A similar proof of the previous theorem can be found in [64, Theorem 4.38]. Due to its connection to the primal problem in (L1), this geometrical interpretation is also called *primal*. Theorem 3.2.2 gives a clear answer, why (L1) does not deliver a sparser solution in case of the example in (1.1.2): considering Figure 3.2, one may see, that a_1 is not contained in a proper face of $A\mathcal{C}^n_\triangle$, therefore, the first component of each solution x^* of (L1) is always 0. Further, the vector Ax_0 is only contained in a one-dimensional face of $A\mathcal{C}^3_\triangle$.

With the previous theorem, one can infer when the set

$$\mathcal{P} \equiv \{Ax^* : x^* \in \mathcal{C}^n_\triangle \text{ solves (L1) uniquely}\}$$

coincides with $A\mathcal{C}^n_\triangle$ for a given matrix $A \in \mathbb{R}^{m\times n}$. In Figure 3.3, one may see that under certain circumstances that $\mathcal{P} \neq A\mathcal{C}^n_\triangle$ for a corresponding matrix A. Further, the set $\mathcal{P}$ is not a convex polytope since some faces are missing. But if A is in global general position, the statement changes. Before this is shown, the following remark motivates the introduction of a related term.

Remark 3.2.3 The assumption that $A \in \mathbb{R}^{m\times n}$ is in global general position is an even stronger condition than generally needed for recoverability since it also considers pairs $(I,s) \in \mathcal{S}_{n,k}$ which do not generate proper faces F in the sense that $\text{conv}(\{s_i a_i\}_{i\in I}) \in \mathcal{F}_{k-1}(A\mathcal{C}_\triangle^n)$. For instance, consider $A \in \mathbb{R}^{2\times 3}$ with $a_1 = e_1, a_3 = e_2, a_2 = (a_1+a_2)/\|a_1+a_2\|_2$, then A being in general position with respect to $(\{1,3\},[1,1]^T)$ does not influence the recoverability since $\text{conv}(\{a_1,a_3\})$ is not contained in any proper face of $A\mathcal{C}_\triangle^3$.

Definition 3.2.4 *Let $A \in \mathbb{R}^{m\times n}, m < n$, and let k be a positive integer. Then A is said to be in* general position with respect to all $(k-1)$-faces *if for all $(I,s) \in \mathcal{S}_{n,k}$ with $F \in \mathcal{F}_{(k-1)}(A\mathcal{C}_\triangle^n)$ such that $\text{conv}(\{s_i a_i\}_{i\in I}) \subset F$, the matrix A is in general position with respect to (I,s).*

The previous concept is introduced for the sake of brevity and is rather of theoretical nature to give a weaker condition than global general position. It characterizes individual recoverability with regard to the term general position. With Proposition 3.1.4 and Theorem 3.2.2, the following corollary holds.

Corollary 3.2.5 *Let $A \in \mathbb{R}^{m\times n}, m < n$, with $\text{rk}(A) = r$. The matrix A is in general position with respect to all $(r-1)$-faces if and only if*

$$A\mathcal{C}_\triangle^n = \{Ax^* : x^* \in \mathcal{C}_\triangle^n \text{ solves (L1) uniquely}\}.$$

Note that for all $A \in \mathbb{R}^{m\times n}, m < n$, it follows that $A\mathcal{C}_\triangle^n = \{Ax^* : x^* \in \mathcal{C}_\triangle^n \text{ solves (L1)}\}$. In context with the optimization problem in (L1), general position is a condition primarily associated with uniqueness. Consequently, a face F of $A\mathcal{C}_\triangle^n$ does uniquely correspond to a pair $(I,s) \in \mathcal{S}_{n,k}$. In Section 3.4 below, this connection is addressed in detail.

Remark 3.2.6 For a given full rank matrix $A \in \mathbb{R}^{m\times n}, m < n$, Corollary 3.2.5 implies that the set

$$\mathcal{P} \equiv \{Ax^* : x^* \in \mathcal{C}_\triangle^n \text{ solves (L1) uniquely}\}$$

is a convex polytope if and only if all facets of $A\mathcal{C}_\triangle^n$ can be associated with maximal recoverable supports of A. Further, the requirement that A is in general position with respect to all $(m-1)$-faces implies that each facet of $\mathcal{P}$ is a *simplex*: such a polytope $\mathcal{P}$ is called *simplicial*. Note that the convex polytope in Figure 3.3 is also simplicial, although its corresponding matrix is not in general position with all 1-faces. In the situation of Corollary 3.2.5, if a matrix $A \in \mathbb{R}^{m\times n}, m < n$, with $\text{rk}(A) = r$ is in general position with respect to all $(r-1)$-faces, then the projected cross-polytope $A\mathcal{C}_\triangle^n$ is simplicial.

Finally, the previous observation can be used to identify the missing piece which prevents the equivalence between general position and neighborliness.

Corollary 3.2.7 *Let $A \in \mathbb{R}^{m\times n}, m < n$, such that $A\mathcal{C}_\triangle^n$ is k-neighborly for a positive integer k. Then for all $l \leq k$, the matrix A is in general position with respect to all $(I,s) \in \mathcal{S}_{n,l}$.*

Proof. The assertion holds with Theorem 3.2.1 and Theorem 3.2.2. □

The converse of the previous corollary does not hold: a recoverable support $(I,s) \in \mathcal{S}_{n,k}$ of $A \in \mathbb{R}^{m\times n}, m < n$, with k as a positive integer, can not necessarily be associated with a face of $A\mathcal{C}_\triangle^n$.

3.3 Polar Interpretation of Basis Pursuit

In this section, a second geometrical interpretation of basis pursuit is considered. To that end, the polar set needs to be introduced, cf. [109, Example 11.19]. For any set $Y \in \mathbb{R}^m$ with $0 \in Y$, the polar of Y is defined by

$$Y^* \equiv \{v \in \mathbb{R}^m : \langle v, x\rangle \leq 1 \text{ for all } x \in Y\}.$$

Note that the polar set is closed, convex and the origin is contained, i.e. $0 \in Y^*$. For applying polar sets on polytopes, consider a polytope P with $0 \in \text{relint}(P)$. The set P^* is also a polytope, see [92, Section 5.3], named *polar polytope* of P. As shown in [73, Section 3.4.4], the mapping

$$\Psi : \mathcal{F}(P) \to \mathcal{F}(P^*), F \mapsto F^* = \{w \in P^* : \langle w, b\rangle = 1 \text{ for all } b \in F\}$$

is one-to-one inclusion-reversing, which means that all faces $F_1, F_2 \in \mathcal{F}(P)$ satisfy $F_1 \subset F_2$ if and only if $\Psi(F_2) \subset \Psi(F_1)$. The polytopes P and P^* are said to be *dual to each other*.

For an arbitrary matrix $A \in \mathbb{R}^{m\times n}, m < n$, the polar polytope of the projected cross-polytope $A\mathcal{C}^n_\triangle$ is considered in this section. This was first envisaged in [104]. The polar polytope

$$(A\mathcal{C}^n_\triangle)^* = \{w \in \mathbb{R}^m : \langle w, b\rangle \leq 1 \text{ for all } b \in A\mathcal{C}^n_\triangle\}$$

can be linked directly to the optimality conditions in Corollary 2.1.7: for all $w \in \mathbb{R}^m$ with $\|A^T w\|_\infty \leq 1$ it follows that $w \in (A\mathcal{C}^n_\triangle)^*$, since for all $b \in A\mathcal{C}^n_\triangle$, with $y \in \mathbb{R}^m, \|y\|_1 \leq 1$, such that $b = Ay$, it follows that

$$\langle w, b\rangle = \langle A^T w, y\rangle \leq \|A^T w\|_\infty \|y\|_1 \leq \|A^T w\|_\infty.$$

Hence, for a given $x^* \in \mathbb{R}^n$, the polar of $A\mathcal{C}^n_\triangle$ contains all elements of the feasible set corresponding to the dual problem of (L1), which is

$$\max_w \langle w, Ax^*\rangle \text{ subject to } \|w^T A\|_\infty \leq 1.$$

A deeper insight to the construction of the polar of a projected cross-polytope is given in the following remark.

Remark 3.3.1 Let $A \in \mathbb{R}^{m\times n}$ with $m < n$, let k be a positive integer, and $F \equiv \text{conv}(\{s_i a_i\}_{i\in I})$ for $(I, s) \in \mathcal{S}_{n,k}$ with $\pm a_j \notin F$ for all $j \in I^c$ such that $F \in \mathcal{F}_{(k-1)}(A\mathcal{C}^n_\triangle)$. Theorem 3.2.2 states that (I, s) is a recoverable support of A. In Section 3.2, it is shown that a recoverable support (I, s) of A with size k can be associated with a $(k-1)$-dimensional face of $A\mathcal{C}^n_\triangle$. Let $w \in \mathbb{R}^m$ be a dual certificate of (I, s). Every $b \in F$ can be represented by $b = \sum_{i\in I} q_i s_i a_i$ for $q \in \mathbb{R}^I$ with $\sum_{i\in I} q_i = 1$ and it further holds that $\langle w, b\rangle = \sum_{i\in I} q_i \langle w, s_i a_i\rangle = 1$. Consequently, the polar face F^* contains all dual certificates w such that $\text{conv}(\{s_i a_i\}_{i\in I}) \subset H_w$, i.e. $F^* = \{w \in \mathbb{R}^m : F \subset H_w\}$. This means that a recoverable support also defines a face of $(A\mathcal{C}^n_\triangle)^*$.

Theorem 3.3.2 *Let $A \in \mathbb{R}^{m\times n}, m < n$ with rank r, and $(I, s) \in \mathcal{S}_{n,k}$ for a positive integer $k \leq r$. Then*

$$F^* \equiv \{w \in \mathbb{R}^m : H_w \supset \text{conv}(\{s_i a_i\}_{i\in I}), \pm a_j \notin H_w \ \forall j \in I^c\}$$

is an $(r-k)$-dimensional face of $(A\mathcal{C}^n_\triangle)^*$ if and only if (I, s) is a recoverable support of A with size k.

Proof. If $F^* \in \mathcal{F}_{r-k}((A\mathcal{C}^n_\triangle)^*)$ and $w \in F^*$, then $a_i^T w = s_i$ for $i \in I$ and A_I is injective. Further, for $j \in I^c$ it follows that $|a_j^T w| \neq 1$ and $w \in (A\mathcal{C}^n_\triangle)^*$ which implies $|a_j^T w| < 1$. The converse direction is shown in Remark 3.3.1. □

Please note, for a given full rank matrix $A \in \mathbb{R}^{m\times n}, m < n$, and $x^* \in \mathbb{R}^n$ with the support I, it is not sufficient to assume that

$$\bar{F}^* \equiv \left\{ w \in (A\mathcal{C}^n_\triangle)^* : A_I^T w = \operatorname{sign}(x^*)_I \right\} \in \mathcal{F}_{(m-|I|)}((A\mathcal{C}^n_\triangle)^*) \tag{3.3.1}$$

such that $x^* \in \mathbb{R}^n$ is the unique solution of (L1). This is discussed in the following remark.

Remark 3.3.3 Consider the Mercedes-Benz matrix $A \in \mathbb{R}^{3\times 4}$, cf. Section 2.5, and $(I, s) \in \mathcal{S}_{4,3}$ with $I \equiv \{1, 2, 3\}$ and $s \equiv [1, -1, 1]^T$. Indeed, the corresponding $\bar{F}^* = \{w \equiv (A_I^T)^{-1}s\}$ from (3.3.1) is zero-dimensional, but it follows that $a_4^T w = -1$, since for $v \in \operatorname{rg}(A^T)$ with $v = [1, -1, 1, \alpha]^T$ and $\alpha \in \mathbb{R}$ if and only if $\alpha = 1$, cf. Proposition 2.5.13. Hence A, I, and s do not satisfy the strict source condition and (I, s) is not a recoverable support of A. As one may see in Figure 3.1, the polytope $A\mathcal{C}^4_\triangle$ is not simplicial.

3.4 Adjoint Polar Interpretation of Basis Pursuit

Another geometrical perspective arises directly by considering the optimality conditions in Corollary 2.1.7. Just as a quick reminder, for a matrix $A \in \mathbb{R}^{m\times n}, n < m$, a vector $x^* \in \mathbb{R}^n$ with $I = \operatorname{supp}(x^*)$ solves (L1) if and only if there is $w \in \mathbb{R}$ such that

$$A_I^T w = \operatorname{sign}(x^*)_I \text{ and } \|A_{I^c}^T w\|_\infty \leq 1.$$

With the set $\operatorname{Sign}(x^*)$ as the subdifferential of the ℓ_1-norm at x^*, the optimality conditions can also be stated as the expression $\operatorname{Sign}(x^*) \cap \operatorname{rg}(A^T) \neq \emptyset$. Note that for all $x^* \in \mathbb{R}^n$, the set $\operatorname{Sign}(x^*)$ is a subset of the hypercube $C^n \equiv [-1, +1]^n$, in the following also called *n-cube*. One can simply deduce that $\bigcup_{x^*\in\mathbb{R}^n} \operatorname{Sign}(x^*) = C^n$. To explore x^* which solves (L1), one can alternatively consider the intersection $C^n \cap \operatorname{rg}(A^T)$. All recoverable supports of A can be characterized with this perspective.

Before characterizing recoverable supports with respect to the n-cube, a crucial observation concerning the connection between such regarded pairs (I, s) and C^n needs to be documented.

Lemma 3.4.1 *Let k and n be positive integers with $k \leq n$. Then the function*

$$\begin{aligned} \Phi : \mathcal{S}_{n,k} &\to \mathcal{F}_{n-k}(C^n) \\ (I, s) &\mapsto \left\{ v \in C^n : v = \sum_{i\in I} s_i e_i + \sum_{j\in I^c} q_j e_j,\ q_j \in (-1, 1) \right\} \end{aligned}$$

is bijective.

Proof. First, the surjectivity is proved. Every $(n-k)$-dimensional face F of C^n can be assigned to a pair $(I, s) \in \mathcal{S}_{n,k}$ since k entries in $v \in F$ are fixed to ± 1, i.e. $v_i = s_i$ for $i \in I$, and the other entries can achieve a magnitude between -1 and 1, more precisely $v_j \in (-1, 1)$ for $j \in I^c$. Hence $\mathcal{F}_{n-k}(C^n) \subset \Phi\mathcal{S}_{n,k}$ and, trivially, it follows that $\Phi\mathcal{S}_{n,k} \subset \mathcal{F}_{n-k}(C^n)$; this means that the function Φ is surjective.

Let $(I,s),(\bar{I},\bar{s}) \in \mathcal{S}_{n,k}$, $I \neq \bar{I}$, then it follows that $\Phi(I,s) \neq \Phi(\bar{I},\bar{s})$ and Φ is injective. □

The following lemma shows that, for each $(I,s) \in \mathcal{S}_{n,k}$, the relative interior of $\Phi(I,s)$ is the set

$$\operatorname{relint}(\Phi(I,s)) = \{v \in \Phi(I,s) : \|v_{I^c}\|_\infty < 1\}.$$

Lemma 3.4.2 *Let $A \in \mathbb{R}^{m\times n}, m < n$, let $(I,s) \in \mathcal{S}_{n,k}$ for a positive integer $k \leq n$, and let $v \in \operatorname{rg}(A^T) \cap C^n$ with $v_I = s$. Then $\|v_{I^c}\|_\infty < 1$ if and only if $v \in \operatorname{relint}(\Phi(I,s))$.*

Proof. It follows easily that $\operatorname{relint}(\Phi(I,s)) \subset \{v : \|v_{I^c}\|_\infty < 1\}$. Let $\|v_{I^c}\|_\infty < 1$ and let $w \in \mathbb{R}^m$ satisfy $A^T w = v$. By [108, Theorem 6.4] it is obvious that

$$\operatorname{relint}(\Phi(I,s)) = \{v \in \Phi(I,s) \ : \ \forall y \in \Phi(I,s)\ \exists \gamma > 1 \text{ such that } \gamma v + (1-\gamma)y \in \Phi(I,s)\}.$$

Choose $\epsilon \equiv 1 - \|v_{I^c}\|_\infty$ and $\delta > 0$ such that $2\delta \leq \epsilon(1+\delta)$. For example, the number δ can be chosen with some $\bar{\epsilon} > 0$ such that $2\bar{\epsilon}^{-1} \leq \epsilon$ and $\delta \equiv (\bar{\epsilon}+1)^{-1}$ with given ϵ. Let $y \in \Phi(I,s)$, then for $\gamma \equiv 1+\delta > 1$ it follows that

$$\gamma v_I + (1-\gamma)y_I = \gamma s + (1-\gamma)s = 1$$

and

$$\begin{aligned}\|\gamma v_{I^c} + (1-\gamma)y_{I^c}\|_\infty &\leq |\gamma|\|v_{I^c}\|_\infty + |1-\gamma|\|y_{I^c}\|_\infty \\ &\leq (1+\delta)(1-\epsilon) + \delta = 1 + 2\delta - \epsilon(1+\delta) \\ &\leq 1.\end{aligned}$$

Hence, $v \in \operatorname{relint}(\Phi(I,s))$. □

Finally, a further characterization of recoverable supports can be achieved.

Theorem 3.4.3 *Let $A \in \mathbb{R}^{m\times n}, m < n$, with $\operatorname{rk}(A) = r$ and let $(I,s) \in \mathcal{S}_{n,k}$ for $k \leq r$ such that A_I is injective. Then the following statements are equivalent.*

- *The pair (I,s) is a recoverable support of A with size k.*
- *For $F \equiv \Phi(I,s) \in \mathcal{F}_{n-k}(C^n)$, it follows that $\operatorname{relint}(F) \cap \operatorname{rg}(A^T) \neq \emptyset$.*
- *For $F \equiv \Phi(I,s)$, there is $G \in \mathcal{F}_{r-k}(C^n \cap \operatorname{rg}(A^T))$ with $G \subset F$ and there is at least one $v \in G$ with $\|v_{I^c}\|_\infty < 1$.*

Proof. Let (I,s) be a recoverable support of A with size k. With Lemma 3.4.1, the set $F \equiv \Phi(I,s)$ is an $(n-k)$-dimensional face of C^n. With $w \in \mathbb{R}^m$ denoting a dual certificate of (I,s) and Lemma 3.4.2, it follows that $v \equiv A^T w$ is an element of the relative interior of F since $\|v_{I^c}\|_\infty < 1$; hence $v \in \operatorname{relint}(F) \cap \operatorname{rg}(A^T)$.
Let $F \equiv \Phi(I,s)$ be an $(n-k)$-dimensional face of C^n. Then there is an $(r-k)$-dimensional face G of $C^n \cap \operatorname{rg}(A^T)$ with $G \subset F$ and $v \in G$ such that $\|v_{I^c}\|_\infty < 1$ since $\operatorname{relint}(F) \cap \operatorname{rg}(A^T) \neq \emptyset$. Finally, consider the r-dimensional polytope $P \equiv C^n \cap \operatorname{rg}(A^T)$ and an $(r-k)$-dimensional face G of P with $G \subset F \equiv \Phi(I,s)$. For $v \in G$ with $\|v_{I^c}\|_\infty < 1$ there is $w \in \mathbb{R}^m$ such that $A^T w = v \in F$, and there are $q_j \in (-1,+1)$ for all $j \in I^c$ such that it follows

$$A^T w = \sum_{i\in I} s_i e_i + \sum_{j \in I^c} q_j e_j.$$

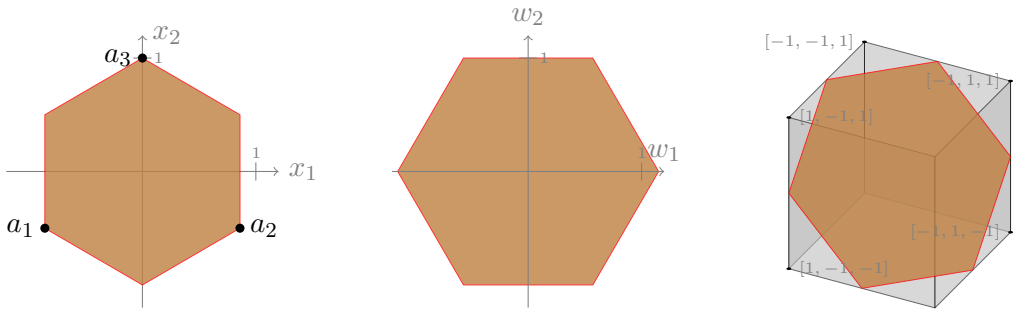

Figure 3.4: Three geometrical interpretations of (L1) with the Mercedes-Benz matrix $A \in \mathbb{R}^{2\times 3}$: the projected cross-polytope $A\mathcal{C}^2_\triangle$ (left), the polar interpretation $(A\mathcal{C}^2_\triangle)^*$ (center), and the adjoint polar interpretation $C^3 \cap \mathrm{rg}(A^T)$ (right).

One can deduce that $A_I^T w = s$ and $\|A_{I^c}^T w\|_\infty < 1$. Further, the submatrix A_I is injective since I has the cardinality k and G is $(r-k)$-dimensional. The pair (I, s) is a recoverable support of A with size k. □

Summarizing, Theorem 3.2.2, Theorem 3.3.2, and Theorem 3.4.3 give an extensive list of geometrical interpretations of the optimization problem in (L1). For a given matrix $A \in \mathbb{R}^{m\times n}, m < n$, all $x^* \in \mathbb{R}^n$ which solve (L1) can be associated to

- pre-images of elements in a projected cross-polytope,
- dual certificates in the polar of a projected cross-polytope,
- faces of the hypercube intersected with a lower-dimensional affine subspace,
- faces of the intersection of the hypercube with a lower-dimensional affine subspace.

Obviously, the last two points only differ in the dimension of the considered object.

In the following sections, all introduced geometrical interpretations are used to evaluate the number of recoverable supports as well as the maximal possible number of recoverable supports, i.e. Λ and Ξ, respectively. Before, the impact on the intersection of the hypercube under the assumption of general position is examined for the rest of this section. Note that in Remark 3.3.1 a guide to construct $(A\mathcal{C}^n_\triangle)^*$ from $A\mathcal{C}^n_\triangle$ is given; this construction can be complemented by mapping the polar polytope with A^T since it follows that

$$\begin{aligned} A^T(A\mathcal{C}^n_\triangle)^* &= \{A^T w : \langle A^T w, x^*\rangle \leq 1 \text{ for all } x^* \in \mathcal{C}^n_\triangle\} \\ &= \{A^T w : \|A^T w\|_\infty \leq 1\} \\ &= C^n \cap \mathrm{rg}(A^T). \end{aligned}$$

In the following remark, the geometrical situation is considered if $A \in \mathbb{R}^{m\times n}, m < n$, is not in general position with respect to certain pairs in $\mathcal{S}_{n,k}, k \leq m$.

Remark 3.4.4 Let $A \in \mathbb{R}^{m\times n}, m < n$, have full rank, let $(I, s) \in \mathcal{S}_{n,k}$ for a positive integer $k \leq m$ such that $\{s_i a_i\}_{i\in I}$ is linearly independent, and assume $F \in \mathcal{F}_{k-1}(A\mathcal{C}^n_\triangle)$ with $F \supset \mathrm{conv}(\{s_i a_i\}_{i\in I})$. If A is in general position with respect to (I, s), then there exists $w \in \mathbb{R}^m$ such that $a_i^T w = s_i$ for all $i \in I$ and $|a_j^T w| < 1$ for all $j \notin I$. Assume that A is not in general position with respect to (I, s), then for all $w \in \mathbb{R}^m$ there is $j_0 \in I^c$ such that $|a_{j_0}^T w| = 1$. This means that the intersection $\Phi(I, s) \cap \mathrm{rg}(A^T)$ is a subset of a

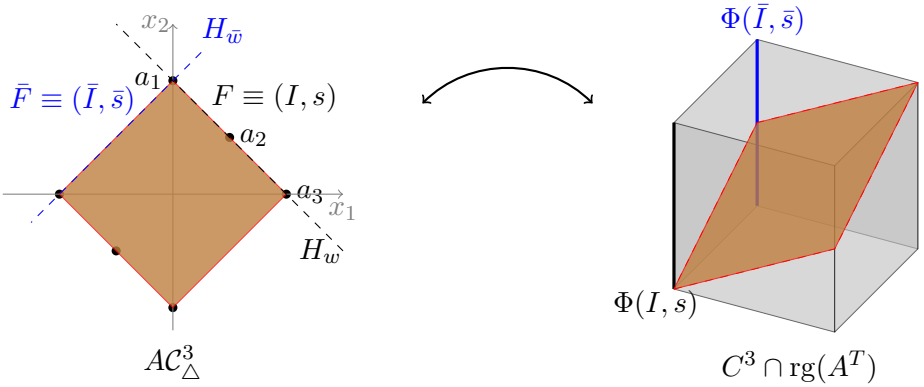

Figure 3.5: Relationship between the projected cross-polytope $A\mathcal{C}^3_\triangle$ and $C^3 \cap \mathrm{rg}(A^T)$. The faces $F \in \mathcal{F}_1(A\mathcal{C}^3_\triangle)$ and $\bar{F} \in \mathcal{F}_1(A\mathcal{C}^3_\triangle)$ can be mapped via Φ to vertices of the polytope $C^3 \cap \mathrm{rg}(A^T)$ and vertices of C^3. The intersection of $\mathrm{relint}(\Phi(I, s))$ and $\mathrm{rg}(A^T)$ is empty, but the rgA^T intersects the relative interior of $\Phi(\bar{I}, \bar{s})$.

lower-dimensional face of C^n and the dimension of $\Phi(I, s) \cap \mathrm{rg}(A^T)$ is smaller than the dimension of $\Phi(I, s)$. Figure 3.5 illustrates this situation for $(I, s) = (\{1, 3\}, [1, 1]^T)$ and the matrix

$$A = \begin{pmatrix} 1 & 1/2 & 0 \\ 0 & 1/2 & 1 \end{pmatrix}.$$

The hyperplane H_w with $w = [1, 1]^T$ contains the face $\mathrm{conv}(\{e_1, e_2\})$ of $A\mathcal{C}^3_\triangle$ and it follows that $a_3^T w = 1$. Hence, the element $A^T w$ is a vertex of C^3. Moreover, the matrix A is not in general position with respect to (I, s). In contrast, for $\bar{w} = [1, -1]^T$, the hyperplane $H_{\bar{w}}$ contains the face $\mathrm{conv}(\{e_1, -e_2\})$ of $A\mathcal{C}^3_\triangle$ and it follows that $a_3^T \bar{w} = 0$. The vector $A^T \bar{w}$ is an element of an edge of C^3 and A is in general position with respect to $(\{1, 2\}, [1, -1]^T)$.

Remark 3.4.5 An intersection of an m-dimensional linear subspace with C^n is called *regular* if no $(n - m - 1)$-dimensional face of the n-cube is intersected by the considered subspace. For example, if $A \in \mathbb{R}^{m \times n}, m < n$, is in general position with all $(m - 1)$-faces, then the intersection $C^n \cap \mathrm{rg}(A^T)$ is regular. The same holds if A is in global general position since this condition is stronger. Moreover, the intersection $C^n \cap \mathrm{rg}(A^T)$ is regular if and only if A is in general position with respect to all $(m - 1)$-faces.
Proposition 2.1.8 states that recoverable supports can be shrunk with respect to their size. If a matrix A is in general position with respect to all $(m-1)$-faces, each recoverable support (I, s) of A with size m can be shrunk to, in total, m recoverable supports with size $(m - 1)$: each $i \in I$ can be excluded from I such that the emerging $(I \backslash \{i\}, \bar{s})$, with $\bar{s}_j = s_j$ for all $j \in I \backslash \{i\}$, is a recoverable support of A with size $(m - 1)$. Hence, each recoverable support with size m is connected with m recoverable supports of size $(m-1)$: assume for a moment that $P \equiv C^n \cap \mathrm{rg}(A^T)$ is a regular intersection, then each vertex of P is connected with m vertices of P. Since P is m-dimensional, such a polytope is called *simple*. The present remark anticipates the methodology in Section 3.5 and is advanced in Lemma 3.5.2.

Remark 3.4.6 Consider a matrix $A \in \mathbb{R}^{m \times n}, m < n$. As mentioned above, it follows that $A^T(A\mathcal{C}^n_\triangle)^* = C^n \cap \mathrm{rg}(A^T)$ which brings a characterization of $w \in \mathbb{R}^m$ belonging to

$(A\mathcal{C}^n_\triangle)^*$. Since only the point of view, but not the property of the elements, is changed in regarding $C^n \cap \mathrm{rg}(A^T)$ instead of $(A\mathcal{C}^n_\triangle)^*$, both polytopes have isomorphic face lattices.

3.5 Partial Order of Recoverable Supports

For a recoverable support with size k, the construction of a recoverable support with a lower size than k can be adapted from the proof of Proposition 2.1.8. In particular, recoverable supports of A with each size can be derived by considering all maximal recoverable supports of A. Therefore, the question of the identification of all recoverable supports of A is reduced to the identification of all maximal recoverable supports. So far, the question whether all maximal recoverable supports have the same size has been concealed; in this section this question is approached. Most of the results in the present section are published in [84].

The following proposition states requirements how to enlarge a recoverable support.

Proposition 3.5.1 *Let $A \in \mathbb{R}^{m\times n}, m < n$, and let (I, s) be a recoverable support of A with size k. If for a dual certificate $w \in \mathbb{R}^m$ of (I, s) there is $y \in \ker(A_I^T)$ such that $\|A_{I^c}^T(w + y)\|_\infty = 1$ and for $J = \{i : |a_i^T(w + y)| = 1\}$ the submatrix A_J is injective, then $(J, A_J^T(w + y))$ is a recoverable support of A with size strictly larger than k.*

Proof. The assertion follows from Corollary 2.1.11 or by contradiction using Proposition 2.1.8. □

Considering Proposition 2.1.8 and Proposition 3.5.1, the recoverable supports of a fixed matrix can be equipped with a partial order: for two recoverable supports $S_1 = (I, s)$ and $S_2 = (J, \bar{s})$, the relationship $S_1 \leq S_2$ is defined if $I \subset J$ and $s_I = \bar{s}_I$. In other words, the set of all recoverable supports of A forms a partially ordered set, respectively a lattice, and can be visualized via a Hasse Diagram, see Remark 3.5.5 below. To that end, in the following two recoverable supports $S_1 = (I, s)$ and $S_2 = (J, \bar{s})$ are said to be *adjacent* if $S_1 \leq S_2$ and $|I| = |J| - 1$.

Moreover, Proposition 2.1.8 states directly a link between the number of recoverable supports with size k and with size $(k - 1)$, which is also considered in Remark 3.4.5.

Lemma 3.5.2 *Let $A \in \mathbb{R}^{m\times n}, m < n$, and let k be a positive integer with $\Lambda(A, k) \neq 0$. Then there exists a positive, real number $\lambda_k \leq 2(n - k + 1)$ such that*

$$\lambda_k \Lambda(A, k - 1) = k\Lambda(A, k).$$

Proof. In this proof, the Hasse diagram of all recoverable supports is considered, and the number of edges between all recoverable supports of A with size k and with size $(k-1)$ is calculated from the perspective of all recoverable supports with size k and all recoverable supports with size $(k - 1)$.
Each recoverable support with size k, which exists by assumption, is adjacent to k recoverable supports with size $(k-1)$, since Proposition 2.1.8 states for each $i \in I$ that the pair $(I_i, s^{(i)})$ with $I_i \equiv I\backslash\{i\}$ and $s^{(i)}_{I_i} \equiv s_{I_i}$ is a recoverable support with size $(k - 1)$ if (I, s) is a recoverable support. Let $\lambda_k \in \mathbb{R}_+$ denote the number of recoverable supports with size k which are adjacent to the recoverable supports with size $(k - 1)$ on average. Then it follows that $\lambda_k\Lambda(A, k - 1) = k\Lambda(A, k)$. Finally, consider $(J, \bar{s})$ as a recoverable support with size $(k - 1)$, then $|J| = (k - 1)$ and $|J^c| = (n - k + 1)$, which means that not more than $(n - k + 1)$ entries can be used for enlarging $(J, \bar{s})$ to a recoverable support (I, s) of

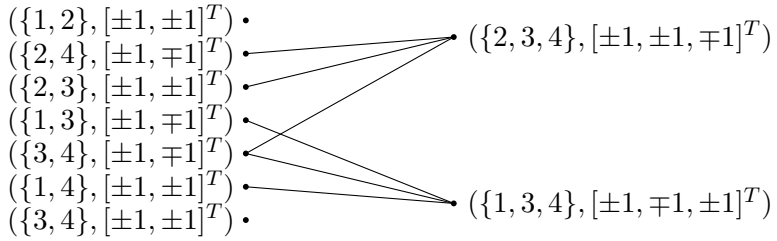

Figure 3.6: Partially ordered set of all recoverable supports with size 2 and 3 for the matrix $A \in \mathbb{R}^{3\times4}$ in Remark 3.5.5.

A with size k. Each new entry $s_j, j \in I \cap J$, of the arising recoverable support (I, s) can adopt both signs: a positive or a negative sign. Hence $\lambda_k \leq 2(n-k+1)$. □

Consider a matrix $A \in \mathbb{R}^{m\times n}$ and a positive integer k such that $\Lambda(A,k) = 2^k\binom{n}{k}$, which means all $(I,s) \in \mathcal{S}_{n,k}$ are recoverable supports and one can deduce that $\Lambda(A,k-1) = 2^{k-1}\binom{n}{k-1}$. Then

$$\lambda_k = 2k\binom{n}{k}\binom{n}{k-1}^{-1} = 2(n-k+1),$$

which emphasizes that λ_k achieves its maximal value if $\Lambda(A,k)$ and $\Lambda(A,k-1)$ achieve their trivial upper bound. Obviously, it follows that $\lambda_k \geq \Lambda(A,k-1)^{-1}$ in the situation of Lemma 3.5.2. Before caring about the question whether all maximal recoverable supports have the same size, a further conclusion is documented concerning the *recoverability curve*.

Definition 3.5.3 *For a given matrix $A \in \mathbb{R}^{m\times n}, m < n$, the mapping*

$$k \mapsto \left[2^k\binom{n}{k}\right]^{-1}\Lambda(A,k)$$

is named recoverability curve.

The recoverability curve states the ratio between the actual number of recoverable supports of A with size k and the total number of pairs $(I,s) \in \mathcal{S}_{n,k}$. It is often used to visualize global and individual recovery, see for instance [29, 53, 126]. With Lemma 3.5.2, a crucial property of this curve can be stated.

Proposition 3.5.4 *Let $A \in \mathbb{R}^{m\times n}, m < n$, then the recoverability curve is monotonically nonincreasing.*

Proof. Let $\Lambda(A,k) \neq 0$ for a positive integer $k \leq m$ and assume that k satisfies

$$\left[2^{k-1}\binom{n}{k-1}\right]^{-1}\Lambda(A,k-1) > \left[2^k\binom{n}{k}\right]^{-1}\Lambda(A,k),$$

then it follows that $\lambda_k > 2(n-k+1)$ which is a contradiction to Lemma 3.5.2. □

Finally, the size of maximal recoverable supports is examined in the following remark.

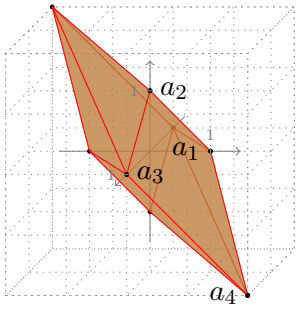

Figure 3.7: Polytope $A\mathcal{C}^4_\triangle$ with $A \in \mathbb{R}^{3\times 4}$ from Remark 3.5.5.

Remark 3.5.5 Consider the matrix

$$A = \begin{pmatrix} 1 & 0 & 0 & 2 \\ 0 & 1 & 0 & -2 \\ 0 & 0 & 1 & 1 \end{pmatrix},$$

then the recoverable supports of A can be computed by considering every element in $\mathcal{S}_{4,k}$ for all $k \leq 3$. Figure 3.6 visualizes the lattice of recoverable supports: conspicuously, the four recoverable supports $S_{1,2} = (\{1,2\}, [\pm 1, \pm 1]^T)$ and $S_{3,4} = (\{3,4\}, [\pm 1, \pm 1]^T)$ with size 2 can not be enlarged. Indeed, neither for $I \supset \{1,2\}$ with $s \equiv [\pm 1, \pm 1, \pm 1]^T$ or $s \equiv [\pm 1, \pm 1, \mp 1]^T$ nor for $I \supset \{3,4\}$ with $s \equiv [\pm 1, \pm 1, \pm 1]^T$ or $s \equiv [\mp 1, \pm 1, \pm 1]^T$, a dual certificate $w \in \mathbb{R}^m$ of (I, s) can be found; hence, all considered S_i are maximal recoverable supports. Nevertheless, it follows that $\Lambda(A, 3) \neq 0$ since $(\{2,3,4\}, [1,1,-1]^T)$ is a recoverable support of A.

The previous remark shows that there is at least one matrix, more precisely a full spark matrix, whose maximal recoverable supports have different sizes. Considering the primal geometrical interpretation in Theorem 3.2.2, one may see that some projected cross-polytopes have facets which have the property that the maximal recoverable supports of a corresponding matrix have different sizes. Figure 3.7 shows $A\mathcal{C}^n_\triangle$ with the matrix A from Remark 3.5.5 as an example that not all matrices have maximal recoverable supports with the same size. There are other, also famous, polytopes which can be used as counterexamples, for example $A\mathcal{C}^{12}_\triangle$ as the rhombicuboctahedron. However, one can deduce directly that matrices $A \in \mathbb{R}^{m\times n}, m < n$, with rank r and which are in general position with respect to all $(r-1)$-faces have maximal recoverable supports with the same size.

Proposition 3.5.6 *Let $A \in \mathbb{R}^{m\times n}, m < n$ be in general position with respect to all $(m-1)$-faces. Then (I, s) is a recoverable support of size m if and only if (I, s) is a maximal recoverable support of A.*

Proof. If a recoverable support (I, s) has size m, then it is a maximal recoverable support, cf. Corollary 2.1.11. Vice versa, as all facets of $A\mathcal{C}^n_\triangle$ are simplices, all recoverable supports have size m. □

Proposition 3.5.6 can also be applied to matrices in global general position. Note that there are also matrices A which are not in general position with respect to all $(\mathrm{rk}(A)-1)$-

faces but whose maximal recoverable supports have all the same size: the matrix

$$A \equiv \begin{pmatrix} 1 & 1/2 & 0 \\ 0 & 1/2 & 1 \end{pmatrix}$$

is not in general position with respect to $(\{1,3\},[1,1]^T)$, but all its maximal recoverable supports have the size 2. Figure 3.5 illustrates $A\mathcal{C}^3_\triangle$ on the left-hand side, see also Remark 3.2.3.

One could get the impression that the set of maximal recoverable supports can be connected to *oriented matroids* [20]. For the rest of Section 3.5, the terms concerning oriented matroids are introduced. Likewise it is shown that the set of maximal recoverable supports is not a set of signed circuits of an oriented matroid. The introduction follows [20, Section 3]. Let E be any set, then a *signed subset* of E is a signed set whose support is contained in E, i.e. a signed subset can be identified with an element of $\{-1,0,1\}^E$. For $X \in \{-1,0,1\}^E$ let

$$\begin{aligned} X^+ &\equiv \{e \in E : \operatorname{sign}(X(e)) = 1\}, \\ X^- &\equiv \{e \in E : \operatorname{sign}(X(e)) = -1\}, \text{ and} \\ \underline{X} &\equiv X^+ \cup X^-. \end{aligned}$$

Definition 3.5.7 *Let E be a set. A collection $\mathcal{C}$ of signed subsets of E is called the set of* signed circuits of an oriented matroid on E *if and only if the following axioms are satisfied:*

(C0) $\emptyset \notin \mathcal{C}$,

(C1) $\mathcal{C} = -\mathcal{C}$,

(C2) for all $X, Y \in \mathcal{C}$ *with* $\underline{X} \subset \underline{Y}$ *it follows that* $X = Y$ *or* $X = -Y$,

(C3) for all $X, Y \in \mathcal{C}$ *with* $X \neq -Y$ *and* $e \in X^+ \cap Y^-$, *there is* $Z \in \mathcal{C}$ *with* $Z^+ \subset (X^+ \cup Y^+)\backslash\{e\}$ *and* $Z^- \subset (X^- \cup Y^-)\backslash\{e\}$.

The following proposition shows that the set of maximal recoverable supports of a matrix $A \in \mathbb{R}^{m\times n}, m < n$, is not necessarily a set of signed circuits of an oriented matroid on $\{-1,0,+1\}^n$.

Proposition 3.5.8 *For $A \in \mathbb{R}^{m\times n}, m < n$, consider the set*

$$\begin{aligned} \mathcal{M}(A) \equiv \{v \in \{-1,0,1\}^n : v_I = s, v_j = 0 \text{ for } j \in I^c \\ \text{and } (I,s) \text{ as a maximal recoverable support of } A\}. \end{aligned}$$

Then $\mathcal{M}(A)$ is not a set of signed circuits of an oriented matroid on $\{-1,0,+1\}^n$.

Proof. In this proof, a counterexample is given which shows that $\mathcal{M}(A)$ is not a set of signed circuits of an oriented matroid on $\{-1,0,+1\}^n$. Among other axioms, the set $\mathcal{M}(A)$ needs to satisfy the *weak elimination axiom* (C3), saying for all $x, y \in \mathcal{M}(A), x \neq -y$, and $i_0 \in \{i : x_i = +1\} \cap \{j : y_j = -1\}$, there is $z \in \mathcal{M}(A)$ such that

$$\begin{aligned} &\text{if } z_i = +1, \quad \text{then } x_i = +1 \text{ or } y_i = +1, \text{ and } i \neq i_0, \text{ and} \\ &\text{if } z_j = -1, \quad \text{then } x_j = -1 \text{ or } y_j = -1, \text{ and } j \neq i_0. \end{aligned} \tag{3.5.1}$$

Let $A \in \mathbb{R}^{4\times 5}$ be the Mercedes-Benz matrix from Remark 2.5.12. Then each $v \in \mathcal{M}(A)$ is also a 4-sparse vector in $C^5 \cap \mathrm{rg}(A^T)$. With Proposition 2.5.13 it also follows that $v \in \mathcal{M}(A)$ if and only if there is exactly one index i_0 such that $v_{i_0} = 0$ and it follows that $\sum_{i=1}^{n} v_i = 0$. Choose $x, y \in \mathcal{M}(A)$ with $x = [+1, +1, -1, 0, -1]^T$ and $y = [-1, +1, -1, 0, +1]^T$, then for $i_0 = 1$ only two vectors can be constructed via (3.5.1): the vectors $z^{(1)} = [0, +1, -1, 0, +1]^T$ and $z^{(2)} = [0, +1, -1, 0, -1]^T$. But since $\sum_{i=1}^{n} z_i^{(1)} = 1$ and $\sum_{i=1}^{n} z_i^{(2)} = -1$, it follows that $z^{(1)}, z^{(2)} \notin \mathcal{M}(A)$. This proves the assertion. □

In the situation of Proposition 3.5.8, let $A \in \mathbb{R}^{m\times n}, m < n$, be in general position with respect to all $(m-1)$-faces. Then $\mathcal{M}(A)$ is still not a set of signed circuits of an oriented matroid on $\{-1, 0, +1\}^n$, since the counterexample in the proof of Proposition 3.5.8 is already in general position with respect to all 4-faces.

Please note that with the same counterexample $A \in \mathbb{R}^{4\times 5}$ as in the proof of Proposition 3.5.8, one can also see that the same $\mathcal{M}(A)$ is not a set of covectors of an oriented matriod: following the definition in [20, Section 4.1], one axiom requires that for $X, Y \in \mathcal{M}(A)$ it follows that $(X \circ Y) \in \mathcal{M}(A)$ with

$$(X \circ Y)_i = \begin{cases} X_i & , \text{ if } X_i \neq 0 \\ Y_i & , \text{ else} \end{cases} , \text{ for } i \in \{1, ..., n\}.$$

Since $z = [+1, -1, +1, -1, +1]^T$ is not a recoverable support, but $x = [+1, -1, 0, -1, +1]^T$ and $y = [-1, -1, +1, +1, 0]^T$ are; the same argument holds if $\mathcal{M}(A)$ is extended to all recoverable supports of A and not only maximal recoverable supports.

Remark 3.5.9 In the situation of the proof of Proposition 3.5.8, the vectors z_1 and z_2 are still recoverable supports of A but with size 3: for example for z_1, one can choose $v = [-\frac{1}{2}, +1, -1, -\frac{1}{2}, +1]^T$ and with Proposition 2.5.13 there exists $w \in \mathbb{R}^4$ such that $A^T w = v$ and the conditions in (2.1.13) are satisfied for $I \equiv \{2, 3, 5\}$. Interpreting x, y, z_1, z_2 as faces of the hypercube C^n, e.g. z_1 can be regarded as the two-dimensional face $\Phi(I, [+1, -1, +1]^T)$, the faces with respect to x and y share a common three-dimensional face which also contains the faces with respect to z_1 and z_2. It appears to be, that with the weak elimination axiom, one can get a face that lies between the considered faces: take for example x and $\bar{y} = [0, -1, +1, +1, -1]^T$, whose faces share a common facet of C^n, then one may get $z_3 = [+1, 0, -1, +1, -1]^T$ with the weak elimination axiom. This situation might be a good starting point for developing an algorithm which computes all maximal recoverable supports.

3.6 Number of Recoverable Supports for Specific Matrices

In this section, the results from the previous sections are used to give values of $\Lambda(A, k)$ for specific matrices A and positive integer k. This is done by adapting results concerning simple and simplicial polytopes.

3.6.1 Minimal Number of Recoverable Supports

Before considering specific matrices, the question is considered whether there is a lower bound on $\Lambda(A, k)$ with respect to k. A simple example: Theorem 3.4.3 suggests that the set of recoverable supports can be associated with the hypercube $C^n \equiv [-1, +1]^n$ being cut by a lower-dimensional affine subspace which contains the origin. It is obvious that

a two-dimensional plane touches C^3 in at least two edges and two facets, i.e. $\Lambda(A,2) \geq 2, \Lambda(A,1) \geq 2$ for all $A \in \mathbb{R}^{2\times 3}$ and $\mathrm{rg}(A^T)$ is associated with that plane.

As seen in the previous sections, one can design a matrix $A \in \mathbb{R}^{m\times n}, m < n$, such that the set

$$\mathcal{P} \equiv \{Ax^* : x^* \in \mathcal{C}^n_\triangle \text{ solves (L1) uniquely}\}$$

can not be represented as a convex polytope, e.g. the set $\mathcal{P}$ on the right-hand side in Figure 3.3 is only the union of two convex sets. In general, one can give a lower bound on the number of recoverable supports only with $\Lambda(A,k) \geq 0$ for $1 < k \leq \mathrm{rk}(A)$; an open conjecture is $\Lambda(A,1) \geq 2\mathrm{rk}(A)$.

But as shown in Corollary 3.2.5, the concept of general position plays a crucial role: if A is in global general position or A is in general position with respect to all $(k-1)$-faces for $k \leq \mathrm{rk}(A)$, is it possible to establish a sharper lower bound on $\Lambda(A,k)$? This particular question can be answered with results from the field of convex polytopes. As seen in the previous sections, the condition of general position with respect to all $(k-1)$-faces, $k \leq \mathrm{rk}(A)$, is figured prominently since otherwise $\mathcal{P} = \{Ax^* : x^* \in \mathcal{C}^n_\triangle \text{ solves (L1) uniquely}\}$, or each other geometrical interpretation, is not a convex polytope. The following proposition is adapted directly from [9, Corollary 2].

Proposition 3.6.1 *Let $A \in \mathbb{R}^{m\times n}, m < n$, with $\mathrm{rk}(A) = r$ and let A be in general position with respect to all $(r-1)$-faces. Then $\Lambda(A,r) \geq 2^r$.*

Further in the cited work, Bárány and Lovász give a geometrical interpretation when the lower bound is achieved: the intersection $C^n \cap \mathrm{rg}(A^T)$ is an r-dimensional parallelepiped if and only if $\Lambda(A,r) = 2^r$.

An additional work in this field, the *lower bound conjecture*, is proved in [10, 11] and concerns simple and centrally symmetric polytopes. The following proposition contains this result for recoverable supports.

Proposition 3.6.2 *Let $A \in \mathbb{R}^{m\times n}, m < n$, with $\mathrm{rk}(A) = r$ and let A be in general position with respect to all $(r-1)$-faces. Then*

$$\Lambda(A,r) \geq (r-1)\Lambda(A,1) - (r+1)(r-2),$$
$$\Lambda(A,k) \geq \binom{r}{r-k+1}\Lambda(A,1) - \binom{r+1}{r-k-1}(r-k) \text{ for } 2 \leq k < r.$$

Applying the previous proposition requires the knowledge of the number of recoverable supports with size 1 a priori, but this can be evaluated by considering all $2n$ pairs $(I,s) \in \mathcal{S}_{n,1}$. Further, for large r, in the situation of Proposition 3.6.2, one can assume that there are $2n$ recoverable supports of A with size 1, which means that $(r-1)\Lambda(A,1)-(r+1)(r-2)$ is always positive.

Remark 3.6.3 Proposition 3.6.1 and Proposition 3.6.2 have in common that they both state a lower bound on $\Lambda(A, \mathrm{rk}(A))$, but the differences should be explained. Proposition 3.6.1 applies with regard to regular intersections of C^n by a lower-dimensional plane containing the origin. As stated in Remark 3.4.5, the plane intersects the n-cube C^n in no $(n - \mathrm{rk}(A) - 1)$-dimensional face of C^n. This can be provided by assuming that A is in general position with respect to all $(\mathrm{rk}(A) - 1)$-faces.
Proposition 3.6.2 holds if a polytope P is simple, which is given if $P \equiv C^n \cap \mathrm{rg}(A^T)$ is a regular section, cf. Remark 3.4.5. Both statements have different qualities: assuming a

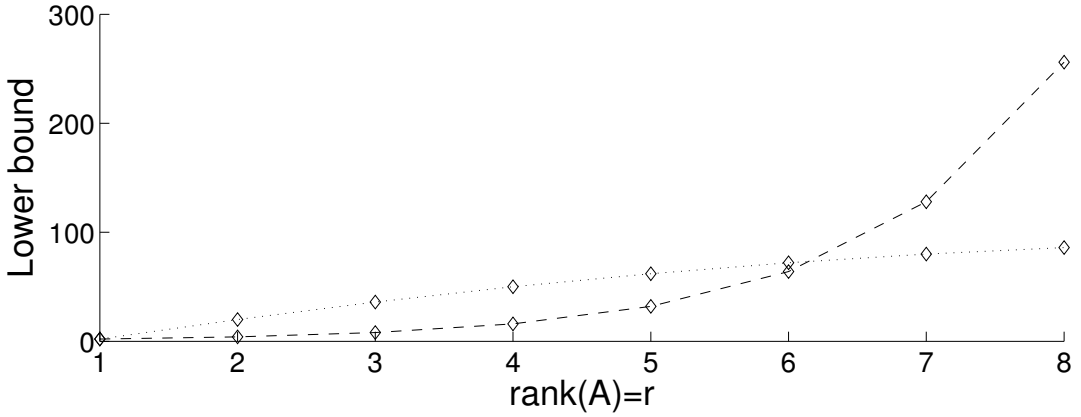

Figure 3.8: Comparison of the results in Proposition 3.6.1 (dashed) and Proposition 3.6.2 (dotted) for $n = 10$ and $\Lambda(A, 1) = 20$ for all matrices $A \in \mathbb{R}^{m\times n}, m < n$, with rank r being in general position with respect to all $(r-1)$-faces. The y-axis gives the lower bound on the number of maximal recoverable supports of a matrix with rank r.

full rank matrix $A \in \mathbb{R}^{m\times n}, m < n$, satisfies $\Lambda(A, 1) = 2n$, the lower bound in Proposition 3.6.1 is larger than the lower bound stated in Proposition 3.6.2 if m is close to n; vice versa, Proposition 3.6.1 gives a weaker bound if $m \ll n$. Figure 3.8 displays this observation for $n = 10$.

3.6.2 Stating the Number of Recoverable Supports with a priori Assumptions

In this section, a linear relationship between the number of recoverable supports with different sizes is considered. If, say, a full rank matrix $A \in \mathbb{R}^{m\times n}, m < n$, is in general position with respect to all $(m-1)$-faces then results from the convex polytope theory can be translated directly into the context of recoverable supports, such as the *Euler-Poincaré formula* [105],

$$\sum_{k=1}^{m}(-1)^{k-1}\Lambda(A, k) = 1 - (-1)^m, \tag{3.6.1}$$

which shows a linear relationship between the number of recoverable supports with different sizes. Recall $\Lambda(A, k) = f_{k-1}(A\mathcal{C}^n_\triangle)$ for all $k \leq m$ if $A \in \mathbb{R}^{m\times n}, m < n$, is in general position with respect to all $(m-1)$-faces. For the rest of the present section and without further mentioning, it is assumed that a matrix $A \in \mathbb{R}^{m\times n}, m < n$, has full rank. The results can be easily adapted to matrices with a lower rank.

Through the assumption that A is general position with respect to all $(m-1)$-faces, the polytope is even simplicial, which leads to the *Dehn-Sommerville equations* [114], stated in the following theorem.

Theorem 3.6.4 *Let $A \in \mathbb{R}^{m\times n}, m < n$, be in general position with respect to all $(m-1)$-faces. Then for all $k \leq m$ it follows that*

$$\sum_{j=k}^{m}(-1)^{j-1}\binom{j}{k}\Lambda(A, j) = (-1)^{m-1}\Lambda(A, k).$$

A relationship between $\Lambda(A,m)$ and $\Lambda(A,m-1)$ can be deduced directly.

Corollary 3.6.5 *Let $A \in \mathbb{R}^{m\times n}, m<n$, be in general position with respect to all $(m-1)$-faces. Then it follows that*

$$m\Lambda(A,m) = 2\Lambda(A,m-1).$$

Proof. It follows that $[(-1)^{m-1}-(-1)^{m-2}]\Lambda(A,m-1) = (-1)^{m-1}m\Lambda(A,m)$, which proves the assertion. □

If, in the situation of Theorem 3.6.4, the value $\Lambda(A,m)$ is known, then $\Lambda(A,m-1)$ can be calculated easily. This argument can not be continued: for $k=m-2$, Theorem 3.6.4 does not imply a linear relationship between $\Lambda(A,m), \Lambda(A,m-1)$ and $\Lambda(A,m-2)$, but only between $\Lambda(A,m)$ and $\Lambda(A,m-1)$.

Remark 3.6.6 The Dehn-Sommerville equations form a linear system of equations with rank $\lfloor \frac{m}{2} \rfloor$ with $\lfloor\cdot\rfloor$ as the *floor function*. Please note that the following convention for the binomial coefficient is chosen:

$$\binom{n}{k} \equiv 0 \text{ if } n<k. \tag{3.6.2}$$

Following [132, Section 8.6], consider $M \in \mathbb{R}^{\{0,\dots,\lfloor\frac{m}{2}\rfloor\}\times\{0,\dots,m\}}$ with entries $m_{i,j} = \binom{m+1-i}{m+1-j} - \binom{i}{m+1-j}$ and assume for a matrix $A\in\mathbb{R}^{m\times n}, m<n$, the vector

$$\Lambda(A) \equiv (1, \Lambda(A,1), \dots, \Lambda(A,m))^T \in \mathbb{R}^{\{0,\dots,m\}}$$

is completely known. Then the linear system of equations $M^T g = \Lambda(A)$ coincides with the Dehn-Sommerville equations and can be solved uniquely. Note that $\Lambda(A)$ has an index equal to 0: for interpretation, the vector $x^* = [0,\dots,0]^T \in \mathbb{R}^n$ also solves (L1) uniquely and one may settle $\Lambda(A,0)=1$. For $I \equiv \{0,\dots,\lfloor\frac{m}{2}\rfloor\}$, the submatrix M_I^T is a lower triangular, square matrix with no value 0 on the diagonal. Therefore, the submatrix M_I^T is invertible. If the values $\Lambda(A,k)$ for $k=1,..,\lfloor\frac{m}{2}\rfloor$ are known, one can state all values $\Lambda(A,k)$.

With Remark 3.6.6, one may calculate, for example, the recoverability curve without calculating all recoverable supports; it is sufficient to calculate the recoverable supports of A up to the size $\lfloor m/2\rfloor$ with m as the rank of the considered matrix A. But since the considered matrix M has a huge condition number and its entries may not be computed exactly, this method needs to be handled carefully. For $A\in\mathbb{R}^{10\times 15}$ whose entries are independent standard normally distributed random variables, Figure 3.9 shows estimated recoverability curve when the values $\Lambda(A,k)$ for $k\leq 5$ are estimated via Monte Carlo experiments. It shows the estimated recoverability curve for $\Lambda(A,k)$, $k\leq 5$, estimated via a Monte Carlo experiment with 100 samples per sparsity (black) and 1000 samples per sparsity (green). The actual recoverability curve is also given (red), as well as the result of the Monte Carlo experiment with 1000 samples per sparsity k (blue). The full description of the experiment can be found on page 110 of the present thesis. In this situation, for the condition number $\kappa(M_I^T)$ of the submatrix of M^T with $I=\{0,\dots,\lfloor\frac{m}{2}\rfloor\}$ from Remark 3.6.6, it follows that $\kappa(M_I^T)\approx 4\cdot 10^5$; one may say the considered problem is ill-conditioned. As one may observe in Figure 3.9, the curves do not distinguish extremely, the ℓ_2-error between the exact recoverability curve and the estimated and interpolated recoverability curves are both around 10^{-1}. For the case in which 100 samples are considered, the

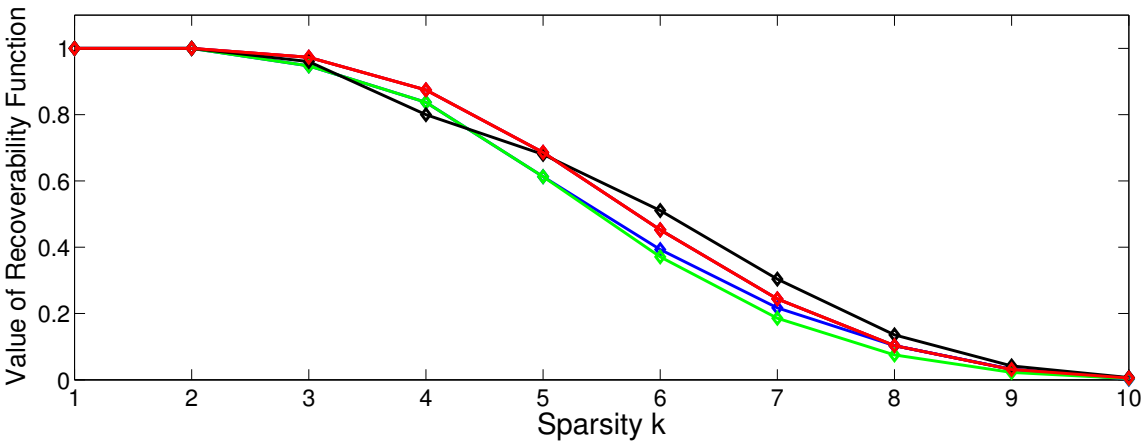

Figure 3.9: Comparison of the different results on the recoverability curve for $A \in \mathbb{R}^{10\times 15}$ whose entries are independent standard normally distributed random variables. The exact recoverability curve is given in red. A Monte Carlo experiment with 1000 samples per sparsity is illustrated in blue. In black and green, the results are given for $\Lambda(A,k), k \leq 5$, estimated via a Monte Carlo experiment with 100 samples per sparsity and 1000 samples per sparsity, respectively, and their remaining values are calculated via the method suggested in Remark 3.6.6.

estimated and interpolated recoverability curve even delivers a smaller ℓ_2-error to the actual recoverability curve than considering only the estimated recoverability curve from the Monte Carlo experiments; but this difference is only around 10^{-10}.

3.6.3 Equiangular Tight Matrices

In this section, equiangular and tight matrices are considered, cf. Section 2.5. Remember, since a frame is considered as a matrix, in the following, both terms are considered as equivalent. Immediately, one can state the following corollary from Theorem 2.5.2 and the Welch bound (2.5.2).

Corollary 3.6.7 *Let $A \in \mathbb{R}^{m\times n}, 1 < m < n$, be equiangular, tight, and have ℓ_2-normalized columns, then*

$$\Lambda(A,k) = 2^k \binom{n}{k} \text{ for } 1 \leq k < \frac{1}{2}\left(1 + \sqrt{\frac{m(n-1)}{n-m}}\right).$$

The previous corollary states that equiangular, tight matrices achieve the maximal possible number of recoverable supports up to a certain size. One may have recognized from Proposition 2.5.11 that minimally redundant matrices, i.e. $m = n-1$, play a particular role for equiangular, tight matrices. For matrices as the Mercedes-Benz matrix, one can state the number of recoverable supports with each size; the following proposition states this value for n odd. The even case can be proved with the same methods and is stated in the following corollary. Please note the convention in (3.6.2) and that $\mathbf{1}_n \in \mathbb{R}^n$ is the vector with all entries equal to 1.

Proposition 3.6.8 *Let $n > 2$ be a positive, odd integer and $A \in \mathbb{R}^{n-1\times n}$ be an equiangular, tight, ℓ_2-normalized matrix with* $\ker(A) = \operatorname{span}(\mathbf{1}_n)$. *Then*

$$\begin{aligned}
\Lambda(A,k) =& 2^k\binom{n}{k} \text{ for } k \leq \frac{n-1}{2},\\
\Lambda(A,k) =& \sum_{i=-1}^{\frac{n-5}{2}}\left\{\sum_{j=0}^{\frac{n-3}{2}}(-1)^{j+i+1}\binom{j}{n-1-k}\binom{n-2-i}{n-1-j}\right\}2^{i+1}\binom{n}{i+1}\\
&+\sum_{i=-1}^{n-1}(-1)^{\frac{n+1}{2}+i}\binom{n-2-i}{n-1-k}\binom{k-i-2}{k-\frac{n+1}{2}}2^{i+1}\binom{n}{i+1}\\
&\text{for } \frac{n-1}{2} \leq k < n-2,\\
\Lambda(A,n-2) =& \frac{(n+1)(n-1)}{4}\binom{n}{\frac{n-1}{2}},\\
\Lambda(A,n-1) =& \frac{n+1}{2}\binom{n}{\frac{n-1}{2}}.
\end{aligned}$$

Proof. The proof is not realized with respect to an increasing k: the first half of the values of k are considered first, then $k = n-1$ and after that the rest is considered. Remark 3.6.9 below explains why this procedure is used.
The case $k \leq (n-1)/2$ can be verified by considering Corollary 3.6.7.
The value $\Lambda(A, n-1)$ is constructed combinatorially. As A satisfies $\ker(A) = \operatorname{span}(\mathbf{1}_n)$, Proposition 2.5.13 implies that an $(n-1)$-sparse vector $v \in \operatorname{rg}(A^T)$ can be constructed by considering $\sum_{i=1}^n v_i = 0$. Moreover, every vector $v \in \mathbb{R}^n$ with $\sum_{i=1}^n v_i = 0$ is an element of $\operatorname{rg}(A^T)$. This means that an $(n-1)$-sparse vector in $\operatorname{rg}(A^T) \cap \{-1, 0, +1\}^n$ has necessarily one entry equal to 0. The construction of an $(n-1)$-sparse vector can be done by choosing $J \subset \{1, ..., n\}$ with $|J| = (n-1)/2$; there are $\binom{n}{(n-1)/2}$ different possibilities choosing J. Next, choose $j \notin J$ which gives $(n+1)/2$ different possibilities. For each J and j consider $I = \{1, ..., n\}\backslash\{j\}$ and $s \in \{-1, +1\}^I$ with $s_i = 1$ for $i \in J$ and $s_k = -1$ for $k \in I\backslash J$. Then the vector $v \in \mathbb{R}^n$ with $v_i = s_i, i \in I$, and $v_j = 0, j \notin I$, is an element of $\operatorname{rg}(A^T)$. Together, there are $\frac{n+1}{2}\binom{n}{(n-1)/2}$ vectors constructed, which is the number of $(n-1)$-sparse vectors in $\operatorname{rg}(A^T) \cap \{-1, 0, +1\}^n$.
Since $\Lambda(A, n-1) \neq 0$ and each recoverable support with size $(n-1)$ is adjacent to $(n-1)$ recoverable supports with size $(n-2)$, one needs to identify the mean value λ_{n-1} in Lemma 3.5.2. Observe that from the previous paragraph of this proof, one can imply that A is in general position to all $(n-2)$-faces. Corollary 3.6.5 leads to $\Lambda(A, n-2) = 2^{-1}(n-1)\Lambda(A, n-1)$. Finally, the remaining values $\Lambda(A, k)$ can be derived with the Dehn-Sommerville equations, cf. Remark 3.6.6. □

Remark 3.6.9 Consider the situation in Proposition 3.6.8. Besides the case $k \leq (n-1)/2$, the proof of Proposition 3.6.8 contains three different methods to achieve the entire result.

1. On the basis of the values $\Lambda(A, k)$ for $k \leq (n-2)/2$ from Corollary 3.6.7, the values for $\Lambda(A, n-2)$ and $\Lambda(A, n-1)$ can be also derived by the Dehn-Sommerville equations in Remark 3.6.6. But first, it needs to be shown that $A\mathcal{C}_\triangle^n$ is simplicial. That is why the combinatorial proof for $\Lambda(A, n-1)$ is important.

2. The value for $\Lambda(A, n-1)$ is proved combinatorially using Proposition 2.5.13. Obviously, the number $\Lambda(A, n-2)$ can be derived using the same strategy. Choose $J \subset \{1, ..., n\}, |J| = (n-1)/2$, and $j_1, j_2 \notin J$. Then with $I \equiv \{1, ..., n\} \backslash \{j_1, j_2\}$ and $v \in \{-1, +1, \}^n$ with $v_i = -1$ for $i \in J$, $v_l = 1$ for $l \in J \backslash I$ and $v_{j_1} = v_{j_2} = 1/2$ it follows that $v \in \mathrm{rg}(A^T)$ with $\|v_{I^c}\|_\infty < 1$.
   Theoretically, this method can be used to calculate the remaining values $\Lambda(A, k), k < n-2$, but this is very difficult since with decreasing k, the number of possibilities to arrange $v \in \mathbb{R}^n$ with $\sum_{i=1}^n v_i = 0$ increases and may become confusing.

3. The lattice introduced in Section 3.5 is used to derive $\Lambda(A, n-2)$ from the knowledge about $\Lambda(A, n-1)$. So far, it is not clear how this result can be generalized for arbitrary k such that one can give λ_k with $\lambda_k \Lambda(A, k-1) = k\Lambda(A, k)$. Even estimating λ_k is difficult; in [84] this was done by the observation $\lambda_k \geq 2(m-k-1)$ for $A \in \mathbb{R}^{m \times n}, m < n$.

The following corollary gives the number of recoverable supports on the analogy of Proposition 3.6.8 with an even number of columns. The proof is similar to the proof in the previous proposition.

Corollary 3.6.10 *Let $n > 2$ be a positive, even integer and $A \in \mathbb{R}^{n-1 \times n}$ be an equiangular, tight, ℓ_2-normalized matrix with* $\ker(A) = \mathrm{span}(\mathbf{1}_n)$. *Then*

$$\begin{aligned} \Lambda(A, k) &= 2^k \binom{n}{k} \text{ for } k \leq \frac{n}{2} - 1, \\ \Lambda(A, n-2) &= \frac{n}{2} \binom{n}{\frac{n}{2}}, \\ \Lambda(A, n-1) &= 0. \end{aligned}$$

Note that there are no recoverable supports of size $(n-1)$ if the Mercedes-Benz matrix A has an even number of columns. Therefore, the polytope $AC_\triangle^n$ is not simplicial and, in contrast to Proposition 3.6.8, the result in [73, Section 9.5.1] can not be used to state $\Lambda(A, k)$ for $n/2 \leq k < n-2$. This implies that for each $(I, s) \in \mathcal{S}_{n,n-1}$ the matrix A is not in general position with respect to (I, s). In other words, the $(n-1)$-dimensional plane $\mathrm{rg}(A^T)$ intersects with the vertices but not with the edges of the n-cube. In Figure 3.1 the Mercedes-Benz matrix is illustrated for $n = 4$.

If a matrix A satisfies the requirement in Proposition 3.6.8, the given intersection is a *hyper-simplex*, i.e. the intersection of a unit cube and a hyperplane which is orthogonal to one vertex of the cube. In the present case, another requirement is that the center of the cube, the origin, is contained in the hyperplane. The values of Λ in Proposition 3.6.8 can be achieved for such matrices with an even number of columns.

Proposition 3.6.11 *Let $n > 2$ be even and consider $v \in \mathbb{R}^n$ such that for exactly one $j_0 \in \{1, ..., n\}$ it follows that $v_{j_0} = 0$ and $v_i = 1$ for $i \neq j_0$. Further let $A \in \mathbb{R}^{n-1 \times n}$ be*

equiangular, ℓ_2-normalized, tight and $\ker(A) = \operatorname{span}(v)$*. Then*

$$\begin{aligned}
\Lambda(A,k) =& 2^k \binom{n}{k} \text{ for } k \leq \frac{n}{2} - 1,\\
\Lambda(A,k) =& \sum_{i=-1}^{\frac{n-4}{2}} \left\{ \sum_{j=0}^{\frac{n-2}{2}} (-1)^{j+i+1} \binom{j}{n-2-k} \binom{n-2-i}{n-1-j} \right\} 2^{i+1} \binom{n}{i+1}\\
&+ \sum_{i=-1}^{\frac{n-4}{2}} (-1)^{\frac{n}{2}+i} \binom{n-2-i}{n-2-k} \binom{k-i-1}{k-\frac{n}{2}-1} 2^{i+1} \binom{n}{i+1}\\
&\text{for } \frac{n}{2} \leq k < n-2,\\
\Lambda(A,n-2) =& \frac{(n-2)n}{4} \binom{n}{\frac{n}{2}},\\
\Lambda(A,n-1) =& \frac{n}{2} \binom{n}{\frac{n}{2}}.
\end{aligned}$$

Proof. This proof can be realized similar to Proposition 3.6.8. Note that $w \in \operatorname{rg}(A^T)$ if and only if $\sum_{i=1, i\neq j_0} w_i = 0$. □

3.6.4 Gaussian Matrices

In compressed sensing, random matrices are often considered. In this section, a special class is the object of interest: *Gaussian matrices.*

Definition 3.6.12 *Let $A \in \mathbb{R}^{m\times n}$. If all entries of A are independent standard normally distributed random variables, then A is called* Gaussian*.*

It is known that the probability that normally distributed random points in $\mathbb{R}^m$ are not in general position, i.e. no $m+1$ points are affinely dependent, is negligible [6]. To that end, it is said that a Gaussian matrix is in global general position with *high probability.* Further, for such a Gaussian matrix $A \in \mathbb{R}^{m\times n}, m < n$, and $x^* \in \mathbb{R}^n$ which solves (L1), one can imply immediately via the strict source condition that, with high probability, the vector x^* is the unique solution of (L1).

Gaussian matrices have been examined in an asymptotic regime which is considered in the end of this section. This section begins with a result on the expected number of maximal recoverable supports adapted from [86, Proposition 2.2]. Note that with Proposition 3.5.6 all maximal recoverable supports of a Gaussian matrix have the same size.

Proposition 3.6.13 *Let $A \in \mathbb{R}^{m\times n}, m < n$, be Gaussian. Then, with the Gauss error function* erf*, the expected value of the number of maximal recoverable supports is*

$$\mathbb{E}(\Lambda(A,m)) = 2^m \binom{n}{m} \sqrt{\frac{2m}{\pi}} \int_0^\infty e^{-mt^2/2} \left[\operatorname{erf}\left(\frac{t}{\sqrt{2}} \right) \right]^{n-m} dt.$$

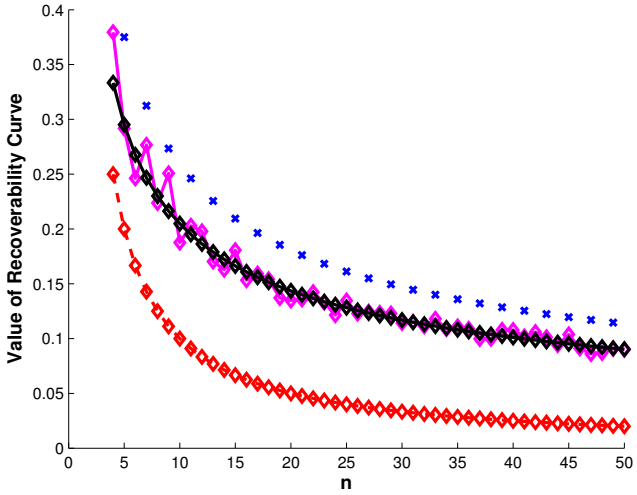

Figure 3.10: Comparison of the recoverability curves for maximal recoverable supports of different minimally redundant matrices with varying n: the Mercedes-Benz matrix (blue) with n odd, the estimated value for the expected value for Gaussian matrices (black), the expected value for Gaussian matrices (black) estimated via Monte Carlo experiment with 1000 samples per n (magenta), and the corresponding lower bound from Proposition 3.6.1 (red).

Remark 3.6.14 In [86, Proposition 2.5] also a lower bound on $\mathbb{E}(\Lambda(A,m))$ is given via estimating the Gauss error function:

$$\mathbb{E}(\Lambda(A,m)) \geq \binom{n}{n-m} 2^n \left(\frac{1}{\pi}\arctan\frac{1}{\sqrt{m}}\right)^{n-m},$$

where equality holds for $m = n-1$.
In comparison to the matrices in Proposition 3.6.8 and Proposition 3.6.11, respectively, one can expect that a Gaussian, minimally redundant matrix has less maximal recoverable supports than the matrices in the propositions mentioned above, cf. Figure 3.10.

Similarly to Corollary 3.6.5, one can state the expected number of recoverable supports of a Gaussian matrix with size $(m-1)$.

Corollary 3.6.15 *Let $A \in \mathbb{R}^{m\times n}, m < n$, be a Gaussian matrix. Then*

$$\mathbb{E}(\Lambda(A,m-1)) = \frac{m}{2}\mathbb{E}(\Lambda(A,m)).$$

Additionally, Lonke derived an asymptotic result [86, Corollary 3.4] for other faces of the emerging polytope. For the rest of this section, let $f(n,m,k)$ denote the expected number of recoverable supports of a Gaussian matrix $A \in \mathbb{R}^{m\times n}$ with size k.

Corollary 3.6.16 *Let m and k be fixed, positive integers with $k < m$. Then*

$$\lim_{n\to\infty} f(n,m,k)(2n)^{-k}k! = 1.$$

Since for a Gaussian matrix $A \in \mathbb{R}^{m\times n}, m < n$, the number $f(n,m,k)$ denotes the expected number of recoverable supports of A with size k, with k as a positive integer,

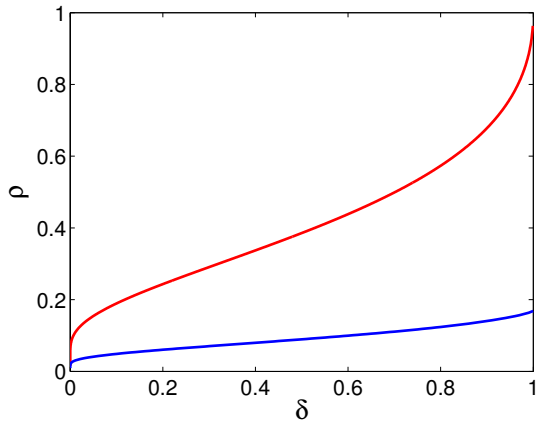

Figure 3.11: Phase transition curves in Theorem 3.6.17 and Theorem 3.6.18: ρ_S (blue) and ρ_W (red).

the author's words in [86, Section 3] can be used to describe the situation in the previous corollary: the value $\Lambda(A,k)$ 'tends to concentrate near the value $[2^k\binom{n}{k}]$, which bounds it from above'. Hence, for large n, Gaussian matrices seem to be good candidates as recovery matrices; but the previous corollary does not include maximal recoverable supports. However, Donoho established a more comprehensive result [50]: it considers in advance defined explicit functions $\rho_S, \rho_W : (0,1] \to [0,1]$ which can be used to give the expected number of k-dimensional faces of $A\mathcal{C}_\triangle^n$ in an asymptotic regime, with A being Gaussian. The functions ρ_S, ρ_W base on the results in [2] and depend on the number of k-dimensional faces of the cross-polytope $\mathcal{C}_\triangle^n$ and angles between different faces of $\mathcal{C}_\triangle^n$. Both functions are illustrated in Figure 3.11.

Theorem 3.6.17 *[50, Theorem 1] Let $\delta \in (0,1)$, $\rho < \rho_S(\delta)$, and let n, m be positive integers with $m \geq \delta n$. Then the probability that $f(n,m,k) = 2^k\binom{n}{k}$ tends to 1 for $k = 1, ..., \lfloor \rho m + 1 \rfloor$ as n tends to infinity.*

The previous result is shown for projected cross-polytopes and states that, for large n, the projected cross-polytope is expected to be at least $\lfloor \rho m + 1 \rfloor$-neighborly for a corresponding δ in dependency of the desired redundancy δ. Moreover, a weaker result considering individual recovery has been stated.

Theorem 3.6.18 *[50, Theorem 2] Let $\delta \in (0,1]$ and $n, m = m(n)$ be positive integers, where m dependents on n with $\lim_{n\to\infty} m(\delta n)^{-1} = 1$. Then for a sequence $\{k_l\}_{l\in\mathbb{N}}$ with $\lim_{n\to\infty} k_n(m\rho)^{-1} = 1$ for $\rho < \rho_W(\delta)$, it follows that*

$$f(n,m,k_n) = 2^{k_n}\binom{n}{k_n}(1+o(1)).$$

The function ρ_W defines the so-called *phase transition* which states in an asymptotic regime for Gaussian matrices $A \in \mathbb{R}^{k/\rho_W(\delta)\times n}$ for sufficiently large n and an arbitrary, positive integer k the abrupt transition between the regimes in which every k-sparse vector is the unique solution of (L1) and no k-sparse vector is the unique solution of (L1) [4, Theorem II]. In contrast, in a non-asymptotic case, Proposition 3.6.13 implies that the expected number of maximal recoverable supports of a Gaussian matrix is strictly larger than 0.

In summary, Gaussian matrices appear to be good candidates for recovery matrices. For sufficiently large n, the primal geometrical interpretation can be used to get satisfying results on recoverability in an asymptotic regime. In a non-asymptotic regime, random intersections of C^n give a few new results on the explicit expected number of maximal recoverable supports of Gaussian matrices.

3.6.5 Upper Bound on the Number of Recoverable Supports

With Section 3.6.3, the maximal number of recoverable supports of a matrix can be stated if A is a minimally redundant matrix. For a general matrix $A \in \mathbb{R}^{m\times n}, m < n$, it appears to be more difficult to calculate the number of recoverable supports of A in accurate time. Therefore, it is of special interest to develop upper bounds for $\Lambda(A,k)$ with $k \leq m$. Trivially, one can deduce $\Lambda(A,k) \leq 2^k\binom{n}{k}$. In this section, a method to construct an upper bound is presented by using previously introduced ideas.

As seen in Lemma 3.5.2, for a given matrix $A \in \mathbb{R}^{m\times n}$ with $m < n$ and $\Lambda(A,k) \neq 0$ for a positive integer k, there is $\lambda_k > 0$ such that

$$\lambda_k \Lambda(A,k-1) = k\Lambda(A,k) \text{ with } \lambda_k \leq 2(n-k+1). \tag{3.6.3}$$

In the following proposition, a lower bound for λ_k is assumed to state a non-trivial upper bound for the number of recoverable supports. After the following proposition, matrices are mentioned which satisfy this lower bound for λ_k.

Proposition 3.6.19 *Let $A \in \mathbb{R}^{m\times n}, m < n$, with $\Lambda(A,l) \neq 0$ for a positive integer $l \leq m$, and let λ_k from (3.6.3) satisfy $2(m-k+1) \leq \lambda_k$ for all $k \leq l$. Then it follows that*

$$\Lambda(A,k) \leq 2^{k-l}\binom{m}{l}^{-1}\binom{m}{k}\Lambda(A,l).$$

Proof. By applying (3.6.3) iteratively, it follows that

$$\begin{aligned}\Lambda(A,k) &\leq \frac{k+1}{2(m-k)}\Lambda(A,k+1) \leq \frac{(k+2)(k+1)}{2^2(m-k)(m-k-1)}\Lambda(A,k+2)\\ &\leq \frac{l!(m-l)!}{2^{l-k}k!(m-k)!}\Lambda(A,l) = 2^{k-l}\binom{m}{l}^{-1}\binom{m}{k}\Lambda(A,l).\end{aligned}$$

□

For a matrix $A \in \mathbb{R}^{m\times n}$ which satisfies the requirements in Proposition 3.6.19 with $\Lambda(A,l) \neq 0$ for $l \leq m$, the potential upper bound from the previous proposition may exceed the value $2^k\binom{n}{k}$ for some k. Instead, for a more realistic upper bound,

$$\Lambda(A,k) \leq \min\left\{2^k\binom{n}{k}, 2^{k-l}\binom{m}{l}^{-1}\binom{m}{k}\Lambda(A,l)\right\}. \tag{3.6.4}$$

should be considered.

Let $U(n,m,k)$ denote the upper bound in (3.6.4). In Figure 3.12, the result from the previous proposition is verified for a known number of recoverable supports from the previous sections. The upper bound is compared to Monte-Carlo experiments for two Gaussian matrices $A \in \mathbb{R}^{50\times n}$ with $n = 51$ and $n = 100$, respectively, in the sense that the

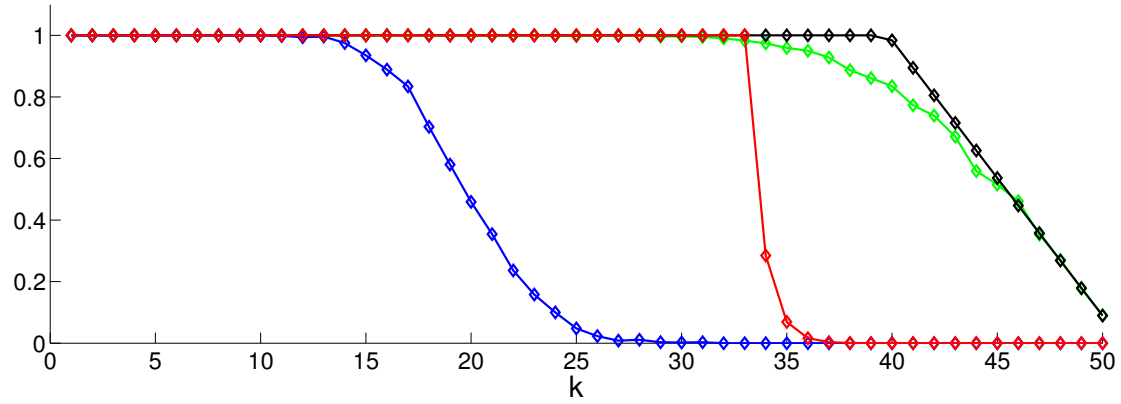

Figure 3.12: Comparison of the upper bound in (3.6.4). In blue, the estimated recoverability curve for a Gaussian matrix $A \in \mathbb{R}^{50\times 100}$ is given which is estimated via a Monte Carlo experiment. The corresponding expected upper bound from (3.6.4) with $\Lambda(A, 50) = 3.73 \cdot 10^{28}$ from Proposition 3.6.13 is illustrated in red. The green line represents the estimated recoverability curve for a Gaussian matrix $A \in \mathbb{R}^{50\times 51}$ which is estimated via a Monte Carlo experiment, and the black line represents the corresponding expected upper bound in (3.6.4) with $\Lambda(A, 50)$ from Proposition 3.6.13.

estimated values of $\Lambda(A, k)$ and $U(n, 50, k)/(2^k\binom{n}{k})$ are compared for all $k \leq 50$. Details can be found on page 111 of the present thesis. One may observe that $U(n, 50, k)/(2^k\binom{n}{k})$ and the estimated recoverability curve diverge in dependency of the distance between n and m. However, the upper bound still appears to be a good result for the redundancy $m/n = 1/2$; for $n = 100$, the ℓ_2-distance between both curves, considered as fifty-dimensional vectors, is around 2, for $n = 51$ the ℓ_2-distance is around 0.3.

The lower bound on λ_k in (3.6.3) is motivated by Proposition 3.5.1 and the observation that, for some $A \in \mathbb{R}^{m\times n}, m < n$, and $(I, s) \in \mathcal{S}_{n,k-1}$, the null space $\ker(A_I^T)$ has the dimension $(m - k + 1)$. Hence, every single basis element of this null space may be used to enlarge a recoverable support (I, s) of A and the enlarging can be done in at least two directions each. So far, a characterization of matrices $A \in \mathbb{R}^{m\times n}$ which satisfy $\lambda_k \geq 2(m - k + 1)$ is not known, but it is conjectured that Gaussian matrices satisfy this lower bound with high probability. Note that it does not mean that λ_k is equal to $2(m - k + 1)$: the bound only considers the case in which one basis element is used to enlarge the recoverable support, a linear combination of basis elements may also be used to enlarge. If that was possible, the number λ_k would be strictly larger than $2(m-k+1)$.

Remark 3.6.20 To examine the values λ_k in (3.6.3), some a priori knowledge about $\Lambda(A, k)$ for all $k \leq m$ is necessary, but even Monte Carlo experiments can give further insights. Figure 3.13 illustrates values of certain λ_k, a full description of the experiment can be found on page 111 in the present thesis. In the upper graphic, the values $\{\lambda_k\}_{k=2}^{10}$ of a Gaussian matrix $A^{(1)} \in \mathbb{R}^{10\times 15}$ are shown in blue. Note that such a small matrix is considered because the values $\Lambda(A, k)$ can be calculated exactly in appropriate time. The estimated values of $\{\lambda_k\}_k$, denoted by $\{\tilde{\lambda}_k\}_k$, are calculated using estimates of $\{\Lambda(A, k)\}_{k=1}^{10}$ via a Monte Carlo experiment with 1000 samples per sparsity k. In green, the values $\tilde{\lambda}_k$ are presented. One may observe that the estimated values are close to the exact values, the ℓ_2-error is $\|(\lambda_k)_k - (\tilde{\lambda}_k)_k\|_2 \approx 2$. In the lower graphic, the estimated values of $\{\lambda_k\}_k$ of a Gaussian matrix $A^{(2)} \in \mathbb{R}^{100\times 150}$ are presented, in which all $\Lambda(A^{(2)}, k)$

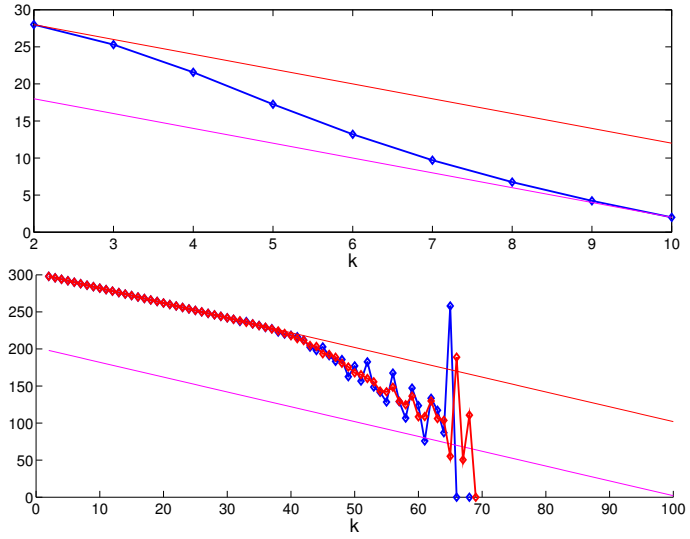

Figure 3.13: Values of λ_k for certain matrices. Top: values of a Gaussian matrix $A \in \mathbb{R}^{10\times 15}$ with exact values (blue) and estimated values via a Monte Carlo experiment (green). Bottom: estimated values of a Gaussian matrix $A \in \mathbb{R}^{100\times 150}$ via Monte Carlo experiment with 1000 samples per k (blue) and 10000 samples per k (red).

are estimated via a Monte Carlo experiment with 1000 samples per k (blue) and 10000 samples per k (red). One may observe that both estimated values violate their upper and lower bounds, given in red and magenta, respectively.

3.7 Maximal Number of Recoverable Supports

In this section, the number $\Xi(m, n, k)$, introduced in the beginning of the present chapter, is considered. It states the maximal possible number of recoverable supports of $A \in \mathbb{R}^{m\times n}, m < n$, with size k. Besides examining properties on Ξ, a matrix $A \in \mathbb{R}^{m\times n}, m < n$, satisfying

$$\Lambda(A, k) = \Xi(m, n, k)$$

is of special interest; such a matrix A is already introduced as a *recovery matrix*, cf. Section 2.5.

Up to now, relatively little is known about recovery matrices. In Corollary 3.6.10, an $(m \times n)$-matrix is given which has zero maximal recoverable supports; the question arises of whether the number $\Xi(m, n, k)$ is also 0 for some instances m, n, and k.

Proposition 3.7.1 *For all $k \leq m < n$ it follows that $\Xi(m, n, k) \neq 0$.*

Proof. Fix k, m, and n and choose $I \equiv \{1, ..., k\}, s \in \{-1, +1\}^I$. In this proof an $(m \times n)$-matrix is constructed such that (I, s) is a recoverable support of this matrix with size k. For arbitrary $w \in \mathbb{R}^m \backslash \{0\}$, set $B \in \mathbb{R}^{m\times k}$ with columns $b_i \equiv e_i w_i s_i$ for $i = 1, ..., k-1$ and $b_k \equiv s_k \sum_{j=k}^{m} e_i w_i$, with $e_i \in \mathbb{R}^m$ as the i-th element of the standard basis. Further, consider $A \in \mathbb{R}^{m\times n}$ with $A_I = (B^\dagger)^T$ and

$$a_{i,j} = \frac{1}{w_i n} \text{ for } j \in I^c.$$

It follows that

$$Bs = \sum_{i=1}^{k} b_i s_i = \sum_{i=1}^{k-1} e_i w_i s_i s_i + \sum_{j=k}^{m} e_j w_j s_k s_k = w$$

and further $s = B^\dagger Bs = B^\dagger w$ which implies $A_I^T w = s$.
Finally, for $j \in I^c$ it follows that

$$\left|a_j^T w\right| = \left|\sum_{i=1}^{m} a_{i,j} w_i\right| = \left|\sum_{i=1}^{m} \frac{1}{n}\right| = \frac{m}{n} < 1.$$

Hence, the pair (I, s) is a recoverable support of A with size k, which means that $\Lambda(A, k) \geq 2$. Consequently, it is $\Xi(m, n, k) \geq 2$. □

Note that $I \equiv \{1, ..., k\}$ in the proof of the previous proposition is only chosen to keep the proof simple, a different subset $I \subset \{1, ..., n\}, |I| = k$, can also be chosen, but then the indices need to be adapted.

Obviously, if $A \in \mathbb{R}^{m \times n}, m < n$, satisfies $\Lambda(A, k) = 2^k \binom{n}{k}$ for a positive integer k, then A is a perfect candidate for recovering all vectors with sparsity k or less via (L1). But what if A satisfies $\Xi(m, n, k) = \Lambda(A, k)$, but $\Lambda(A, k) < 2^k \binom{n}{k}$: is A also a perfect candidate for recovering $(k-1)$-sparse vectors via (L1) or is it possible that a different matrix $\bar{A}$ can achieve a larger value $\Lambda(\bar{A}, k-1) > \Lambda(A, k-1)$? So far, the answer to this question is not answered in general, but in Section 3.6.3 it is shown that one matrix $A \in \mathbb{R}^{n-1 \times n}$ satisfies $\Xi(n, n-1, k) = \Lambda(A, k)$ for all $k \leq n-1$. The following proposition states two results concerning recovery matrices. Both results were published in [84].

Proposition 3.7.2 *Let $m < n$, then for all positive integers $k \leq m$, it follows that*

$$k\Xi(m, n, k) \leq 2(n - k + 1)\Xi(m, n, k - 1).$$

Further, the mapping

$$k \mapsto \left[2^k \binom{n}{k}\right]^{-1} \Xi(m, n, k)$$

is monotonically nonincreasing.

Proof. Assume there is $k \leq m$ for $A, \bar{A} \in \mathbb{R}^{m \times n}$ with $\Xi(m, n, k-1) = \Lambda(A, k-1), \Xi(m, n, k) = \Lambda(\bar{A}, k)$, and $k\Lambda(\bar{A}, k) > 2(n-k+1)\Lambda(A, k-1)$. Then it holds that

$$\frac{2(n-k+1)}{k}\Lambda(A, k-1) < \Lambda(\bar{A}, k) \leq \frac{2(n-k+1)}{k}\Lambda(\bar{A}, k-1),$$

which is a contraction to $\Xi(m, n, k-1) = \Lambda(A, k-1)$.
The second assertion can be proved similarly. □

It should be emphasized that several matrices $A \in \mathbb{R}^{m \times n}$ may satisfy $\Xi(m, n, k) = \Lambda(A, k)$ for a positive integer k. For example for n even, different matrices which satisfy $\Xi(n-1, n, k) = \Lambda(A, k)$ for all $k \leq n-1$ are given in Theorem 3.7.9 below. Further for a positive integer k, it is possible that a matrix $A \in \mathbb{R}^{m \times n}$ which satisfies $\Xi(m, n, k) = \Lambda(A, k)$ does not satisfy $\Xi(m, n, k+1) = \Lambda(A, k+1)$.

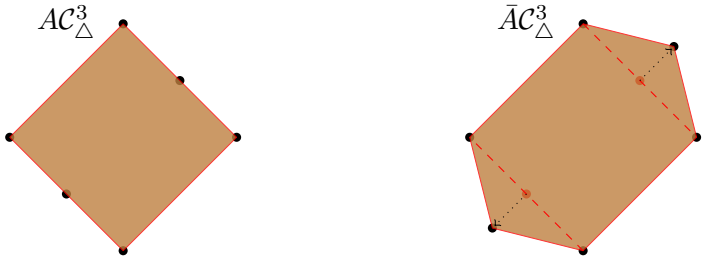

Figure 3.14: Illustration of the proof in Theorem 3.7.3: a matrix $\bar{A}$ being in general position with respect to a specific $(I, s) \in \mathcal{S}_{n,k}$ is constructed out of a matrix A, which is not in general position with respect to that pair (I, s). On the left-hand side the projected cross-polytope regarding A is illustrated, on the right-hand side the projected cross-polytope regarding $\bar{A}$ is illustrated.

3.7.1 Necessary Conditions on Recovery Matrices

In this section two necessary conditions on recovery matrices are stated. To that end, only full rank matrices are considered. The first condition can be derived using further ideas of the geometrical interpretation. An illustration of the proof of the following theorem is given in Figure 3.14.

Theorem 3.7.3 *Let $A \in \mathbb{R}^{m\times n}, m < n$, and for some positive integer $k \leq m$ let A satisfy $\Xi(m, n, k) = \Lambda(A, k)$. Then A is in general position with respect to all $(k-1)$-faces.*

Proof. Since $A\mathcal{C}^n_\triangle$ is one of the polytopes with the largest possible number of $(k-1)$-dimensional faces with $2n$ vertices, by [73, Section 10.1.1] it follows that $A\mathcal{C}^n_\triangle$ is simplicial. The rest of the proof is done by contradiction: assume that one $(k-1)$-dimensional face is not in general position with respect to an appropriate $(I, s) \in \mathcal{S}_{n,k}$.
Without loss of generality, let $(I, s) \in \mathcal{S}_{n,k}$ such that $F \equiv \operatorname{conv}(\{s_i a_i\}_{i\in I})$ is a $(k-1)$-dimensional face of $A\mathcal{C}^n_\triangle$ and let $a_{j_0} \in F$ for $j_0 \notin I$. Further, assume for a moment that a_{j_0} is the only additional vertex on F, i.e. $\pm a_l \notin F$ for all $l \notin I \cup \{j_0\}$. This means that A is not in general position with respect to (I, s). Moreover, it follows that a_{j_0} is in the convex hull of all vertices $s_i a_i, i \in I$. Consider the matrix $\bar{A} \in \mathbb{R}^{m\times n}$ with columns $\bar{a}_i = a_i$ for all $i \neq j_0$, and $\bar{a}_{j_0} = \gamma a_{j_0}$ with $\gamma > 1$ sufficiently large. Then $\operatorname{conv}(\{s_i a_i\}_{i\in I})$ is in the interior of $\bar{A}\mathcal{C}^n_\triangle$ and not a face of $\bar{A}\mathcal{C}^n_\triangle$; moreover, for each $l \in I$, the sets $F_l \equiv \operatorname{conv}(\{s_i a_i\}_{i\in I\setminus\{l\}} \cup \{a_{j_0}\})$ are $(k-1)$-dimensional faces of $\bar{A}\mathcal{C}^n_\triangle$ and it follows that $\Lambda(A, k) < \Lambda(\bar{A}, k)$.
The same reasoning as in the last paragraph holds if $-a_j \in F$; the arguments remain the same if more than one additional vertex lay on F. Finally, if $F \supset \operatorname{conv}(\{s_i a_i\}_{i\in I})$ is a $(k-1)$-dimensional face and $\pm a_j \in F$ for $j \in I^c$, choose $\bar{I} \subset I \cup \{j\}$ such that $F = \operatorname{conv}(\{s_i a_i\}_{i\in \bar{I}})$ with $s_j = \pm 1$. The rest of the proof runs as before. □

Figure 3.14 illustrates the idea of the proof of the previous theorem for $k = m$. On the left-hand side, the polytope $A\mathcal{C}^3_\triangle$, which is also considered in Figure 3.5, is not a potential candidate for a recovery matrix since some faces can not be identified with recoverable supports; in contrast on the right-hand side, the polytope $\bar{A}\mathcal{C}^3_\triangle$ is a better candidate since all faces can be used for recovery.

Note that, with the same argument as in the proof of the previous theorem, a matrix A can be constructed which is in global general position; but this effects that any pair $(I, s) \in \mathcal{S}_{n,k}$ which is not involved in recovery via Theorem 3.2.2 is also in general position.

This means that global general position is not a necessary property for recovery matrices.

A further necessary condition on recovery matrices is taken from [96, Section 23] where the neighborliness of centrally symmetric polytopes is considered. The following theorem gives a necessary condition for global recovery.

Theorem 3.7.4 *Let $A \in \mathbb{R}^{m\times n}, m < n$, in general position with respect to all $(m-1)$-faces. If A satisfies $\Lambda(A,k) = 2^k\binom{n}{k}$ for $k \leq m$, then*

$$\begin{aligned} k &\leq \left\lfloor \frac{m}{2} \right\rfloor && \text{if } m = n-1, \\ k &\leq \left\lfloor \frac{m+1}{3} \right\rfloor && \text{if } m < n-1. \end{aligned}$$

With respect to the previous theorem, in the case of minimally redundant matrices the Mercedes-Benz matrices achieve the maximal possible k such that $\Lambda(A,k) = 2^k\binom{n}{k}$, cf. Proposition 3.6.8 and Corollary 3.6.10. The difference between both is that, for n odd the Mercedes Benz matrix is in general position with respect to all $(n-1)$-faces, while in case n even it is not. But in Proposition 3.6.11 a matrix is given which also achieves the maximal k for n even. So far, for the case $m < n-1$ no matrix A is known which achieves $\Lambda(A,k) = 2^k\binom{n}{k}$ for $k = \lfloor \frac{1}{3}(m+1) \rfloor$. With respect to the previous theorem, such a matrix would be a perfect candidate for being a recovery matrix. But so far, the existence of such a corresponding polytope is debatable: McMullen and Shepard conjectured [96, Section 26] that a centrally symmetric polytope with $2(m+l)$ vertices, $l \geq 1$, is at most $\lfloor \frac{m+l-1}{l+1} \rfloor$-neighborly, where neighborliness still excludes antipodal vertices, but this conjecture is refuted [75].

3.7.2 Explicit Maximal Numbers of Recoverable Supports

In the field of convex polytopes, a central question is: what is the maximal number of k-dimensional faces of an m-dimensional polytope P if P has $v > m$ vertices and what properties does such a polytope have, cf. [73, Chapter 10]. As stated in [73, Section 10.1.1], such a polytope is simplicial. Keeping in mind the recent results in the present chapter, for a recovery matrix $A \in \mathbb{R}^{m\times n}$ the desired polytope

$$\mathcal{P} \equiv \{Ax^* : x^* \in \mathcal{C}^n_\triangle \text{ solves (L1) uniquely}\}$$

is necessarily simplicial, cf. Theorem 3.7.3. The maximal number of k-dimensional faces of an m-dimensional polytope P is given in [94] and is achieved if P is a cyclic m-polytope with v vertices. In general, cyclic polytopes are not centrally symmetric, which means that the result in [94] does not hold for Ξ. So far, a direct adaption to the upper bound theorem to centrally symmetric polytopes is not known, cf. [14].

However, a few numbers for Ξ can be stated directly using the Euler-Poincaré formula in (3.6.1).

Proposition 3.7.5 *Let $n > 1$ be an integer. Then it follows that*

$$\Xi(1,n,1) = 2,\ \Xi(m,n,1) = 2n \text{ for } 1 < m < n,\ \Xi(2,n,2) = 2n \text{ for } n > 2,$$

and

$$\Xi(3,n,k) = \begin{cases} 6n-6, & \text{if } k = 2, \\ 4n-4, & \text{if } k = 3, \end{cases} \quad \text{for } n > 3.$$

Further, for $n > 4$ it follows that

$$\Xi(4, n, 3) < 4n^2 - 8n \text{ and } \Xi(4, n, 4) < 2n^2 - 4n.$$

Proof. Consider the Euler-Poincaré formula in (3.6.1). For $A \in \mathbb{R}^{m\times n}, m < n$, satisfying $\Xi(m, n, k) = \Lambda(A, k)$, the polytope $A\mathcal{C}^n_\triangle$ is simplicial. If $m = 1$, then $\Lambda(A, 1) = 2$ and further $\Xi(1, n, 1) = 2$. Moreover, one can easily place $n \neq 1$ points in $\mathbb{R}^m$ such that n points plus their mirrored points are vertices of a polytope, therefore, $\Xi(m, n, 1) = 2n = 2\binom{n}{1}$. For $m = 2$, one can deduce that $0 = \Lambda(A, 1) - \Lambda(A, 2) = 2n - \Lambda(A, 2)$, hence $\Xi(2, n, 2) = 2n$. Please note that $2\Lambda(A, m - 1) = m\Lambda(A, m)$ since $A\mathcal{C}^n_\triangle$ is simplicial. Hence, for $m = 3$ it follows that

$$2 = \Lambda(A, 1) - \Lambda(A, 2) + \Lambda(A, 3) = 2n - \frac{1}{3}\Lambda(A, 2),$$

and further $\Xi(3, n, 2) = 6n - 6$ and $\Xi(3, n, 3) = 4n - 4$. Finally, Theorem 3.7.4 implies $\Lambda(A, 2) < 2n(n-1)$ for $m = 4$, which proves the upper bounds on $\Xi(4, n, 3)$ and $\Xi(4, n, 4)$. □

The case $\Xi(1, n, 1) = 2$ can be verified without the Euler-Poincaré formula: if $A \in \mathbb{R}^{1\times n}, n > 1$, then $w_{1,2} = \pm\|A^T\|^{-1}_\infty$ are the only vectors which satisfy $|A^T_I w| = 1$ and $\|A^T_{I^c} w\|_\infty < 1$ for $I \subset \{1, ..., n\}$ with $|I| = 1$. So far, even for $m = 4$ the value of $\Xi(m, n, k), k \geq 2$, can not be stated without an inequality. A corresponding open question is stated in [14] for centrally symmetric polytopes, in which also reasonable upper bounds [14, Proposition 2.1, Proposition 2.2] are given. These are stated in the following proposition.

Proposition 3.7.6 *Let $m < n$, then*

$$\Xi(m, n, 2) \leq 2n^2(1 - 2^{-m}),$$
$$\Xi(m, n, k) \leq \frac{2n}{2n-1}(1 - 2^{-m})\binom{2n}{k} \text{ for } k \leq \left\lfloor \frac{m}{2} \right\rfloor.$$

It follows easily that $\Xi(n, m, k) \leq 2^k\binom{n}{k}$. Comparing this trival upper bound to the result in Proposition 3.7.6 for $k = 2$, the upper bound $2n^2(1 - 2^{-m})$ is smaller than $2n(n - 1)$ if $m \leq \log_2(n)$. Hence, for $m \ll n$ this upper bound is useful.

Remark 3.7.7 It is not easy to continue the proof of Proposition 3.7.5 for $m \geq 5$ by using the same argument. Let $A \in \mathbb{R}^{m\times n}, m < n$, such that A is in general position with respect to all $(m - 1)$-faces.
Following [73, Section 10.1.1], for $m = 5$, one can state that

$$\Lambda(A, 3) = 4\Lambda(A, 2) - 10\Lambda(A, 1) + 20,$$
$$\Lambda(A, 4) = 5\Lambda(A, 2) - 15\Lambda(A, 1) + 30,$$
$$\Lambda(A, 5) = 2\Lambda(A, 2) - 6\Lambda(A, 1) + 12,$$

which means, if $\Lambda(A, 2) = 2n(n-1)$, then $\Lambda(A, k) = \Xi(5, n, k)$ for $k = 3, 4, 5$ and $\Lambda(A, 1) = 2n$. This is a possible scenario since the necessary condition in Theorem 3.7.4 is not broken. For $m = 6$ this argument changes. Although with the Dehn-Sommerville equation one can state

$$\Lambda(A, 4) = 5\Lambda(A, 1) - 5\Lambda(A, 2) + 3\Lambda(A, 3),$$
$$\Lambda(A, 5) = 6\Lambda(A, 1) - 6\Lambda(A, 2) + 3\Lambda(A, 3),$$
$$\Lambda(A, 6) = 2\Lambda(A, 1) - 2\Lambda(A, 2) + \Lambda(A, 3),$$

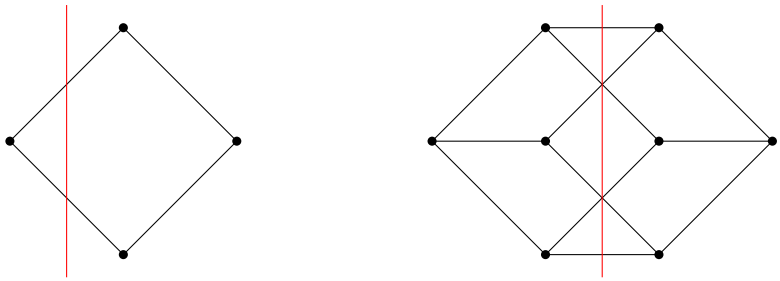

Figure 3.15: Illustration of the intersection of a hyperplane and edges of the cube $[0,+1]^n$ for $n = 2$ (left) and $n = 3$ (right) from Remark 3.7.10. Both graphics sketch how the edges of the corresponding cube are intersected by a hyperplane (red) which cuts the most edges.

but since $3 > \lfloor \frac{1}{3}(m+1) \rfloor$, it follows that $\Lambda(A,3) < 2^3\binom{n}{3}$, and the previous inequalities can only be used to estimate $\Xi(6,n,k)$.

It is long overdue to adapt the result from Corollary 3.6.7 to Ξ.

Corollary 3.7.8 *Let $1 < m < n$ then for $k < \frac{1}{2}\left(1 + \sqrt{\frac{m(n-1)}{n-m}}\right)$ it follows that*

$$\Xi(m,n,k) = 2^k\binom{n}{k}$$

if there is an equiangluar, tight matrix $A \in \mathbb{R}^{m\times n}$ with ℓ_2-normalized columns.

In comparison to the case $m < n-1$, the experiences from Section 3.6 suggest that the case of minimally redundant matrices appears to be easy. Indeed, for $m = n-1$ one can state directly a non-trivial upper bound on $\Xi(n-1,n,n-1)$ with the same argument as in Proposition 3.6.8.

Theorem 3.7.9 *Let $n > 2$ be a positive, odd integer. Then $A \in \mathbb{R}^{n-1\times n}$ satisfies $\Xi(n-1,n,k) = \Lambda(A,k)$ for each $k \leq n-1$ if A is an equiangular, tight matrix with ℓ_2-normalized columns and $\ker A = \operatorname{span}(\mathbf{1}_n)$.*
Let $n > 2$ be a positive, even integer and $v \in \mathbb{R}^n$ such that for $v_i = 0$ for exactly one index $i \in \{1,...,n\}$ and $v_j = 1$ for $j \neq i$. Then $A \in \mathbb{R}^{n-1\times n}$ satisfies $\Xi(n-1,n,k) = \Lambda(A,k)$ for each $k \leq n-1$ if A is an equiangular, tight matrix with ℓ_2-normalized columns and $\ker A = \operatorname{span}(v)$.

Proof. In this proof, only the case for n odd is considered; the other case can be proved similar to Proposition 3.6.11.
Let n be odd. From Corollary 3.7.8 and Corollary 3.6.7, it follows that $\Xi(n-1,n,k) = \Lambda(A,k)$ for $k \leq (n-1)/2$. As every $\Lambda(A,k)$ for $k \geq (n+1)/2$ depends linearly on $\{\Lambda(A,k)\}_{k=1}^{(n-1)/2}$ with positive coefficients, cf. Remark 3.6.6, and $\Lambda(A,k), k \leq (n-1)/2$, are chosen maximally, there is no other matrix $\bar{A} \in \mathbb{R}^{n-1\times n}$ with $\Lambda(\bar{A},k) > \Lambda(A,k)$ for $k \geq (n+1)/2$. □

Remark 3.7.10 A different approach to evaluate $\Xi(n-1,n,n-1)$ can be adapted from [101]. In this work, the author answers the question how many edges of the n-dimensional unit cube $C_+^n \equiv [0,+1]^n$ can be cut maximally by a hyperplane. To that end, he established

a partial order on the set of edges: let $e \equiv (v^{(1)}, v^{(2)})$ denote an edge which connects two vertices $v^{(1)}, v^{(2)} \in C_+^n$ in the sense that $v_i^{(1)} = v_i^{(2)}$ holds for all but exactly one index, then for two edges $e_1 = (v^{(1)}, v^{(2)}), e_2 = (v^{(3)}, v^{(4)})$ it follows that $e_1 < e_2$ if $v_i^{(3)} = v_i^{(2)}$ for all indices i with $v_i^{(2)} = 1$. If for two edges e_1, e_2 it follows that $e_1 < e_2$, then it is said they are *comparable*; if this relation can not be stated for two vertices, then both vertices are *non-comparable*. Further, in [101] a *rank function* r on the set of edges of C_+^n is defined such that $r(e)$ is the number of entries in $v^{(1)}$ which are equal to 1 for $e = (v^{(1)}, v^{(2)}) \in \mathcal{F}_1(C_+^n)$. Obviously, the set of vertices with the same rank consists of non-comparable edges. Baker's generalization [8] of Sperner's lemma [115] states that any set of non-comparable edges has at most Q elements, where $Q = \max_i e(i)$ and $e(i)$ is the number of elements of rank i. Further, the author proves that the set of edges being cut by a hyperplane consists of non-comparable edges [101, Lemma 2]. Therefore, the maximal number of edges being cut by a hyperplane is $Q = \max_i e(i)$, where $e(i)$ is the number of edges of rank i. Since C_+^n is a simple polytope, for example for $n \geq 5$ it follows that $e(0) = 1, e(1) = n, e(2) = n(n-1)$, etc, and the maximum is achieved at $e(n - \lfloor \frac{n}{2} \rfloor) = (n - \lfloor \frac{n}{2} \rfloor)\binom{n}{\lfloor \frac{n}{2} \rfloor}$.
The proof in [101] describes, that no hyperplane can cut C_+^n in more than $(n - \lfloor \frac{n}{2} \rfloor)\binom{n}{\lfloor \frac{n}{2} \rfloor}$ edges. In Figure 3.15, the partial order sets for $n = 2$ (left) and $n = 3$ (right) are illustrated, the red lines illustrate the hyperplanes, which cut the set of the most non-comparable edges. For $n = 2$, it is obvious that the hyperplane does not cut C_+^n through its center; this means that, in general, the realized intersection of the n-cube does not contain the origin. Therefore, the result in [101] states only an upper bound on the number $\Xi(n-1, n, n-1)$. But as described in Proposition 3.6.8 and Proposition 3.6.11, there are minimally redundant matrices A such that $\Lambda(A, n-1) = (n - \lfloor \frac{n}{2} \rfloor)\binom{n}{\lfloor \frac{n}{2} \rfloor}$. It follows that

$$\Xi(n-1, n, n-1) = \left(n - \left\lfloor \frac{n}{2} \right\rfloor\right) \binom{n}{\lfloor \frac{n}{2} \rfloor}.$$

Remark 3.7.11 The result in Remark 3.7.10 suggests that the proof in [101] can be adapted to $\Xi(m, n, m)$ with $m < n - 1$. But, for say $m = n - 2$, neither establishing a partial order on $\mathcal{F}_2(C_+^n)$ such that non-comparable two-dimensional faces arise nor establishing the partial order from two different initial vertices does lead to satisfying results.

3.7.3 Non-trivial Upper Bound on the Maximal Number of Recoverable Supports

In this section, a non-trivial upper bound on Ξ is constructed. Proposition 3.6.19 states an a priori upper bound on the number of recoverable supports and similar to that proposition, for positive integer $m, n, m < n$, an upper bound on $\Xi(m, n, k)$ can be established in dependency of $\Xi(m, n, k)$ for some $l \geq k$.

Corollary 3.7.12 *Let m, n, k be positive integer, then for all $l \leq k$ it follows that*

$$\Xi(m, n, k) \leq 2^{k-l} \binom{m}{l}^{-1} \binom{m}{k} \Xi(m, n, l).$$

The disadvantage of the upper bound in the previous corollary is that it can only be used if for the integers m, n, and k the value $\Xi(m, n, l)$ is known for some $l \geq k$. The only known $\Xi(m, n, k)$ is for $m = n - 1$ which is fully covered by Theorem 3.7.9.

In this section, a simplicial m-dimensional polytope P with $2n$ vertices is constructed which is k-neighborly for $k \leq \lfloor \frac{1}{3}(m+1) \rfloor$ and $|\mathcal{F}_{k+1}(P)|$ is close to $2^k \binom{n}{k}$ for $\lfloor \frac{1}{3}(m+1) \rfloor < k < \frac{n}{2}$. The disadvantage of the constructed polytope P is that one can not verify that P is centrally symmetric; however, the constructed polytope can only be used to state an upper bound.

In advance, the *pseudo-power* of a positive integer needs to be introduced. The following representation is unique and known as the *k-binomial expansion* of n.

Lemma 3.7.13 *[85] Let n and k be positive integers with $n \geq k$. Then there exists a positive integer l and a sequence $\{c_i\}_{i=l}^{k}$ with $1 \leq l \leq c_l < ... < c_{k-1} < c_k$ such that*

$$n = \sum_{i=l}^{k} \binom{c_i}{i}.$$

Definition 3.7.14 *Let n, k, and l be positive integers with $n \geq k \geq l$, and $\{c_i\}_{i=l}^{k}$ with $l \leq c_l < ... < c_{k-1} < c_k$ satisfy $n = \sum_{i=l}^{k} \binom{c_i}{i}$. Then the* pseudo-power of n and k *is defined as*

$$\partial^k(n) \equiv \sum_{i=l}^{k} \binom{c_i + 1}{i + 1}.$$

Further a sequence $h \equiv \{h_i\}_{i=0}^{m}$ of non-negative integers $h_i \in \mathbb{N}$ is called M-sequence *if $h_0 = 1$ and $h_{k-1} \geq \partial^k(h_k)$ for $1 \leq k \leq m$.*

Using M-sequences, simplicial polytopes can be fully characterized. The so-called *g-Theorem*, introduced in the following theorem, states sufficient and necessary conditions for a sequence of non-negative integers to be a sequence whose entries are the numbers of faces of a simplicial polytope. For the rest of this section, a *modified f-vector* is a non-negative sequence $\tilde{f} = \{\tilde{f}_i\}_{i=0}^{m}$ whose i-th entry is the number of $(i-1)$-dimensional faces of an m-dimensional polytope. It is realized as a column vector. Please note that this term is slightly different from the usual use of f-vectors in convex polytopes, cf. [73]. With the notations introduced in the beginning of the present chapter, it follows that $\tilde{f}_i = f_{i-1}$ for $0 \leq i \leq m$. In the following, the entry $\tilde{f}_0$ is always set to 1, one may interpret this as the number of empty sets which is an improper face of a polytope.

Theorem 3.7.15 *[19, 116] Let M be a matrix with entries $m_{i,j} = \binom{m+1-i}{m+1-j} - \binom{i}{m+1-k}$ for $0 \leq i \leq \lfloor \frac{m}{2} \rfloor, 0 \leq j \leq m$. Then $\tilde{f}$ is the modified f-vector of an m-dimensional, simplicial polytope if and only if the unique solution $\bar{g}$ of $M^T g = \tilde{f}$ is an M-sequence.*

In the situation of Theorem 3.7.15, one can immediately construct a simplicial polytope which provides some necessary conditions of $A\mathcal{C}_{\triangle}^{n}$, for A as a recovery matrix. This construction is given in the following corollary. But Theorem 3.7.15 only characterizes simplicial polytopes, which means that a centrally symmetric polytope P is simplicial if the solution of $M^T g = \tilde{f}$ is an M-sequence with $\tilde{f}$ as the modified f-vector of P, but the converse does not hold. However, an upper bound on the number of recoverable supports can be stated which is given in the following corollary. For $m = n-1$ a similar construction, as in the following corollary, coincides with the results in Theorem 3.7.9.

Corollary 3.7.16 *Let $k \leq m < n-1$ and consider the sequence $\{\bar{f}_i\}_{i=0}^{\lfloor \frac{m}{2} \rfloor}$ with*

$$\bar{f}_i = \begin{cases} 2^i \binom{n}{i}, & 0 \leq i \leq \lfloor \frac{m+1}{3} \rfloor, \\ 2^i \binom{n}{i} - 2, & i = \lfloor \frac{m+1}{3} \rfloor + 1, \\ \frac{2(n-i+1)}{i} \bar{f}_{i-1}, & \lfloor \frac{m+1}{3} \rfloor + 2 \leq i \leq \lfloor \frac{m}{2} \rfloor. \end{cases}$$

If the recursively constructed sequence $\{g_i\}_{i=0}^{\lfloor \frac{m}{2} \rfloor}$ with

$$g_i = \bar{f}_i - \sum_{j=0}^{i-1} \left[\binom{m+1-j}{m+1-i} - \binom{j}{m+1-i} \right] g_j, \ i \leq \lfloor \frac{m}{2} \rfloor,$$

is an M-sequence, then

$$\Xi(m,n,k) \leq \sum_{j=0}^{\lfloor \frac{m}{2} \rfloor} \left[\binom{m+1-j}{m+1-k} - \binom{j}{m+1-k} \right] g_j.$$

Proof. The statement follows immediately with Theorem 3.7.15. □

Remark 3.7.17 So far, it is an open question whether the sequence $\{g_i\}$ in Corollary 3.7.16 is an M-sequence. However, no example has been found so far which proves that $\{g_i\}$ is not an M-sequence.
In the situation of Corollary 3.7.16, the resulting polytope is constructed with an initial vector $\bar{f}$ which also states the first half of the modified f-vector of the constructed polytope. It is constructed such that for $k \leq \lfloor \frac{m+1}{3} \rfloor$ the resulting polytope has $2^k \binom{n}{k}$ faces of dimension $(k-1)$, and for $k = \lfloor \frac{m+1}{3} \rfloor + 1$, it reaches almost its trivial upper bound $2^k \binom{n}{k}$ faces. The rest is inspired by Lemma 3.5.2. In context to the partial order in Lemma 3.5.2, it means that a recoverable support can not be enlarged with respect to each available entry. This construction does not violate Theorem 3.7.4.

3.8 Remarks and Future Work

In the present chapter, a connection with compressed sensing and convex polytopes is made. However, this work can rather be seen as an initial spark, there is a lot of work to do in this direction. A strategy to examine how to design a recovery matrix with arbitrary redundancy is to decrease the number of measurements from $(n-1)$ one-by-one and examine each case separately. The case $m = n-1$, which is fully described in this section, is a first attempt to run this strategy.

Many results concerning convex polytopes and discrete geometry are not mentioned in the present chapter. For example, the fact could be exploited that there is a constant $c > 0$ such that for any centrally-symmetric m-polytope P it follows that [61]

$$\log f_0(P) \cdot \log f_{m-1}(P) \geq cm.$$

This means that one can give a lower bound on the number of maximal recoverable supports if $A \in \mathbb{R}^{m \times n}, m < n$, is in general position for all $(m-1)$-faces. It follows that $\Lambda(A,m) \geq e^{cm/\log(2n)}$ for $c > 0$.
Further, one may ask whether Dvoretzky's theorem [55] gives additional insights. As

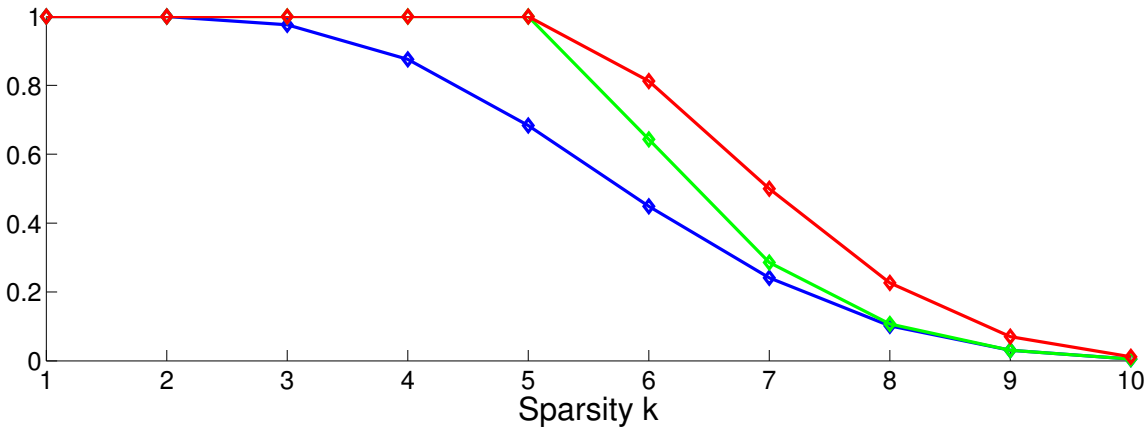

Figure 3.16: Comparison of different upper bounds in Chapter 3 in terms of recoverability for $A \in \mathbb{R}^{10\times 15}$ from Figure 2.1. The exact recoverability curve (blue), as well as the upper bound in Corollary 3.7.16 (red), the upper bound from Proposition 3.6.19 with given initial number $\Lambda(A, 10)$ (magenta).

stated in [131], the intersection of the n-cube with a k-dimensional subspaces, for $k \ll n$, can be "very spherical", which implies it has a huge number of vertices.

Improving the Upper Bound in Corollary 3.7.16
One open task is to achieve a better upper bound than stated in Corollary 3.7.16. The first step in this direction could be to examine λ_k in (3.6.3) to get a better intuition on the connection between $\Lambda(A, k-1)$ and $\Lambda(A, k-2)$.

Designing Recovery Matrices out of Centrally Symmetric Polytopes
A closer look to recent developments [12, 13] on the number of faces of centrally symmetric polytopes may also bring potential recovery matrices. Obviously, for a given r-dimensional, centrally symmetric polytope P with $2n$ vertices, each antipodal set of n vertices forms the columns of an $(m \times n)$-dimensional matrix with rank r. The authors of [12, 13] investigate the *symmetric moment curve*, cf. [14, Section 1], which, hopefully, leads to a similar upper bound as in the more general case of simplicial polytopes, in which the convex hull of n distinct points on the *moment curve* leads to a *cyclic polytope* [94]. Cyclic polytopes are simplicial polytopes with the highest number of k-dimensional faces for $0 \leq k < m$ if the dimension of the considered cyclic polytope is m.

In [12, Corollary 1.4] a centrally symmetric m-polytope P with N vertices is constructed such that

$$f_{k-1}(P) \geq (1 - (\delta_k)^m) \binom{N}{k} \text{ with } \delta_k \approx (1 - 5^{-k+1})^{5/(24k+4)}.$$

The construction is done by considering the symmetric moment curve. Further, this bound has been improved [13, Corollary 5.4]: for a fixed k and arbitrarily large N and m there is a centrally symmetric m-dimensional polytope with N vertices and

$$f_{k-1}(P) \geq \left(1 - k^2 \left(2^{-3/20k^2 2^k}\right)^m\right) \binom{N}{k}.$$

In the corresponding proof [13, Theorem 5.2], for fixed integers $l \geq 1, k \geq 3$, and Υ as a k-independent family of subsets of $\{1, ..., l\}$, a polytope $P \subset \mathbb{R}^{2k(l+1)}$ is constructed which

is k-neighborly, has $2|\Upsilon|$ vertices, taken from the symmetric moment curve, and at most dimension $2k(l+1) - 2l\lfloor (k+1)/3 \rfloor$. To determine a k-independent family Υ of subset of $\{1, ..., l\}$, the authors of [13] propose the deterministic algorithm in [65] which delivers Υ with $|\Upsilon| > 2^{l/5(k-1)2^k}$. Further, to get the desired number N of vertices, an additional integer $t \geq 2$ is introduced such that $N = 2t|\Upsilon|$; geometrically, each point of Υ, and its mirrored point, is replaced by a cluster of t points. Therefore, this construction does not deliver a perfect construction for arbitrary matrices since the number of vertices N is large. Further, the appropriate matrix does not have full rank.

However, the result in [13, Theorem 5.2] implies that a matrix $A \in \mathbb{R}^{m \times n}$ with rank $r < m$ can be constructed with $\Lambda(A, k) = 2^k \binom{n}{k}$ for $k \in \Omega(m)$, and with redundancy

$$\frac{r}{n} < \frac{r}{t} 2^{-\frac{m-2k}{10k(k-1)2^k}}$$

for some t. This appears to be interesting for recovery matrices, but so far it is not known whether such a matrix is in general position to all $(r-1)$-faces – if not, with the idea in Theorem 3.7.3, the recoverability of the corresponding matrix might be improved. Further, a computationally tractable algorithm for designing $A \in \mathbb{R}^{m \times n}$ with given m and n needs to be found. In my opinion, this is a problem whose solution process might give promising insights.

Improving the Upper Bound in Corollary 3.7.16

In Section 3.7.3, at least two open problems remain. The first one is to verify whether the sequence $\{g_i\}_{i=0}^{\lfloor \frac{m}{2} \rfloor}$ in Corollary 3.7.16 is an M-sequence. So far, one can only verify algorithmically whether a certain sequence is an M-sequence, but up to now, all generated sequences $\{g_i\}_{i=0}^{\lfloor \frac{m}{2} \rfloor}$ I considered were verified as M-sequences.

The second problem is to adapt Theorem 3.7.15 to centrally symmetric, simplicial polytopes. Since proving Theorem 3.7.15 requires advanced knowledge in commutative algebra and algebraic geometry, one can expect that the restriction on centrally symmetric polytopes is not less difficult. However, necessary conditions whether a polytope is centrally symmetric and simplicial already exist [117] which can be used to decide whether a polytope is not centrally symmetric and simplicial.

A further task is to examine whether the upper bound in Proposition 3.6.19 can be improved by considering Theorem 3.7.15. Maybe considering the resulting system of equations as a system of linear Diophantine equations may lead to further results.

Designing an (Heuristic) Algorithm to Calculate All Maximal Recoverable Supports

As mentioned in Remark 3.5.9, the weak elimination axiom for signed circuits of oriented matroids might be a good starting point to design a new method which calculates all maximal recoverable supports. To evaluate all maximal recoverable supports, one needs to check each pair $(I, s) \in \mathcal{S}_{n,m}$ respectively $2^{m-1}\binom{n}{m}$ pairs $(I, s) \in \mathcal{S}_{n,m}$ due to symmetry. Initial tests showed that at most 32 testings – instead of 40 testings – were required if two maximal recoverable supports are given for a Gaussian matrix $A \in \mathbb{R}^{4 \times 5}$ generated via Marsaglias' ziggurat algorithm initialized by using the value 1 in Matlab R2007a. The idea is the following. Take $S_1 \equiv (\{1,3,4,5\}, [+1,-1,-1,-1]^T), S_2 \equiv (\{1,2,3,4\}, [+1,+1,+1,-1]^T)$ and consider all sets $(I, s) \in \mathcal{S}_{5,4}$ which can be generated via the weak elimination axiom of signed circuits of an oriented matriod, cf. [20, Definition 3.2.1]. Out of S_1 and S_2, the

pairs

$$\begin{aligned} & (\{2,3,4,5\},[-1,-1,+1,-1]^T), \\ S_3 \equiv\ & (\{2,3,4,5\},[-1,-1,+1,-1]^T), \\ & (\{1,2,3,5\},[+1,-1,-1,-1]^T), \\ S_4 \equiv\ & (\{1,2,3,5\},[-1,-1,-1,-1]^T) \end{aligned}$$

can be generated, with S_3 and S_4 being maximal recoverable supports. From S_1 and $-S_4 \equiv (\{1,2,3,5\},[+1,+1,+1,+1]^T)$ one can generate four other maximal recoverable supports whereby twelve testings are required, and so on. Please note, that this example may not give the smallest number of required testings. Developing this method for general $A \in \mathbb{R}^{m\times n}$, $m < n$, might give new insights into the partial order of all recoverable supports, cf. Section 3.5, and may answer the question which is the smallest number of required testings with this method. Additionally, for stopping the presented method, the number $\Lambda(A,m)$ is required so far, but it may be that the partially ordered set of the recoverable supports as well as the partially ordered set of the edges of the cube C^n give a different stopping criterion.

Extending Results on the Number of Recoverable Supports of A if $A\mathcal{C}^n_\triangle$ is not a convex polytope

Several results in the present chapter require that, for a matrix $A \in \mathbb{R}^{m\times n}, m < n$, it follows that

$$A\mathcal{C}^n_\triangle = \mathcal{P} \equiv \{Ax^* : x^* \in \mathcal{C}^n_\triangle \text{ solves (L1) uniquely}\}.$$

This is not always the case, for example if $A\mathcal{C}^n_\triangle$ is not simplicial. In this situation, the set $\mathcal{P}$ is not a convex polytope. However, the geometrical interpretation $C^n \cap \mathrm{rg}(A^T)$ can still be considered since it represents the sufficient and necessary conditions for solving (L1) uniquely. The question arises, whether the results on the basis of the $A\mathcal{C}^n_\triangle = \mathcal{P}$ can be transfered to the more general case $C^n \cap \mathrm{rg}(A^T)$.

CHAPTER 4

Verifying Exact Recovery

In this chapter, the algorithmic verification of unique solutions of basis pursuit, analysis ℓ_1-minimization, and analysis $\ell_{1,2}$-minimization, respectively, is considered. In the following, let $A \in \mathbb{R}^{m\times n}, m < n, D \in \mathbb{R}^{n\times p}$, and let k be a positive integer. Please note that the matrix D can have an arbitrary number of columns. In the first section, *test instances* are constructed which can be used to evaluate pre-defined tasks. More precisely, in Section 4.1.1 a recoverable support of a given matrix A with a desired size k is constructed. In Section 4.1.2 a matrix A is constructed such that a given pair $(I, s) \in \mathcal{S}_{n,k}$ is a recoverable support of A and a given $w \in \mathbb{R}^m$ is a dual certificate of (I, s). Finally, in Section 4.1.2 a vector x^* is constructed which has a desired sparsity corresponding to the problems in (L1), (AL1), and (AL12), respectively. The test instances in the Sections 4.1.1 and 4.1.3 can be used, for example, to evaluate different solvers for (L1), the test instances in Section 4.1.2 can be used to examine, for example in Monte Carlo experiments, how many considered test instances are unique solutions of the corresponding optimization problem. In Section 4.2, methods to check whether a given vector $x^* \in \mathbb{R}^n$ solves (L1) and (AL1), respectively, uniquely. Computational results on both methods are also done in this section. Furthermore, the recovery condition in Proposition 2.1.1 is used to guarantee that a given vector $x^* \in \mathbb{R}^n$ solves (AL12) uniquely. In Section 4.3, all the methods for (L1) and (AL1) in Section 4.2 are used to study the applicability of compressed sensing to computed tomography.

The conditions in Proposition 2.1.1 for analysis $\ell_{1,2}$-minimization and in Theorem 2.1.3 for analysis ℓ_1-minimization suggest that the term sparsity needs to be adapted to the corresponding optimization problems. Similar to (L1), the adapted term of sparsity for (AL1) and (AL12), respectively, is defined with regard to the non-zero terms of the (outer) sum of the corresponding optimization problem.

Definition 4.0.1 *Let $D \in \mathbb{R}^{n\times p}$, then it is said that the vector $x \in \mathbb{R}^n$ has D-*sparsity *k if $|D^T x|_0 = k$.*
*Let $D \in \mathbb{R}^{n\times pn}$ for $p \in \mathbb{N}$, then it is said that $x \in \mathbb{R}^n$ has D-ℓ_2-*sparsity *k if $|D^T x|_{0,2} = k$ with*

$$|y|_{0,2} \equiv \left| \left\{ i \in \{1, ..., n\} : \sqrt{\sum_{j=0}^{p-1} y_{i+jn}^2} \neq 0 \right\} \right| \text{ for } y \in \mathbb{R}^{pn}.$$

If $D^T \in \mathbb{R}^{2n\times n}$ models the two-dimensional derivate forward operator, which is given below, one can detect the difference between D-ℓ_2-sparsity and D-sparsity: the D-ℓ_2-sparsity of a vector $x \in \mathbb{R}^n$ counts the number of indices i such that $x_i = x_{i+1}$ and

$x_i = x_{i+n}$, while the D-sparsity of x counts the number of indices i such that $x_i = x_{i+1}$ or $x_i = x_{i+n}$. Observe, if x has D-ℓ_2-sparsity k, then it has at least D-sparsity $2k$.

As described in Chapter 1, analysis ℓ_1-minimization and analysis $\ell_{1,2}$-minimization are often considered in image processing with $D^T \in \mathbb{R}^{2n\times n}$ as the two-dimensional derivate forward operator. In this context, both problems (AL1) and (AL12) are also called anisotropic total variation minimization and isotropic total variation minimization, respectively. In the following, a vector $x \in \mathbb{R}^n$ is called *image* if $\sqrt{n} \in \mathbb{N}$. The two-dimensional derivate forward operator D^T is applied on square images respectively pixel arrays $X \in \mathbb{R}^{N\times N}$ with columns $x_1, .., x_N$ which are transformed to an N^2-dimensional vector via

$$X \mapsto (x_1^T, ..., x_N^T)^T.$$

For an approximation of the continuous gradient, the derivate forward operator needs to be equipped with a boundary condition which determines what values occur outside of the domain $\{1, ..., N\} \times \{1, .., N\}$. The most common conditions are the *zero boundary condition*, where it is assumed that all values outside of $\{1, ..., N\} \times \{1, ..., N\}$ are set to 0, and the *Neumann boundary condition*, where is is assumed that outside of $\{1, ..., N\} \times \{1, ..., N\}$, the image is continued constantly, this means that

$$X_{k,j} \equiv X_{N,j}, X_{j,k} \equiv X_{j,N} \text{ for } k > N, 1 \leq j \leq N.$$

For a positive integer $N, n \equiv N^2$, and $D \in \mathbb{R}^{n\times 2n}$ with D^T as two-dimensional derivate forward operator equipped with zero boundary condition, the matrix D has columns $\{d_i\}_{i=1}^{2n}$ such that for each $x \in \mathbb{R}^n$, it follows that

$$d_i^T x = \begin{cases} x_{i+1} - x_i & \text{if } i \leq n, i/N \notin \mathbb{N}, \\ -x_i & \text{if } i \leq n, i/N \in \mathbb{N}, \\ x_{i+N-n} - x_{i-n} & \text{if } n < i \leq 2n - N, \\ -x_{i-n} & \text{if } i > 2n - N, \end{cases}$$

and for D^T equipped with Neumann boundary condition, the matrix D has columns $\{d_i\}_{i=1}^{2n}$ such that for each $x \in \mathbb{R}^n$, it follows that

$$d_i^T x = \begin{cases} x_{i+1} - x_i & \text{if } i \leq n, i/N \notin \mathbb{N}, \\ 0 & \text{if } i \leq n, i/N \in \mathbb{N}, \\ x_{i+N-n} - x_{i-n} & \text{if } n < i \leq 2n - N, \\ 0 & \text{if } i > 2n - N. \end{cases}$$

Neumann boundary conditions are considered for example in [37, 70]. Note that using Neumann boundary conditions in anisotropic total variation minimization implies that the D-sparsity of every $x \in \mathbb{R}^n$ with $N \equiv \sqrt{n} \in \mathbb{N}$ is at most $2N(N-1)$. The following lemma gives a necessary condition on the value of the D-sparsity.

Lemma 4.0.2 *Let $D \in \mathbb{R}^{n\times p}$ have full column rank and let $x \in \mathbb{R}^n$ have D-sparsity $k \neq 0$. Then*

$$\begin{aligned} p - n < k \leq p, \text{ if } n \leq p, \\ 0 \leq k \leq p, \text{ if } n > p. \end{aligned}$$

Proof. In this proof, only the case $n \leq p$ is shown, the other case can be proved similarly. Consider $D^T x \equiv v$ and observe that $v \in \mathbb{R}^p$ has $(p-k)$ entries equal to 0. If $k \leq p-n$, then it immediately holds $x = 0$. □

Note that a boundary condition can also be selected for isotropic total variation minimization. But in contrast to D-sparsity in anisotropic total variation minimization, for each D-ℓ_2-sparsity k with $1 \leq k \leq n$ for zero boundary condition and $1 \leq k < n$ for Neumann boundary condition, an image $x \in \mathbb{R}^n$ with the desired D-ℓ_2-sparsity can be found.

4.1 Test Instances

In this section, methods for constructing test instances are designed. In Section 4.1.1, for a given underdetermined matrix A and a positive integer k, an algorithm to calculate a recoverable support of A with size k is given. In Section 4.1.2, vectors with D-sparsity and $D-\ell_2$-sparsity are constructed. Finally, in Section 4.1.3, a matrix A is given such that for a given $(I,s) \in \mathcal{S}_{n,k}$ and $w \in \mathbb{R}^m$, the pair (I,s) is a recoverable support of A with size k and w is a dual certificate of (I,s).

4.1.1 Construction of Recoverable Supports

Finding a k-sparse vector $x^* \in \mathbb{R}^n$ which is the unique solution of (L1) for a given matrix $A \in \mathbb{R}^{m \times n}, m < n$, is a challenging task, especially if not each pair $(I,s) \in \mathcal{S}_{n,k}$ is a recoverable support of A. In contrast, if it is known that k satisfies $\Lambda(A,k) = 2^k \binom{n}{k}$ for a given $A \in \mathbb{R}^{m \times n}, m < n$, then one can easily take an arbitrary k-sparse vector or project an arbitrary vector onto the subset of k-sparse vectors. With Corollary 3.0.2 such a vector solves (L1) uniquely. But this procedure can not be used for, say, finding a maximal recoverable support of a Gaussian matrix $A \in \mathbb{R}^{n-1 \times n}$: as the expected number of maximal recoverable supports tends to 0 for huge n, cf. Proposition 3.6.13, both methods may not find a maximal recoverable support in appropriate time. However, with the results in Section 3.5, for a given matrix $A \in \mathbb{R}^{m \times n}, m < n$ and $k \leq m$ such that $\Lambda(A,k) > 0$, an algorithm can be designed which generates a recoverable support $(I,s) \in \mathcal{S}_{n,k}$ of A with size k. This algorithm is published in [84].

The pseudo-code of the following method is outlined in Algorithm 1. Please note that the pseudo-code only describes the basic algorithm, this means that details for implementation and an error output for the while loop are missing. In other words, the algorithm can be implemented as stated in Algorithm 1 but it may not terminate if no control is established which terminates the while loop. Let $A \in \mathbb{R}^{m \times n}, m < n$, have rank r and consider a positive integer $k \leq r$. In the following, a pair $(I,s) \in \mathcal{S}_{n,k}$ and $w \in \mathbb{R}^m$ are constructed such that (I,s) is a recoverable support of A with size k and w is a dual certificate of (I,s). The method is based on Proposition 3.5.1, which gives an instruction how to enlarge a recoverable support. Prior to enlarge a recoverable support, an initial recoverable support, which in this case means a recoverable support with size 1, needs to be found.

Proposition 4.1.1 *Let $A \in \mathbb{R}^{m \times n}, m < n$, and $k \in \{1, ..., n\}$ such that for all $j \neq k$ it holds $\|a_j\|_2 \leq \|a_k\|_2$. Then for $s \in \{-1, +1\}$, the pair $(\{k\}, s)$ is a recoverable support of A with size 1 if and only if for any $j \neq k$ with $\|a_j\|_2 = \|a_k\|_2$ it follows that $a_j \neq a_k$.*

Input : $A \in \mathbb{R}^{m\times n}, k \leq \operatorname{rank}(A)$
Output: Recoverable Support (I, s) of A with size k

1 $a_k = \arg\max_{a_i} \|a_i\|_2^2$
2 $w \leftarrow \|a_k\|_2^{-2} a_k$
3 $s \leftarrow A^T w$
4 $I \leftarrow \{k\}$
5 $I^c \leftarrow \{1, ..., n\} \backslash \{k\}$
6 **while** $|I| < k$ **do**
7 *Choose a vector* $y \in \ker A_I^T$
8 *Choose* $\gamma \in \mathbb{R}$ *such that* $\|A_{I^c}^T(w + \gamma y)\|_\infty = 1$
9 $J \leftarrow \{i : |a_i^T(w + \gamma y)| = 1\}$
10 **if** $|J| \leq k$ and A_J has full rank **then**
11 $I \leftarrow J$
12 $I^c \leftarrow \{1, ..., n\} \backslash I$
13 $w \leftarrow w + \gamma y$
14 $s \leftarrow A^T w$
15 **else** *Return to line 7*
16 **end**

Algorithm 1: Computing a recoverable support of a given matrix A with a desired size k

Proof. Let $(\{k\}, s)$ be a recoverable support of A and, without loss of generality, let $s = +1$. Assume that $a_j = a_k$ for $j \neq k$, then for all y orthogonal to a_k, i.e. $a_k^T y = 0$, it holds $|\|a_k\|_2^{-2} a_j^T a_k + a_j^T y| = 1$. This is a contradiction to Corollary 2.1.13 with x^* chosen such that $\{k\} = \operatorname{supp}(x^*)$ and $s = \operatorname{sign}(x_k^*)$.
For the converse direction, let $a_j \neq a_k$ with $\|a_j\|_2 = \|a_k\|_2$. With the Cauchy-Schwarz inequality and $w \equiv \|a_k\|_2^{-2} a_k$ it follows that

$$|a_k^T w| = 1 \text{ and } |a_j^T w| = \frac{|a_j^T a_k|}{\|a_k\|_2^2} < \frac{\|a_j\|_2^2}{\|a_k\|_2} = 1.$$

Further, for any a_i which satisfies $\|a_i\|_2 < \|a_k\|_2$, the inequality $|a_i^T w| < 1$ holds. Trivially, the submatrix $A_{\{k\}}$ has full rank and, with $s = a_k^T w$, the pair $(\{k\}, s)$ is a recoverable support of A with size 1. □

Remark 4.1.2 If all columns of the matrix A have the same norm and are pairwise linearly independent, i.e. for all $j \neq i$ there is no $\alpha \in \mathbb{R}$ such that $a_j = \alpha a_i$, then Proposition 4.1.1 states that each column can be used to generate a recoverable support, hence $\Lambda(A, 1) = 2n$. The other way around, for $\Lambda(A, 1) = 2n$ it is not necessary that all columns of A have the same norm: as long as each column is a vertex of $A\mathcal{C}_\triangle^n$, there are $2n$ recoverable supports with size 1 no matter what norm each column has.
Further note, that only one particular recoverable support with size 1 is considered in Proposition 4.1.1: the one whose column has the largest norm. Obviously, there are more recoverable supports, even if the columns do not have the same norm.
Despite Proposition 4.1.1 generates recoverable supports in dependency of the column with the largest norm, it covers a huge class of matrices: it excludes only matrices in which at least two columns a_i, a_j have both the largest norm over all columns and $a_i = a_j$.

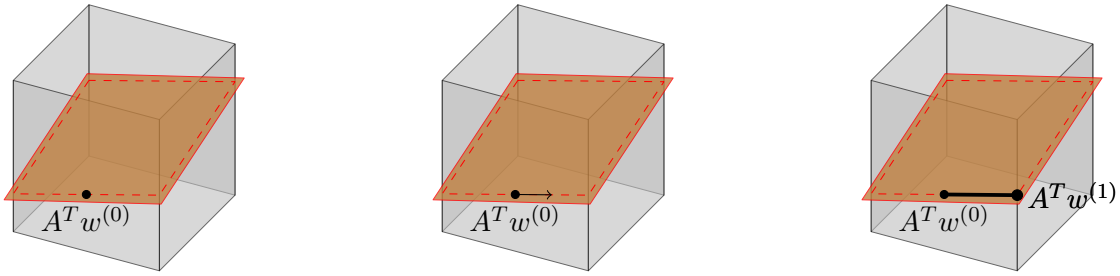

Figure 4.1: Illustration of Algorithm 1 for the case $n = 3, m = 2$. The brown parallelepiped represents the range of a matrix $A^T \in \mathbb{R}^{3\times 2}$ which intersects C^3. On the left-hand side, the point $A^T w^{(0)}$ represents the initial recoverable support in the sense that $w^{(0)}$ is its dual certificate. In the center picture, the arrow at $A^T w^{(0)}$ represents the considered direction in the first iterative of Algorithm 1. On the right-hand side, the initial recoverable support is enlarged, represented by $A^T w(1)$, where $w^{(1)}$ is the new dual certificate.

The algorithm in Algorithm 1 works as follows. With Proposition 4.1.1, a recoverable support of A with size 1 is determined. This recoverable support, denoted by $(\{k\}, s)$, is enlarged via Proposition 3.5.1 if there is an element y orthogonal to a_k and the submatrix consisting of all columns a_j with

$$|\|a_k\|_2^{-2} a_j^T a_k + a_j^T y| = 1 \text{ for } j \in \{1, ..., n\} \tag{4.1.1}$$

is injective. Then, the enlarged recoverable support is a pair (I, s) where I is union of all indices j satisfying (4.1.1) and $s \in \{-1, +1\}^I$ with $s_i = \|a_k\|_2^{-2} a_i^T a_k + a_i^T y$. This procedure is continued iteratively with non-trivial null space elements $y \in \ker(A_I^T)$, until the desired sparsity is achieved.

With Theorem 3.4.3, a geometrical interpretation of the Algorithm 1 can be stated. Consider the hypercube C^n and the m-dimensional subspace $\mathrm{rg}(A^T) \subset \mathbb{R}^n$. Obviously, the intersection $C^n \cap \mathrm{rg}(A^T)$ is not empty. Choosing the initial recoverable support $(\{k\}, s)$ with size 1 may be interpreted geometrically as the element $\|a_k\|_2^{-2} A^T a_k \in \mathbb{R}^n$ which is on a facet of C^n. Following the enlargement in Proposition 3.5.1, a recoverable support (I, s) is enlarged by considering the point $A^T w \in \mathbb{R}^n$, with a corresponding dual certificate $w \in \mathbb{R}^m$, which lays on the $(n - |I|)$-dimensional face $\Phi(I, s)$ of C^n. The mapping $\gamma \mapsto A^T(w + \gamma y)$ for $\gamma \in \mathbb{R}$ and $y \in \ker(A_I^T)$ may be interpreted as *walking along* the range of A^T and the face $\Phi(I, s)$ with respect to a direction y, and with line 8 in Algorithm 1 a lower-dimensional face of C^n, whose intersection with $\mathrm{rg}(A^T)$ is not empty, is met. Figure 4.1 illustrates this interpretation for $n = 3, m = 2$: on the left-hand side, one may see the initial recoverable support of size 1 laying on a facet of C^3, in the center the direction y is illustrated, on the right-hand side, one may see the enlarged recoverable support which is represented by $A^T w^{(1)}$.

Since in Algorithm 1 the iterative *walks* from a face of C^n to a lower-dimensional face in each iteration step, one may estimate that a recoverable support with size k can be computed in at least $(k - 1)$ steps. In fact, a precise statement can not be given since it is possible that the algorithm *walks* from a t-dimensional face to a $(t - 2)$-dimensional face. Experience shows that mostly $(k - 1)$ iterations are required. In Figure 4.2, time and iteration numbers are given for constructing recoverable supports of $A \in \mathbb{R}^{n-1\times n}$ with all sizes $1 \leq k \leq n - 1$, with A as the Mercedes-Benz matrix (top) or a Gaussian matrix (bottom) with $n = 155$ (left) and $n = 555$ (right). Please note that the y-axis is scaled logarithmically to the base 10 to represent the results clear and consistent. One

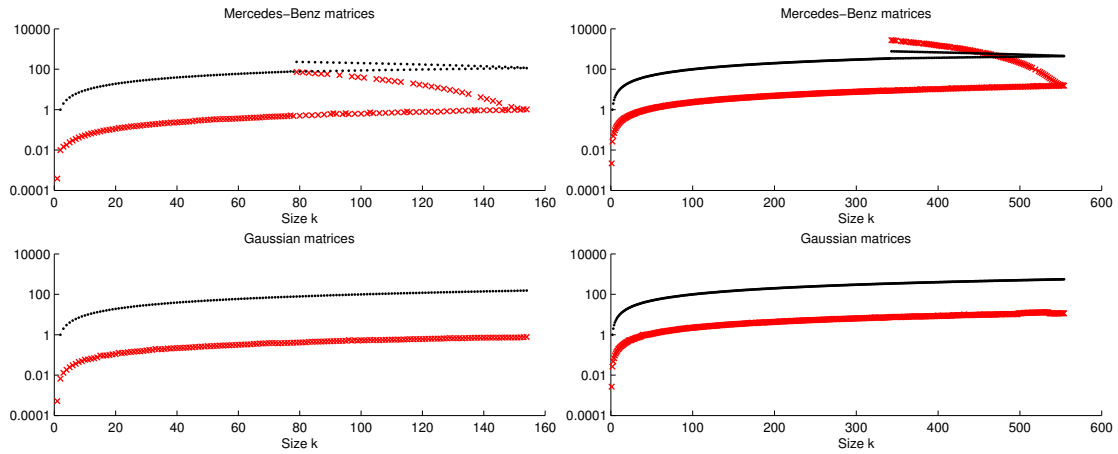

Figure 4.2: The results on time duration (red) and iteration number (black) for constructing a recoverable support of $A \in \mathbb{R}^{n-1\times n}$ with size $k, 1 \leq k \leq n-1$, for A as a Mercedes-Benz matrix (top) or a Gaussian matrix (bottom) with $n = 155$ (left) and $n = 555$ (right).

may observe, that the required number of iterations for Gaussian matrices behaves almost linearly in dependency of the size of the desired recoverable support. To get a recoverable support with size k, mostly only $(k-1)$ iterations are required. For Mercedes-Benz matrices, one may observe that up to $k = 75$ $(n = 155)$ and $k = 340$ $(n = 555)$, respectively, the number of iteration also almost behaves linearly and $(k-1)$ iterations are required. For $k > 76$ $(n = 155)$ and $k > 340$ $(n = 555)$, respectively, the required number of iterations alternates between more than k iterations are required (k odd) and less than $(k-1)$ iterations are required (k even) to compute a recoverable support. This is caused by the fact that the dimension of the considered face of C^n is not increased by 1 in one iteration step, but increased by an integer strictly larger than 1. Fortunately, this decreases the number of required iterations for k even, but increases the number of required iterations for k odd, since the algorithm walks to a face of dimension strictly smaller than $(n-k)$.

Algorithm 1 is outlined with considerable freedom in line 7 and line 8. For instance, a null space element of A_I^T for a given index set $I \subset \{1, ..., n\}$ is chosen by computing an orthonormal basis of $\ker(A_I^T)$ and try each basis element as a potential candidate for y to enlarge the recoverable support. If a potential basis element y is chosen in line 7, it may happen that the `if`-statement in line 10 is violated and a different basis element needs to be considered. Since in each iteration step the index set I is updated by adding new indices, the orthonormal basis of $\ker(A_I^T)$ is generated by a rank-one-update to a QR decomposition in each iteration step, see for instance [69]. Choosing γ in line 8 is done by considering $v = A^T w$ and $z = A^T y$ for a recoverable support (I, s) and a dual certificate w of (I, s), choosing $t \in \mathbb{R}^{2n}$ with

$$t_j = \frac{1 - v_j}{z_j}, t_{j+n} = -\frac{1 + v_j}{z_j}, i = 1, ..., n,$$

and by considering the index $i_{max} = \min_{i\in\{1,...,2n\}} |t_i|$. Then $\gamma = t_{i_{max}}$ guarantees $\|A^T(w + \gamma y)\|_\infty \leq 1$.

Since in each iteration step, one may try all basis elements of $\ker(A_I^T)$, i.e. all $(m-l)$ basis elements with $|I| = l$ for a full rank matrix $A \in \mathbb{R}^{m\times n}$ with $m < n$, a recoverable support with size k can be given in at most $(\mathrm{rk}(A)k - k^2)/2$ iterations. But, so far, such

an instance could not be constructed; from experience, the algorithm requires $(k-1)$ iterations. Please note, that in the current version of this algorithm it may be possible that a recoverable support with size k can not be found. To forestall such a scenario, the results in Section 3.5 give a solution to that problem: one can complement the algorithm for example with the shrinking in Proposition 2.1.8, but so far such an addition has not been not necessary. Moreover, such an addition may increase the total runtime of the algorithm.

Note that the proposed algorithm is deterministic, this means with a given particular input, Algorithm 1 will always produce the same output. This may be seen as a disadvantage, for example if one is interested in calculating several, pairwise different k-sparse vectors. In such a case, one may adapt the algorithm, for instance, such that it starts with a randomly chosen initial recoverable support instead of the recoverable support proposed in Proposition 4.1.1. This method has not been tested so far, but it may happen that, despite different recoverable supports are chosen as initial recoverable supports, the algorithm delivers the same recoverable supports. Note that the total number of recoverable supports is the main topic in Section 3.6.

4.1.2 Constructions of Test Instances for Exact Recovery via Alternating Projections

The algorithm introduced in Section 4.1.1 generates recoverable supports of each given matrix; such a construction is required if the unique solution $x^* \in \mathbb{R}^n$ of (L1) for a given matrix $A \in \mathbb{R}^{m\times n}, m < n$, with a desired sparsity k is used, for example, to compare different solvers for basis pursuit. In some experiments, as for example estimating the recoverability of a given matrix in dependency of the sparsity via a Monte Carlo experiment, only vectors with a desired sparsity need to be constructed; such experiments are discussed in Section 3.6.2. Constructing a k-sparse vector $x \in \mathbb{R}^n$ with $k \leq n$ is easy: either one takes an arbitrary index set $I \subset \{1, ..., n\}$ of cardinality k and places arbitrary non-zero values on x_I while the rest is set to 0, or one takes an arbitrary vector $v \in \mathbb{R}^n$ and projects it via $\Sigma_k : \mathbb{R}^n \to \mathbb{R}^n$, with $I_k(x)$ as the index set with the k largest values of x in absolute value and

$$\begin{aligned}(\Sigma_k x)_i &= x_i, \quad \text{for } i \in I_k(x),\\ (\Sigma_k x)_j &= 0, \quad \text{for } j \notin I_k(x),\end{aligned}$$

onto the subset of all k-sparse vectors.

Input : $D \in \mathbb{R}^{n\times p}$, $v \in \mathbb{R}^p$
Output: $x \in \mathbb{R}^n$ with D-sparsity k

```
while k ≠ |v|_0 do
    v ← Σ_k v
    v ← D†Dv
end
Determine x solving D^T x = v
```

Algorithm 2: Constructing a vector $x^* \in \mathbb{R}^n$ with D-sparsity k

Let $A \in \mathbb{R}^{m\times n}, m < n$, and $D \in \mathbb{R}^{n\times p}$. For analysis ℓ_1-minimization, one can construct a vector $x \in \mathbb{R}^n$ with D-sparsity k via *alternating projections*, see for instance [15]. Usually, the method of alternating projections is an iteration method to find an element in the

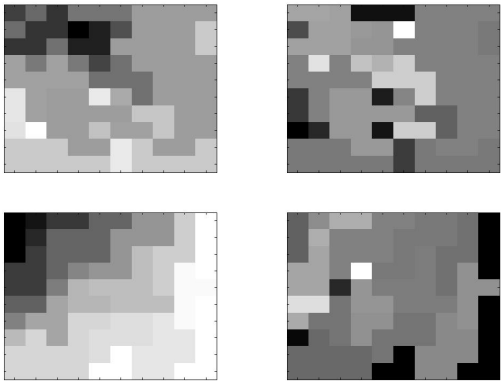

Figure 4.3: Generated images with D-sparsity 100 with $D^T \in \mathbb{R}^{200\times 100}$ as the two-dimensional derivate forward operator. On the left-hand side, the images are generated via alternating projections; on the right-hand side the projection in (4.1.2) is used with I chosen similar to the result from alternating projections. The upper row shows images with an initial vector with entries drawn from the standard normal distribution, the row below shows images generated with an initial vector containing values drawn from the uniform distribution on the interval $(0, 1)$.

non-empty intersection of two (or more) convex sets via projecting orthogonally onto each set successively in each iteration. However, recent developments show that alternating projections still converges for sparse optimization problems with affine constraints [16]. To that end, for a positive integer k an element

$$v \in \mathrm{rg}(D^T) \cap \{\bar{v} \in \mathbb{R}^p : |\bar{v}|_0 = k\}$$

is searched via alternating projections. The algorithm is outlined in Algorithm 2. The idea behind the presented method is that an arbitrary vector of dimension p is projected alternatingly between the subset of all k-sparse vectors and the range of D^T until a projected vector is in the intersection of both sets – the method requires that the intersection of all k-sparse sets and the range of D^T is not empty. A vector x in line 5 can be found since $v \in \mathrm{rg}(D^T)$ with $\mathrm{rg}(D^T) = \mathrm{rg}(D^\dagger)$ in finite dimension. The algorithm is considered in [80].

The authors in [97, Section 2.2] propose a different approach: a projection of an arbitrary vector $\bar{v} \in \mathbb{R}^n$ onto the null space of $D_{I^c}^T$ for a given $D \in \mathbb{R}^{n\times p}$ and a given $I \subset \{1, ..., p\}$ with $|I| = k$. Hence, one considers

$$x = \left(\mathrm{Id} - (D_{I^c}^T)^\dagger D_{I^c}^T\right)\bar{v}. \tag{4.1.2}$$

Note that after using this projection, it must be ensured that x has D-sparsity k since the projection only guarantees $|D^T x|_0 \leq k$. The disadvantage of this method is that the index set I must be chosen carefully: for example for the two-dimensional derivate forward operator $D^T \in \mathbb{R}^{2n\times n}$ with zero boundary condition and for an image $x \in \mathbb{R}^n$, if the index n is an element of the support of $D^T x$ then $2n$ is necessarily also an element of the support of $D^T x$.

In Figure 4.3 both introduced methods, alternating projections and the projection in (4.1.2), are compared for $D^T \in \mathbb{R}^{200\times 100}$ as the two-dimensional derivate forward operator. Both images have D-sparsity 100 and are generated in Matlab as follows. A vector $v \in$

$\mathbb{R}^{200}$ is constructed via `randn` (top) and `rand` (bottom), respectively, and the vector $\bar{v} \in \mathbb{R}^{100}$ with $\bar{v}_i = v_i$ for $1 \leq i \leq 100$ is set. Both vectors are used as initial vectors; the vector v is used for alternating projections, the vector $\bar{v}$ is used for the projection in (4.1.2). The alternating projections method generates the desired image in a few iterations. Furthermore, after generating $x_1 \in \mathbb{R}^{100}$ via alternating projections with the initial vector v, the set $I \equiv \{i : |d_i^T x_1| > 10^{-8}\}$ is chosen. The index set I has cardinality 100. By using I, the projection in (4.1.2) is considered which leads to a vector $x_2 \in \mathbb{R}^{100}$. Note that $D^T x_1$ and $D^T x_2$ have the same support and the same sparsity. For Figure 4.3 both vectors x_1 and x_2 have been transformed to a (10×10)-image each, a linear grayscale colormap is used. Considering the images generated with an initial vector with entries drawn from the standard normal distribution (top), one may observe that both methods produce vectors with similar structure. In contrast, in the row below, the images generated with an initial vector containing values drawn from the standard uniform distribution on the open interval $(0, 1)$ differ widely in their structure: the image generated via alternating projections is structured such that from the upper left corner to the lower right corner the values go from the smallest value to the highest value, while in the image generated via (4.1.2) no such structure can be guessed. This effect can be seen on images with D-sparsities of all sizes if they are generated via alternating projections and with an initial vector generated via `rand` in Matlab. So far, an explanation to this effect is missing.

Input : $D \in \mathbb{R}^{n \times pn}$, $v \in \mathbb{R}^n$
Output: $x \in \mathbb{R}^n$ with D-ℓ_2-sparsity k

1 $v \leftarrow D^T v$
2 **while** $k \neq |v|_{0,2}$ **do**
3 *Set* $t \in \mathbb{R}^n$ *with* $t_i = \sqrt{\sum_{j=0}^{p-1} v_{i+jn}^2}$
4 *Set* $I \subset \{1, ..., n\}$ *with the largest* k *entries of* t *in absolute value*
5 $v_{j+in} \leftarrow 0$ *for* $j \notin I$, $i = 0, ..., p-1$
6 $v \leftarrow D^\dagger D v$
7 **end**
8 *Determine* x *solving* $D^T x = v$

Algorithm 3: Constructing Test Instance with desired D-ℓ_2-sparsity

Algorithm 2 can be adapted to D-ℓ_2-sparsity. With a similar motivation as for finding an element with a certain D-sparsity, for a positive integer k one can search for an element

$$v \in \mathrm{rg}(D^T) \cap \{\bar{v} \in \mathbb{R}^p : |\bar{v}|_{0,2} = k\}$$

via alternating projections. The adaption of Algorithm 2 to $D - \ell_2$-sparsity is outlined in Algorithm 3. The idea behind Algorithm 3 is that, in each iteration, instead of taking the largest entries of $|v|$, as in Algorithm 2, the k largest entries of $t \in \mathbb{R}^n$ with $t_i = \sqrt{v_i^2 + ... + v_{i+pn}^2}$ are considered for $D \in \mathbb{R}^{n \times pn}, p \in \mathbb{N}$, and only these indices remain, see line 5 in Algorithm 3.

Further, one can adopt the idea in (4.1.2) to D-ℓ_2-sparsity. For a given $D \in \mathbb{R}^{n \times pn}$, take $\bar{I} \subset \{1, ..., n\}$ with a desired cardinality $|\bar{I}| = k$ and consider $I \equiv \{i + vn : i \in \bar{I}, v = 0, ..., p-1\}$, as well as the projection onto the null space of $D_{I^c}^T$, i.e. for arbitrary $v \in \mathbb{R}^n$ consider

$$x = (\mathrm{Id} - (D_{I^c}^T)^\dagger D_{I^c}^T) v. \tag{4.1.3}$$

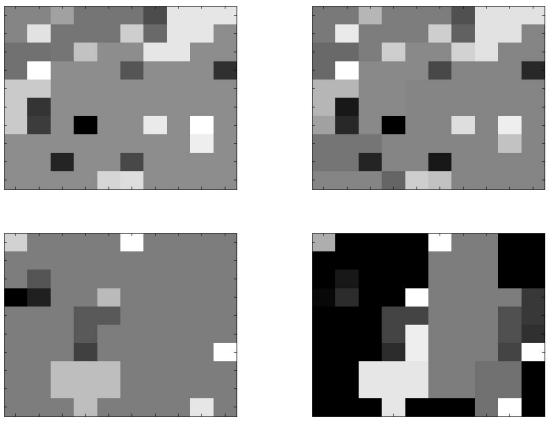

Figure 4.4: Generated images of size (10×10) with D-ℓ_2-sparsity 60 via alternating projections (left) and via the projections in (4.1.3) (right) with I chosen similar to the result from alternating projections. The upper row shows images generated with an initial vector with entries drawn from the standard normal distribution. The row below shows images generated with an initial vector containing values drawn from the uniform distribution on the open interval $(0, 1)$.

The disadvantage of this method is that the index set I must be chosen carefully: for example if $n = 4$ and D^T is the two-dimensional derivate forward operator $D^T \in \mathbb{R}^{2n \times n}$ with the Neumann boundary condition, then there is only one index set with cardinality 3, namely $I = \{1, 2, 3\}$, which leads to the D-ℓ_2-sparsity 3.

In Figure 4.4, alternating projections and the projection in (4.1.3) are compared for $D^T \in \mathbb{R}^{200 \times 100}$ as the two-dimensional derivate forward operator. All images have D-ℓ_2-sparsity 60, where the D-ℓ_2-sparsity of $y \in \mathbb{R}^n$ is approximated by

$$\left| \left\{ i \in \{1, ..., n\} : \sqrt{(d_i^T y_i)^2 + (d_{i+n}^T y)^2} > 10^{-8} \right\} \right|.$$

The images are generated in Matlab as follows. A vector $v \in \mathbb{R}^{200}$ is constructed via `randn` (top) respectively `rand` (bottom) and is used as an initial vector for alternating projections and for the projection in (4.1.3). In the light of past experience and taking into account that no iterative in line 2 of Algorithm 3 has a $D - \ell_2$-sparsity strictly smaller than n, the function $|\cdot|_{0,2}$ is approximated by

$$|v|_{0,2} \approx \left| \left\{ i : \sqrt{(d_i^T y_i)^2 + (d_{i+n}^T y)^2} > 10^{-8} \right\} \right| \ \forall\ v \in \mathbb{R}^n.$$

After generating $x_1 \in \mathbb{R}^{100}$ via alternating projections with the initial vector v, the set $\bar{I} \equiv \{i \in \{1, ..., n\} : \sqrt{(d_i^T x_1)^2 + (d_{i+n}^T x_1)^2} > 10^{-8}\}$ is considered which has cardinality 60. For $I \equiv \bar{I} \cup \{i + n : i \in \bar{I}\}$, the projection in (4.1.3) is considered which leads to a vector x_2. For the graphics in Figure 4.4, all vectors have been transformed to images of the size (10×10) each, a linear grayscale colormap is used. First, one may observe that, in contrast to the anisotropic total variation minimization in Figure 4.3, there is no optical difference between images generated with alternating projections and via the projection in (4.1.3). Note, that the images on the left-hand side let guess that they have a larger D-ℓ_2-sparsity than their analogue counterpart on the right-hand side; this

is caused by the choice of the threshold 10^{-8} in $\bar{I}$: for some indices i it follows that $\sqrt{(d_i^T x_1)^2 + (d_{i+n}^T x_1)^2} \approx 10^{-7}$. Decreasing this threshold does not eliminate this effect: if 10^{-q} for $q \in \mathbb{N}$ is set as a threshold, alternating projections may produce instances such that $\left\{ i : \sqrt{(d_i^T x_1)^2 + (d_{i+n}^T x_1)^2} \approx 10^{-q+1} \right\} \neq \emptyset$. This effect may also happen for the projections for D-sparsity, but this did not occur in most realized experiments.

Since a while-loop is used in Algorithm 3, for implementation it is advisable to stop the iteration after Q iterations, where Q is a self-chosen positive integer. Based on experiences, the value Q should be chosen large. For example, in the experiments in Figure 4.4, it is $Q \equiv 100n$, which was not large enough in several experiments. An additional strategy is to stop the iteration and restart the alternating projections method with a new starting point v. Since in each iteration in Algorithm 3, the D-ℓ_2-sparsity of the iterative v remains equal or is decreased with respect to the previous iteration, a further addition to the algorithm is to include a second positive integer $k_1 \leq k$ for the desired sparsity k and consider the largest k_1 entries in line 4, instead of taking the largest k entries. This is motivated by the observation that even for large Q, the desired D-ℓ_2-sparsity is not reached, but the iterative has a D-ℓ_2-sparsity close to the desired D-ℓ_2-sparsity. This effect was often observed with different choices of the D-ℓ_2-sparsity. The additional strategy avoids this effect by stopping the iteration at the desired iteration k. Since some vectors v are not favorable for being initial vectors, because their required iteration number exceeds the self-chosen value Q, this strategy is an appropriate supplement.

Remark 4.1.3 For (L1), (AL1), and (AL12), all projections onto the space of their corresponding sparsity are realized via setting all but the largest entries in absolute value to 0. For example at anisotropic total variation minimization, the idea behind the consecutive projections in Algorithm 2 is that the D-sparsity of the iterative v decreases. But it may happen that in one iteration the iterative v has D-sparsity $(k-1)$, instead of the desired D-sparsity k. In this situation, setting the smallest entries in absolute value to 0 has no effect: these entries are already 0. This can be avoided by the following method. Assume for example that a vector of D-sparsity k is desired. In each iteration step, before the iterative v is projected onto the set of k-sparse vectors, save the iterative, $v_1 \leftarrow v$, and project v onto the space of k-sparse vectors. If $|v|_0 < k$, discard v and project v_1 onto the space of $(k+1)$-sparse vectors, $v \leftarrow \Sigma_{k+1} v_1$. If it still holds that $|v|_0 < k$, discard v and project v_1 onto the space of $(k+2)$-sparse vectors and continue this procedure until the projected iterative v satisfies $|v|_0 \geq k$.

4.1.3 Construction of ℓ_2-Normalized Matrices for Desired Recoverable Supports

In Section 4.1.1, the construction of a recoverable support of a given matrix and a desired size is presented. Hence, sparsity and matrix are predetermined, support and sign of a potential solution, as well as a dual certificate of (I, s), can be constructed via Algorithm 1. Vice versa, one may be interested in designing a matrix $A \in \mathbb{R}^{m \times n}, m < n$, such that a given pair $(I, s) \in \mathcal{S}_{n,k}$ is a recoverable support of A and a given vector $w \in \mathbb{R}^m$ is a dual certificate of (I, s). In Proposition 3.7.1, such a matrix is designed to show that for each triple (m, n, k), it follows that $\Xi(m, n, k) \neq 0$. One may regard the designed matrix in this proposition as unfavorable since most columns indexed by the given index set I consist of only one non-zero entry and all columns not indexed by I are equal, i.e. $a_i = a_j$ for

all $i, j \notin I$. It is rather uncommon that such a matrix is used to, say, compare different solvers for basis pursuit. But obviously, this construction is kept simple.

With the method introduced in the present section, one can construct an ℓ_2-normalized matrix $A \in \mathbb{R}^{m\times n}$ such that for a given $(I, s) \in \mathcal{S}_{n,k}$ and a given $w \in \mathbb{R}^m$ it follows that

$$A_I \text{ is injective, } A_I^T w = s, \text{ and } \|A_{I^c}^T w\|_\infty < 1,$$

provided $\|w\|_2 \geq 1$.

Lemma 4.1.4 *Let $w \in \mathbb{R}^m$. Then there is $a \in \mathbb{R}^m$ with $a^T w = \pm 1$ and $\|a\|_2 = 1$ if and only if $\|w\|_2 \geq 1$.*

Proof. With $a \equiv \pm w/\|w\|_2$ it follows that $a^T w = \pm 1$ and $\|a\|_2 = 1$. Vice versa, it follows that

$$1 = |a^T w| \leq \|a\|_2 \|w\|_2 = \|w\|_2.$$

□

The previous lemma shows that dual certificates of recoverable supports of ℓ_2-normalized matrices have at least an ℓ_2-norm equal to 1. This can also be seen in Figure 3.4 where, for the Mercedes-Benz matrix $A \in \mathbb{R}^{2\times 3}$, the projected cross-polytope $A\mathcal{C}_\triangle^3$ (left) and its polar polytope $(A\mathcal{C}_\triangle^3)^*$ (center), which consists of all dual certificates of recoverable supports of A, are given. Moreover, for a given pair $(I, s) \in \mathcal{S}_{n,k}$, the previous lemma shows that one can not construct a real, ℓ_2-normalized matrix A with $A_I^T w = s$ for arbitrary $w \in \mathbb{R}^m$.

Input : $k, m, n \in \mathbb{N}, k \leq m < n$, $w \in \mathbb{R}^m$ with $\|w\|_2 > 1$, $I \subset \{1, ..., n\}, |I| = k$, $s \in \{-1, 0, 1\}^n$, s k-sparse
Output: $A \in \mathbb{R}^{m\times n}$ with ℓ_2-normalized columns $\{a_i\}_{i=1}^n$

Set $w^\dagger \leftarrow \|w\|_2^{-2} w$
Choose $\{n_i\}_{i=1}^n \subset \mathbb{R}^m$ *such that* $n_i^T w = 0, \|n_i\|_2 = 1$ *and each subset of* $\{n_i\}_{i=1}^n$ *with* m *elements is linearly independent.*
Choose $y \in \mathbb{R}^n$ *with* $I^c \subset \operatorname{supp}(y)$ *and* $\|y\|_\infty < 1$
for $i \in I$ **do**
  $a_i \leftarrow s_i w^\dagger + \sqrt{1 - \|w^\dagger\|_2^2} n_i$
end
for $j \in I^c$ **do**
  $a_j \leftarrow y_j w^\dagger + \sqrt{1 - y_j^2 \|w^\dagger\|_2^2} n_j$
end

Algorithm 4: Computing a matrix $A \in \mathbb{R}^{m\times n}$ with ℓ_2-normalized columns such that for given $(I, s) \in \mathcal{S}_{n,k}$, $w \in \mathbb{R}^m, m < n$, the pair (I, s) is a recoverable support of A and w is a dual certificate of (I, s)

In Algorithm 4, a method is given which computes a matrix $A \in \mathbb{R}^{m\times n}$ with ℓ_2-normalized columns such that for a given pair $(I, \bar{s}) \in \mathcal{S}_{n,k}$ and a given $w \in \mathbb{R}^m$ with $\|w\|_2 > 1$ satisfying $k \leq m < n$, the pair $(I, \bar{s})$ is a recoverable support of A and w is the corresponding dual certificate. Note that for $w \in \mathbb{R}^m$ with $\|w\|_2 = 1$ the algorithm delivers a matrix whose columns are pairewise linear dependent, i.e. there is $\alpha \in \mathbb{R}$ such that $a_i = \alpha a_j$ for $i \neq j$. Further note that in Algorithm 4, instead of considering

$\bar{s} \in \{-1,+1\}^I$, the vector $s \in \{-1,0,+1\}^n$ with $s_i = \bar{s}_i$ for $i \in I$, and $s_j = 0$ for $j \notin I$ is considered. The algorithm is outlined with considerable freedom in line 2. A proposal how to implement this statement is based on the idea of considering all $(m-1)$ linearly independent and ℓ_2-normalized elements which are orthogonal to a given $w \in \mathbb{R}^m$ and taking n linear combinations with random coefficients. The following proposition shows that the output from Algorithm 4 is an ℓ_2-normalized matrix A such that the input parameter $(I,s) \in \mathcal{S}_{n,k}$ is a recoverable support of A and the other input parameter is a dual certificate of (I,s).

Proposition 4.1.5 *Let $k \leq m < n$ and let $I \subset \{1,...,n\}, |I| = k$, $s \in \{-1,0,+1\}^n$ be k-sparse and $w \in \mathbb{R}^m$ with $\|w\|_2 > 1$. Then the matrix $A \in \mathbb{R}^{m\times n}$ which is generated via Algorithm 4 with columns $(a_i)_{i=1}^n$ is real, has full rank, and it follows that*

$$a_i^T w = s_i \text{ for } i \in I,\ |a_j^T w| < 1 \text{ for } j \in I^c, \text{ and } \|a_i\|_2 = 1 \text{ for } 1 \leq i \leq n.$$

Proof. Since $\|w\|_2 > 1$, it follows that $\|w^\dagger\|_2 = \|w\|_2^{-1} < 1$, hence, all columns are real. Further, each subset of $(a_i)_{i=1}^n$ with m or less elements is linearly independent since each subset of $\{n_i\}_{i=1}^n$ with m or less elements is linearly independent; the matrix A has full rank. Finally, since $w^\dagger$ is orthogonal to all n_i, it follows that

$$\begin{aligned} a_i^T w &= s_i \underbrace{(w^\dagger)^T w}_{=1} + \sqrt{1-\|w^\dagger\|_2^2}\underbrace{n_i^T w}_{=0} = s_i \text{ for all } i \in I, \\ |a_j^T w| &= \left| y_j (w^\dagger)^T w + \sqrt{1-y_j^2\|w^\dagger\|_2^2} n_i^T w \right| = |y_j| < 1 \text{ for all } j \in I^c, \end{aligned}$$

and

$$\begin{aligned} \|a_i\|_2^2 &= \left\| s_i w^\dagger + \underbrace{\sqrt{1-\|w^\dagger\|_2^2}}_{>0} n_i \right\|_2^2 \\ &= \|w^\dagger\|_2^2 + \left(1 - \|w^\dagger\|_2^2\right) = 1 \text{ for all } i \in I, \\ \|a_j\|_2^2 &= y_j^2\|w^\dagger\|_2^2 + (1-y_j^2\|w^\dagger\|_2^2) = 1 \text{ for all } j \in I^c. \end{aligned}$$

□

4.2 Testing Exact Recovery

In this section, for a given matrix $A \in \mathbb{R}^{m\times n}, m < n$, methods to test whether a vector $x^* \in \mathbb{R}^n$ solves (L1), (AL1) for given $D \in \mathbb{R}^{n\times p}$, and (AL12) for given $D \in \mathbb{R}^{n\times pn}, p \in \mathbb{N}$, respectively, are presented. The methods base on the optimality conditions in Section 2.1 and are implemented by using the software package Mosek [5] in Matlab. With given $b_l, b_u \in \mathbb{R}^f, c, l, u \in \mathbb{R}^f$ and $B \in \mathbb{R}^{f\times g}$, the corresponding optimality conditions for (L1) and (AL1) are formulated as linear optimization problems in the form of

$$\min_x \{c^T x : b_l \leq Bx \leq b_u, l \leq x \leq u\}.$$

Note that in this situation, the relation $\leq$ is considered component-by-component. In this representation, the Matlab routine `mosekopt` uses Mosek's primal-dual interior-point method to solve the considered optimization problem. Further, the routine `mosekopt` can also handle *conic optimization problems*, where for $\mathcal{C}$, for instance, as a quadratic cone, the additional restriction $x \in \mathcal{C}$ is added to the considered linear optimization problem, cf. [1, Section 7.6.1]. This formulation is used for the condition on (AL12) from Proposition 2.1.1.

In the following, the symbol $\mathbf{1}_n$ denotes an n-dimensional vector with entries equal to 1.

4.2.1 Basis Pursuit

For a given matrix $A \in \mathbb{R}^{m\times n}, m < n$, and a given vector $x^* \in \mathbb{R}^n$, a method which can be used to decide whether x^* solves (L1) uniquely is presented in this section. The most straightforward way to study recoverability is to check whether the computed solution of (L1) agrees with the original x^*. As for example described in [93, Section 8.5], the problem (L1) can be formulated as a linear program: it is equivalent to the optimization problem

$$\min_{\alpha,\beta\in\mathbb{R}^n} \mathbf{1}_n^T\beta \text{ subject to } A\alpha = Ax^*, -\beta \leq \alpha \leq \beta. \tag{L1p}$$

If a pair (α^*, β^*) solves (L1p), it has the smallest value $\sum_{i=1}^n \beta_i^*$ such that $A\alpha^* = Ax^*$ and $|\alpha_i^*| \leq \beta_i^*$ for $i = 1, ..., n$. For a previously determined $\epsilon > 0$, the vector x^* can be stated as a solution of (L1) if $\|x^* - \alpha^*\|_2/\|x^*\|_2 \leq \epsilon$. This method was used in several experiments as for Gaussian matrices, see for instance [53], or for matrices modeled for computed tomography [81]. The main advantage of solving (L1p) is its simplicity, it does not call for sophisticated derivations. But considering this optimization problem has two disadvantages . First, the accuracy ϵ may cause that some solutions x^* are not verified as solutions because ϵ is chosen too small, while some x^* may be verified as solutions, despite they are no solutions, because ϵ was chosen too large. The second disadvantage is that, for certain matrices and vectors x^*, the computed solution (α^*, β^*) is not the only solution of (L1p) and, hence, it is not the only solution of (L1). In this case, if $\|\alpha^* - x^*\|_2/\|x^*\|_2 > \epsilon$, one can only guarantee that x^* is not the unique solution of (L1), but it is still possible that x^* also solves (L1). Vice versa, one can not guarantee that x^* is the unique solution of (L1) if $\|\alpha^* - x^*\|_2/\|x^*\|_2 \leq \epsilon$.

The following method is based on Corollary 2.1.11 which gives a condition for unique solutions of basis pursuit. Let $(I, s) \in \mathcal{S}_{n,k}$ and $k \leq m < n$. Further, let $A \in \mathbb{R}^{m\times n}, m < n$, and assume that the submatrix A_I has full rank. The conditions in Theorem 2.1.3 suggest that solving

$$\min_{w\in\mathbb{R}^m} \|A_{I^c}^T w\|_\infty \text{ subject to } A_I^T w = s \tag{4.2.1}$$

is an adequate method to verify whether (I, s) is a recoverable support of A: if w^* solves (4.2.1) and $\|A_{I^c}^T w^*\|_\infty < 1$, then (I, s) is a recoverable support of A. Problem (4.2.1) can be formulated as follows. For a given $A \in \mathbb{R}^{m\times n}, m < n$, and $(I, s) \in \mathcal{S}_{n,k}$, for $\xi \in \mathbb{R}^m$ and $\nu \in \mathbb{R}$, the problem (4.2.1) is equivalent to

$$\begin{aligned} \min_{\xi,\nu} \nu \text{ subject to } \quad & -\nu\mathbf{1}_{n-k} \leq A_{I^c}^T\xi \leq \nu\mathbf{1}_{n-k}, \\ & A_I^T\xi = s. \end{aligned} \tag{L1d}$$

For a solution (ξ^*, ν^*), it follows that ν^* is the smallest positive number such that

$$-\nu^* \leq a_j^T\xi^* \leq \nu^* \text{ for } j \in I^c \text{ and } a_i^T\xi^* = s_i \text{ for } i \in I.$$

With Theorem 2.1.3, one can state, if $\nu^* < 1$ and A_I is injective, then the pair (I, s) is a recoverable support of A. Note that the condition in Theorem 2.1.3 is also necessary: if A_I is not injective or $\nu^* \geq 1$, then x^* is not a unique solution. However, if $\nu^* = 1$, one can still deduce that x^* is one solution of (L1), cf. Corollary 2.1.7. In [80] and [84] this formulation was used to verify whether pairs $(I, s) \in \mathcal{S}_{n,k}$ are recoverable supports of certain matrices. The method concerning (L1d) has a disadvantage: verifying $\nu^* < 1$ is difficult. For a verification algorithm, one can choose a sufficiently small $\bar{\epsilon} > 0$ and check whether $\nu^* \leq 1 - \bar{\epsilon}$ holds. But choosing $\bar{\epsilon}$ too large may cause that some unique solutions x^* of (L1) are not verified as such.

For the rest of the present section, the results from [84] are presented, the results in [80] are presented in Section 4.3. The following experiment and results are published in [84], in which both methods, (L1p) and (L1d), were compared for Gaussian matrices. Note that, in general, it is not easy to compare the methods concerning (L1p) and (L1d) because via (L1p) one can only verify whether the corresponding solver returns the input parameter x^* as a solution, while (L1d) can be used to verify whether such x^* solves basis pursuit uniquely. But with regard to Section 3.6.4, the situation changes since Gaussian matrices are in global general position: if x^* solves (L1p) with a Gaussian matrix A, then, with high probability, the vector x^* is the unique solution of (L1). In the following, a similar setup as in [53] was used: for fixed $n \equiv 1600$ and varying $m \leq n$, several Gaussian matrices $A \in \mathbb{R}^{m \times n}$ were generated and for certain sparsities $k \leq m$, it was tested whether both methods produce the same results. Additionally, a time comparison of both methods was done. More precisely, for each triple $(n, m_i, k_{i,j})$ with $m_i = 40i, i = 1, ..., 40$ and $k_{i,j} = (m_i j)/40, j = 1, ..., 40$, the following testing was done in Matlab. Generate a Gaussian matrix $A \in \mathbb{R}^{m_i \times 1600}$ and choose an index set I, with $|I| = k_{i,j}$, randomly by choosing I uniformly over the index set $\{1, ..., 1600\}$. Assure whether the submatrix A_I has full rank through the Matlab function `rank`; if A_I is not injective, then for all $s \in \{-1, +1\}^I$, the pair (I, s) is not a recoverable support of A. If A has full rank, choose $s \in \{-1, +1\}^I$ randomly by generating a random $k_{i,j}$-dimensional vector v via `randn` and set $s \equiv \text{sign}(v)$. Solve (4.2.1) via the formulation (L1d) and the Matlab routine `mosekopt`. If (ξ^*, ν^*) is the computed optimal solution and if $\nu^* \leq 1 - 10^{-12}$, then it is said that (I, s) is a recoverable support of A. Next, consider $x^* \in \mathbb{R}^n$ such that $\text{supp}(x^*) = I$ and $\text{sign}(x^*_I) = s$ hold. With the same matrix A, solve (L1) via (L1p) and `mosekopt` in Matlab. If the optimal computed solution α^* satisfies $\|x^* - \alpha^*\|_2 / \|x^*\|_2 < 10^{-5}$, it is judged that x^* is the solution of (L1) and (I, s) as a recoverable support of A. For each pair $(m_i, k_{i,j})$ this procedure was repeated 50 times.

The experiments were done with Matlab R2012b employed on a desktop computer with 4 CPUs, each Intel® Core™ i5-750 with 2.67GHz, and 5.8 GB RAM. At Mosek 6, the routine `mosekopt` was used to solve (L1p) and (L1d).

Figure 4.5 displays averaged results on recoverability from the experiment described in the previous paragraph: both graphics show how many recoverable supports are identified with respect to the total number of trials. On the left-hand side, the results on (L1p) are displayed, and on the right-hand side, the results on (L1d) are shown. One may observe the misfit between both graphics: the results on (L1p) are not accurate enough to fulfill the desired tolerance of 10^{-5}. Relaxing the threshold from $\epsilon = 10^{-5}$ to $\epsilon = 10^{-3}$ leads to almost identical results as given on the right-hand side of Figure 4.5. It appears to be more difficult to state a criterium a priori for (L1p) than for (L1d) to decide whether a pair (I, s) is a recoverable support. Alternatively, one may consult a comparison of the supports I and $\text{supp}(\alpha^*)$ as a criterium for (L1p); however, since one can assume that,

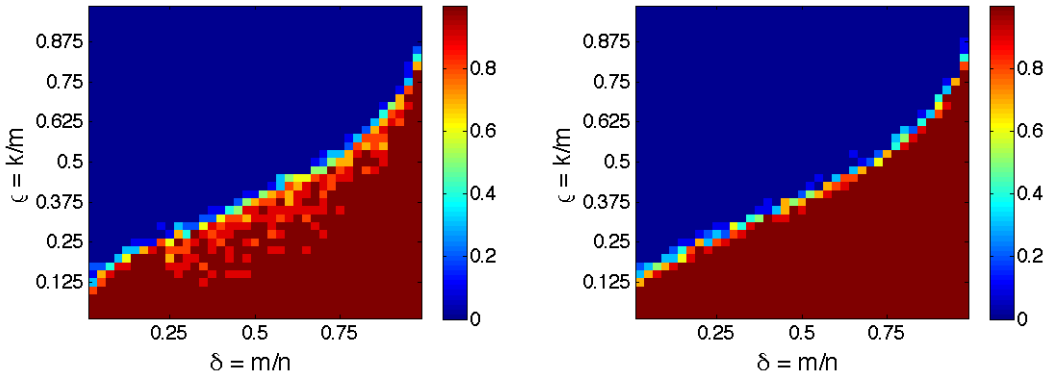

Figure 4.5: Averaged results from Monte Carlo experiments whether a randomly chosen pair $(I, s) \in \mathcal{S}_{n,k}$ is a recoverable support of a Gaussian matrix, algorithmically decided with (L1p) (left) and (L1d) (right). The values reach from 0 (none of the instances are recoverable supports) to 1 (all instances are recoverable supports).

due to numerical effects, α^* has entries equal to 0 but some close to 0, a different tolerance needs to be chosen a priori to determine the support of $\operatorname{supp}(\alpha^*)$. This means that the problem of defining a threshold a priori is only suspended.

In perspective to previous experiments, as in [53], the results are as expected. Further, one may observe a phase transition between 1 to 0. This phase transition is also displayed by ρ_W in Figure 4.5, cf. Theorem 3.6.18. The performance of both methods, (L1p) and (L1d), are measured by taking the time Mosek needed to solve each problem. Additionally for (L1d), it was measured how long it took to compute the rank of A_I; since only Gaussian matrices are considered, which are full rank matrices with probability 1 [24], this test could have been skipped; however, the duration of computing the rank is included, since the test shall be presented without any restrictions to specific test problems. Skipping the testing of the rank would have saved about 0.7 percent of the entire run time of the test. In dependency of $\delta = m_i/1600$ and $\rho = k_{i,j}/m_i$, Figure 4.6 (top) shows the averaged duration of solving (4.2.1) via (L1d) and calculating the rank of the corresponding submatrix divided by the averaged duration of solving (L1) via (L1p). One may observe that all quotients in the plot are less than 1 which means that solving (4.2.1) was always faster than solving (L1) via (L1p). Figure 4.6 (bottom) gives the duration of time for both methods. One may observe that the duration of both methods increase with an increasing δ, while for (L1p) it appears to depend also on ρ and δ. Moreover, the contours of ρ_W in Figure 4.5 can be seen for (L1p): on average, in case that $k_{i,j}$ is close to $\rho_W(m_i/n)m_i$ one may regard that solving (L1) via (L1p) takes longer than for any other $k_{i,j}$.

Further, one may observe a transition at $\delta = 0.25$ where the quotients rapidly decrease. So far, this effect can not be explained. In total, solving (4.2.1) appears to be a faster alternative for calculating the recoverability for Gaussian matrices: it is more than three times faster than using (L1p).

4.2.2 Analysis ℓ_1-Minimization / Anisotropic Total Variation Minimization

For a given matrix $A \in \mathbb{R}^{m\times n}, m < n$, a given matrix $D \in \mathbb{R}^{n\times p}$, and a given vector $x^* \in \mathbb{R}^n$, three methods are presented in this section, which can be used to decide whether

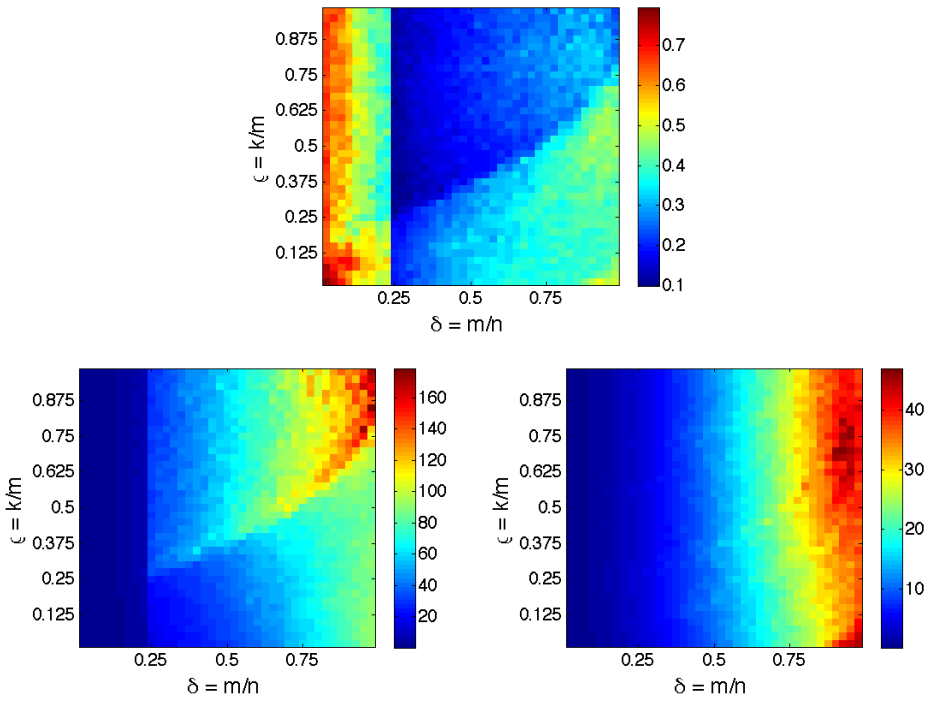

Figure 4.6: Comparison of time duration using (L1p) and (L1d). Top: time duration of solving (L1p) divided by the time duration of solving (L1d) with an additional injectivity check. Bottom: comparison of duration performances between solving (L1p) (left) and solving (L1d) with an additional injectivity check (right) in seconds.

x^* solves

$$\min_y \|D^T y\|_1 \text{ subject to } Ay = Ax^* \tag{AL1}$$

uniquely. The problem (AL1) is called *analysis ℓ_1-minimization*, and if D^T is the two-dimensional derivate forward operator, the problem (AL1) is also called *anisotropic total variation minimization*. Similarly to basis pursuit, as considered in the previous section, one can easily formulate (AL1) as a linear program: for $\alpha \in \mathbb{R}^n, \beta \in \mathbb{R}^p$ consider

$$\min_{\alpha,\beta} \mathbf{1}_p^T \beta \text{ subject to } A\alpha = Ax^*, -\beta \leq D^T\alpha \leq \beta. \tag{AL1p}$$

If a pair (α^*, β^*) solves (AL1p), the smallest value $\sum_{i=1}^p \beta_i^*$ is found such that $A\alpha^* = Ax^*$ and $|d_i^T\alpha^*| \leq \beta_i$, with d_i as the i-th column of D. For previously chosen $\epsilon > 0$, the vector x^* can be stated as a solution of (AL1) if $\|x^* - \alpha^*\|_2 \leq \epsilon$. Comparing (AL1p) with (L1p) in Section 4.2.1, one may observe that both problems appear to be similar. The problems on the threshold ϵ remain the same as described in Section 4.2.1. However, one can state the question whether it is possible to formulate (AL1) in form of (L1). In fact, assume that $DD^\dagger$ is the identity matrix, then substituting $z = D^T y$ and considering $(D^T)^\dagger z = y$ leads to

$$\min_z \|z\|_1 \text{ subject to } AD^\dagger z = Ax^*. \tag{4.2.2}$$

The disadvantage of the optimization problem (4.2.2) is that finding a solution of the linear system $Ay = Ax^*$ is restricted to elements in the range of D since y needs to satisfy $(D^T)^\dagger z = y$. As for basis pursuit, Theorem 2.1.3 states sufficient and necessary conditions for a given $x^* \in \mathbb{R}^n$ being the unique solution of (AL1). The verification whether a given $x^* \in \mathbb{R}^n$ with $I \equiv \{i : d_i^T x^* \neq 0\}$ and $k \equiv |I|$ solves (AL1) uniquely can be realized via the following optimization problem: for $\xi \in \mathbb{R}^m, \tau \in \mathbb{R}^{p-k}$, and $\nu \in \mathbb{R}$ consider

$$\begin{aligned} \min_{\xi,\tau,\nu} \nu \text{ subject to } \quad & A^T\xi + D_{I^c}\tau = -D_I \text{sign}(D_I^T x^*), \\ & -\nu\mathbf{1}_{p-k} \leq \tau \leq \nu\mathbf{1}_{p-k}. \end{aligned} \tag{AL1d}$$

For (ξ^*, τ^*, ν^*) as a solution of (AL1d) with an input parameter $x^* \in \mathbb{R}^n$, the vector x^* solves (AL1) uniquely if $\nu^* < 1$ and $\ker(A) \cap \ker(D_{I^c}^T) = \{0\}$. Similar experiments to the Donoho and Tanner's phase transition experiment [53] were done for analysis ℓ_1-minimization in [97, Section 6.1] with D as a random tight frame [56].

In the following, an experiment is described in which the methods in (AL1p), (AL1d) as well as (4.2.2) via (L1d) are compared with respect to time duration. The experiment is similar to the experiment in Section 4.2.1; but the difference, as well as to the experiment in [97], is that the size of the matrix $D \in \mathbb{R}^{n\times p}$ and the D-sparsity vary while the redundancy of $A \in \mathbb{R}^{m\times n}$ is fixed to $m/n = 1/2$. For fixed $p \equiv 1600$ and varying $n = \delta p$ and $k = \rho p$ with $\delta = i/40, i \in \{1, ..., 37\}$ and $\rho = j/40, j \in \{1, ..., 40\}$, the experiment was done in Matlab as follows. Compute a random tight frame $D \in \mathbb{R}^{n\times p}$ as proposed in [120], choose a Gaussian matrix $A \in \mathbb{R}^{n/2\times n}$ via `randn` and choose an index set $I, |I| = k$, randomly by choosing I uniformly over the subset $\{1, ..., 1600\}$. Note that $\delta < 1$, this means that D^T is an overdetermined matrix. Lemma 4.0.2 shows that $k > p-n$ or $k = 0$; hence, if $k \leq p-n$, the procedure is aborted for the instance (δ, ρ). Next, choose $y \in \mathbb{R}^n$ drawn randomly from the standard normal distribution and set $x^* \in \mathbb{R}^n$ via the projection onto the null space of $D_{I^c}^T$ in (4.1.2). Make sure that x^* has D-sparsity k. First solve (AL1p). Then assure that $(AD^\dagger)_I$ is injective and solve (4.2.2) via (L1d). Finally, verify that $\ker(A) \cap \ker(D_{I^c}^T) = \{0\}$.

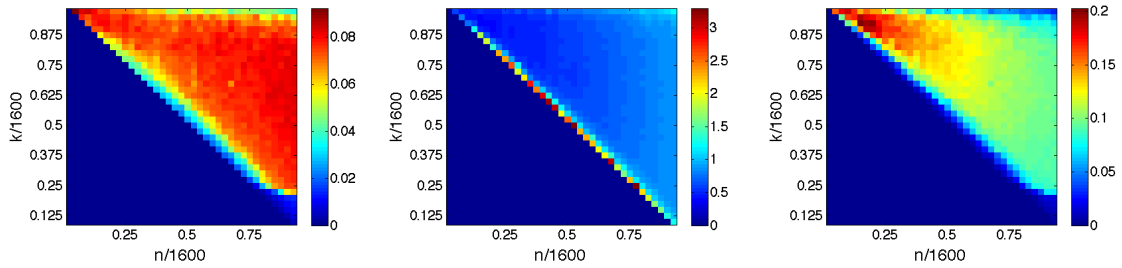

Figure 4.7: Comparison of time duration of all three presented methods for solving analysis ℓ_1-minimization with Gaussian matrices $A \in \mathbb{R}^{n/2 \times n}$ and random tight frames $D \in \mathbb{R}^{1600 \times n}$ with varying n and vectors $x^* \in \mathbb{R}^n$ with varying D-sparsity k. Presented as quotients of results on (AL1d) divided by (AL1p) (left), on (AL1d) divided by (4.2.2) via (L1p) (center), and on (4.2.2) via (L1d) divided by (AL1p) (right).

This can be done by checking whether the matrix $X^T \equiv [A^T, D_{I^c}]^T$ has full rank, for example with a QR decomposition $X = QR$ and checking whether no entry on the diagonal of R is 0. If $\ker(A) \cap \ker(D_{I^c}^T) = \{0\}$, then solve (AL1d). All three optimization problems are solved with the Mosek routine `mosekopt` in Matlab. For each pair (δ, ρ), this procedure is done $M \equiv 50$ times. The focus on these experiments lays on the time duration of solving each optimization problem. Therefore, only the time is measured which Mosek requires to solve the considered optimization problem. Results on recoverability can be found in [97, Section 6] for similar test instances.

The timing experiment was run in Matlab 7.13 (R2011b) using Mosek 6.0 on Dell Precision T3610 with Intel Xeon CPU E5-1620 (10 MB cache, up to 3.70GHz) and 16 GB RAM.

In Figure 4.7, the results on the comparison are presented in the following form: on the left-hand side, the time duration of (AL1d) divided by the time duration of (AL1p) is given in dependency of δ and ρ; in the center, the time duration of (AL1d) divided by the time duration of solving (4.2.2) is given in dependency of δ and ρ; on the right-hand side, the time duration of solving (4.2.2) divided by the time duration of (AL1p) is given in dependency of δ and ρ. In the comparison on the left-hand side and on the right-hand side, one may observe that using the optimality conditions from Section 2.1 is always faster than solving analysis ℓ_1-minimization via (AL1p). On average, solving (AL1d) is more than eighteen times faster than using (AL1p) and solving (4.2.2) via (L1d) is more than thirteen times faster than using (AL1p). Comparing (AL1d) and (4.2.2), one may observe that for a fixed n at a D-sparsity close to $(1600 - n)$, solving (4.2.2) is faster than (AL1d), for a D-sparsity not close to $(1600 - n)$, using (AL1d) is faster. On average, the method concerning (AL1d) is faster than the method concerning (4.2.2). In total, the experiments show that using (AL1d) to verify whether a given vector is the unique solution of analysis ℓ_1-minimization is the fastest considered method, for A being Gaussian and D as a random tight frame.

4.2.3 Analysis $\ell_{1,2}$-Minimization / Isotropic Total Variation Minimization

In the following, for given matrices $A \in \mathbb{R}^{m \times n}, m < n, D \in \mathbb{R}^{n \times pn}, p \in \mathbb{N}$, and a given vector $x^* \in \mathbb{R}^n$, a method is presented which can be used to guarantee that a given x^*

solves

$$\min_y \sum_{i=1}^{n} \left(\sum_{j=0}^{p-1} (d_{i+jn}^T y)^2 \right)^{1/2} \quad \text{subject to } Ay = Ax^* \tag{AL12}$$

uniquely. The problem (AL12) is called *analysis $\ell_{1,2}$-minimization*, and if D^T is the two-dimensional derivate forward operator, the problem (AL12) is also called *isotropic total variation minimization*. Similarly to the previous two sections, this method is compared to a straightforward approach, which is described first.

The problem (AL12) can be formulated as a conic quadratic optimization problem and can also be solved via the Mosek routine `mosekopt` in Matlab. For $\alpha, \beta \in \mathbb{R}^n, \gamma \in \mathbb{R}^{pn}$, the problem (AL12) can be formulated as

$$\begin{aligned} \min_{\alpha,\beta,\gamma} \mathbf{1}_n^T \beta \quad & \text{subject to} \\ & A\alpha = Ax^*, \\ & -\gamma_i \leq d_i^T \alpha \leq \gamma_i \text{ for all } i = 1, ..., pn, \\ & \beta_i \geq \sqrt{\gamma_i^2 + ... + \gamma_{i+(p-1)n}^2} \text{ for } i = 1, ..., n. \end{aligned} \tag{AL12p}$$

If the triple $(\alpha^*, \beta^*, \gamma^*)$ solves (AL12p), then the smallest value

$$\sum_{i=1}^{n} \sqrt{\sum_{j=0}^{p-1} (\gamma_{i+jn}^*)^2}$$

such that $A\alpha^* = Ax^*$, and $|d_j^T \alpha^*| \leq \gamma_j^*$ for $j = 1, .., pn$ is found. For a previously determined $\epsilon > 0$, the vector x^* can be stated as a solution of (AL12) if $\|x^* - \alpha^*\|_2 / \|x^*\|_2 \leq \epsilon$. As in Section 4.2.1 and 4.2.2, this method has the problem that one can not guarantee that x^* is the unique solution of (AL12).

In contrast to basis pursuit and analysis ℓ_1-minimization, the problem (AL12) is not a linear program and no necessary conditions on unique solutions are known so far. However, one can apply Proposition 2.1.1 to get sufficient conditions on a given $x^* \in \mathbb{R}^n$ such that x^* is the unique solution of (AL12) for $A \in \mathbb{R}^{m \times n}, m < n$, and $D \in \mathbb{R}^{n \times pn}, p \in \mathbb{N}$. But note that Proposition 2.1.1 does not guaranteed that a vector $x^* \in \mathbb{R}^n$ is not the unique solution of (AL12) if the conditions in Proposition 2.1.1 are not satisfied. In the notation of Proposition 2.1.1, the problem (AL12) can be adapted to Proposition 2.1.1 as follows. Consider a finite sequence of bounded, linear operators $\{\Phi_i\}_{i=1}^n$ such that

$$\begin{aligned} \Phi : \mathbb{R}^n \to \prod_{i=1}^{n} \mathbb{R}^p, \; x \mapsto (\Phi_1 x, ..., \Phi_n x), \\ \text{and } \Phi_i x = (d_i^T x, ..., d_{i+(p-1)n}^T x), i = 1, ..., n, \end{aligned}$$

where $\Phi_i x$ is p-dimensional for all $i = 1, ..., n$. For $\bar{V} \equiv (\bar{V}_1, ..., \bar{V}_p) \in \mathbb{R}^{n \times p}$ with $\bar{V}_i \in \mathbb{R}^n$ for $i = 1, ..., p$, the adjoint of Φ at $\bar{V}$ is given by

$$\Phi^* \bar{V} = -\sum_{j=0}^{p-1} D_{I_j} \bar{V}_{j+1} \text{ with } I_j \equiv \{1 + jn, ..., n + jn\}.$$

Note that in case of isotropic total variation minimization, one may observe that the discretization of the total variation in the continuous setting leads to the same results, see

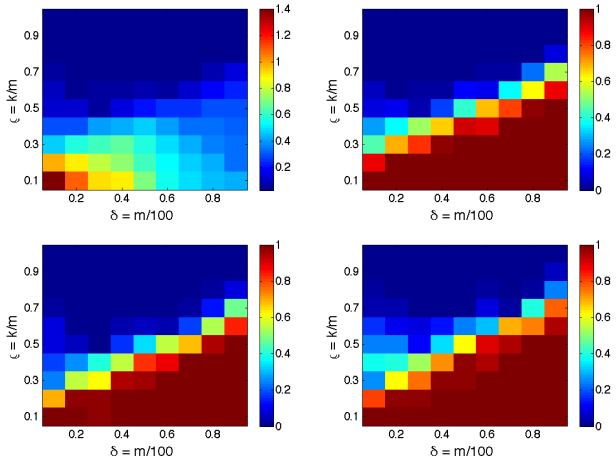

Figure 4.8: Time comparison (in seconds) of the optimization problems (AL12p) and (AL12d) with Gaussian matrices $A \in \mathbb{R}^{m\times 100}$ for varying m and $x^* \in \mathbb{R}^{100}$ with varying D-ℓ_2-sparsity k. Top left: Time duration using (AL12d) and the injectivity check divided by time duration using (AL12p). Top right: Number of identified unique solutions x^* with D-ℓ_2-sparsity k (via (AL12d) and the injectivity check) divided by the number of considered samples ($M \equiv 50$). Bottom left: Number of identified unique solutions x^* with D-ℓ_2-sparsity k (via (AL12p) and identification threshold 10^{-3}) divided by the number of considered samples ($M \equiv 50$). Bottom right: Number of identified unique solutions x^* with D-ℓ_2-sparsity k (via (AL12p) and identification threshold 10^{-1}) divided by the number of considered samples ($M \equiv 50$).

for instance [37]. To apply the conditions in Proposition 2.1.1 to a given $x^* \in \mathbb{R}^n$ and a given $A \in \mathbb{R}^{m\times n}, m < n$, consider the index set

$$I \equiv \left\{ i \in \{1, ..., n\} : \sqrt{(d_i^T x^*)^2 + ... + (d_{i+(p-1)n}^T x^*)^2} \neq 0 \right\} \tag{4.2.3}$$

and $V \in \mathbb{R}^{n\times p}$ with

$$V_{i,j} = \begin{cases} \frac{d_{i+(j-1)n}^T x^*}{\sqrt{(d_i^T x^*)^2 + ... + (d_{i+(p-1)n}^T x^*)^2}} & i \in I, \\ 0 & i \in I^c \end{cases}, \text{ for } j = 1, ..., p. \tag{4.2.4}$$

Now, the sufficient conditions in Proposition 2.1.1 can be formulated as a conic quadratic optimization problem. For $j = 1, .., p$, let $D^{(j)} \in \mathbb{R}^{n\times n}$ denote the matrix with columns $d_i^{(j)} \equiv d_{i+(j-1)n}, i = 1, ..., n$, and $k \equiv |I|$. For $\alpha \in \mathbb{R}^n, \beta \in \mathbb{R}^{n-k}, \tau \in \mathbb{R}$, and $\{\gamma_j\}_{j=1}^p \subset \mathbb{R}^{n-k}$ consider with $\bar{V}_j \in \mathbb{R}^I, \bar{V}_{i,j} = V_{i,j}, i \in I, j = 1, ..., p$, from (4.2.4), the optimization problem

$$\begin{aligned} \min_{\alpha,\beta,\gamma,\eta,\tau} \tau \quad & \text{subject to} \\ & A^T\alpha - \textstyle\sum_{j=1}^p D_{I^c}^{(j)} \gamma_j = \sum_{j=1}^p D_I^{(j)} \bar{V}_j, \\ & -\tau \leq \beta_i \leq \tau \text{ for all } i = 1, ..., n-k, \\ & \beta_i \geq \sqrt{\gamma_{1,i}^2 + ... + \gamma_{p,i}^2} \text{ for all } i = 1, ..., n-k. \end{aligned} \tag{AL12d}$$

For the smallest τ^* in (AL12d) the conditions in Proposition 2.1.1 are satisfied if $\tau^* < 1$ and A restricted to $\{y \in \mathbb{R}^n : d_j^T y = 0, ..., d_{j+(p-1)n}^T y = 0, j \in I^c\}$ is injective.

In the following, an experiment concerning isotropic total variation minimization is described. In this experiment, both optimization problems (AL12p) and (AL12d) are

compared with regard to the number of identified vectors x^* to solve (AL12) uniquely and with regard to time duration. The experiment is similar to the described experiment in Section 4.2.1. The two-dimensional derivate forward operator D^T is equipped with the Neumann boundary condition. For each $m \in \{10, 20, ..., 90\}$ and $k \in \{jm/10 : j = 1, ..., 10\}$, consider a Gaussian matrix $A \in \mathbb{R}^{m\times 100}$ and a vector $x^* \in \mathbb{R}^{100}$ with D-ℓ_2-sparsity k. The element $x^* \in \mathbb{R}^{100}$ with the desired D-ℓ_2-sparsity is constructed via Algorithm 3 and an initial vector whose entries are drawn from the standard normal distribution. Then the optimization problem (AL12p) is solved by the Mosek routine `mosekopt` in Matlab. If the computed, optimal solution α^* satisfies $\|\alpha^* - x^*\|_2/\|x^*\|_2 \leq 10^{-3}$, then it is said that x^* solves (AL12) via (AL12p). Next, consider the index set I as in (4.2.3) and solve (AL12d) with $V \in \mathbb{R}^{n\times 2}$ from (4.2.4). If the optimal computed solution τ^* satisfies $\tau^* \leq 1 - 10^{-12}$ and A restricted to $\{y \in \mathbb{R}^n : d_j^T y = 0, d_{j+n}^T y = 0, j \in I^c\}$ is injective, then x^* is said to solve (AL12) uniquely via (AL12d). For each pair (m, k), this procedure is repeated $M \equiv 50$ times.

The timing experiment was run in Matlab 7.13 (R2011b) using Mosek 6.0 on Dell Precision T3610 with Intel Xeon CPU E5-1620 (10 MB cache, up to 3.70GHz) and 16 GB RAM.

In Figure 4.8, the results on the previously described experiment are displayed. The graphic at the top on the left-hand side gives the comparison of time duration as the quotient of time duration using (AL12d) and the injectivity check divided by the time duration using (AL12p). Note that, with the exception that the values in the lower left corner, all quotients are less than 1, which means that solving (AL12d) is faster than solving (AL12p). On average, using (AL12d) is more than four times faster than using (AL12p). Further, in Figure 4.8, one can see how many instances with respect to m and k were identified as unique solutions via (AL12d) (top right) and (AL12p) (bottom). The graphics at the bottom of Figure 4.8 show the number of identified unique solutions with respect to the total number of samples ($M \equiv 50$) with the threshold 10^{-3} (left), as described above, and if the threshold 10^{-1}, instead of 10^{-3}, is considered (right). First, one may observe a phase transition between the regime in which all $x^* \in \mathbb{R}^{100}$ solve (AL12) uniquely and no $x^* \in \mathbb{R}^{100}$ solve (AL12) uniquely. Further, one may observe that both graphics give almost similar results. For $m = 10, 20, 30$ and small k, it is noticeable that both graphics differ considerably from each other: considering the problem (AL12d), the number of identified unique solutions is monotonically nonincreasing, for the problem (AL12p) such a statement can not be made. The situation changes if the threshold is relaxed to 10^{-1}: at $m = 10, 20, 30$ and small k the number of identified unique solutions does not differ in both optimization problems, but beyond the phase transition curve, one may observe that far more solutions are identified than by using the threshold 10^{-3} or by using the optimization problem (AL12p).

In total, the optimization problem (AL12d) seems to be a good candidate to guarantee that a given vector solves isotropic total variation minimization uniquely: it is faster and more stable than the considered straightforward approach in (AL12p). But please note that as long as the conditions in Proposition 2.1.1 are not proved as necessary conditions, this test can only guarantee that a given vector is the unique solution of isotropic total variation minimization, and not that a vector is not the unique solution.

4.3 Application to Computed Tomography

Both total variation methods, isotropic and anisotropic total variation minimization, are often considered in image processing since images consist mostly of piecewise constant components. That implies that they have a small D-ℓ_2-sparsity and D-sparsity, respectively, with D^T as the two-dimensional derivate forward operator. Connecting compressed sensing to the application *computed tomography* is a growing field in research. In [80], a quantitative study is published in which similar experiments as in the previous sections were done: vectors with a corresponding sparsity are tested for solving basis pursuit, anisotropic total variation minimization, and isotropic total variation minimization uniquely. In contrast, matrices which are used for computed tomography are considered. The results on basis pursuit, anisotropic total variation minimization, and isotropic total variation minimization are presented in the present section and have been achieved in cooperation with Jakob S. Jørgensen and Dirk A. Lorenz. My contribution consisted mainly in establishing and proving the optimality conditions for unique solutions of all three problems, and developing the method for constructing the test instances as they are presented in Section 4.1.2. Further, I built first prototypes for the uniqueness verification tests and alternating projections methods. Before the results are presented, the image model concerning computed tomography is presented.

4.3.1 Imaging Model

Computed tomography is a classical example for an ill-posed inverse problem. In order to obtain an image of the interior of some object, x-rays are sent through the considered object. Due to correlation with matter, some x-rays may be absorbed; the probability of absorption depends on the wavelengths of the x-rays, and atomic number, thickness, and density of the matter. In the present thesis, a simple model is considered in which x-rays of a single wavelength with known intensity I_0 are used. Further, it is assumed that the x-rays follow straight lines through the object. In this model, a single x-ray has the intensity I after passing the object following the line L. From the Lambert-Beer law, see for instance [30], the resulting problem is to determine a function f such that

$$\int_L f(y)dy = -\ln\left(\frac{I}{I_0}\right). \tag{4.3.1}$$

The matter is represented by the so-called linear attenuation coefficient f, the value $f(y)$ describes how much x-rays are absorbed at a spatial coordinate y. Recovering f through (4.3.1) depends on how many different measurements I are given. Further, it should be noted that determining f is badly conditioned: if the right-hand side of (4.3.1) is disturbed by noise, its solution f^η may not be in a neighborhood of the true solution f. But since in this thesis the ideal case, that no noise is added on the measured data, is considered, this fact is neglected. For a more detailed mathematical introduction into computed tomography, the reader may consult [98]. Please note that the assumption behind the Lambert-Beer law does include only a single wavelength of the x-rays and does not include scattered radiation.

Receiving information about the insight of an object without cutting it up is a big advantage of computed tomography. It is of interest for material science, geoscience, and in medical diagnosis. Computed tomography is a huge improvement in non-invasive medical diagnosis, but the risk of radiation-induced cancer caused by x-rays should not be

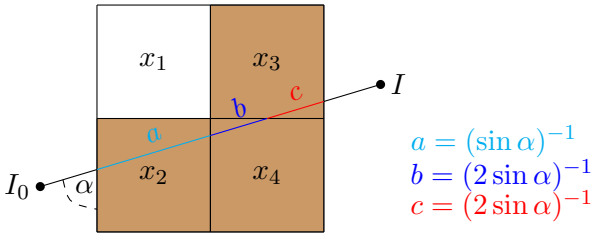

Figure 4.9: Line segment method: a line intersects the image $X \in \mathbb{R}^{2\times 2}$. Here, all four pixel arrays have a size length 1. The symbols a, b, and c describe the length of the segment of the line from I_0 to I intersecting with x_2, x_4, and x_3, respectively. For the given line, the arising linear system is $-\ln(I/I_0) = ax_2 + cx_3 + bx_4$ with an angle α. The pixel arrays which intersect with the line from I_0 to I are colored in brown.

underestimated [48, 113]. Therefore, it is of interest to lower the x-ray intensity a patient is given. But since reducing the intensity may cause that the reconstructed f has bad image quality [28, 30], advanced methods need to be considered.

Classical methods, such as the *filtered back-projection*, are based on inverting the Radon transform [107], which describes how the image is transformed into line integral measurements as in the Lambert-Beer law. These methods have many advantages including low computational time but require a large number of measurements and high x-ray dose, respectively. A different class of methods, known as *algebraic methods*, is based on discretizing the image into, for example, pixels, and modeling the x-rays as a discrete linear operator. In the present section, the x-rays are modeled as rows of an underdetermined matrix A. One needs to determine x^* from the measured data b with $b = Ax^*$, where x^* represents the attenuation coefficient of the considered object. The considered problem is a discrete linear inverse problem. In this sense, algebraic methods are close to the standard compressed sensing setup.

With the function

$$p(x) = \begin{cases} n, & x \in [-\frac{1}{2}, \frac{1}{2}) \\ 0, & \text{else} \end{cases},$$

each image $x \in \mathbb{R}^n$ can be considered as a continuous function via a piecewise constant interpolation

$$f(y) = \frac{1}{n}\sum_{j=1}^{n} x_j p(y-j).$$

Consider m measurements of the form in (4.3.1). Then for a line L_i and the measurement I_i, $i = 1, ..., m$, it follows that

$$b_i \equiv -\ln\left(\frac{I_i}{I_0}\right) = \int_{L_i} f(y)dy = \frac{1}{n}\sum_{j=1}^{n} x_j \int_{L_i} p(y-j)dy.$$

Define

$$a_{i,j} \equiv \frac{1}{n}\int_{L_i} p(y-j)dy, \tag{4.3.2}$$

which describes the length of the line L_i passing the j-th component of a pixel array, cf. Figure 4.9. The element $a_{i,j}$ is the (i,j)-th entry of a matrix $A \in \mathbb{R}^{m\times n}$, with n as the number of pixels and m as the total number of measurements. A solution of the linear

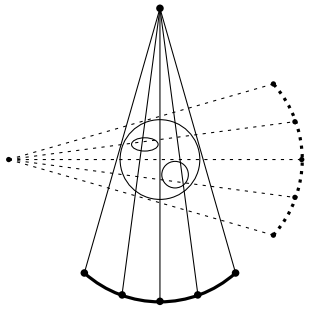

Figure 4.10: Illustration of fan-beam computed tomography for two-dimensional objects. Two projection views are illustrated.

system of equations $Ay = b$ may describe the attenuation coefficient of the considered matter. More precisely, if there exists exactly one solution x^*, then x^* describes the attenuation coefficient of the considered matter. This discretization method is known as the *line-intersection method*, see for instance [112].

Since $a_{i,j}$ in (4.3.2) describes the length of certain line segments, designing the matrix $A = (a_{i,j})_{i,j}$ is equivalent to arranging the lines passing the considered object. A source circles around the object and from certain positions (*projection views*) it sends a determined number of lines L_i through the object in form of a fan-beam. Figure 4.10 illustrates this procedure; it simulates the so-called *fan-beam computed tomography* in which the radiation source circles around the considered object and measures the intensity on the other side of the object. The projection views are equiangular acquired from 360 degrees around the object. The intersection of the fan beams from all projection views has the shape of a disk; therefore, instead of considering an $(N \times N)$-image, a pixel array of the shape of a disk is considered. After transferring this pixel array to a vector, it follows that $n \approx \pi N^2/4$, in the following such a vector is called *disk-shaped image*. Here, the detector has the shape of a circular arc with the center at the radiation source; that is why all lines L_i have the same distance to the detector. In the following experiments, the distance between the radiation source and the detector is set to $2N$. The detector has $2N$ cells for measuring the intensity I_i of a line L_i after passing the object. The fan angle is set to 28.07 degrees. The number of projection views is denoted by N_v. Finally, the number of measurements is $m \equiv 2NN_v$. This means that, for considering a matrix $A \in \mathbb{R}^{m \times n}$ with entries as in (4.3.2), less than $\pi N/8$ projection views are necessary to obtain $m < n$. In the following, consider $N_v^{\text{suf}} \equiv \lceil \pi N/8 \rceil$ which gives the number of samples such that the considered linear system of equations $Ay = b$ has only one solution.

In the following sections, experiments are presented which are designed to study the applicability of computed tomography in a compressed sensing setup. The main goal is to examine whether one may observe a relationship between the number of projection views N_v, the existence of a unique solution of basis pursuit, anisotropic total variation minimization, or isotropic total variation minimization, respectively, and the corresponding sparsity. The rate of considered vectors are recovered via (L1), (AL1), and (AL12), respectively, is called *reconstruction rate*. All experiments were done by Jakob S. Jørgensen and published in the joint work [80]. The following graphics in the present chapter are taken from [80]. The development of the methods used to perform the following experi-

ments were mainly my contribution and are described in the previous sections. The timing experiments were run in Matlab 7.13 (R2011b) using Mosek 6.0 on a Lenovo ThinkPad T430s with Intel Core i5-3320M processor (3 MB cache, up to 3.30 GHz) and 8 GB RAM, restricted to a single core.

4.3.2 Results on Basis Pursuit

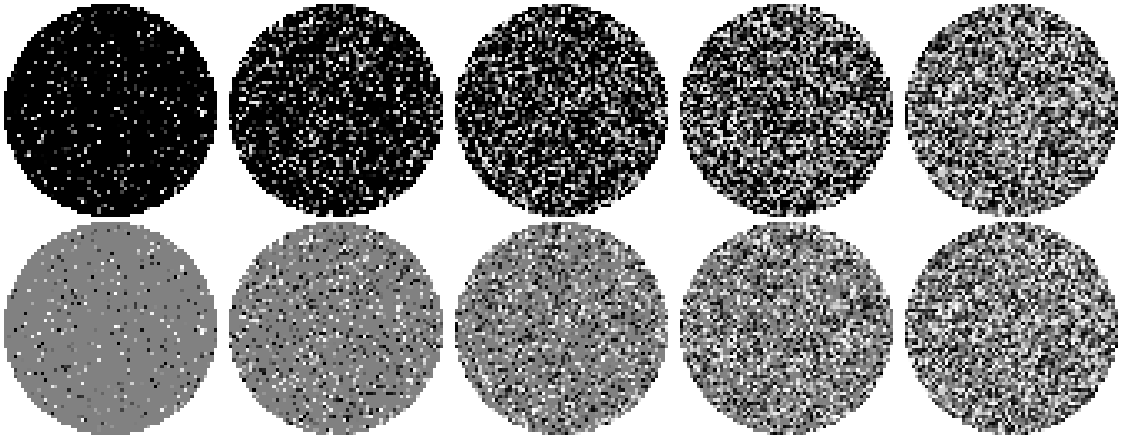

Figure 4.11: Image classes with with certain sparsities: Spikes (top) and signed-spikes (bottom) with relative sparsity $\kappa = 0.1, 0.3, 0.5, 0.7, 0.9$ from left to right. Images generated by Jakob S. Jørgensen.

The following section coincides with the corresponding section in [80]. For basis pursuit, test images are constructed as described in Section 4.1.2. In detail, images of the size 64×64 are considered, this means that $N \equiv 64$ and $n = 3228$, and for varying relative sparsity $\kappa = 0.025, 0.05, 0.1, 0.2, ..., 0.8, 0.9$, where the relative sparsity κ is defined as the sparsity k of the considered image divided by the total number of pixels of the image, hence $\kappa \equiv k/n$. More precisely, in the experiments, the sparsities $k = \lceil 3228\kappa \rceil$ are considered. Following the approach in [21], the test images are built with k non-zero entries on random position with values drawn randomly from a uniform distribution on $(0, 1)$, this class is called *spikes*, or drawn randomly from a uniform distribution on $(-1, +1)$, which is called *signed-spikes*. Both image classes are also considered in [81]. In Figure 4.11, examples for images of the class spikes (top) and of the class signed-spikes (bottom) are given. For each relative sparsity κ and each introduced image class, one hundred disk-shaped images $x^* \in \mathbb{R}^{3228}$ with sparsity $k = \lceil 3228\kappa \rceil$ are generated and for each number of projection views $N_v = 1, ..., 26$, matrices $A \in \mathbb{R}^{128N_v \times 3228}$ with entries as in (4.3.2) are generated with the function `fanbeamtomo` from the Matlab package AIR Tools [77]. For each disk-shaped image x^* and each matrix A, the optimization problem (L1) is solved via (L1p); if the computed, optimal solution $\bar{x}$ satisfies $\|\bar{x} - x^*\|_2 / \|x^*\|_2 \leq 10^{-4}$, then it is declared that x^* is recovered via basis pursuit. In Figure 4.12 (top), the reconstruction rate in dependency of the relative sampling N_v/N_v^{suf} and the relative sparsity κ is given. Further for the same matrix A and the same disk-shaped image x^*, the conditions in Theorem 2.1.3 are verified via (L1d). If the computed, optimal solution α^* of (L1d) satisfies $\|A_{I^c}^T \alpha^*\|_\infty \leq 1 - 10^{-12}$, it is declared that x^* is recovered via basis pursuit. In Figure 4.12 (bottom), the reconstruction rate in dependency of the relative sampling N_v/N_v^{suf} and the relative sparsity κ is given for both image classes.

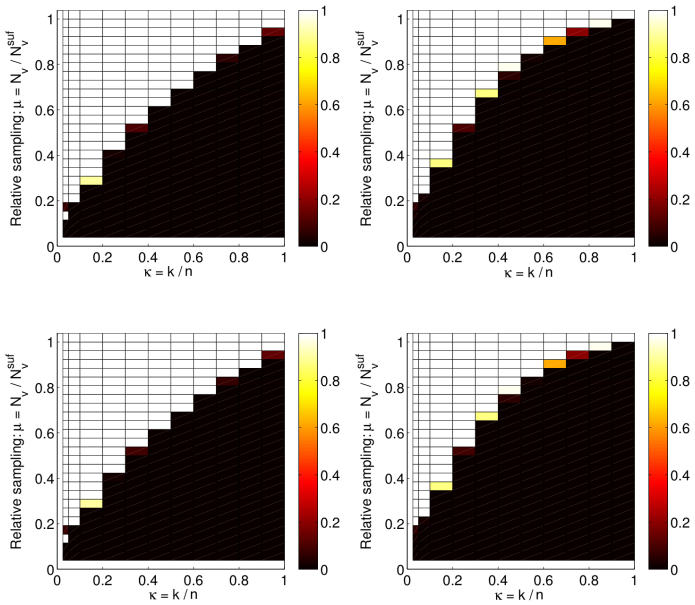

Figure 4.12: Results on the reconstruction rate via basis pursuit in dependency of relative sparsity and relative sampling. In the top row, the recovery is considered for (L1p), the recovery via (L1d) is considered in the bottom row. On the left-hand side, spike images are considered; on the right-hand side, signed spikes images are considered. The reconstruction rate extents from 0 (no instance is declared as a solution) to 1 (all instances are declared as solutions).

In Figure 4.11, the results on the described experiments are given. One may observe that solving (L1) via (L1p) and checking the conditions in Theorem 2.1.3 via (L1d) coincides. Note that the experiments in Section 4.2.1 give the same result, but in these experiments Gaussian matrices are considered, which imply that, with high probability, a solution of basis pursuit is the unique solution of basis pursuit. In contrast, no such theoretical statement for matrices which model the measurements in computed tomography is known. However, the empirical results on the present experiment coincide. Further, one may observe a sharp phase transition in both image classes for most instances. This means that either all images with a common relative sparsity can be recovered via (L1) with a matrix A which possesses a certain relative sampling, or none of the images with a relative sparsity can be recovered via (L1) with a matrix A which is modeled with a certain relative sampling. Hence, a clear relationship between the number of projection views N_v, the existence of a unique solution of basis pursuit and sparsity can also be observed for matrices modeled as in Section 4.3.1.

As in Section 4.2.1, experiments for comparing the computational time of (L1p) and (L1d) were done for $A \in \mathbb{R}^{2NN_v \times n}$ with varying positive integers N, N_v and with entries as in (4.3.2). The matrix A is generated with the function `fanbeamtomo` from the Matlab package AIR Tools [77]. For $N = 32, 64, 128$, disk-shaped images of the class signed-spikes are generated with relative sparsities $\kappa = 0.1, 0.3, 0.5, 0.7, 0.9$. For each size N and each

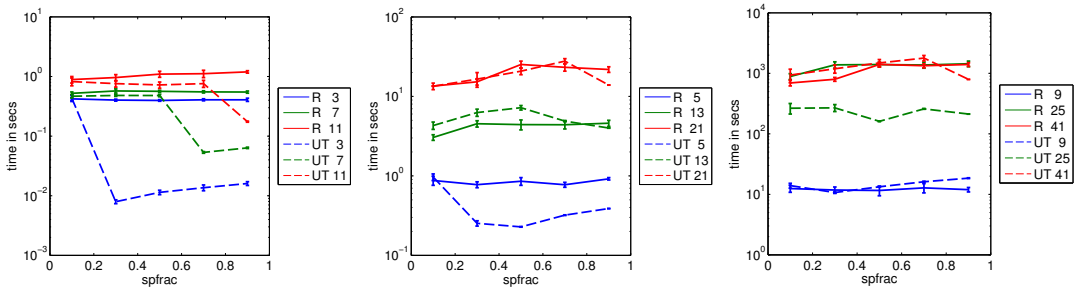

Figure 4.13: Computational time comparison for $N = 32$ (left), $N = 64$ (center), and $N = 128$ (right). The lines show the results on different projection views via solving (L1p) (R) and (L1d) (UT).

κ, ten instances are generated. Further, the matrix $A \in \mathbb{R}^{2NN_v \times n}$ is generated with

$$N_v = \begin{cases} 3, 7, 11 & \text{if } N = 32, \\ 5, 13, 21 & \text{if } N = 64, \\ 9, 25, 41 & \text{if } N = 128. \end{cases}$$

The experiment is run similarly as the previous experiment in the present section, the results are given in Figure 4.13. In contrast to the experiment in Section 4.2.1, no clear tendency can be made which of both optimization problems does deliver a faster verification for unique solutions. One may observe that for $N = 32$, the uniqueness test (L1d) is faster than solving (L1) with (L1p), but for $N = 64$, and $N = 128$ no such statement can be made since in some cases solving (L1p) is faster than using the uniqueness check (L1d). Comparing the present results with the results in Section 4.2.1, one may suggest that Gaussian matrices provide certain properties which bring an advantage to the uniqueness verification in (L1d) over (L1p). Alternatively, the considered CT-matrices may provide certain properties which disadvantage the uniqueness verification in (L1d) over (L1p).

4.3.3 Results on Anisotropic Total Variation Minimization

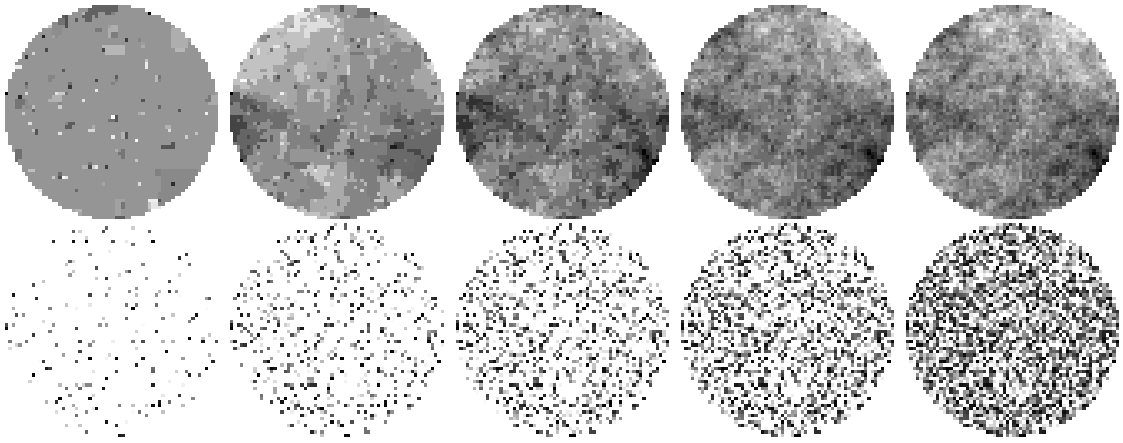

Figure 4.14: Image classes with certain D-sparsities: Generated via alternating projections (top) and of the uniform truncated image class (bottom) with relative D-sparsity $\kappa = 0.1, 0.3, 0.5, 0.7, 0.9$ from left to right, where D^T is the two-dimensional deriviate forward operator. Images generated by Jakob S. Jørgensen.

The following section coincides with the corresponding section in [80]. The present experiment is similar to the experiment in Section 4.3.2. For anisotropic total variation minimization, test images are constructed, as described in Section 4.1.2, via alternating projections. In [80] and also in the following, the matrix D^T models the two-dimensional deriviate forward operator with Neumann boundary conditions. In this setting, the *relative D-sparsity* κ is defined as the D-sparsity k of the disk-shaped image divided by the total number of pixels of the image, hence $\kappa \equiv k/n$. Further, images of the size 64×64 are considered, therefore $N \equiv 64$ and $n \equiv 3228$, and for varying relative D-sparsity $\kappa = 0.025, 0.05, 0.1, 0.2, ..., 1.9$. More precisely, in the present experiments, the D-sparsities $k = \lceil 3228\kappa \rceil$ are considered. Note that, in contrast to the relative sparsity in Section 4.3.2, the relative D-sparsity can be larger than 1 and has the upper bound 2. In Figure 4.14 (top) images with different D-sparsities are generated via alternating projections. For each relative D-sparsity κ, one hundred disk-shaped images $x^* \in \mathbb{R}^{3228}$ with corresponding D-sparsity k are generated via Algorithm 2 with an initial vector whose entries are drawn from the standard normal distribution. Further, for each number of projection views $N_v = 1, ..., 26$, matrices $A \in \mathbb{R}^{128N_v \times 3228}$ with entries as in (4.3.2) are generated via the function `fanbeamtomo` from the Matlab package AIR Tools [77]. For each disk-shaped image x^* and each matrix A, the optimization problem (AL1) is solved via (AL1p); if the computed, optimal solution $\bar{x}$ satisfies $\|\bar{x} - x^*\|_2 / \|x^*\|_2 \leq 10^{-4}$, then it is declared that x^* is recovered via anisotropic total variation minimization. In Figure 4.15 (left), the reconstruction rate in dependency of the relative sampling N_v/N_v^{suf} and the relative D-sparsity κ is given. Further, for the same matrix A and the same x^*, the conditions in Theorem 2.1.3 are verified via (L1d). If the computed, optimal solution ν^* of (AL1d) satisfies $\nu^* \leq 1 - 10^{-12}$, it is declared that x^* is recovered via anisotropic total variation minimization. In Figure 4.15 (right), the reconstruction rate in dependency of the relative sampling N_v/N_v^{suf} and the relative D-sparsity κ is given.

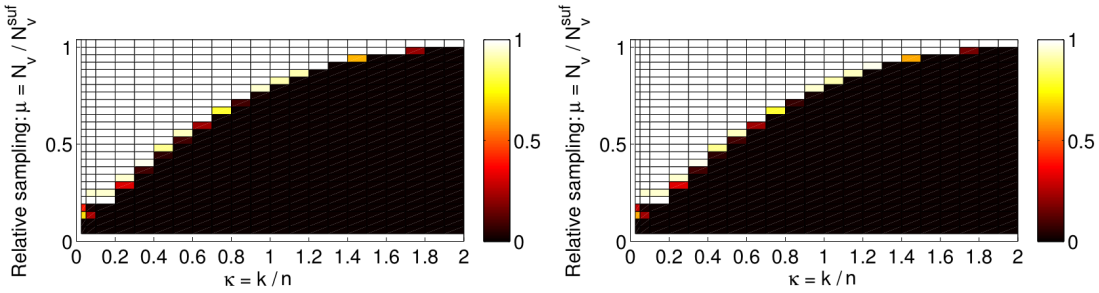

Figure 4.15: Results on the reconstruction rate via anisotropic total variation minimization in dependency of relative D-sparsity and relative sampling for images generated via alternating projections. On the left-hand side, recovery is considered via (AL1p), on the right-hand side the recovery via (AL1d) is considered. The reconstruction rate extents from 0 (no instance is declared as a solution) to 1 (all instances are declared as solutions).

In Figure 4.15 the results on the described experiments are given. One may observe that the number of identified solutions of (AL1) via (AL1p) coincides with the number of identified unique solutions by checking the conditions in Theorem 2.1.3 via (AL1d). Further, a sharp phase transition may be observed in most instances. This means that either all images with a common relative D-sparsity can be recovered via (AL1) with a matrix A which possesses a certain relative sampling, or none of the images with a relative D-sparsity can be recovered via (AL1) with a matrix A which is modeled with a certain

relative sampling. Hence, a clear relationship between the number of projection views N_v, the existence of a unique solution of anisotropic total variation minimization and D-sparsity can also be observed for matrices modeled as in Section 4.3.1.

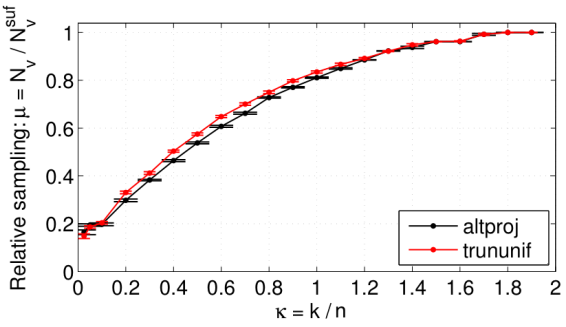

Figure 4.16: Comparison of the phase transition with images generated via alternating projections (black) and with images of the truncated uniform image class (red).

In [80], two other image classes are considered. Similarly to the *spikes* image class in Section 4.3.2, images with non-negative entries are also considered. Such an image is generated via alternating projections, as previously described in the present section, and its values are shifted by the smallest positive constant such that the emerging image is non-negative. The experiment as described in the present section remains the same. The results coincide with the results in Figure 4.15 which is not surprising since in anisotropic total variation minimization the signs of the entries of an image have no direct influence on recovery, but the differences of two neighboring pixels do have, which is not changed by shifting them with a constant. The result for a third considered image class is more surprising. The so-called *truncated uniform* image class is generated heuristically by partitioning the interval $[0, 1]$ into F intervals where the intervals $I_1, ..., I_{F-1}$ have predetermined length in dependency of D^T and the desired relative D-sparsity. Let $\{f_k\}_{i=1}^F$ denote the midpoints of each corresponding interval and assign each entry of the image to the value f_k with the probability of the length of the corresponding interval F_k. In mean, the emerging image has the desired relative D-sparsity. Details can be found in [80]. As one may observe in Figure 4.14, the images appear to have different properties than the images generated via alternating projections: for example, the images generated via alternating projections appear to have more constant-valued plateaus than the images from the truncated uniform class. As described in [80], for images of the truncated uniform class a phase transition may also be observed. Furthermore, as one may observe in Figure 4.16, the phase transition is similar to the phase transition of the images generated via alternating projections. One may conclude that the phase transition for anisotropic total variation minimization mostly depends on D-sparsity and not on the properties of an image class.

As in Section 4.2.2, experiments which compare the computational time of (AL1p) and (AL1d) were done for $A \in \mathbb{R}^{2NN_v \times n}$ with varying positive integers N, N_v and entries as in (4.3.2). Each matrix A is generated with the function `fanbeamtomo` from the Matlab package AIR Tools [77]. For $N = 32, 64, 128$, disk-shaped images are generated, as described above, via Algorithm 2 with relative D-sparsities $\kappa = 0.1, 0.7, 1.3, 1.9$. For each size and each κ, ten instances are generated. Further, the matrix $A \in \mathbb{R}^{2NN_v \times n}$ is

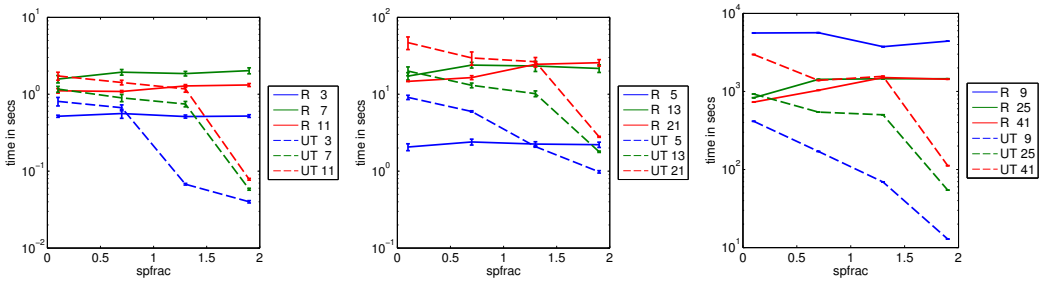

Figure 4.17: Computational time comparison for $N = 32$ (left), $N = 64$ (center), and $N = 128$ (right). The lines show the results on different projection views via solving (AL1p) (R) and (AL1d) (UT).

generated with

$$N_v = \begin{cases} 3, 7, 11 & \text{if } N = 32, \\ 5, 13, 21 & \text{if } N = 64, \\ 9, 25, 41 & \text{if } N = 128. \end{cases}$$

The experiment is run as the previous experiment in the present section, the results are given in Figure 4.17. Similarly to the experiments in Section 4.3.2, no clear tendency can be made which of both optimization problems deliver a faster verification for unique solutions. In contrast, the experiment in Section 4.2.2 shows that the uniqueness test (AL1d) is faster than considering (AL1p) if a Gaussian matrix A and a random tight frame D are considered. One may observe that for $N = 32$, the uniqueness test (AL1d) is faster than solving (AL1) with (AL1p), but for $N = 64$ no such statement can be given since in some cases solving (AL1p) is faster than using the uniqueness check (AL1d). This is similar to the experiments in Section 4.3.2. But one may observe that for large D-sparsities, the uniqueness test (AL1d) is faster than solving (AL1) with (AL1p). As in Section 4.3.2, in comparison to Section 4.2.2, one may suggest that Gaussian matrices and random tight frames provide certain properties which bring an advantage to the uniqueness check (AL1d) over (AL1p).

4.3.4 Results on Isotropic Total Variation Minimization

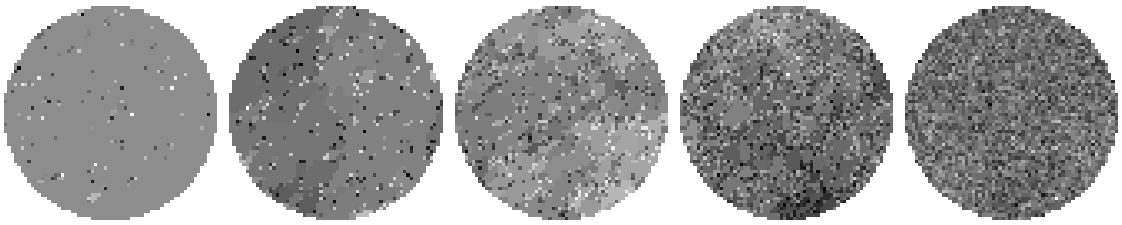

Figure 4.18: Image classes with certain $D-\ell_2$-sparsities: Generated via alternating projections with relative $D-\ell_2$-sparsity $\kappa = 0.1, 0.3, 0.5, 0.7, 0.9$ from left to right, where D^T is the two-dimensional deriviate forward operator. Images generated by Jakob S. Jørgensen.

The following section coincides with the corresponding section in [80]. The present experiment is similar to the experiments in the previous sections. For isotropic total variation minimization, test images are constructed, as described in Section 4.1.2, via

alternating projections. In [80], and also in the following, the matrix D^T models the two-dimensional deriviate forward operator with Neumann boundary conditions, the *relative* $D-\ell_2$*-sparsity* κ is defined as the $D-\ell_2$-sparsity k of the disk-shaped image divided by the total number of pixels of the image. In this setting, square images of the size 64×64 with varying relative $D-\ell_2$-sparsity $\kappa = 0.025, 0.05, 0.1, 0.2, ..., 0.9$ are considered and transfered to disk-shaped images $x^* \in \mathbb{R}^{3228}$. More precisely, in the present experiments, the $D-\ell_2$-sparsities $k = \lceil 3228\kappa \rceil$ are considered. Figure 4.18 shows images with different $D-\ell_2$-sparsities which are generated via Algorithm 3. For each relative $D-\ell_2$-sparsity κ, one hundred disk-shaped images $x^* \in \mathbb{R}^{3228}$ with corresponding $D-\ell_2$-sparsity k are generated via Algorithm 3. For Algorithm 3, an initial vector whose entries are drawn from the standard normal distribution is chosen. Further, for each number of projection views $N_v = 1, ..., 26$, matrices $A \in \mathbb{R}^{128N_v \times 3228}$ with entries as in (4.3.2) are generated via the function `fanbeamtomo` from the Matlab package AIR Tools [77]. For each disk-shaped image x^* and each matrix A, the optimization problem (AL12) is solved via (AL12p); if the computed, optimal solution $\bar{x}$ satisfies $\|\bar{x} - x^*\|_2 / \|x^*\|_2 \leq 10^{-3}$, then it is declared that x^* is recovered via isotropic total variation minimization. In Figure 4.19 (left), the reconstruction rate in dependency of the relative sampling N_v/N_v^{suf} and the relative $D-\ell_2$-sparsity κ is given. Further, for the same matrix A and the same x^*, the conditions in Proposition 2.1.1 are verified via (AL12d). If the computed, optimal solution τ^* of (AL12d) satisfies $\tau^* \leq 1 - 10^{-12}$, it is declared that x^* is recovered via isotropic total variation minimization. In Figure 4.19 (right), the reconstruction rate in dependency of the relative sampling N_v/N_v^{suf} and the relative $D-\ell_2$-sparsity κ is given.

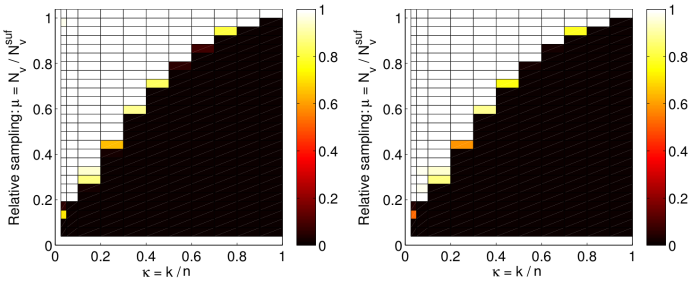

Figure 4.19: Results on the reconstruction rate via isotropic total variation minimization in dependency of relative $D-\ell_2$-sparsity and relative sampling for disk-shaped images generated via alternating projections. On the left-hand side, recovery is considered via (AL12p), on the right-hand side the recovery via (AL12d) is considered. The reconstruction rate extents from 0 (no instance is declared as a solution) to 1 (all instances are declared as solutions).

In Figure 4.19 the results on the described experiments are given. One may observe that the number of identified solutions of (AL12) via (AL12p) almost coincides with the number of identified unique solutions by checking the conditions in Proposition 2.1.1 via (AL12d). Further, a sharp phase transition may be observed, which means that either almost all images with a relative $D-\ell_2$-sparsity can be recovered via (AL12) with a matrix A which possesses a certain relative sampling, or none of the images with a relative $D-\ell_2$-sparsity can be recovered via (AL1) with a matrix A which possesses a certain relative sampling. Hence, a clear relationship between the number of projection views N_v, the existence of a unique solution of isotropic total variation minimization, and $D-\ell_2$-sparsity can also be observed for matrices modeled as in Section 4.3.1. One may conclude that the phase transition for isotropic total variation minimization mostly depends on $D-\ell_2$-sparsity.

Again, it should be emphasized that the conditions in Proposition 2.1.1 are only sufficient conditions for unique solutions of analysis $\ell_{1,2}$-minimization. A proof that the considered sufficient conditions coincide with necessary conditions is still missing. This means that, in contrast to the experiments in the previous sections, if the conditions are not satisfied, the considered vector may still be the unique solution of analysis $\ell_{1,2}$-minimization. In other words, the uniqueness test concerning (AL12d) may exclude some unique solutions, which may explain the difference between the graphic on the left-hand side and on the right-hand side of Figure 4.19.

4.4 Remarks and Future Work

In the present chapter, results from the previous chapters are captured and extended with an algorithmic implementation. However, there are still open questions which may be concerned in the future. Further, it should be emphasized that computed tomography can be connected differently to compressed sensing. For example in [103], results from compressed sensing are considered for *discrete tomography*.

Generalize Algorithm 1 to Analysis ℓ_1-minimization
The generalization of the conditions for unique solutions of basis pursuit, in the form of the conditions for unique solutions of analysis ℓ_1-minimization, suggests that a generalization of Algorithm 1 can be made straight forward such that one can generate a vector x^* with a desired D-sparsity which solves (AL1) uniquely for given $A \in \mathbb{R}^{m\times n}, m < n$ and $D \in \mathbb{R}^{n\times p}$. In contrast, a generalization to isotropic total variation minimization appears to be more difficult since the indices of a vector are closer related to each other. This means that less degrees of freedom are available.

Connecting Algorithm 1 with Uniqueness Test
Algorithm 1 is designed to generate a recoverable support of an arbitrary matrix and arbitrary size. One might state the question, whether it is possible to verify that a given pair $(I, s) \in \mathcal{S}_{n,k}$ is a recoverable support of a given full rank matrix $A \in \mathbb{R}^{m\times n}$ with Algorithm 1. This question can partly be answered positively: if $k = m$, then Algorithm 1 can be easily adapted such that one can verify that $\Phi(I, s) \cap \operatorname{rg}(A^T) \neq \emptyset$. For $I \equiv \{i_1, ..., i_m\}$, in each iteration j of the adapted algorithm, an iterative $v^{(j)}$ *walks along* the range of A^T with $-1 \leq v_l^{(j)} \leq 1$ for $l = i_1, .., i_j$ and $-\infty \leq v_l^{(j)} \leq \infty$ for $l > i_j$. Since A_I is injective and squared, a clear statement to uniqueness can be made. In contrast to Algorithm 1, the iterative $v^{(j)}$ is not necessarily an element of the cube C^n. That is why for $k < m$, it may happen that $v^{(k)} \notin C^n$ but $Pv^{(k)} \in \operatorname{relint}(\Phi(I, s))$ with P as the orthogonal projection P onto C^n. Methods as HOC [87] may also benefit from the development of such an algorithm since such a verification may be faster than solving the corresponding linear system in HOC. For a comprehensive study, a comparison with the previously introduced uniqueness test in Section 4.2.1 and also with the result in Corollary 2.1.13 needs to be done.

Exploring the Partial Order Set of all Recoverable Supports with Algorithm 1
Algorithm 1, as presented in Section 4.1.1, is a deterministic algorithm, this means with the same input, it generates the same recoverable support. Instead of using the initial vector proposed in Proposition 4.1.1, one may use a random 1-sparse vector as an initial vector. This adaption may generate different recoverable supports of the same matrix A with size k, but one needs to verify that the initial 1-sparse vector x^* solves (L1) uniquely.

With such an adaptation, one may generate particulately the partially ordered set of recoverable supports of A by using several values of k.

Extensive Phase Transition Experiments for Analysis ℓ_1-minimization
In addition to the experiment in Section 4.2.2, a comprehensive study for varying $m/n, n/p$, and k/p may give further insights to the phase transition of analysis ℓ_1-minimization.

Computed Tomography Experiments with Larger Images
The results given in Figure 4.17 show that for larger N, the method involving (AL1d) is significantly faster than the straightforward approach with (AL1p). It would be interesting whether for larger N the method (AL1d) is always faster.

Phase Transition Experiments Computed Tomography with Randomly Chosen Projection Views
The experiments in the Sections 4.3.2 and 4.3.3 are performed with equiangular projection views. Since randomness plays a particular role in compressed sensing, it would be interesting what kind of phase transition occurs if the position of the projection views are chosen randomly on the trajectory around the considered object.

Design a CT-Matrix such that Every Image can be Recovered
With a fixed integer n and the conditions in Theorem 2.1.3, one may state the question whether one can construct a CT-matrix $A \in \mathbb{R}^{m\times n}, m < n$, with entries as in (4.3.2), such that all images $x^* \in \mathbb{R}^n$ up to a certain sparsity or D-sparsity solve (L1) respectively (AL1) uniquely. Such a matrix A would be a good candidate for computed tomography in a compressed sensing setup.

CHAPTER 5

Conclusion

In the present thesis, several aspects of exact recovery in compressed sensing are considered. On the basis of the sufficient and necessary conditions of unique solutions for basis pursuit, two questions are addressed: firstly, how to identify unique solutions of basis pursuit, analysis ℓ_1-minimization and analysis $\ell_{1,2}$-minimization, and secondly, how many different unique solutions do exist for basis pursuit which only differ in their support and their sign pattern. Both topics can be used to evaluate the benefit of compressed sensing in several applications. The joint work with Jakob Jørgensen is a perfect example: in our study we considered matrices which model the measurement process in computed tomography and observed a phase transition between the regime in which all images with the corresponding sparsity can be recovered via basis pursuit, anisotropic total variation and isotropic total variation, respectively, and the regime in which no image with corresponding sparsity can be recovered. The observed phase transition depends on number of measurements and the corresponding sparsity of the image. Moreover, we surprisingly observed a universality of the phase transition at anisotropic total variation because different image structures delivered almost the same phase transition. The results in Chapter 4 suggest that the decision whether a given vector is the unique solution of basis pursuit or analysis ℓ_1-minimization can be made relatively easy if the sufficient and necessary conditions are considered. The only parameter which needs to be chosen a priori is the threshold which is used to decide whether the optimal value of (L1d) and (AL1d), respectively, is strictly less than 1. However, experiences show that such a threshold can be chosen as $1 - 10^{-12}$. In contrast, solving both problems straightforwardly leads to a more difficult choice of the threshold which decides whether a solution of (L1p) or (AL1p) is the desired solution x^* of basis pursuit and anisotropic ℓ_1-minimization, respectively.

Furthermore, in the thesis at hand an extensive overview into the geometry of basis pursuit is given which deals with the second question from above: how many different unique solutions exist for basis pursuit. In the present work, the geometrical interpretations established by Donoho [49] and Plumbley [104], respectively, are taken up and complemented by the interpretation of the sufficient and necessary conditions of basis pursuit. This additional interpretation relates solutions of basis pursuit to the faces of the n-cube $C^n \equiv [-1, +1]^n$ in $\mathbb{R}^n$ being cut by a lower-dimensional affine space. All three geometrical interpretations are studied and embedded in the context of convex polytopes. The result is a comprehensive insight into the geometry of basis pursuit as it has not been published yet. Different to the approaches of constructing recovery matrices in Chapter 2, in which the mutual coherence condition and the restricted isometry property are considered, the hope for the geometrical interpretations consists in designing a convex polytope or a corresponding intersection from which a recovery matrix can be derived. By

considering both perspectives, a recovery matrix $A \in \mathbb{R}^{n-1\times n}$ is derived which satisfies $\Xi(n-1,n,k) = \Lambda(A,k)$ for all $k < n$. But a general answer to the maximal number of recoverable supports for matrices of arbitrary size, as well as a concrete specification is not given in this thesis. So far, no design for a recovery matrix is known and, in general, the maximal value which can be achieved by the recoverability curve for an arbitrary sparsity k and for $m \times n$ matrices is still an open question. Nevertheless, this thesis provide the foundations on how to tackle these open problems geometrically. On the one side, a non-trivial upper bound on the number of recoverable supports is given and further working steps on how to improve this bound are sketched. On the other side, the recovery matrix for $m = n-1$ is given and the transition from $m = n-1$ and $m = n-2$ may give further insights in how to deal with high redundancy; especially since the necessary conditions in Theorem 3.7.4 only consider the two cases $m = n-1$ and $m < n-1$. Further, recent constructions on centrally-symmetric polytopes [12, 13] may give a first attempt of a deterministic recovery matrix.

Such results may bring euphoric hopes to questions in basis pursuit. The theory of convex polytopes may not deliver all answers to questions in compressed sensing, but, since a problem like basis pursuit can be interpreted as an application for high-dimensional geometry, their theoretical impact should not be underestimated. Especially by studying the design of recovery matrices and by constructing centrally-symmetric polytopes, as well as by constructing the intersections of the n-cube with an affine space, the research fields of convex polytopes and compressed sensing may benefit from each other. This thesis is a contribution to bind together both fields.

Description of Experiments

In the following, experiments are described which are not described in the main part of the present thesis. More experiments mostly correspond to graphs.

Computed Tomography Experiment in Chapter 1

The experiments in Figure 1.1 are done in Matlab and executed as follows. The matrix $A \in \mathbb{R}^{320\times 812}$ models the x-ray computed tomography measurements, as described in Section 4.3. It models the following. A radiation source circles around the considered object and at five discrete locations the x-rays are sent through the body in form of a fan-beam. On the other side of the body, a detector measures the remaining intensity of the x-rays in 64 detector arrays. The locations on the circle are chosen in equiangular distances. The matrix A is built with the Matlab package AIR Tools [77]. If b is the measured data, the smallest ℓ_2-norm solution is $A^\dagger b$. The smallest ℓ_1-norm solution is solved via (L1p) from Section 4.2.1 in Mosek [5].

Comparison of the Recovery Conditions in Chapter 2

The experiments in Figure 2.1 are done in Matlab and executed as follows. Generate the random matrix $A \in \mathbb{R}^{10\times 15}$ with the RandStream generator and the type 'mt19937ar' and normalize the columns. Then compute the mutual coherence $\mu(A)$ of A. Then for each $k \leq 10$, compute all $2^k\binom{15}{k}$ pairs $(I,s), I \subset \{1,...,15\}, |I| = k, s \in \{-1,+1\}^I$, and for each pair check the recoverability via the considered recovery conditions. The strict source condition can be checked via the method in Section 4.2, Fuchs' condition, the exact recovery condition and the condition involving $\mu(A)$ can be computed straight forward. With Theorem 2.2.3, the null space property of order k is satisfied if all pairs $(I,s), I \subset \{1,...,15\}, |I| = k, s \in \{-1,+1\}^I$ satisfy the strict source condition.

Comparison of Estimated Recoverability Curve when calculated with the Dehn-Sommerville Equation

The experiments in Figure 3.9 are done in Matlab and executed as follows. Generate the random matrix $A \in \mathbb{R}^{10\times 15}$ with the RandStream generator and the type 'mt19937ar' and normalize the columns. Then for each $k \leq 10$, compute all $2^k\binom{15}{k}$ pairs $(I,s), I \subset \{1,...,15\}, |I| = k, s \in \{-1,+1\}^I$, and for each pair check the recoverability via the strict recovery condition and count the number of recoverable supports. The result is the vector $\{\Lambda(A,k)\}_{k=1}^{10}$. Next, run a Monte Carlo experiment: for each $k \leq 10$, choose M pairs $(I,s) \in \mathcal{S}_{15,k}$ and check the recoverability via the strict recovery condition. The Monte Carlo experiments in Figure 3.9 are realized with $M = 100$ and $M = 1000$ samples. Each

time, a recoverable support is identified, increase a counter variable, which is initialized in dependency of k, by $1/M$. The result is a vector $\{R(M,k)\}_{k=1}^{10}$ with $R(M,k) \leq 1$ for each k; to estimate the number of recoverable supports with size k, consider $\{2^k\binom{15}{k}R(M,k)\}_{k=1}^{10}$. To evaluate the procedure in Remark 3.6.6, consider $\{2^k\binom{15}{k}R(M,k)\}_{k=1}^{5}$ and interpolate the remaining numbers via the supposed linear system of equations. The result is a vector $\{C(M,k)\}_{k=1}^{10}$, where $C(M,k) = 2^k\binom{15}{k}R(M,k)$ for $k \leq 5$. To compare the estimated recoverability curves with the exact recoverability curve, the vector $\{\left[2^k\binom{15}{k}\right]^{-1}C(M,k)\}_{k=1}^{10}$ is regarded. In Figure 3.9, the red line represents the actual recoverability curve, in green the curve $k \mapsto \left[2^k\binom{15}{n}\right]^{-1}C(1000,k)$ is illustrated, and in black one can see the same with $\left[2^k\binom{15}{n}\right]^{-1}C(100,k)$. In magenta, the Monte Carlo experiments $k \mapsto R(1000,k)$ are given.

Comparison of Estimated Recoverability Curve via Monte Carlo Experiments and Expected Upper Bound from Proposition 3.6.19

The Monte Carlo experiments in Figure 3.12 are done in Matlab and executed as follows. Generate the random matrix $A^{(1)} \in \mathbb{R}^{50\times 100}$ with the RandStream generator and the type 'mt19937ar'. For each $k \leq 50$, choose 1000 pairs $(I,s) \in \mathcal{S}_{100,k}$ and check the recoverability via the strict recovery condition. Each time, a recoverable support is identified, increase a counter variable, which is initialized in dependency of k, by $1/1000$. The result is a vector $\{R(k)\}_{k=1}^{50}$ with $R(k) \leq 1$. Next, calculate the proposed upper bound $U(k), 1 \leq k \leq 50$, in from Proposition 3.6.19 with $\Lambda(A,50) = 3.73 \cdot 100^{28}$ – this is the value for the expected number of recoverable supports of $A \in \mathbb{R}^{50\times 100}$ with size 50 when A is Gaussian, cf. Proposition 3.6.13 – and consider compare each component $\left[2^k\binom{100}{k}\right]^{-1}U(k)$ (red) with $R(k)$ (blue) Repeat this procedure with $A^{(2)} \in \mathbb{R}^{50\times 51}$ generated with the RandStream generator and the type 'mt19937ar'. The upper bound is colored in black, the Monte Carlo experiment in green.

Comparison of the Values λ_k in Section 3.6.5

The experiments in Figure 3.13 are done in Matlab and executed as follows. Generate the random matrix $A^{(1)} \in \mathbb{R}^{10\times 15}$ with the RandStream generator and the type 'mt19937ar' and normalize the columns. Then for each $k \leq 10$, compute all $2^k\binom{15}{k}$ pairs $(I,s), I \subset \{1,...,15\}, |I| = k, s \in \{-1,+1\}^I$, and for each pair check the recoverability via the strict recovery condition and count the number of recoverable supports. The result is the vector $\{\Lambda(A,k)\}_{k=1}^{10}$. Consider $\{\lambda_k\}_{k=2}^{10}$ with $\lambda_k \equiv k\Lambda(A^{(1)},k)/\Lambda(A^{(1)},k-1)$. In the upper graphics of Figure 3.13, the values λ_k are illustrated in blue. Next, run a Monte Carlo experiment: for each $k \leq 10$, choose 1000 pairs $(I,s) \in \mathcal{S}_{15,k}$ and check the recoverability via the strict recovery condition. Each time, a recoverable support is identified, increase a counter variable, which is initialized in dependency of k, by $1/1000$. The result is a vector $\{R(M,k)\}_{k=1}^{10}$ with $R(M,k) \leq 1$ for each k; to estimate the number of recoverable supports with size k, consider $\{2^k\binom{15}{k}R(M,k)\}_{k=1}^{10}$. Consider $\{\tilde{\lambda}_k\}_{k=2}^{10}$ with $\tilde{\lambda}_k \equiv 2(15-k+1)R(k)/R(k-1)$. If $R(k-1) = 0$, the value λ_k is set to zero. In the upper graphics of Figure 3.13, the values $\tilde{\lambda}_k$ are illustrated in green. For the lower graphics, generate the random matrix $A^{(2)} \in \mathbb{R}^{100\times 150}$ with the RandStream generator and the type 'mt19937ar' and normalize the columns. Run two Monte Carlo experiments: for each $k \leq 100$, choose

M pairs $(I, s) \in \mathcal{S}_{150,k}$ and check the recoverability via the strict recovery condition. The Monte Carlo experiments are realized with $M = 1000$ and $M = 10000$ samples. Each time, a recoverable support is identified, increase a counter variable, which is initialized in dependency of k, by $1/M$. The result is a vector $\{R(M,k)\}_{k=1}^{1000}$ with $R(M,k) \leq 1$. In blue and red, the values $\lambda_k \equiv 2(150-k+1)R(1000,k)/R(1000,k-1)$ respectively $\tilde{\lambda}_k \equiv 2(150-k+1)R(10000,k)/R(10000,k-1)$ are illustrated. Additionally, in thin red and magenta lines, the upper respectively lower bounds on λ_k are given.

Index

Adjacent, 55

Cross-polytope
    projected, 44

Dual Certificate, 24, 39

General Position, 41
    k-faces, 47
    global, 41

Image, 89
    disk-shaped, 117

M-sequence, 82
Matrix
    equiangular, 33
    Gaussian, 67
    recovery, 33, 74, 76
    tight, 31
Modified f-vector, 82

Oriented Matroid, 58

Phase transition, 70
Polytope
    dual, 48
    polar, 48
    simple, 54
    simplicial, 48
Pseudo-power, 82

Reconstruction Rate, 117
Recoverability Curve, 56
Recoverable Support, 39
Redundancy, 1
Regular Intersection, 54
Robustness, 6

Sign pattern, 9
Stability, 6

Bibliography

[1] *The MOSEK optimization toolbox for MATLAB manual. Version 6.0 (Revision 148)*, 2012.

[2] F. Affentranger and R. Schneider. Random projections of regular simplices. *Discrete & Computational Geometry*, 7:219–226, 1992.

[3] B. Alexeev, J. Cahill, and D. G. Mixon. Full spark frames. *Journal of Fourier Analysis and Applications*, 18(6):1167–1194, 2012.

[4] D. Amelunxen, M. Lotz, M. B. McCoy, and J. A. Tropp. Living on the edge: Phase transitions in convex programs with random data. *Information and Inference*, 3(3):224–294, 2014.

[5] MOSEK ApS. MOSEK optimization software, version 6, 2011. http://www.mosek.com.

[6] E. M. Arkin, A. Fernández-Anta, J. S. B. Mitchell, and Mosteiro M. A. Probabilistic bounds on the length of a longest edge in delaunay graphs of random points in d-dimensions. *Computational Geometry*, 48(2):134–146, 2015.

[7] F. Bach, R. Jenatton, J. Mairal, and G. Obozinski. Convex optimization with sparsity-inducing norms. In S. Sra, S. Nowozin, and S. J. Wright, editors, *Optimization for Machine Learning*, pages 1–35. MIT Press, 2011.

[8] K. A. Baker. A generalization of Sperner's lemma. *Journal of Combinatorial Theory*, 6(2):224–225, 1969.

[9] I. Bárány and L. Lovász. Borsuk's theroem and the number of facets of centrally symmetric polytopes. *Acta Mathematica Hungarica*, 40(3–4):323–329, 1982.

[10] D. W. Barnette. The minimum number of vertices of a simple polytope. *Israel Journal of Mathematics*, 10(1):121–125, 1971.

[11] D. W. Barnette. A proof of the lower bound conjecture for convex polytopes. *Pacific Journal of Mathematics*, 46(2):349–354, 1973.

[12] A. Barvinok, S.J. Lee, and I. Novik. Centrally symmetric polytopes with many faces. *Israel Journal of Mathematics*, 195:457–472, 2013.

[13] A. Barvinok, S.J. Lee, and I. Novik. Explicit constructions of centrally symmetric k-neighborly polytopes and large strictly antipodal sets. *Discrete & Computational Geometry*, 49:429–443, 2013.

[14] A. Barvinok and I. Novik. A centrally symmetric version of the cyclic polytope. *Discrete & Computational Geometry*, 39:76–99, 2008.

[15] H. Bauschke, D. Luke, H. Phan, and X. Wang. Restricted normal cones and the method of alternating projections: theory. *Set-Valued and Variational Analysis*, pages 431–473, 2013.

[16] H. Bauschke, D. Luke, H. Phan, and X. Wang. Restricted normal cones and sparsity optimization with affine constraints. *Foundations of Computational Mathematics*, 14(1):63–83, 2014.

[17] H. H. Bauschke and P. L. Combettes. *Convex Analysis and Monotone Operator Theory in Hilbert Spaces*. Springer-Verlag, 2011.

[18] J. J. Benedetto and J. D. Kolesar. Geometric properties of grassmannian frames for $\mathbb{R}^2$ and $\mathbb{R}^3$. *EURASIP Journal on Advances in Signal Processing*, 2006.

[19] L. J. Billera and C. W. Lee. Sufficiency of McMullen's conditions for f-vectors of simplicial polytopes. *Bulletin of the American Mathematical Society*, 2:181–185, 1980.

[20] A. Björner, M. Las Vergnas, B. Sturmfels, N. White, and G. Ziegler. *Oriented Matroids*. Cambrigde University Press, 1993.

[21] J.D. Blanchard, C. Cartis, and J. Tanner. Compressed sensing: How sharp is the restricted isometry property. *SIAM Review*, 53(1):105–125, 2011.

[22] P. Bloomfield and W. L. Steiger. *Least absolute deviations: theory, applications, and algorithms*. Birkhäuser, 2010.

[23] T. Blumensath and M. Davies. Iterative hard thresholding for compressed sensing. *Applied and Computational Harmonic Analysis*, 27(3):265–274, 2009.

[24] T. Blumensath and M. Davies. Sampling theorems for signals from the union of finite-dimensional linear subspaces. *IEEE Transactions on Information Theory*, 55(4):1872–1882, 2009.

[25] F. F. Bonsall. A general atomic decomposition theorem and Banach's closed range theorem. *The Quarterly Journal of Mathematics*, 42:9–14, 1991.

[26] J. Bourgain, S. Dilworth, K. Ford, S. Konyagin, and D. Kutzarova. Explicite constructions of RIP matrices and related problems. *Duke Mathematical Journal*, 159(1):145–185, 2011.

[27] J. N. Bradley and C. M. Brislawn. Compression of fingerprint data using the wavelet vector quantization image compression algorithm. Technical report, Los Alamos Nat. Lab, 1992.

[28] R. A. Brooks and G. DiChiro. Statistical limitations in x-ray reconstructive tomography. *Medical Physics*, 3:237–249, 1976.

[29] A. M. Bruckstein, D. L. Donoho, and M. Elad. From sparse solutions of systems of equations to sparse modeling of signals and images. *SIAM Review*, 51(1):34–81, 2002.

[30] T. M. Buzug. *Computed Tomography. From Photon Statistics to Modern Cone-Beam CT.* Springer, 2008.

[31] T. Tony Cai and A. Zhang. Sharp RIP bound for sparse signal and low-rank matrix recovery. *Applied and Computational Harmonic Analysis*, 35:74–93, 2013.

[32] E. Candès and Y. Plan. A probabilistic and RIPless theory of compressed sensing. *IEEE Transactions on Information Theory*, 57(11):7235–7254, 2011.

[33] E. Candès, J. Romberg, and T. Tao. Stable signal recovery from incomplete an inaccurate measurements. *Communications on Pure and Applied Mathematics*, 59(8):1207–1223, 2006.

[34] E. Candès and T. Tao. Decoding by linear programming. *IEEE Transactions on Information Theory*, 51(12):4203–4215, 2005.

[35] E. Candès and T. Tao. Near-optimal signal recovery from random projections: Universal encoding strategies? *IEEE Transactions on Information Theory*, 52(12), Dec 2006.

[36] P. G. Casazza and G. Kutynoik, editors. *Finite Frames - Theory and Applications.* Springer, 2010.

[37] A. Chambolle. An algorithm for total variation minimization and applications. *Journal of Mathematical Imaging and Vision*, 20:89–97, 2004.

[38] V. Chandrasekaran, B. Recht, P. A. Parrilo, and A. S. Willsky. The convex geometry of linear inverse problems. *Foundations of Computational Mathematics*, 12(6):805–849, 2012.

[39] M. Cho and W. Xu. Precisely verifying the null space conditions in compressed sensing: A sandwiching algorithm. *http://arxiv.org/abs/1306.2665*, 2013.

[40] O. Christensen. *Frames and Bases - An Introductory Course.* Birkhäuser, 2008.

[41] P. G. Ciarlet. *Linear and Nonlinear Functional Analysis with Applications.* SIAM, 2013.

[42] R. E. Cline. Representations for the generalized inverse of a partitioned matrix. *Journal of the Society for Industrial and Applied Mathematics*, 12(3):588–560, 1964.

[43] A. Cohen, W. Dahmen, and R. DeVore. Compressed sensing and best k-term approximation. *Journal of American Mathematical Society*, 22:211–231, 2009.

[44] J.H. Conway, R.H. Hardin, and N.J.A. Sloane. Packing lines, planes, etc.: packings in Grassmannian spaces. *Experimental Mathematics*, 5(2):139–159, 1996.

[45] A. d'Aspremont and L. El Ghaoui. Testing the nullspace property using semidefinite programming. *Mathematical Programming*, 127(1):123–144, February 2011.

[46] I. Daubechies, M. Defrise, and C. De Mol. An iterative thresholding algorithm for linear inverse problems with a sparsity constraint. *Communications in Pure and Applied Mathematics*, 57(11):1413–1457, 2003.

[47] M. Davenport. *Random observations on random observations: Sparse signal acquisition and processing.* PhD thesis, Rice University, 2010.

[48] A. B. de Gonzalez, M. Mahesh, K.-P. Kim, M. Bhargavan, R. Lewis, F. Mettler, and C. Land. Projected cancer risks from computed tomographic scans performed in the united states in 2007. *Archives of Internal Medicine*, 169:2071–2077, 2009.

[49] D. L. Donoho. Neighborly polytopes and sparse solution of underdetermined linear equations. Technical report, Statistics Departement Stanford University, 2004.

[50] D. L. Donoho. High-dimensional centrally-symmetric polytopes with neighborliness proportional to dimension. *Discrete & Computational Geometry*, 35(4):617–652, 2006.

[51] D. L. Donoho and M. Elad. Optimally sparse representation in general (non-orthogonal) dictionaries via ℓ^1 minimization. *Proceedings of the National Academy of Science of the United States of America*, 100:2197–2202, 2003.

[52] D. L. Donoho and X. Huo. Uncertainty principles and ideal atomic decomposition. *IEEE Transactions on Information Theory*, 47(7):2845–2862, 2001.

[53] D. L. Donoho and J. Tanner. Observed universality of phase transitions in high-dimensional geometry, with implications for modern data analysis and signal processing. *Philosophical Transactions of the Royal Society A: Mathematical, Physical and Engineering Sciences*, 367(1906):4273–4293, 2009.

[54] C. Dossal. A necessary and sufficient condition for exact sparse recovery by ℓ_1 minimization. *Comptes Rendus de l'Académie des Sciences - Series I*, 350:117–120, 2012.

[55] D. Dvoretzky. Some results on convex bodies and Banach spaces. *Proc. Internat. Symp. Linear Spaces*, pages 123–160, 1961.

[56] M. Ehler. Random tight frames. *Journal of Fourier Analysis and Applications*, 18(1):1–20, 2012.

[57] M. Elad. *Sparse and Redundant Representations - From Theory to Applications in Signal and Image Processing.* Springer, 2010.

[58] M. Elad and A. M. Bruckstein. A generalized uncertainty principle and sparse representation in pairs of bases. *IEEE Transactions on Information Theory*, 48:2558–2567, 2002.

[59] Y. C. Eldar and G. Kutynoik, editors. *Compressed Sensing - Theory and Applications.* Cambridge, 2012.

[60] M. Fickus, D. G. Mixon, and J. C. Tremain. Steiner equiangular tight frames. *Linear Algebra and its Applications*, 436(5):1014–1027, 2012.

[61] T. Figel, J. Lindenstrauss, and V.D. Milman. The dimension of almost spherical sections of convex bodies. *Acta Mathematica*, 139:53–94, 1977.

[62] M. Fornasier. Numerical methods for sparse recovery. In Massimo Fornasier, editor, *Theoretical Foundations and Numerical Methods for Sparse Recovery*, volume 9 of *Radon Series on Computational and Applied Mathematics*. De Gruyter, 2010.

[63] S. Foucart and R. Gribonval. Real versus complex null space properties for sparse vector recovery. *Computes Rendus de l'Académie des Sciences*, 348(15):863–865, 2010.

[64] S. Foucart and H. Rauhut. *A mathematical introduction to compressed sensing*. Birkhäuser, 2013.

[65] G. Freiman, E. Lipkin, and L. Levitin. A polynomial algorithm for constructing families of k-independent sets. *Discrete Mathematics*, 70:137–147, 1988.

[66] J.-J. Fuchs. On sparse representations in arbitrary redundant bases. *IEEE Transactions on Information Theory*, 50(6), June 2004.

[67] M. R. Garey and D. S. Johnson. *Computers and Intractability - A Guide to the Theory of NP-Completeness*, volume A Series of Books in the Mathematical Science. W. H. Freeman and Company, San Francisco, 1979.

[68] S. Gerschgorin. Über die Abgrenzung der Eigenwerte einer Matrix. *Bulletin de l'Académie des Sciences de l'URSS. Classe des sciences mathématiques et na*, 6:749–754, 1931.

[69] G. H. Golub and C. F. van Loan. *Matrix Computations*. John Hopkins, third edition, 1996.

[70] M. Grasmair. Linear convergence rates for Tikhonov regularization with positively homogeneous functionals. *Inverse Problems*, 27, 2011.

[71] M. Grasmair, M. Haltmeier, and O. Scherzer. Necessary and sufficient conditions for linear convergence of ℓ^1-regularization. *Communications on Pure and Applied Mathematics*, 64(2):161–182, 2011.

[72] R. Gribonval and M. Nielsen. Highly sparse representations from dictionaries are unique and independent of the sparseness measure. *Applied and Computational Harmonic Analysis*, 22(3):335–355, 2007.

[73] B. Grünbaum. *Convex Polytopes*. Number 221 in Graduate Texts in Mathematics. Springer, second edition, 2003.

[74] J. Hadamard. Sur les problèmes aux dérivées partielles et leur signification physique. *Princeton University Bulletin*, 13:49–52, 1902.

[75] E. R. Halsey. *Zonotopal complexes on the d-cube*. PhD thesis, University of Washington, 1972.

[76] M. Haltmeier. Stable signal reconstruction via ℓ_1-minimization in redundant, non-tight frame. *IEEE Transactions on Signal Processing*, 61(2):420–429, 2013.

[77] P.C. Hansen and M. Saxild-Hansen. AIR Tools: A MATLAB package of algebraic iterative reconstruction methods, 2012. www2.compute.dtu.dk/ pcha/AIRtools/.

[78] M. N. Istomina and A. B. Pevnyi. The Mercedes Benz frame in the n-dimensional space [in russian]. *Vestnik Syktyvkar. Gos. Univ. Ser*, 1:219–222, 2006.

[79] X. Jin, L. Li, Z. Chen, L. Zhang, and Y. Xing. Anisotropic total variation for limited-angle CT reconstruction. In *IEEE Nuclear Science Symposium Conference Record (NSS/MIC)*, pages 2232–2238, 2010.

[80] J. S. Jørgensen, C. Kruschel, and D. A. Lorenz. Empirical phase transition in computed tomography using reconstruction and uniqueness testing. *Inverse Problems in Science and Engineering*, 2014.

[81] J. S. Jørgensen, E. Y. Sidky, P. C. Hansen, and X. Pan. Empirical average-case relation between undersampling and sparsity in x-ray CT. *Inverse Problems and Imaging*, 2015. to appear.

[82] M. Joswig and T. Theobald. *Polyhedral and Algebraic Methods in Computational Geometry*. Universitext. Springer, 2013.

[83] A. Juditsky and A. Nemirovski. On verifiable sufficient conditions for sparse signal recovery via ℓ_1 minimization. *Mathematical Programming Series B*, 127:57–88, 2011.

[84] C. Kruschel and D. A. Lorenz. Computing and analyzing recoverable supports for sparse reconstruction. *Advances in Computational Mathematics*, 2015. to appear.

[85] J. Kruskal. The number of simplices in a complex. In Richard Bellmann, editor, *Mathematical Optimization Techniques*, pages 251–278. University of California Press, 1963.

[86] Y. Lonke. On random section of the cube. *Discrete & Computational Geometry*, 23:157–169, 2000.

[87] D. A. Lorenz, M. E. Pfetsch, and A. M. Tillmann. Solving Basis Pursuit: Subgradient algorithm, heuristic optimality check and solver comparison. *Optimization Online*, 2014.

[88] D. A. Lorenz, S. Schiffler, and D. Trede. Beyond convergence rates: exact recovery with the Tikhonov regularization with sparsity constraints. *Inverse Problems*, 27(8), 2011.

[89] M. Lustig, D. Donoho, and L. M. Pauly. Sparse MRI: The application of compressed sensing for rapid MR imaging. *Magnetic Resonance in Medicine*, 58(6):1182–1195, 2007.

[90] S. Mallat. *A Wavelet Tour of Signal Processing: The Sparse Way*. Academic Press, 2009.

[91] V. N. Malozemov and A. B. Pevnyi. Equiangular tight frames. *Journal of Mathematical Sciences*, 157:789–815, 2009.

[92] J. Matoušek. *Lectures on Discrete Geometry*. Springer, 2002.

[93] J. Matoušek and B. Gärtner. *Understanding and Using Linear Programming*. Springer, 2007.

[94] P. McMullen. The maximum numbers of faces of a convex polytope. *Mathematika*, 17:179–184, 1970.

[95] P. McMullen and G. C. Shephard. *Convex Polytopes and the upper bound conjecture*. Number 3 in London Mathematical Society Lecture Note. Cambridge University Press, 1971.

[96] P. McMullen and G.C. Shephard. Diagrams for centrally symmetric d-polytopes. *Mathematika*, 15:123–138, 1968.

[97] S. Nam, M. E. Davies, M. Elad, and R. Gribonval. The cosparse analysis model and algorithms. *Applied and Computational Harmonic Analysis*, 34(1):30–56, 2013.

[98] F. Natterer. *The Mathematics of Computerized Tomography*. John Wiley & Sons, 1986.

[99] D. Needell and R. Ward. Near-optimal compressed sensing guarantees for total variation minimization. *IEEE Transactions on Image Processing*, 22(10):3941–3949, 2013.

[100] Y. Nesterov and A. Nemirovskii. *Interior Point Polynomial Algorithms in Convex Programming*. SIAM, 1994.

[101] P. E. O'Neil. Hyperplane cuts of an n-cube. *Discrete Mathematics*, 1(2):193–195, 1971.

[102] V.M. Patel, G.R. Easley, D.M. Healy, and R. Chellappa. Compressed synthetic aperture radar. *IEEE Journal of Selected Topics in Signal Processing*, 4(2):244–254, 2010.

[103] S. Petra and C. Schnörr. Average case recovery analysis of tomographic compressive sensing. *Linear Algebra and its Applications*, 441(15):168–198, 2014.

[104] M. D. Plumbley. On polar plytopes and the recovery of sparse representations. *IEEE Transactions on Information Theory*, 53(9), Sept 2007.

[105] H. Poincaré. Sur la généralisation d'un théorème d'Euler relatif aux polyèdres. *Comptes Rendus de l'Académie des Sciences*, 177:144–145, 1893.

[106] G. Pope and H. Bölcskei. Sparse signal recovery in Hilbert spaces. In *Proc. of IEEE International Symposium on Information Theory (ISIT)*, pages 1463–1467, 2012.

[107] J. Radon. Über die Bestimmung von Funktionen durch ihre Integralwerte längs gewisser Mannigfaltigkeiten. *Ber. Verh. Sächs. Akad.*, 69:262–277, 1917.

[108] R. T. Rockafellar. *Convex Analysis*. Princeton University Press, 1972.

[109] R. Tyrrell Rockafellar and Roger J-B Wets. *Variational Analysis*. Number 317 in Grundlehren der mathematischen Wissenschaften. Springer, 2004.

[110] M. Rosenfeld. In praise of the gram matrix. In Ronald L. Graham and Jaroslav Nešetřil, editors, *The Mathematics of Paul Erdös II*, volume 14 of *Algorithms and Combinatorics*, chapter VI, pages 318–323. Springer Berlin Heidelberg, 1997.

[111] L. Rudin, S. Osher, and E. Fatemi. Nonlinear total variation based noise removal algorithms. *Physica D: Nonlinear Phenomena*, 60:259–268, 1992.

[112] R. L. Siddon. Fast calculation of the exact radiological path for a three-dimensional CT array. *Medical Physics*, 12:252–255, 1985.

[113] R. Smith-Bindman, J. Lipson, R. Marcus, K.-P. Kim, M. Mahesh, R. Gould, A. B. de Gonzalez, and D. L Miglioretti. Radiation dose associated with common computed tomography examinations and the associated lifetime attributable risk of cancer. *Archives of Internal Medicine*, 169:2078–2086, 2009.

[114] D. Sommerville. The relations connecting the angle sums and volume of a polytope in space of n dimensions. *Proceedings of the Royal Society*, pages 103–119, 1927.

[115] E. Sperner. Ein Satz über Untermengen einer endlichen Menge. *Mathematische Zeitschrift*, 7:544–548, 1928.

[116] R. P. Stanley. The number of faces of simplicial convex polytopes. *Advances in Mathematics*, 35:236–238, 1980.

[117] R. P. Stanley. On the number of faces of centrally-symmetric simplicial polytopes. *Graphs and Combinatorics*, 3:55–66, 1987.

[118] T. Strohmer and R. W. Heath Jr. Grassmannian frames with applications to coding and communication. *Applied and Computational Harmonic Analysis*, 14(3):257–275, 2003.

[119] B. L. Sturm, B. Mailhe, and M. D. Plumbley. On theorem 10 in 'On polar polytopes and the recovery of sparse representations'. *IEEE Transactions on Information Theory*, 59(8):5206–5209, Aug 2013.

[120] Z. Tan, Y. C. Eldar, A. Beck, and A. Nehorai. Smoothing and decomposition for analysis sparse recovery. *IEEE Transactions on Signal Processing*, 62(7):1762–1774, 2014.

[121] A. M. Tillmann and Marc E. Pfetsch. The computational complexity of the restricted isometry property, the nullspace property, and related concepts in compressed sensing. *IEEE Transactions on Information Theory*, 60(2):1248–1259, 2014.

[122] J. Tropp. Recovery of short, complex linear combinations via ℓ_1 minimization. *IEEE Transactions on Information Theory*, 51:1030–1051, 2006.

[123] J. A. Tropp. Greed is good: Algorithmic results for sparse approximation. *IEEE Transactions on Information Theory*, 50(10):2231–2242, Oct 2004.

[124] J. A. Tropp. Just relax: Convex programming methods for identifying sparse signals in noise. *IEEE Transactions on Information Theory*, 52(3):1030–1051, 2006.

[125] J. Trzasko and A. Manduca. Highly undersampled magnetic resonance image reconstruction via homotopic ℓ_0-minimization. *IEEE Transactions on Medical Imaging*, 28(1):106–121, 2009.

[126] Y. Tsaig and D. L. Donoho. Breakdown of local equivalence between sparse solution and ℓ^1 minimization. *Signal Processing*, 86(3):533–548, 2006.

[127] S. Vaiter, G. Peyré, C. Dossal, and J. Fadili. Robust sparse analysis regularization. *IEEE Transactions on Information Theory*, 59(4):2001–2016, 2013.

[128] L. R. Welch. Lower bounds on the maximum cross correlation of signals. *IEEE Transactions on Information Theory*, 20(3):397–399, 1974.

[129] J. Wright, A. Y. Yang, A. Ganesh, S. Shankar Sastry, and Y. Ma. Robust face recognition via sparse representation. *IEEE Transactions on Pattern Analysis and Michine Intelligence*, 31(2):1–18, 2009.

[130] Y. Zhang. Theory of compressive sensing via ℓ_1-minimization: a non-RIP analysis and extensions. Technical report, Rice University, Houston, 2008.

[131] C. Zhong. *Strange Phenomena in convex and discrete geometry.* Springer-Verlag, 1996.

[132] G. M. Ziegler. *Lectures on Polytopes.* Number 152 in Graduate Texts in Mathematics. Springer, 1995.